

Oral Presentations

Saturday, June 25, 2022

Neuro-oncology 1

OPR-001

Patient and carer involvement in the formulation of the clinical questions: the Guideline on Palliative Care (PC) in Adults with Glioma

S. Veronese¹, A. Solari², E. Bertocchi³, B. Lissoni⁴, L. De Panfilis⁵, G. Dalla Verde¹, R. Rudà⁶, A. Silvani⁷, R. Merli⁸, A. Pace⁹

¹ Palliative care and research department, Fondazione FARO, Turin, Italy, ² Fondazione IRCCS Istituto Neurologico Carlo Besta, Milano, Italy, ³ Palliative care unit – Azienda USL - IRCCS di Reggio Emilia, Reggio Emilia, Italy, ⁴ Hospice and Palliative Care Unit, Niguarda Hospital, Milan, Italy, ⁵ Bioethics Unit, Azienda USL - IRCCS di Reggio Emilia, Reggio Emilia, Italy, ⁶ Department of Neuro-oncology, City of Health and Science and University of Turin, Turin, Italy, ⁷ Unit of Neuro-Oncology, Fondazione IRCCS Istituto Neurologico Carlo Besta Milan, Milan, Italy, ⁸ Unit of Neurosurgery, Papa Giovanni XXXIII hospital, Bergamo, Italy, ⁹ Neuro-Oncology Unit, IRCCS-Regina Elena National Cancer Institute, Rome, Italy

Background and aims: In 2017, the European Association for Neuro-Oncology (EANO) published the guideline for palliative care (PC) in adults with glioma. The Italian Society of Neurology (SIN), the Italian Association for Neuro-Oncology (AINO), and the Italian Society for Palliative Care (SICP) joined forces to update and adapt these guidelines to the Italian context; and (herein presented) to involve patients and carers in the formulation of the clinical questions.

Methods: Semi-structured interviews with glioma patients and focus group meetings (FGMs) with family carers of deceased patients. Participants rated the importance of 10 pre-specified intervention topics produced by the guideline panel, shared their experience, and suggested additional topics. Interviews and FGMs were audio-recorded, transcribed, coded and analysed (framework and content analysis).

Results: We held 20 interviews and five FGMs (28 carers). Both groups considered communication and psychological support as the most important topics, and reported difficulties in dealing with behavior and personality changes. Patients emphasized the impact of focal neurological and cognitive deficits. Carers focused on the preservation of functioning via rehabilitation and social support. Both affirmed the importance of a dedicated health care path and patient's involvement in the decision-making process.

Conclusion: Interviews and FGMs were well informative but emotionally demanding. Participants confirmed the importance of the 10 intervention topics, with no additional issues identified. Our findings strengthen the importance of a comprehensive care approach, and of addressing the needs of both parties (patients and family carers).

Disclosure: Nothing to disclose.

OPR-002

MRI response assessment in glioblastoma patients treated with dendritic cell-based immunotherapy

J. Heugenhauer¹, M. Galijasevic², S. Mangesius², G. Goebel³, J. Buchroithner⁴, F. Erhart⁵, J. Pichler⁶, G. Widhalm⁵, G. Stockhammer¹, S. Iglseider¹, C. Freyschlag⁷, S. Oberndorfer⁸, K. Bordihn⁹, G. Von Campe¹⁰, T. Czech⁵, B. Surböck¹¹, T. Urbanic Purkart¹², C. Marosi⁶, T. Felzmann¹³, M. Nowosielski¹

¹ Department of Neurology, Medical University of Innsbruck, Innsbruck, Austria, ² Department of Neuroradiology, Medical University of Innsbruck, Innsbruck, Austria, ³ Department of Medical Statistics, Informatics and Health Economics, Medical University Innsbruck, Innsbruck, Austria, ⁴ University Clinic for Neurosurgery, Kepler University Hospital, Johannes Kepler University, Linz, Austria, ⁵ Department of Neurosurgery, Medical University of Vienna, Vienna, Austria, ⁶ Department of Internal Medicine and Neurooncology, Kepler University Hospital, Johannes Kepler University, Linz, Austria, ⁷ Department of Neurosurgery, Medical University of Innsbruck, Innsbruck, Austria, ⁸ Department of Neurology, University Clinic of St. Pölten, Karl Landsteiner Private University, St. Pölten, Austria, ⁹ Department of Neurosurgery, University Clinic of Salzburg, Paracelsus Private Medical University, Salzburg, Austria, ¹⁰ Department of Neurosurgery, Medical University of Graz, Graz, Austria, ¹¹ Department of Neurology, Klinik Favoriten, Wiener Gesundheitsverbund, Vienna, Austria, ¹² Department of General Neurology and Department of Neuroradiology, Vascular and Interventional Radiology, Medical University of Graz, Graz, Austria, ¹³ Activartis Biotech GmbH, Vienna, Austria

Background and aims: In this post-hoc analysis we compared response assessment criteria (MacDonald, RANO, Vol-RANO, mRANO, Vol-mRANO, iRANO) in newly diagnosed glioblastoma (GB) patients treated with tumor lysate-charged autologous dendritic cells (Audencel) and determined the differences in prediction of progression free survival (PFS) and overall survival (OS).

Methods: 76 patients with newly diagnosed GB enrolled in a multicenter phase II trial receiving standard of care (SOC, n=40) or SOC + Audencel vaccine (n=36) were included. MRI scans were evaluated using MacDonald, RANO, mRANO and iRANO criteria. Tumor volumes (T1 contrast enhancing as well as T2/FLAIR volumes) were calculated by semiautomatic segmentation. To detect differences in PFS among the assessment criteria Kruskal-Wallis-test, for correlation analysis Spearman test were used.

Results: There was a significant difference in median PFS between mRANO (8.6 months) and Vol-mRANO (8.6 months) compared to MacDonald (4.0 months), RANO (4.2 months) and Vol-RANO (5.4 months). For the vaccination arm, median PFS by iRANO was 6.2 months. There was no difference in PFS between SOC and SOC + Audencel using these various response criteria. The best correlation between PFS/OS was detected for mRANO ($r=0.65$) and Vol-mRANO ($r=0.69$, each $p<0.001$). 16/76 patients developed a pure T2/FLAIR progressing disease, 4/36 patients treated with Audencel developed pseudoprogression.

Conclusion: When comparing different response assessment criteria in GB patients treated with dendritic cell-based immunotherapy, best correlation between PFS and OS was observed for mRANO and Vol-mRANO. iRANO was not superior for predicting OS in patients treated with Audencel.

Disclosure: Nothing to disclose.

OPR-003

ABTR-SANO Real-World Pattern of Care Study on Glioblastoma in the Austrian Population. Final results from 2014–2020

S. Oberndorfer¹, A. Woehrer², M. Borkovec², C. Marosi³, F. Payer⁵, T. Urbanic-Purkart⁵, M. Nowosielski⁷, S. Iglseider⁷, G. Stockhammer⁷, W. Kleindienst⁶, C. Florea⁶, A. Hager⁹, A. Tinchon¹, M. Stultschnig⁸, B. Surboeck¹⁰, J. Pichler¹¹, A. Leibetseder¹³, S. Weiss¹², M. Hutterer¹³, L. Seebrecht², T. Roetzer², A. Hainfellner², J. Hainfellner²

¹ Department of Neurology, University Clinic St. Pölten, Austria, ² Division of Neuropathology and Neurochemistry, Medical University of Vienna, Vienna, Austria, ³ Department of Medicine I, Medical University of Vienna, Vienna, Austria, ⁵ Department Neurology, University Clinic Graz, Graz, Austria, ⁶ Department Neurology, CDK-University Clinic Salzburg, Salzburg, Austria, ⁷ Department Neurology, University Clinic Innsbruck, Innsbruck, Austria, ⁸ Department Neurology, Klinikum Klagenfurt, Klagenfurt, Austria, ⁹ Department Neurology, LKH Wr. Neustadt, Wr. Neustadt, Austria, ¹⁰ Department Neurology KFJ, Vienna, Vienna, Austria, ¹¹ Department Internal Medicine, J Kepler University Clinic Linz, Linz, Austria, ¹² Department Neuropathology, J Kepler University Clinic Linz, Linz, Austria, ¹³ Department Neurology, J Kepler University Clinic Linz, Linz, Austria

Background and aims: The Austrian ABTR-SANO Glioblastoma Registry is the first population-based assessment of patterns of care for patients with Glioblastoma across Austrian healthcare institutions. The primary aim is to assess the real world effectiveness of administered therapies.

Methods: Clinical data are collected via a common web-based IT platform “ABTR-SANO Net” since 2014. The database and the ongoing evaluation of clinical parameters, as well as interims analysis are provided in cooperation with a review board. First Outcome analysis, including patients from 2014–2020, was performed at the end of 2021.

Results: 11 centers across Austria are involved, and the data of 1,416 patients (m/f ratio: 1.35, median age: 66 years) were recently analyzed in detail. Age, extent of resection, as well as ECOG was associated with improved survival. Methylated MGMT Status also showed a moderate survival benefit. Patients with re-resection and re-radiation also exhibited improved survival, which however may be attributed to a selection bias. Second line treatment mainly comprised of antiangiogenic treatment, followed by alkylated agents, re-radiation and re-surgery. Median overall survival of all patients was 344 days and clearly age dependent (best for <50 years, worse for >80 years)

Conclusion: This is the first population based outcome analysis of Glioblastoma in Austria. Results regarding prognostic markers and outcome are mostly comparable with international data. Robust population based data are important in order to monitor quality of health care, and to match the data with results from clinical studies.

Disclosure: Nothing to disclose.

OPR-004

Brain Tumour-Related Epilepsy: Impact of Grading and Treatments in a Cohort of Molecularly Defined Lower-Grade Gliomas

F. Bruno¹, A. Pellerino¹, F. Mo¹, E. Muscolino¹,

C. Mantovani², A. Melcarne³, R. Rudà¹, R. Soffietti¹

¹ Department of Neuro-Oncology, University and City of Health and Science Hospital, Turin, Italy, ² Department of Radiation Oncology, University and City of Health and Science Hospital, Turin, Italy, ³ Department of Neurosurgery, University and City of Health and Science Hospital, Turin, Italy

Background and aims: Brain-tumour related epilepsy is associated with lower-grade gliomas (LGGs) in up to 70–90% of cases. Our study aims to identify which factors are related to seizure control in a large cohort of grade 2 and 3 LGGs patients.

Methods: We retrospectively collected clinical data of LGGs patients with history of BTRE. We retained information about seizure-freedom after surgery, adjuvant treatments, and at recurrence.

Results: 280 patients with LGGs diagnosed between 1988 and 2021 were included. Oligodendrogliomas IDH-mutant 1p19q-codeleted, astrocytomas IDH-mutant and IDH-wildtype were 106 (54.9%), 40 (20.7%), and 47 (24.4%), respectively. Grade 2 and 3 tumours were 199 (71.1%) and 81 (28.9%). Gross-total resection (GTR) accounted for 117 (41.8%) cases. In a multivariable model, seizure-freedom after surgery was positively related to age ≥ 40 years (OR 2,173, $p=0.012$) and GTR (OR 2,006, $p=0.022$), and negatively related to temporal lobe location (OR 0.440, $p=0.007$) and grade 2 histology (OR 0.271, $p<0.001$). Similarly, grade 2 histology and temporal lobe location were negative predictors of seizure-freedom after adjuvant treatments (OR 0.169, $p<0.001$, and OR 0.353, $p=0.006$, respectively). FLAIR response to adjuvant treatments (complete/partial vs stable disease/progression) was associated with seizure-freedom (84.2% vs 59.4%, $p=0.040$) regardless of tumour grade. Seizures were a symptom at recurrence in 134 (59.6%) patients. Previous RT significantly reduced the risk of seizures at recurrence (OR 0.343, $p=0.010$).

Conclusion: These data suggest that grade 2 histology increases the risk of seizure persistence after treatment among LGGs. Conversely, GTR and RT are associated with seizure control regardless of tumour grade.

Disclosure: I have no disclosures.

OPR-005

Abstract withdrawn

Cognitive neurology/neuropsychology

OPR-006

Unravelling neural correlates of empathy deficits along Alzheimer's Disease continuum

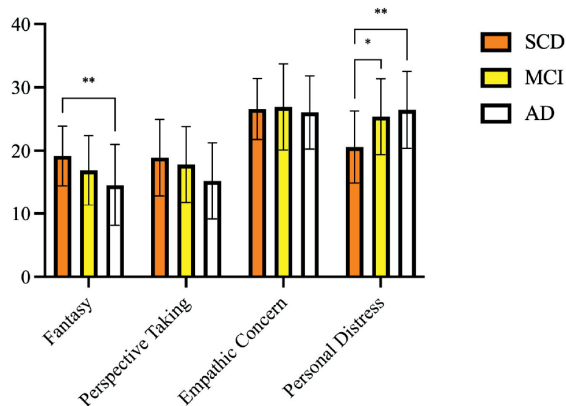
G. Giacomucci¹, G. Galdo¹, C. Polito², V. Berti³, S. Padiglioni⁴, S. Mazzeo¹, M. De Cristofaro⁵, S. Bagnoli¹, B. Nacmias¹, S. Sorbi¹, V. Bessi¹

¹ Department of Neuroscience, Psychology, Drug Research and Child Health, University of Florence, Florence, Italy, ² IRCCS Fondazione Don Carlo Gnocchi, Florence, Italy, ³ Department of Biomedical, Experimental and Clinical Sciences "Mario Serio", University of Florence, Florence, Italy, ⁴ Regional Referral Centre for Relational Criticalities - Tuscany Region, Italy, ⁵ Nuclear Medicine Unit, Azienda Ospedaliero-Universitaria Careggi, Florence, Italy

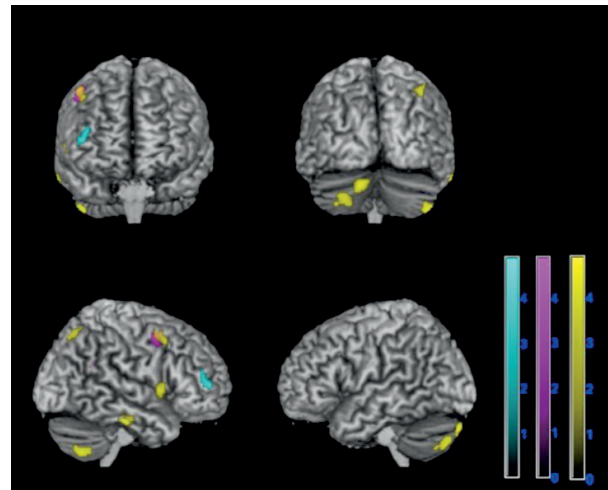
Background and aims: Empathy is the ability to understand (cognitive empathy) and to feel (affective empathy) what others feel. We aimed to assess empathy deficit and neuronal correlates along Alzheimer's Disease (AD) continuum: from Subjective Cognitive Decline (SCD), to Mild Cognitive Impairment (MCI) and to dementia.

Methods: 24 SCD, 41 MCI and 46 AD patients were included. Informer-rated Interpersonal Reactivity Index was used to explore cognitive (Perspective Taking-PT, Fantasy-FT) and affective (Empathic Concern-EC, Personal Distress-PD) empathy, before (T0) and after (T1) cognitive symptoms' onset. Cerebral FDG-PET SPM analysis was used to explore neural correlates underlying empathy deficits.

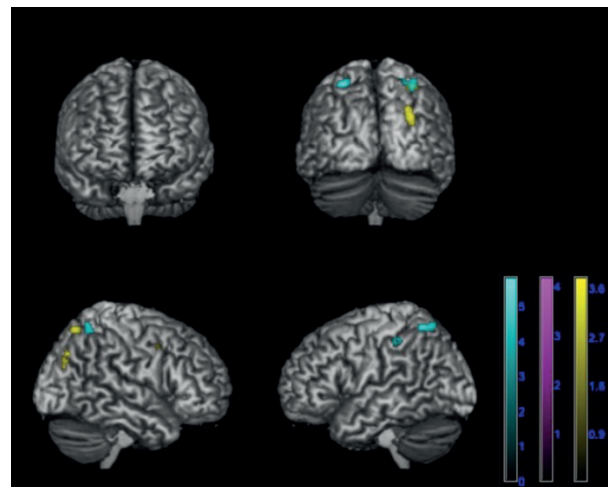
Results: PD-T1 score were higher in AD compared to MCI and to SCD ($p=0.001$). A positive correlation was found between PT-T1 and hmetabolic dysfunction of right middle gyrus (MFG) in MCI and AD. In AD group, a positive correlation between PT-T1 and insula and superior temporal gyrus (STG) metabolism was detected. PD-T1 was negatively correlated with superior parietal lobule metabolism in MCI, and with STG metabolism in AD.



Current empathy assessed by Interpersonal Reactivity Index (IRI) in Subjective Cognitive Decline (SCD), Mild Cognitive Impairment (MCI) and Alzheimer's Disease (AD). * $p<0.05$; ** $p<0.01$.



Positive correlation between cognitive empathy assessed by PT-T1 IRI subscale and brain metabolism in MCI and AD patients at 18F-FDG-PET SPM analysis. Colour grading: Cyan= MCI, Violet=AD, Yellow=MCI & AD.



Negative correlation between emotional contagion assessed by PD-T1 IRI subscale and brain metabolism in MCI and AD patients at 18F-FDG-PET SPM analysis. Colour grading: Cyan= MCI, Violet=AD, Yellow=MCI & AD.

Conclusion: Impairment of cognitive empathy starts at MCI stage, while increase of PD starts from preclinical phases. Our study suggests the presence of a continuum, with a progressive involvement of structures involved in cognitive empathy starting from prodromal stage of AD. Heightened emotional contagion is probably related to derangement of mirror neurons systems in parietal regions in prodromal stage, and to impairment of temporal emotion inhibition system in dementia. Further studies are needed to clarify if empathy deficits might be a predictive feature of a cognitive decline driven by AD.

Disclosure: The authors have nothing to disclose.

OPR-007

Hippocampal microstructural integrity and speed of information processing in multiple sclerosis

D. Mistri¹, L. Cacciaguerra², E. Pagani¹, P. Valsasina¹, A. Meani¹, M. Rocca³, M. Filippi³

¹ Neuroimaging Research Unit, Division of Neuroscience, IRCCS San Raffaele Scientific Institute, Milan, Italy,

² Neuroimaging Research Unit, Division of Neuroscience, IRCCS San Raffaele Scientific Institute, and Vita-Salute San Raffaele University, Milan, Italy, ³ Neuroimaging Research Unit, Division of Neuroscience, and Neurology Unit, IRCCS San Raffaele Scientific Institute, and Vita-Salute San Raffaele University, Milan, Italy

Background and aims: The contribution of hippocampal atrophy to cognitive impairment has been widely described in multiple sclerosis (MS). However, less is known about measures of microstructural damage, which could provide further insights on mechanisms of cognitive dysfunction. Aim of this study was to investigate the association between hippocampal microstructural integrity and information processing speed deficit (IPS) in MS.

Methods: 50 healthy controls (HC) and 117 MS patients underwent 3.0T MRI. Global and subregional hippocampal volumes were assessed with the cross-sectional pipeline of Freesurfer 6.0. Measures of microstructural integrity were obtained using diffusion tensor imaging (i.e. fractional anisotropy [FA], mean diffusivity [MD]) and neurite orientation dispersion and density imaging (NODDI, i.e. neurite density index, orientation dispersion index [ODI]). Symbol Digit Modalities Test (SDMT) was administered to assess IPS, and z-scores were calculated according to normative data. Age- and sex-adjusted linear models were used for between-group comparisons. In MS patients, hierarchical linear regression analysis was run to identify predictors of SDMT z-scores among clinical and MRI variables.

Results: Compared to HC, MS patients showed atrophy of the fimbria ($p < 0.001$) as well as reduced FA and increased MD and ODI compared of the whole hippocampus ($p < 0.004$). Older age (delta R-square=0.189; $p < 0.001$), higher T2-lesion volume (delta R-square=0.055; $p = 0.009$) and higher MD of the fimbria (delta R-square=0.051; $p = 0.010$) were selected as significant predictors of slower IPS measured with SDMT (adjusted R-square=0.273).

Conclusion: The integrity of the fimbria appears to be a critical anatomical correlate of information processing speed performance in MS.

Disclosure: Nothing to disclose.

OPR-008

Cognitive dysfunction in primary and secondary progressive MS: a multiparametric structural and functional MRI study

D. Mistri¹, L. Cacciaguerra², P. Valsasina¹, E. Pagani¹, M. Filippi³, M. Rocca³

¹ Neuroimaging Research Unit, Division of Neuroscience, IRCCS San Raffaele Scientific Institute, Milan, Italy,

² Neuroimaging Research Unit, Division of Neuroscience, IRCCS San Raffaele Scientific Institute, and Vita-Salute San Raffaele University, Milan, Italy, ³ Neuroimaging Research Unit, Division of Neuroscience, and Neurology Unit, IRCCS San Raffaele Scientific Institute, and Vita-Salute San Raffaele University, Milan, Italy

Background and aims: Few cross-sectional studies have been focused on identifying patterns of cognitive impairment in progressive multiple sclerosis (MS) and possible differences between primary progressive (PP) and secondary progressive (SP) MS remain to be determined. Aim of this study was to investigate the contribution of structural and functional MRI abnormalities in explaining cognitive dysfunction in PPMS and SPMS.

Methods: Brain dual-echo, diffusion tensor, 3D T1-weighted, and resting-state (RS) MRI scans were acquired from 183 MS patients (60 PPMS and 123 SPMS) and 75 healthy controls. Cognitive assessment included the Brief Repeatable Battery of Neuropsychological tests; for all cognitive tests z-scores were calculated and used to derive a measure of global cognition (BRB-N z). Hierarchical linear regression analysis was run to assess the association of BRB-N z with clinical and MRI variables.

Results: Compared to PPMS, SPMS showed decreased fractional anisotropy (FA) ($p = 0.012$) in the fornix, and lower RS functional connectivity within the basal ganglia network ($p = 0.005$). No differences between PPMS and SPMS were found in mean BRB-N z (-1.0 and -1.1 respectively; $p = 0.46$). In PPMS patients, decreased FA of the medial lemniscus ($\Delta R^2 = 0.107$; $p = 0.011$) and lower normalized gray matter volume ($\Delta R^2 = 0.287$; $p < 0.001$) were associated with lower BRB-N z (adjusted-R² = 0.364). In SPMS, decreased FA of the fornix ($\Delta R^2 = 0.345$; $p < 0.001$) and lower normalized white matter volume ($\Delta R^2 = 0.045$; $p = 0.034$) were associated with worse cognitive status (adjusted-R² = 0.371).

Conclusion: PPMS and SPMS showed similar patterns and degree of cognitive impairment. However, different structural substrates contribute to explain cognitive dysfunction in these clinical phenotypes of MS.

Disclosure: Nothing to disclose.

OPR-009

Spatial correlations of gray matter atrophy and neurotransmitter maps explain clinical features in multiple sclerosis

A. Fiore¹, P. Preziosa¹, N. Tedone¹, M. Margoni¹, M. Filippi², M. Rocca²

¹ *Neuroimaging Research Unit, Division of Neuroscience, IRCCS San Raffaele Scientific Institute, Milan, Italy,*

² *Neuroimaging Research Unit, Division of Neuroscience, and Neurology Unit, IRCCS San Raffaele Scientific Institute, and Vita-Salute San Raffaele University, Milan, Italy*

Background and aims: In multiple sclerosis (MS), clinically-relevant gray matter (GM) atrophy progresses in a non-random manner, possibly due to the preferential involvement of specific neurotransmitter networks. However, the associations among regional GM atrophy, neurotransmitter distribution and MS clinical manifestations still need to be fully explored.

Methods: Brain 3.0 T MRI scans were acquired from 286 patients with MS (PwMS) and 172 healthy controls (HC). Regional GM volume differences, the cross-correlations between regional GM atrophy and nuclear imaging-derived neurotransmitter maps and their associations with clinical disability, cognitive impairment, fatigue and depression were investigated using voxel-based morphometry and Jspace toolbox.

Results: Compared to HC, PwMS showed a widespread pattern of cortico-subcortical GM atrophy that was spatially correlated with serotonergic, dopaminergic, opioid, noradrenergic, cholinergic and glutamatergic maps ($p < 0.003$). Cognitively-impaired vs cognitively-preserved PwMS had a widespread pattern of GM atrophy that was spatially associated with serotonergic, dopaminergic, opioid, noradrenergic, cholinergic and glutamatergic maps ($p < 0.04$). Compared to mildly-disabled PwMS, those reaching Expanded Disability Status Scale > 3.0 had significant atrophy of deep GM, fronto-temporal and cingulate cortices, hippocampi and cerebellum, which were associated with serotonergic, dopaminergic, and cholinergic maps ($p < 0.02$). Compared to non-fatigued PwMS, those with fatigue had significant atrophy of fronto-temporo-parietal and cingulate cortices, hippocampi and cerebellum, which were associated with the serotonergic, dopaminergic, opioid and glutamatergic maps ($p < 0.03$). No significant GM volume differences and associations with neurotransmitter maps were found according to depression.

Conclusion: GM atrophy in regions belonging to specific neurotransmitter systems may contribute to explain part of MS clinical manifestations, including locomotor disability, cognitive impairment and fatigue.

Disclosure: Nothing to disclose.

OPR-010

Cognitive reserve modulates the impact of frontal lobe damage on executive functioning in multiple sclerosis

P. Preziosa¹, L. Conti¹, E. Pagani¹, M. Filippi², M. Rocca²

¹ *Neuroimaging Research Unit, Division of Neuroscience, IRCCS San Raffaele Scientific Institute, Milan, Italy,*

² *Neuroimaging Research Unit, Division of Neuroscience, and Neurology Unit, IRCCS San Raffaele Scientific Institute, and Vita-Salute San Raffaele University, Milan, Italy*

Background and aims: Early-life enriching experiences may influence frontal lobe maturation and may preserve executive function (EF) integrity in multiple sclerosis (MS). In this study, we investigated the interaction between cognitive reserve, frontal gray matter (GM) atrophy and white matter (WM) tract microstructural abnormalities and their associations with EF in MS patients.

Methods: Frontal GM volumes, lesional volume, fractional anisotropy, mean diffusivity, intracellular volume fraction and orientation dispersion index of frontal WM tracts were quantified in 93 MS patients and 27 matched healthy controls (HC). Cognitive reserve index (CRI), Wisconsin Card Sorting Test (WCST) and Word List Generation (WLG) of the Rao's battery were assessed. Interaction of structural MRI measures and CRI on cognitive performance were explored.

Results: MS patients vs HC showed significant diffuse frontal GM atrophy and WM tract microstructural abnormalities ($p < 0.046$) and worse performances in categories and total errors of WCST and WLG ($p < 0.034$). In MS, higher CRI was correlated with better WLG performance, WCST-categories, frontal gyri volumes and diffusivity measures of frontal WM tracts (r from -0.212 to 0.455 ; $p \leq 0.046$). The combination of demographic, clinical and measures of frontal lobe structural damage significantly explained EF (WLG: $R^2 = 0.44$; $p = 0.022$; WCST categories: $R^2 = 0.33$; $p = 0.010$). Higher CRI explained a further portion of variance in WLG (WLG: $R^2 = 0.50$; $p = 0.002$; $\Delta R^2 = 0.07$; $p = 0.003$).

Conclusion: In MS, CRI is associated with higher frontal GM volumes and higher frontal WM tract microstructural integrity. CRI may contribute to preserve semantic verbal fluency and cognitive flexibility, possibly moderating the effect of frontal lobe structural damage on cognitive performance.

Disclosure: Nothing to disclose.

OPR-011

Functional Cognitive Disorder is a multisystem condition affecting reaction time and metacognition

T. Teodoro ¹, A. Koreki ³, J. Chen ⁵, J. Coebergh ¹,
N. Poole ⁴, J. Ferreira ², M. Edwards ¹, [J. Isaacs](#) ¹

¹ *Atkinson Morley Neurosciences Centre, St George's University Hospitals, London, United Kingdom*, ² *Instituto de Medicina Molecular, Lisbon, Portugal*, ³ *Department of Neuropsychiatry, Keio University, Tokyo, Japan*, ⁴ *South West London and St George's Mental Health NHS Trust, London, United Kingdom*, ⁵ *St George's University, London, United Kingdom*

Background and aims: We hypothesised that FCD is characterised by heightened subjective mental effort, exhausted attentional reserve and metacognitive failure.

Methods: Stroop colour-word task in which attentional demand was varied by task difficulty (congruent/incongruent cues) and the presence of an auditory stimulus (passive/active listening to oddball-type paradigm). We measured subjective mental effort, objective performance, metacognition and EEG-based biomarkers of mental workload (including P300 suppression).

Results: We tested 19 patients with FCD and 23 healthy controls. FCD patients reported higher levels of depression, anxiety, fatigue, pain, sleep disruption, dissociation and obsessiveness. FCD was associated with slower reaction times; however the Stroop effect was similar in both groups. FCD patients reported greater mental workload and poorer self-rated performance when performing the congruent Stroop task in noisy conditions. However, accuracy did not differ between groups in any condition, suggesting that FCD patients are more prone to metacognitive error. Biomarkers of mental workload were similar in both groups, regardless of task difficulty.

Conclusion: In our sample, FCD was characterised by altered mood, somatic complaints, dissociation, and obsessiveness, suggesting syndromic overlap with mood disorders, chronic fatigue and pain. FCD was associated with metacognitive failure in that patients reported high subjective mental effort and poor self-reported performance but were just as accurate as controls. However, FCD patients were slower than controls, providing some objective support for the subjective “brain fog” commonly reported in this condition. We found no evidence of changes in EEG biomarkers of mental workload.

Disclosure: Nothing to disclose.

Cerebrovascular diseases: Acute stroke management

OPR-012

Absence of Susceptibility Vessel Sign in Patients with Malignancy-related Acute Ischemic Stroke

M. Beyeler¹, N. Belachew², M. Kielkopf¹, E. Aleman³, A. Betancourt¹, K. Genceviciute¹, C. Kurmann², B. Birner¹, T. Meinel¹, A. Scutelnic¹, P. Philipp¹, D. Seiffge¹, T. Dobrocky², H. Mattle¹, M. Arnold¹, U. Fischer⁴, T. Pabst⁵, M. Berger⁵, J. Kaesmacher², S. Jung¹

¹ Department of Neurology, Inselspital, Bern University Hospital, and University of Bern, Bern, Switzerland,

² Institute for Diagnostic and Interventional Neuroradiology, Inselspital, Bern University Hospital, and University of Bern, Bern, Switzerland, ³ Department of Neuroradiology, University Hospital, Freiburg, Germany, ⁴ Neurology Department, University Hospital of Basel, University of Basel, Basel, Switzerland, ⁵ Department of Medical Oncology, Inselspital, Bern University Hospital, and University of Bern, Bern, Switzerland

Background and aims: Platelet and fibrin-rich composition of retrieved thrombi in patients with acute ischemic stroke (AIS) are associated with the absence of susceptibility vessel sign (SVS) on MRI and the presence of active malignancy. This study analyzed the direct association between SVS status and the presence of active malignancy in AIS patients that underwent mechanical thrombectomy (MT).

Methods: Single-centered, retrospective and cross-sectional study including consecutive patients with admission MRI treated for AIS with MT between January 2010 and December 2018. SVS status was evaluated on susceptibility weighted imaging (SWI). Adjusted OR (aOR) were calculated to determine the association between the absence of SVS and active and occult malignancy presence. The performance of predictive models with and without SVS status were assessed by calculating the areas under the Receiver Operating Characteristics curve (auROC).

Results: Of the 577 AIS patients with assessable SVS status, 40 (6.9%) had a documented active malignancy and 72 patients (12.5%) showed no SVS. The absence of SVS was strongly associated with active malignancy (aOR 4.85, 95% CI 1.94–12.11) and occult malignancy alone (aOR 11.42, 95% CI 2.36–55.20). The auROC of predictive models, including demographics and common malignancy-biomarkers, decreased from 0.85 to 0.82 when SVS status was excluded (Figure, p=0.07).

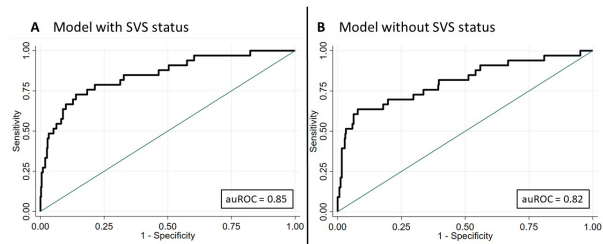


Figure – Comparison of predictive models for active malignancy with and without SVS status.

Conclusion: The absence of SVS on baseline MRI is associated with the presence of active and occult malignancy in patients with AIS eligible for MT. Considering SVS status may increase the chances of detecting paraneoplastic coagulation disorders and occult malignancy in patients with AIS.

Disclosure: Nothing to disclose.

OPR-013

Abstract withdrawn

OPR-014

Acute ischemic stroke in patients with active versus never cancer: characteristics, mechanisms, and stroke recurrence.

G. Costamagna¹, A. Hottinger², H. Milionis³, A. Salerno¹, D. Strambo¹, F. Livio⁴, B. Navi⁵, P. Michel¹

¹ Service of Neurology, Department of Clinical Neurosciences, Lausanne University Hospital and University of Lausanne, Lausanne, Switzerland, ² Services of Neurology and Oncology, Lausanne University Hospital and University of Lausanne, Switzerland, ³ 1st Department of Internal Medicine, University of Ioannina, Medical School, Ioannina, Greece, ⁴ Service of Clinical Pharmacology, Lausanne University Hospital and University of Lausanne, Switzerland, ⁵ Feil Brain and Mind Research Institute and Department of Neurology, Weill Cornell Medicine, New York, NY, United States of America

Background and aims: Acute ischemic stroke (AIS) and cancer are important causes of disability and death. We aimed to estimate the rate of active cancer (AC) in a large cohort of consecutive AIS patients, and to assess demographics, risk factors, mechanisms, and long-term outcomes when compared with never-cancer (NC) AIS patients.

Methods: We retrospectively analyzed data from ASTRAL (Acute-Stroke-Registry-and-Analysis-of-Lausanne) between 01/2003-10/2021. We defined AC according to the standard definition (Khorana, J.Thromb.Haemost, 2018) and included newly-diagnosed cancer within 12 months after the index stroke in the AC group. We performed univariate analysis comparing both groups regarding patients' characteristics, stroke mechanisms, and long-term functional outcomes. Other multivariate logistic regression analyses are ongoing and will be presented at the congress.

Results: Among 5,917 AIS patients, 44.3% were women and the median age was 73.8 years (IQR 21.3). We identified 396 (6.7%) AC patients and 5,521 (93.3%) NC patients. Whereas stroke risk factors were mostly similar between groups (Table), AC patients were more often men and presented with higher pre-stroke modified Rankin Scale scores. Compared to NC patients, AC patients had fewer traditional stroke mechanisms and more multiple/rare mechanisms [OR 7.3 (5.6–9.6)]. In unadjusted analyses, AC patients had a higher rate of stroke recurrence within 3-months as well as increased disability and mortality.

Variable	Study cohort (N=5917)	Active cancer (AC) (N = 396)	Never cancer (NC) (N = 5521)	OR (95% CI)	p-value
Age	73.8 (21.3)	74.3 (16.7)	73.8 (21.8)		0.039
Female sex	2623/5917(44.3%)	154/396 (38.9%)	2469/5521(44.7%)	0.79 (0.64 – 0.97)	0.024
mRS pre-stroke	0 (2)	1(2)	0(2)	1.3 (1.19-1.41)	0.026
Vascular risk factors					
Hypertension	1650/5916 (72.1%)	288/395 (72.9%)	3976/5521 (72.1%)	1.04 (0.83-1.31)	0.71
Atrial fibrillation	1716/5909 (29%)	106/393 (27%)	1610/5516 (29.2%)	0.9 (0.71-1.13)	0.35
Diabetes	1123/5911 (19%)	80/395 (20.2%)	1043/5516 (18.9%)	1.09 (0.84-1.4)	0.51
Dyslipidaemia	4421/5905 (74.9%)	274/393 (69.7%)	4147/5512 (75.2%)	0.76 (0.61-0.95)	0.015
Smoking	1389/5873 (23.7%)	105/389 (27%)	1284/5484 (23.4%)	1.21 (0.96-1.53)	0.16
Coronary disease	1098/5901 (18.6%)	79/391 (20.2%)	1019/5510 (18.5%)	1.12 (0.86-1.44)	0.41
Eject. fraction <35%	320/5917 (5.4%)	18/396 (4.5%)	302/5521 (5.5%)	0.5 (-1.34)	0.43
BMI	25 (5)	24 (5)	25 (5)	0.95 (0.93-0.98)	0.008
Stroke etiologies					
Atherosclerosis	843/5558 (15.2%)	49/370 (13.2%)	794/5188 (15.3%)	0.85 (0.62-1.15)	0.29
Cardioembolism	1714/5558 (30.8%)	88/370 (23.3%)	1628/5188 (31.4%)	0.66 (0.52-0.85)	<0.001
Lucunar	578/5558 (10.4%)	28/370 (7%)	552/5188 (10.6%)	0.64 (0.42-0.96)	0.028
Dissection	227/5558 (4.1%)	3/370 (0.81%)	224/5188 (4.3%)	0.18 (0.06-0.57)	<0.001
PFO-related	191/5558 (3.4%)	3/370 (0.81%)	188/5188 (3.6%)	0.22 (0.07-0.68)	0.004
Rare, including undet. source	325/5558 (5.8%)	94/370 (25.4%)	231/5188 (4.5%)	7.31 (5.59-9.56)	<0.001
Multiple	361/5558 (6.5%)	48/370 (13%)	313/5188 (6%)	2.32 (1.68-3.21)	<0.001
Embolic stroke of undet. source	788/5558 (14.2%)	37/370 (10%)	751/5188 (14.5%)	0.66 (0.46-0.93)	0.017
Undetermined, and/or incomplete work-up	531/5558 (9.6%)	24/370 (6.5%)	507/5188 (9.8%)	0.64 (0.42-0.98)	0.038
Recurrence 3 months	244/5904 (4.1%)	44/394 (11.2%)	200/5510 (3.63%)	3.34 (2.37-4.71)	<0.001
Mortality 7 days	537/5917 (9.1%)	42/396 (10.6%)	495/5521 (9%)	1.2 (0.86-1.68)	0.27
Mortality 3 months	829/5258 (15.8%)	110/350 (31.4%)	719/4908 (14.6%)	2.67 (2.1-3.39)	<0.001
Mortality 12 months	1170/4380 (24.4%)	165/305 (54.1%)	905/4075 (22.2%)	4.13 (3.26-5.23)	<0.001
mRS>2 at 3 months	2149/5028 (40.9%)	194/350 (55.4%)	1955/4908 (39.8%)	1.88 (1.51-2.34)	<0.001

Table 1 - Patient characteristics and results. Continuous and ordinal variables are expressed as medians (with interquartile range, IQR), and categorical variables as absolute counts (with percentage). Results from the univariate analysis in the "AC" and "NC" groups are reported as odds ratio (OR) and 95% confidence interval (CI). "Mortality" refers to mortality for all causes. PFO: patent foramen ovale; mRS (modified Rankin Scale); BMI: Body Mass Index.

Conclusion: Among large contemporary cohort, 6.7% of AIS patients had AC, they were more often men and had worse pre-stroke function than NC patients. In addition, AC patients had more atypical stroke mechanisms, a higher rate of stroke recurrence, and increased long-term disability and mortality.

Disclosure: Nothing to disclose.

OPR-015

Perfusion imaging in large vessel occlusion stroke within 6 hours from onset: from time-window to tissue-window

G. Schwarz¹, E. Agostoni¹, G. Saliou², S. Hajdu², V. Dunet², P. Michel³, D. Strambo³

¹ Department of Neurology and Stroke Unit - ASST Grande Ospedale Metropolitano Niguarda, Milan, Italy,

² Department of Diagnostic and Interventional Radiology, Lausanne University Hospital, Lausanne, Switzerland,

³ Stroke Center, Neurology Service, Lausanne University Hospital and University of Lausanne, Lausanne, Switzerland

Background and aims: Little is known on the role of perfusion imaging for patients treated within early (<6h) time window. We aimed to investigate whether pre-treatment perfusion parameters are associated with outcome in acute ischemic stroke (AIS) patients treated within 6 hours.

Methods: Based on the ASTRAL registry, we retrospectively included consecutive anterior circulation large vessel occlusion (LVO) AIS patients, treated within 6 h and with available baseline perfusion data. We assessed the absence of mismatch according to DEFUSE 3 and DAWN trials criteria, ischemic core and penumbra volumes, and perfusion/core ratio. We evaluated their association with 3-month unfavorable outcome (modified Rankin Scale, mRS>2) via univariate and multivariate logistic regression analysis.

Results: 262 patients were included: 83 (31.7%) and 168 (64.1%) did not meet DEFUSE 3 and DAWN criteria, respectively. Absence of mismatch according to DEFUSE 3 or DAWN criteria was associated with higher probability of unfavorable outcome (respectively 67.1% vs. 31.4%, aOR=2.69, 95% CI=1.22–5.90, p=0.014; and 50.0% vs. 28.9%, aOR=3.46, 95% CI=1.56–7.67, p=0.002; adjusted for age, pre-stroke mRS, baseline NIHSS, blood glucose, ASPECTS, collaterals, time-to-groin-delay, occlusion site and IVT). Ischemic penumbra volume (aOR=0.51, 95% CI=0.30–0.87, p=0.013) and penumbra/core ratio (aOR=0.75, 95% CI 0.60–0.95, p=0.015) were also independently associated with 3-month outcome, but not ischemic core volume (aOR=1.22, 95% CI=0.96–1.58, p=0.104).

Conclusion: The mismatch criteria for the extended time-window EVT are not met in a substantial proportion of early arriving patients and are independently associated with 3-month outcome. Further data confirming these results may suggest a paradigm shift in acute stroke management, from time-window to tissue-window.

Disclosure: The authors have no disclosures to report.

OPR-016

Effect of symptomatic and asymptomatic Covid-19 on safety and outcome of acute ischemic stroke treatments

D. Strambo¹, J. Marto², G. Ntaios³, T. Nguyen⁴, R. Herzig⁵, A. Członkowska⁶, J. Demeestere⁷, O. Mansour⁸, G. Georgiopoulos⁹, R. Nogueira¹⁰, P. Michel², The Global COVID-19 Stroke Registry Investigators

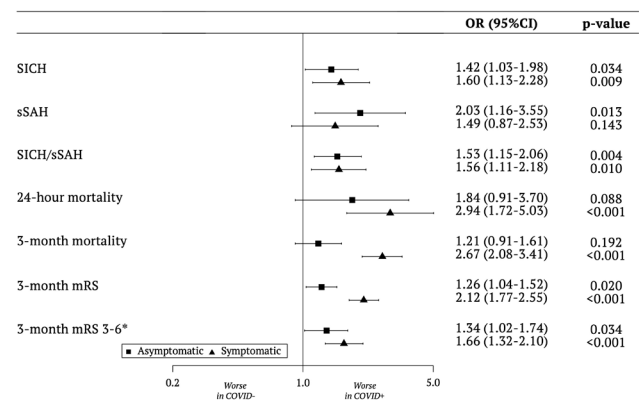
¹ Stroke Center, Neurology Service, Department of Neurological Sciences, Lausanne University Hospital, Lausanne, Switzerland, ² Department of Neurology, Hospital de Egas Moniz, Centro Hospitalar Lisboa Ocidental, Lisbon, Portugal, ³ Department of Internal Medicine, Faculty of Medicine, School of Health Sciences, University of Thessaly, Larissa, Greece, ⁴ Department of Neurology, Radiology, Boston Medical Centre, Boston University School of Medicine, Boston, MA, United States of America,

⁵ Department of Neurology, Comprehensive Stroke Centre, Charles University Faculty of Medicine and University Hospital, Hradec Králové, Czech Republic, ⁶ 2nd Department of Neurology, Institute of Psychiatry and Neurology, Warsaw, Poland, ⁷ Neurology Department, Leuven University Hospital, Leuven, Belgium,

⁸ Alexandria University Hospitals and Affiliated Stroke Network, Alexandria, Egypt, ⁹ Department of Clinical Therapeutics, National and Kapodistrian University of Athens, Greece, ¹⁰ Departments of Radiology, Neurology and Neurosurgery, Grady Memorial Hospital, Atlanta, GA, United States of America

Background and aims: COVID-19 related inflammation, endothelial dysfunction and coagulopathy may increase the bleeding risk and lower the efficacy of revascularization treatments in patients with ischemic stroke (IS). The effect of these pathophysiological processes is possibly related to the disease severity. We aimed to evaluate the safety and outcomes of revascularization treatments in patients with IS and asymptomatic or symptomatic COVID-19.

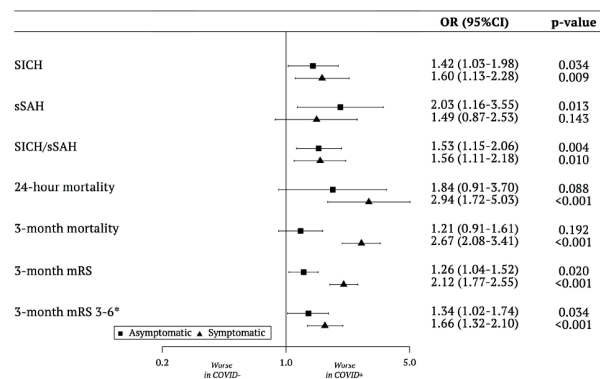
Background and aims: COVID-19 related inflammation, endothelial dysfunction and coagulopathy may increase the bleeding risk and lower the efficacy of revascularization treatments in patients with ischemic stroke (IS). The effect of these pathophysiological processes is possibly related to the disease severity. We aimed to evaluate the safety and outcomes of revascularization treatments in patients with IS and asymptomatic or symptomatic COVID-19.



Methods: Retrospective multicenter cohort study of consecutive IS patients receiving intravenous thrombolysis (IVT) and/or endovascular treatment (EVT) between March-2020 and June-2021, tested for SARS-CoV-2 infection, with or without COVID-19-compatible

symptoms. By multivariate logistic regression analysis, we assessed the association of asymptomatic and symptomatic COVID-19 with bleeding complications and clinical outcomes. Study protocol was registered in ClinicalTrials.gov (NCT04895462).

Results: Among 15,128 revascularized patients from 105 centers, 853 (5.6%) were diagnosed with COVID-19, of whom 395 (46%) were asymptomatic and 454 (54%) symptomatic. 5,848 (38.7%) patients received IVT only, and 9,280 (61.3%) EVT (\pm IVT). As shown in Figure, the hemorrhagic complications similarly increased in both asymptomatic and symptomatic COVID-19 patients, while 24-hour and 3-month mortality was significant increased only in symptomatic COVID-19 patients. Compared to COVID-negative controls, 3-month disability was significantly worse in COVID-19 patients regardless the symptoms of the disease, but it was affected to a larger extent in symptomatic patients.



Conclusion: Ischemic stroke patients with asymptomatic or symptomatic COVID-19 showed higher rates of intracranial bleeding complications and worse clinical outcomes after acute revascularization treatments than contemporaneous non-COVID-19 treated patients.

Disclosure: The authors have no disclosure to report.

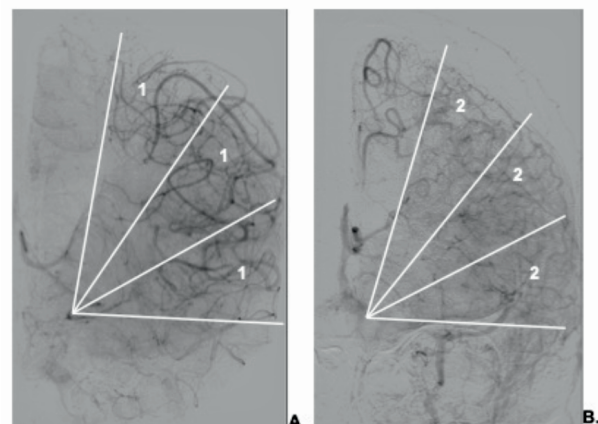
OPR-017

Angiographic evaluation of no-reflow phenomenon in patients with acute ischemic stroke from large vessels occlusion

E. Nicolini¹, M. Iacobucci², M. De Michele¹, A. Falco¹, I. Berto¹, L. Petraglia¹, A. Ciacciarelli¹, D. Toni²
¹ Policlinico Umberto I - Sapienza University of Rome, Stroke Unit, Rome, Italy, ² Sapienza University of Rome, Department of Human Neurosciences, Rome, Italy

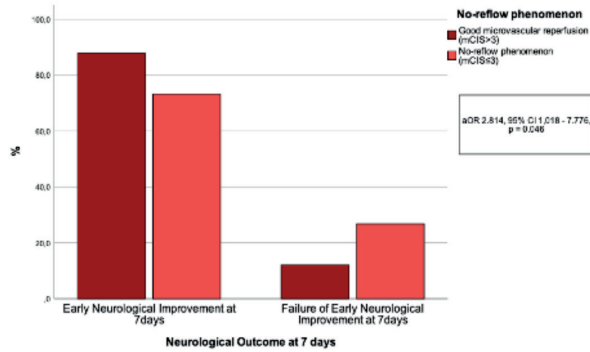
Background and aims: Futile recanalization (FR) is defined as a 90-day mRS 3-6 despite successful recanalization (TICI 2b-3), and account for 29% to 60% of large vessel occlusion (LVO) ischemic stroke (IS) treated with mechanical thrombectomy (MT). Failure of early neurological improvement (fENI) describes patients successfully recanalized but not clinically improving at 24-hours or at 7-days. No-reflow phenomenon (NRP) is a possible cause of FR and fENI, described in global ischemia animal models and human myocardial infarction as deficient microvascular reperfusion. Evidence of NRP in IS patients is scarce. Aim of our study was to identify an angiographic marker of NRP and explore its association with clinical outcome.

Methods: We retrospectively analyzed 185 post-interventional digital subtraction angiographies of anterior circulation LVO IS patients treated with MT. We created a score, dividing middle cerebral artery territory in three segments. For each segment we gave 2 points if the capillary blush was present without any delay, 1 if delayed and 0 if absent. We called our score modified capillary index score (mCIS). We used ROC curve to define $mCIS \leq 3$ as cut-off and marker of NRP.



Post-interventional DSA showing on parenchymal phase (A) delayed contrast washout in all the 3 segments of MCA territory (mCIS 3) and (B) regular contrast washout (mCIS 6) (DSA=digital subtraction angiography; MCA= middle cerebral artery)

Results: NRP was present in 35.1% of patients. mCIS \leq 3 predicted fENI at 24 hours (aOR 2.617, 95% CI 1.192–5.745, $p=0.016$) and at 7 days (aOR 4.601, 95% CI 1.636–12.936, $p=0.004$), but not FR. Moreover, mCIS \leq 3 predicted hemorrhagic transformation (aOR 0.444, 95% CI 1.266–4.717, $p=0.008$).



Conclusion: NRP is poorly investigated in IS patients. Our angiographic marker was able to predict early outcome and could help identifying patients for future research on NRP.

Disclosure: Nothing to disclose.

Muscle and neuromuscular junction disorder

OPR-018

FXR1-related congenital myopathy: expansion of the clinical and genetic spectrum

M. Mroczek¹, C. Longman², M. Farrugia³, S. Kapetanovic Garcia⁴, D. Ardicli⁵, H. Topaloglu⁶, A. Hernández Laín⁷, D. Orhan⁸, M. Alikasifoglu⁹, J. Duff¹⁰, S. Specht¹⁰, K. Nowak¹¹, G. Ravenscroft¹², K. Chao¹³, Z. Valivullah¹³, S. Donkervoort¹⁴, C. Bonnemann¹⁴, V. Straub¹⁰, G. Yoon¹⁵

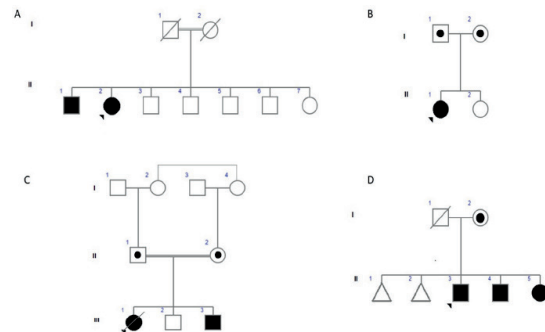
¹ Department of Neurology and Neurophysiology, Balgrist University Hospital, Zurich, Switzerland, ² West of Scotland Regional Genetics Service, Queen Elizabeth University Hospital, Glasgow, United Kingdom, ³ Department of Neurology, Institute of Neurological Sciences, Queen Elizabeth University Hospital, Glasgow, United Kingdom, ⁴ Unidad de ELA y Neuromuscular, Hospital Universitario de Basurto, Bilbao, Spain, ⁵ Department of Pediatric Neurology, Hacettepe University Children's Hospital, 06100 Ankara, Turkey, ⁶ Yeditepe University Department of Pediatrics, İstanbul, Turkey, ⁷ Department of Pathology (Neuropathology), Hospital 12 de Octubre Research Institute (imas12), 28041 Madrid, Spain, ⁸ Department of Pathology, Hacettepe University School of Medicine, Ankara, Turkey, ⁹ Department of Medical Genetics, Hacettepe University Children's Hospital, Ankara, Turkey, ¹⁰ John Walton Muscular Dystrophy Research Centre, Translational and Clinical Research Institute, Newcastle University and Newcastle Hospitals NHS Foundation Trust, Newcastle upon Tyne, United Kingdom, ¹¹ School of Biomedical Sciences, Faculty of Health and Medical Sciences, University of Western Australia, Nedlands, Australia, ¹² Centre of Medical Research, The University of Western Australia and the Harry Perkins Institute for Medical Research, Perth, Western Australia, Australia, ¹³ Center for Mendelian Genomics, Program in Medical and Population Genetics, Broad Institute of MIT and Harvard, Cambridge, MA, United States of America, ¹⁴ Neuromuscular and Neurogenetic Disorders of Childhood Section, National Institute of Neurological Disorders and Stroke, National Institutes of Health, Bethesda, Maryland, United States of America, ¹⁵ Division of Neurology, Department of Paediatrics, The Hospital for Sick Children, University of Toronto, Toronto, Canada

Background and aims: Bi-allelic pathogenic variants in FXR1 have recently been associated with two rare congenital myopathy phenotypes: a severe form associated with hypotonia, long bone fractures, respiratory insufficiency, and infantile death, and a milder form characterized by proximal muscle weakness with survival into adulthood. We report eight patients from four unrelated families with bi-allelic pathogenic variants in exon 15 of FXR1.

Methods: The patients were recruited from the following centres: the Queen Elizabeth University Hospital in

Glasgow, United Kingdom; Hospital de Basurto in Bilbao, Spain; Hacettepe University Children's Hospital in Ankara, Turkey and Hospital for Sick Children in Toronto, Canada. Whole exome sequencing was used to detect variants.

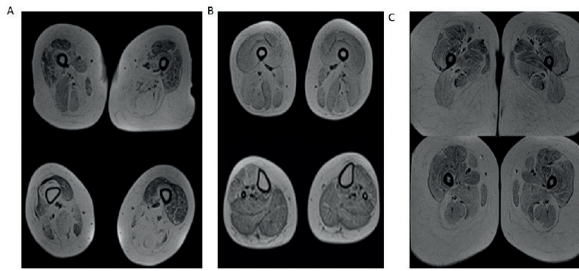
Results: Common clinical features were noted for all patients, which included proximal myopathy, normal serum creatinine kinase levels, and diffuse muscle atrophy with relative preservation of the quadriceps femoris muscle on muscle imaging. Additionally, some patients with FXR1-related myopathy had respiratory involvement and required BiPAP support. Other clinical features observed to varying degrees among the cohort were calf hypertrophy, scoliosis, joint laxity, contractures, and psychiatric symptoms. Muscle biopsy showed multi-minicores and type I fibre predominance.



Pedigrees of all four families



Clinical presentation and muscle biopsies



Muscle MRI of three patients

Conclusion: FXR1-related congenital myopathy is an emerging entity that is clinically recognizable. Phenotypic variability associated with variants in FXR1 can result from differences in variant location and type and is also observed between patients homozygous for the same variant, rendering specific genotype-phenotype correlations difficult. Molecular testing for FXR1 should be considered for patients with a clinical diagnosis of congenital myopathy, especially if cores are observed on muscle biopsy.

Disclosure: Two patients were diagnosed as part of the MYO-SEQ Project. Analysis was provided by the Broad Institute of MIT and Harvard Center for Mendelian Genomics (Broad CMG).

OPR-019

COMET: Efficacy and safety of avalglucosidase alfa in late-onset Pompe disease participants after 97 weeks of treatment

B. Schoser¹, P. Kishnani², J. Díaz-Manera³, H. Kuschlaf⁴, S. Ladha⁵, T. Mozaffar⁶, V. Straub³, A. Toscano⁷, A. Van der Ploeg⁸, K. Berger⁹, P. Clemens¹⁰, Y. Chien¹¹, J. Day¹², S. Ilarioshkin¹³, M. Roberts¹⁴, S. Attarian¹⁵, G. Carvalho¹⁶, Y. Choi¹⁷, S. Erdem-Özdamar¹⁸, O. Goker-Alpan¹⁹, A. Kostera-Pruszczyk²⁰, K. An Haack²¹, N. Thibault²², T. Zhou²², M. Dimachkie on behalf of the COMET Investigator Group²³

¹ Department of Neurology, LMU Klinikum München, München, Germany, ² Division of Medical Genetics, Department of Pediatrics, DUnited Kingdome University Medical Center, Durham, NC, United States of America, ³ John Walton Muscular Dystrophy Research Centre, Newcastle University and Newcastle Hospitals NHS Foundation Trust, Newcastle Upon Tyne, United Kingdom, ⁴ Department of Neurology & Rehabilitation Medicine and Department of Pathology & Laboratory Medicine, University of Cincinnati, Cincinnati, OH, United States of America, ⁵ Gregory W. Fulton ALS and Neuromuscular Center, Barrow Neurological Institute, Phoenix, AZ, United States of America, ⁶ Department of Neurology, University of California, Irvine, Orange, CA, United States of America, ⁷ Department of Clinical and Experimental Medicine, Reference Center for Rare Neuromuscular Disorders, University of Messina, Messina, Italy, ⁸ Center for Lysosomal and Metabolic Diseases, Erasmus MC, University Medical Center, Rotterdam, The Netherlands, ⁹ Division of Pulmonary, Critical Care and Sleep Medicine, NYU Grossman School of Medicine, and the André Cournand Pulmonary Physiology Laboratory, Bellevue Hospital, New York, NY, United States of America, ¹⁰ Department of Neurology, University of Pittsburgh, and Department of Veterans Affairs Medical Center, Pittsburgh, PA, United States of America, ¹¹ Department of Medical Genetics and Pediatrics, National Taiwan University Hospital, Taipei, Taiwan, ¹² Departments of Neurology and Pediatrics, Stanford University, Stanford, CA, United States of America, ¹³ Research Center of Neurology, Moscow, Russian Federation, ¹⁴ Salford Royal NHS Foundation Trust, Salford, United Kingdom, ¹⁵ Referral Centre for Neuromuscular Diseases and ALS, Hôpital La Timone, Marseille, France, ¹⁶ Instituto Chronos de Apoio à Pesquisa, Brasília, DF, Brazil, ¹⁷ Gangnam Severance Hospital, Yonsei University, College of Medicine, Seoul, Korea, ¹⁸ Department of Neurology, Hacettepe University Faculty of Medicine, Ankara, Turkey, ¹⁹ Lysosomal and Rare Disorders Research and Treatment Center (LDRTC), Fairfax, VA, United States of America, ²⁰ Department of Neurology, Medical University of Warsaw, Warsaw, Poland, ²¹ Sanofi Genzyme, Chilly-Mazarin, France, ²² Sanofi Genzyme, Cambridge, MA, United States of America, ²³ University of Kansas Medical Center, Department of Neurology, Kansas City, KS, United States of America

Background and aims: Avalglucosidase alfa (AVAL) is a recombinant human GAA enzyme replacement therapy with increased mannose-6-phosphate content for increased cellular uptake compared with alglucosidase alfa (ALGLU). Here we report efficacy and safety of AVAL in late-onset Pompe disease participants in the extended treatment period (ETP) of COMET (Phase 3; NCT02782741) after a 49-week primary analysis period (PAP).

Methods: At PAP enrollment, participants were treatment-naïve (n=100; age 16–78 years). All 51 participants receiving AVAL 20 mg/kg every other week (qow) in the PAP continued this in the ETP (AVAL arm). Of 49 participants receiving ALGLU 20 mg/kg qow in the PAP, 44 entered the ETP and received AVAL 20 mg/kg qow (switch arm).

Results: Trends for improvement or stabilisation from Baseline to Week 97 were observed for the primary and secondary outcomes of respiratory and motor function, muscle strength, and quality of life in AVAL-arm and switch-arm participants (Table 1). Treatment-emergent adverse events up to the last follow-up are summarised in Table 2 for the periods that participants were receiving AVAL. 17 AVAL-arm and 10 switch-arm participants had treatment-emergent serious AEs (SAEs); 4 and 2 of them, respectively, had treatment-related SAEs. Switch-arm participants showed no safety- or immunogenicity-related concerns.

	Avalglucosidase alfa arm PAP: Avalglucosidase alfa ETP: Avalglucosidase alfa (N=51)	Switch arm PAP: Alglucosidase alfa ETP: Avalglucosidase alfa (N=44)
Primary endpoint		
FVC % predicted (upright)	+2.65 (1.05)	+0.36 (1.12)
Secondary efficacy endpoints		
6MWT distance, m	+18.60 (12.01)	+4.56 (12.44)
MIP % predicted (upright)	+9.97 (1.86)	+5.32 (2.00)
MEP % predicted (upright)	+17.25 (3.26)	+13.90 (3.47)
HHD lower extremity composite score	+145.54 (50.92)	+195.06 (52.73)
QMFT total score	+3.83 (0.84)	+2.16 (0.91)
SF-12 PCS	+3.24 (0.98)	+2.13 (1.03)
SF-12 MCS	+1.62 (1.27)	+2.47 (1.32)
<small>6MWT, 6-minute walk test; ETP, extended treatment period; HHD, hand-held dynamometry; LS, least squares; MCS, Mental Component Score; MEP, maximum expiratory pressure; MIP, maximum inspiratory pressure; PAP, primary analysis period; PCS, Physical Component Score; QMFT, quick motor function test; SE, standard error; SF-12, Short-Form-12.</small>		

Table 1: Least squares mean change (standard error) in primary and secondary outcome measures from Baseline (Week 0) to Week 97.

	Avalglucosidase alfa arm PAP + ETP (N=51)	Switch arm ETP* (N=44)
Any TEAEs, n (%)	50 (98)	42 (95)
TEAEs potentially related to treatment, n (%)	29 (57)	25 (57)
Serious TEAEs, n (%)	17 (33)	10 (23)
Serious TEAEs potentially related to treatment, n (%)	4 (8)	2 (5)
Severe TEAEs, n (%)	11 (22)	9 (20)
TEAEs leading to permanent treatment discontinuation, n (%) [†]	2 (4)	3 (7)
TEAEs leading to death, n (%)	0	1 (2) [‡]
Protocol-defined IARs, n (%) [§]	20 (39)	21 (48)
<small>ETP, extended treatment period; IAR, infusion-associated reaction; PAP, primary analysis period; TEAE, treatment-emergent adverse event. Numbers reported are the number (%) of participants with at least 1 TEAE in each category. *Data for the switch arm are for the ETP only whilst participants were receiving avalglucosidase alfa; this group had received alglucosidase alfa during the PAP. [†]5 participants discontinued treatment during the ETP by Week 97 for AEs (1 event each – treatment-related: ocular hyperaemia, erythema, urticaria, respiratory distress; non-treatment related: acute myocardial infarction, pancreatic adenocarcinoma). [‡]Pancreatic adenocarcinoma considered not related to treatment. [§]Defined as an adverse event that occurred during either the infusion or observation period following the infusion, related or possible related to the investigational treatment.</small>		

Table 2: Summary of treatment-emergent adverse events during avalglucosidase alfa treatment

Conclusion: The data show a sustained treatment effect and continued benefit with AVAL beyond the PAP, and stabilisation of treatment effect after switch from ALGLU to AVAL over 97 weeks, supporting long-term maintenance of clinically meaningful outcomes with AVAL.

Disclosure: Sanofi Genzyme funding. Editorial support was provided by Jane M Gilbert, BSc, CMPP of Elevate Medical Affairs, contracted by Sanofi Genzyme for publication support services. Some COMET 97-week data will be presented at WORLDSymposium 2022.

OPR-020

Ravulizumab Reduces Clinical Deteriorations in Patients with Generalised Myasthenia Gravis

R. Mantegazza¹, A. Meisel², T. Vu³, D. Annane⁴, M. Katsuno⁵, R. Aguzzi⁶, K.N. Beasley⁶, J.F. Howard Jr⁷
¹ *Fondazione IRCCS Istituto Neurologico Carlo Besta, Milan, Italy*, ² *Charité Universitätsmedizin Berlin, Berlin, Germany*, ³ *University of South Florida Morsani College of Medicine, Tampa, FL, United States of America*, ⁴ *Raymond Poincaré Hospital, Garches, France*, ⁵ *Nagoya University, Nagoya, Japan*, ⁶ *Alexion, AstraZeneca Rare Disease, Boston, MA, United States of America*, ⁷ *The University of North Carolina, Chapel Hill, NC, United States of America*

Background and aims: The efficacy and safety of the long-acting terminal complement C5 inhibitor ravulizumab in treating patients with anti-acetylcholine receptor antibody-positive (AChR Ab+) generalised myasthenia gravis (gMG) were demonstrated in the 26-week, phase 3, randomised, double-blind, placebo-controlled CHAMPION MG study (NCT03920293). This analysis of the study data assessed ravulizumab's efficacy in reducing acute clinical deterioration, including life-threatening myasthenic crisis.

Methods: Adults with AChR Ab+ gMG (Myasthenia Gravis Foundation of America Class II–IV and Myasthenia Gravis-Activities of Daily Living score ≥ 6) were randomised (1:1) to intravenous ravulizumab or placebo infusion every 8 weeks after the initial loading dose, for 26 weeks. Clinical deterioration was defined as an MG crisis (weakness severe enough to necessitate intubation or to delay extubation following surgery); significant symptomatic worsening; or administration of rescue therapy if the patient's health was in jeopardy.

Results: The analysis set comprised 175 patients (86 received ravulizumab; 89 received placebo). Fewer clinical-deterioration events occurred in the ravulizumab group (10 events in 8 patients [9.3%]) than in the placebo group (26 events in 15 patients [16.9%]) (Table). Rescue therapy was administered for 10 clinical-deterioration events in the ravulizumab group and 24 events in the placebo group (Table 1).

Outcome	Ravulizumab (n=86)		Placebo (n=89)	
	No. of events	No. of patients (%)	No. of events	No. of patients (%)
Clinical deterioration – total ^a	10	8 (9.3)	26	15 (16.9)
Clinical deterioration – by criterion				
MG crisis ^c	0	0 (0.0)	1	1 (1.1)
Significant symptomatic worsening ^d	1	1 (1.2)	6	5 (5.6)
Rescue therapy (health in jeopardy) ^e	9	7 (8.1)	19	12 (13.5)
Any use of rescue therapy ^f	10	8 (9.3)	24	14 (15.7)

^aThe full analysis set (n=175) comprised all randomised patients who received at least one dose of study drug.

^bAccording to per-protocol criteria; a clinical deterioration event may have met more than one criterion, and patients may have experienced more than one event.

^cDefined as weakness severe enough to necessitate intubation or to delay extubation following surgery; one patient in the placebo group received rescue therapy.

^dWorsening to a score of 3, or a 2-point worsening from baseline, on any one of the individual Myasthenia Gravis-Activities of Daily Living questionnaire items other than double vision or eyelid droop, which in the investigator's assessment was associated with significant symptomatic worsening; one patient in the ravulizumab group and three patients (one patient on two occasions) in the placebo group received rescue therapy.

^eDefined as administration of rescue therapy to a patient whose health, in the opinion of the investigator, would be in jeopardy if rescue therapy were not given.

^fBy patients experiencing clinical deterioration.

Table: Clinical deterioration during the 26-week CHAMPION MG study (full analysis set)^a

Conclusion: Ravulizumab treatment was associated with numerically fewer clinical-deterioration events compared with placebo. These findings support the efficacy of ravulizumab in controlling acute worsening of symptoms in patients with AChR Ab+ gMG.

Disclosure: This study was funded by Alexion, AstraZeneca Rare Disease.

OPR-021

Long-term Safety and Efficacy of Efgartigimod in Patients With Generalised Myasthenia Gravis

A. Meisel¹, V. Bril², T. Vu³, C. Karam⁴, S. Peric⁵, J. De Bleecker⁶, H. Murai⁷, S. Beydoun⁸, M. Pasnoor⁹, A. Guglietta¹⁰, P. Ulrichs¹⁰, C. T'joen¹⁰, K. Utsugisawa¹¹, J. Verschuuren¹², R. Mantegazza¹³, J. Howard¹⁴

¹ Department of Neurology and NeuroCure Clinical Research Center, Charité – Universitätsmedizin Berlin, Berlin, Germany, ² Ellen & Martin Prosserman Centre for Neuromuscular Diseases, University Health Network, Toronto, Ontario, Canada; University of Toronto, Toronto, Ontario, Canada, ³ Department of Neurology, University of South Florida, Morsani College of Medicine, Tampa, Florida, United States of America, ⁴ Penn Neuroscience Center, University of Pennsylvania, Philadelphia, Pennsylvania, United States of America, ⁵ Neurology Clinic, University Clinical Center of Serbia, University of Belgrade, Belgrade, Serbia, ⁶ Ghent University Hospital, Ghent, Belgium, ⁷ Department of Neurology, School of Medicine, International University of Health and Welfare, Tokyo, Japan, ⁸ Keck School of Medicine, University of Southern California, Los Angeles, California, United States of America, ⁹ University of Kansas Medical Center, Kansas City, Kansas, United States of America, ¹⁰ argenx, Ghent, Belgium, ¹¹ Department of Neurology, Hanamaki General Hospital, Hanamaki, Japan, ¹² Department of Neurology, Leiden University Medical Center, The Netherlands, ¹³ Department of Neuroimmunology and Neuromuscular Diseases, Fondazione IRCCS Istituto Neurologico Carlo Besta, Milan, Italy, ¹⁴ Department of Neurology, The University of North Carolina, Chapel Hill, North Carolina, United States of America

Background and aims: Efgartigimod is a human IgG1 antibody Fc-fragment that blocks neonatal Fc receptor. In the ADAPT study, treatment with efgartigimod resulted in clinically meaningful improvement (CMI) in generalised myasthenia gravis (gMG)-specific outcome measures. All patients completing ADAPT were eligible to enroll in its ongoing open-label, 3-year extension, ADAPT+. This study aimed to evaluate the safety, tolerability, and efficacy of efgartigimod in patients with gMG enrolled in ADAPT+.

Methods: Efgartigimod 10 mg/kg was administered intravenously in cycles of once-weekly infusions for 4 weeks, with subsequent cycles initiated based on clinical response. Efficacy was assessed during each cycle utilising MG-ADL and QMG scales, in addition to other secondary analyses.

Results: 90% of ADAPT patients (151/167) entered ADAPT+. As of February 2021, 106 AChR-Ab+/33 AChR-Ab- patients had received ≥ 1 dose of open-label efgartigimod (including 66 ADAPT placebo patients). The mean (SD) study duration was 363 (114) days, resulting in 138 patient-years of observation. The most common adverse events in the overall safety population (n=139) were headache (22.3%; n=31), nasopharyngitis (10.8%; n=15), and diarrhoea (8.6%; n=12), which were mostly mild or

moderate. In cycle 1, CMI was observed in the overall population with a mean change (mean [SE]) of -5.1 (0.32) in MG-ADL and -4.8 (0.36) in QMG, and this magnitude of improvement occurred during each cycle for up to 10 cycles. Clinical improvements correlated with reductions in total IgG and AChR antibodies across all cycles. Additional analyses will be presented.

Conclusion: The results of these analyses suggest long-term treatment with efgartigimod was well tolerated and efficacious.

Disclosure: Multiple relationships financial and non-financial nature for authors AM, VB, CK, SP, JLdB, HM, SB, MP, AG, PU, CT, KU, JV, RM and JFH Jr. stated at point of presentation.

MS and related disorders: NMOSD and pediatric MS

OPR-022

Functional correlates of intelligence quotient and cognitive abilities in pediatric multiple sclerosis

L. Cacciaguerra¹, C. Curatoli², C. Vizzino², P. Valsasina², M. Filippi¹, M. Rocca¹

¹ *Neuroimaging Research Unit, Division of Neuroscience, IRCCS San Raffaele Scientific Institute, and Vita-Salute San Raffaele University, Milan, Italy,* ² *Neuroimaging Research Unit, Division of Neuroscience, IRCCS San Raffaele Scientific Institute, Milan, Italy*

Background and aims: Clinical and cognitive features of pediatric MS differ from adult-onset disease. We evaluated the neuropsychological profile of pediatric MS patients and its association with resting-state functional connectivity (RS-FC) abnormalities in key cognitive and motor networks. **Methods:** In this 3.0 T MRI study, 76 pediatric MS patients underwent a neuropsychological assessment of Wechsler-Intelligence-Scales for Intelligent Quotient [IQ], Semantic/Phonemic Verbal Fluency Test [SVFT/PVFT], Symbol Digit Modalities Test [SDMT], Coding subtest [CD], Block Design subtest [BD], Trial Making Test [TMT-A/B]. Test failure corresponded to a performance <5th percentile of normative values. Twenty-two matched healthy controls (HC) were also enrolled. Seed-based correlation analysis was used to reconstruct RS-FC within executive, language, motor, default-mode and basal ganglia networks. Age- and sex-adjusted between-group comparisons and correlations with cognitive scores were assessed in right-handed patients having good MRI quality (n=58).

Results: In patients, median IQ was 97.5; 18.4% scored below normatives (IQ<84). Patients most commonly failed CD (21.1%), TMT-B (15.8%), TMT-A (10.5%), SDMT (9.2%), PVFT (6.8%), and BD (3.9%). Compared to HC, patients exhibited reduced RS-FC within all explored networks, involving bilateral caudate nucleus and precentral gyrus. Basal ganglia and language networks also showed reduced RS-FC with anterior and posterior cingulate cortices and frontal regions. Decreased caudate RS-FC was associated with higher IQ and PVFT scores and worse performance in CD, while decreased RS-FC between basal ganglia and cingulate cortices was associated with worse SDMT and PVFT scores.

Conclusion: Reduced RS-FC of the caudate contributes to global cognitive efficiency but also to patients' fragility in different cognitive abilities.

Disclosure: Nothing to disclose.

OPR-023

Long-term eculizumab in AQP4+ NMOSD: relapse-risk reduction and safety in PREVENT and its completed open-label extension

A. Berthele¹, D. Wingerchuk², K. Fujihara³, J. Palace⁴, M. Levy⁵, H. Kim⁶, I. Nakashima⁷, C. Oreja-Guevara⁸, K. Wang⁹, S. Shang¹⁰, M. Yountz¹⁰, S. Pittock¹¹

¹ *Department of Neurology, Klinikum rechts der Isar, Technical University of Munich, Munich, Germany,* ² *Department of Neurology, Mayo Clinic, Scottsdale, AZ, United States of America,* ³ *Department of Multiple Sclerosis Therapeutics, Fukushima Medical University, Fukushima City, Japan,* ⁴ *Nuffield Department of Clinical Neurosciences, John Radcliffe Hospital, Oxford, United Kingdom,* ⁵ *Department of Neurology, Massachusetts General Hospital and Harvard Medical School, Boston, MA, United States of America,* ⁶ *Department of Neurology, Research Institute and Hospital, National Cancer Center, Goyang, South Korea,* ⁷ *Department of Neurology, Tohoku Medical and Pharmaceutical University, Sendai, Japan,* ⁸ *Multiple Sclerosis (MS) Center, Hospital Universitario Clinico San Carlos, Madrid, Spain,* ⁹ *Neurology Department, Cheng Hsin General Hospital, Taipei City, Taiwan,* ¹⁰ *Alexion, AstraZeneca Rare Disease, Boston, MA, United States of America,* ¹¹ *Department of Neurology, Mayo Clinic, Rochester, MN, United States of America*

Background and aims: Eculizumab is well tolerated and significantly reduces relapse risk versus placebo in patients with aquaporin-4 immunoglobulin G-positive (AQP4+) neuromyelitis optica spectrum disorder (NMOSD). We report eculizumab's long term relapse-risk-reduction efficacy and safety in AQP4+ NMOSD during PREVENT (NCT01892345) and its completed open label extension (OLE; NCT02003144).

Methods: After receiving eculizumab or placebo during PREVENT, adults with AQP4+ NMOSD could enter the OLE (eculizumab maintenance dose, 1200 mg/2 weeks, with/without concomitant immunosuppressive therapy). Combined PREVENT and OLE (final data cut, 12 July 2021) data were analysed.

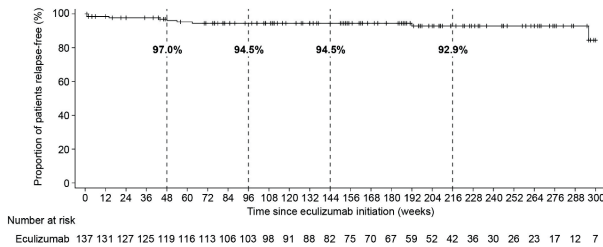
Results: During PREVENT and/or the OLE, 137 patients received eculizumab for a median (range) of 183.4 (0.1–342.0) weeks (3.5 years) and a total of 449.2 patient-years (Table 1). The estimated proportion of adjudicated relapse-free patients at week 216 (4.1 years) was 92.9% (95% CI: 85.9–96.5%; Figure). Nine patients experienced 10 adjudicated relapses (seven during the OLE, including one since the last interim analysis; Table 2). The adjudicated annualized relapse rate was 0.022 (95% CI: 0.012–0.041; Table 1). Rates of treatment-related adverse events and serious adverse events (SAEs)/100 patient-years were 165.3 and 7.0, respectively, versus 167.5 and 24.5 with placebo in PREVENT. The most common SAE was urinary tract infection (5.1% of patients). The serious infection rate was 10.5/100 patient-years with no meningococcal infections. No patients died during the OLE.

Table 1. Eculizumab treatment duration and adjudicated ARR during PREVENT and the OLE.

Variable	Statistic	OLE only			PREVENT + OLE combined
		Placebo/ eculizumab (n = 41)	Eculizumab/ eculizumab (n = 78)	Total eculizumab (n = 119)	Total eculizumab (N = 137)
Treatment duration (weeks)*	Mean (SD)	128.6 (75.5)	117.3 (52.9)	121.2 (61.5)	171.1 (67.1)
	Median	107.1	106.1	106.1	183.4
	Min. max.	0.1, 318.3	11.1, 295.1	0.1, 318.3	0.1, 342.0
	Total PY	101.0	175.4	276.4	449.2
Total number of PY in study period	Sum	101.8	176.0	277.8	451.3
Total number of adjudicated relapses	Sum	3	4	7	10
Number of patients with a total adjudicated relapse count of:					
0	n (%)	39 (95.1)	74 (94.9)	113 (95.0)	128 (93.4)
1	n (%)	1 (2.4)	4 (5.1)	5 (4.2)	8 (5.8)
2	n (%)	1 (2.4)	0 (0)	1 (0.8)	1 (0.7)
3	n (%)	0 (0)	0 (0)	0 (0)	0 (0)
Study-level adjudicated ARR	Rate ^b	0.029	0.023	0.025	0.022
	95% CI ^c	0.010–0.091	0.009–0.061	0.012–0.053	0.012–0.041

Accounting for COVID-19 disruption: for patients who missed two or more infusions consecutively in the OLE owing to COVID-19-related reasons, the time period for the calculation of eculizumab adjudicated ARR excludes the time period when the patient missed eculizumab infusions, to account for the impact of the pandemic. Any relapses occurring during this period was not included in the calculation of eculizumab adjudicated ARR. *Treatment duration = (Date of last study drug dose – Date of first study drug dose) + 1 day. ^bCalculated as the total number of relapses during the study period for all patients, divided by the total number of PY in the study period. ^cWald CI from Poisson regression. ARR, annualized relapse rate; CI, confidence interval; OLE, open-label extension; max., maximum; min., minimum; PY, patient-years; SD, standard deviation.

Figure. Time to first adjudicated relapse during PREVENT and the OLE.



Patients who did not experience an adjudicated on-trial relapse were censored at the end of the study period. For patients who missed two or more consecutive doses owing to COVID-19-related reasons, the study period was truncated to the last dose date prior to the missed doses + 16 days (or + 9 days if in the induction phase), and patients who did not experience an adjudicated on-trial relapse were censored at this date. Tick marks indicate censoring of data. Proportions of patients who were adjudicated relapse-free at weeks 48, 96, 144 and 216 were estimated using the Kaplan-Meier product limit method. OLE, open-label extension.

Table 2. Adjudicated relapses during PREVENT and the OLE.

Patient number	Study during which adjudicated relapse occurred	Eculizumab treatment day of adjudicated relapse onset	Type of adjudicated relapse (severity) ^a
1	OLE (placebo in PREVENT)	15	ON unilateral left (major)
2	PREVENT	18	TM partial (minor)
3	PREVENT	98	ON unilateral right (minor)
1	OLE (placebo in PREVENT)	218	ON unilateral left (major)
4	OLE (eculizumab in PREVENT)	300	ON unilateral; TM partial (major)
5	PREVENT	338	ON bilateral (major)
6	OLE (placebo in PREVENT)	381	Brainstem; TM partial (major)
7	OLE (eculizumab in PREVENT)	433	ON unilateral left; TM partial (major)
8	OLE (eculizumab in PREVENT)	1336	Cerebral; ON bilateral (major)
9	OLE (eculizumab in PREVENT)	2065	ON unilateral left; TM partial (major)

Accounting for COVID-19 disruption: relapses with onset during a dose interruption due to COVID-19 were excluded. ^aSeverity was only determined for relapses of TM or ON. OLE, open-label extension; ON, optic neuritis; TM, transverse myelitis.

Conclusion: The proportion of relapse-free patients remained high (92.9%) through 4.1 years' eculizumab treatment. Long-term eculizumab was well tolerated with no new safety signals. These long-term data confirm eculizumab's sustained benefit/risk profile in AQP4+ NMOSD.

Disclosure: Research funding for this study was provided Alexion, AstraZeneca Rare Disease.

OPR-024

Neuromyelitis optica as an in-vivo model of glymphatic system alterations

L. Cacciaguerra¹, A. Carotenuto², E. Pagani², M. Radaelli³, V. Martinelli³, M. Filippi⁴, M. Rocca⁴

¹ Neuroimaging Research Unit, Division of Neuroscience, IRCCS San Raffaele Scientific Institute, and Vita-Salute San Raffaele University, Milan, Italy, ² Neuroimaging Research Unit, Division of Neuroscience, IRCCS San Raffaele Scientific Institute, Milan, Italy, ³ Neurology Unit, IRCCS San Raffaele Scientific Institute, Milan, Italy, ⁴ Neuroimaging Research Unit, Division of Neuroscience, and Neurology Unit, IRCCS San Raffaele Scientific Institute, and Vita-Salute San Raffaele University, Milan, Italy

Background and aims: Aquaporin-4 is involved in neuromyelitis optica spectrum disorder (NMOSD) autoimmunity and glymphatic functioning. We aimed to assess whether NMOSD patients have glymphatic impairment and its association with clinical disability.

Methods: 34 NMOSD patients and 46 age- and sex-matched healthy controls (HC) from two independent cohorts (exploratory- and validation-dataset) underwent a standardized 3.0 T MRI protocol (T2-, T1-weighted sequences and diffusion tensor imaging). Susceptibility-weighted imaging (SWI) was also acquired in the exploratory-dataset. We evaluated perivascular space (PVS) enlargement and glymphatic system function by calculating the diffusion along perivascular space (DTI-ALPS) index. In the exploration-dataset, SWI was used to draw the regions of interest for DTI-ALPS calculation in areas having veins perpendicular to lateral ventricles. Between-group comparisons, partial correlations and regression models were run to assess associations between DTI-ALPS index, PVS scores, clinical and MRI variables.

Results: The two datasets were similar for demographic and clinical features. In both, NMOSD patients had reduced DTI-ALPS index (p-values: 0.004–0.038). Patients also showed a higher frequency of severe PVS enlargement in the centrum semiovale (29.4 vs. 8.7%, p=0.040). Lower DTI-ALPS index, deep grey matter and cortical volumes predicted NMOSD diagnosis (R²=0.62). Lower DTI-ALPS index, higher number of myelitis, and higher T2-lesion volume associated with worse disability (R²=0.55). Higher PVS scores correlated with global brain and deep grey matter atrophy (r-values: -0.44, -0.36; p-values=0.01–0.046). **Conclusion:** We detected impaired glymphatic system functioning in two independent cohorts of NMOSD patients. It was associated with worse clinical disability, suggesting a correlation with disease pathogenetic mechanisms and their magnitude.

OPR-025

Teriflunomide in paediatric patients with relapsing multiple sclerosis: results from the open-label TERIKIDS extension

T. Chitnis¹, B. Banwell², L. Kappos³, D. Arnold⁴, K. Gücüyener⁵, K. Deiva⁶, S. Saubadu⁷, W. Hu⁸, M. Benamor⁷, A. Le-Halpere⁷, P. Truffinet⁷, M. Tardieu⁶
¹ Massachusetts General Hospital for Children, Boston, MA, United States of America, ² Children's Hospital of Philadelphia, Philadelphia, PA, United States of America, ³ Research Center for Clinical Neuroimmunology and Neuroscience Basel (RC2NB), MS Center and Neurologic Clinic and Policlinic, Departments of Biomedicine and Clinical Research, University Hospital and University of Basel, Basel, Switzerland, ⁴ Montreal Neurological Institute, McGill University, Montreal, Canada, ⁵ Gazi Üniversitesi Tıp Fakültesi Pediatrik Nöroloji Bilim Dalı, Ankara, Turkey, ⁶ Hôpitaux Universitaires Paris-Sud, Paris, France, ⁷ Sanofi, Chilly-Mazarin, France, ⁸ Sanofi, Beijing, China

Background and aims: In the 2-year, randomized, double-blind (DB), phase 3 TERIKIDS study (NCT02201108) of paediatric patients with relapsing MS, teriflunomide numerically reduced relapse risk and significantly reduced new/enlarging T2 and gadolinium-enhancing T1 lesion counts versus placebo (Chitnis T et al, Lancet Neurol 2021;20:1001-11). Here, we report final results from the TERIKIDS open-label extension (OLE).

Methods: Patients who completed DB treatment or qualified for early switch from DB treatment to open-label teriflunomide could continue in the OLE until 192 weeks after initial randomization. All patients in the OLE received teriflunomide at body weight-based dose (14 mg equivalence in adults).

Results: 152 patients from the DB period entered the OLE (teriflunomide, 100/109 [91.7%]; placebo, 52/57 [91.2%]) of which 104 (68.4%) completed the OLE. From DB randomization to the end of OLE, relapse risk was numerically lower for teriflunomide/teriflunomide versus placebo/teriflunomide (hazard ratio [95% CI]: 0.62 [0.39–0.98]; $p=0.11$), as was risk of disability progression sustained for 24 weeks (0.47 [0.23–0.96]). The teriflunomide/teriflunomide group showed reductions versus placebo/teriflunomide for new/enlarging T2 (5.7 vs 11.1; $p=0.001$) and gadolinium-enhancing T1 (1.5 vs 2.7; $p=0.04$) lesion counts per MRI scan. Proportion of patients with treatment-emergent adverse events (TEAEs) during the OLE was lower in the teriflunomide/teriflunomide group (81.0%) versus placebo/teriflunomide (90.4%), as was the proportion with serious TEAEs (teriflunomide/teriflunomide: 14.0%; placebo/teriflunomide: 28.8%). 12 patients discontinued open-label treatment due to TEAEs.

Conclusion: Continuous teriflunomide versus delayed teriflunomide initiation in paediatric patients numerically lowered relapse risk and disability progression, and significantly reduced MRI lesion counts with a manageable safety profile.

Disclosure: Editorial support was provided by Richard Hogan, PhD, and Gleb Baida, PhD of Elevate Medical Affairs, which was sponsored by Sanofi Genzyme.

Ageing and dementia 1

OPR-026

Naturally occurring plasma tau autoantibodies and risk of systemic disease

A. Magalhães, M. Emmenegger, E. De Cecco, M. Carta, K. Frontzek, A. Chincisan, S. Hornemann, A. Aguzzi
Institute of Neuropathology, University of Zurich, Zurich, Switzerland

Background and aims: Microtubule-associated protein tau is highly expressed in neurons and is known to have a role in neurodegenerative diseases, including Alzheimer’s disease. Most research efforts have focused on the function of tau in the nervous system and several clinical trials are exploring the use of tau immunization strategies to prevent progression of neurodegenerative diseases. However, tau protein is not only highly expressed in the brain but also in the kidney and skeletal muscle. A potential role of tau in systemic disease had not been previously explored and so that was the aim of our study.

Methods: Using a high-throughput ELISA (Enzyme-Linked Immunosorbent Assay) screening platform, we probed >20.000 plasma samples of patients visiting a university hospital for the presence of naturally occurring tau autoantibodies. Clinical conditions were classified using ICD-10 (International Classification of Disease and Related Health Problems, 10th revision) codes. Risk ratios and 95% confidence intervals for tau autoimmunity in different systemic disorders were estimated using multivariate log-binomial regression models (including age, sex).

Results: Using data from 21.995 patients, we identified cystitis (RR 1.59, 95% CI 1.14–2.16, p=0.004), other urinary disorders (RR 1.23, 95% CI 1.03–1.45, p=0.018), chronic kidney disease (RR 1.20, 95% CI 1.01–1.41, p=0.033), arterial embolism and thrombosis (RR 1.56, 95% CI 1.02–2.25, p=0.026) and atherosclerosis (RR 1.35, 95% CI 1.09–1.66, p=0.004) as independent predictors of naturally occurring tau autoantibodies.

Conclusion: Tau autoimmunity is associated with vascular, kidney and urinary disorders.

Disclosure: Candoc grant (FK-19-025) of UZH to ADM. Swiss Personalised Health Network (SPHN 2017DRI17), Swiss National Foundation (SNF 179040), the European Research Council (ERC 670958) and the Nomis Foundation to AA.

OPR-027

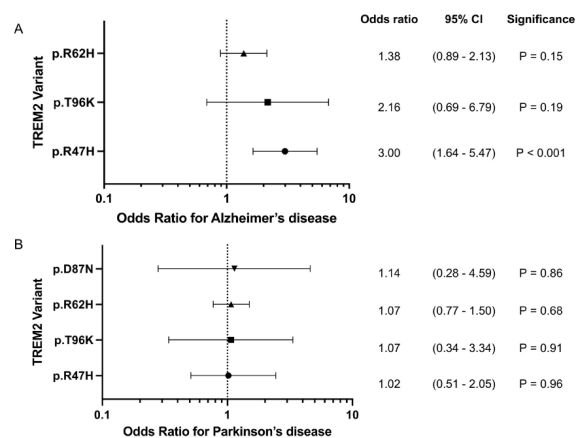
Effect of TREM2 on neurodegenerative diagnosis, cognitive profile and brain structure.

O. Cousins, Z. Chappell, A. Chandra, F. Turkheimer, A. Hodges
Institute of psychology, psychiatry & Neurology, King’s College London, United Kingdom

Background and aims: Microglial genes are risk factors for neurodegenerative diseases, especially variant rs75932628 (p.R47H) TREM2. We investigated the association between different TREM2 variants and neurodegenerative disease and evaluated their association with brain structure and cognition.

Methods: Data was acquired from the UKBIOBANK study, including TREM2 variant carriers: p.R47H (n=1,863), p.T96K (n=665), p.R62H (n=7,988) and p.D87N (n=419), and noncarriers (n=392,373). Risk of Alzheimer’s (AD; n=803) and Parkinson’s (PD; n=1,687) disease was calculated using logistic regression. A subgroup of healthy older adults underwent brain volumetric MRI and cognitive profile. These were compared between carriers of each TREM2 variant and noncarriers.

Results: The p.R47H variant was associated with AD but not PD (Figure 1). Other variants were not associated with either disease. There was no difference in age of onset between p.R47H carriers and noncarriers (median 72 years). There were trend-level associations for reduced putamen (p=0.09), hippocampal (p=0.10) and total brain volumes (p=0.07) in healthy older p.R47H carriers. This was driven by under 65s for the putamen (p=0.09), hippocampal (p=0.10) and total brain volumes (p=0.07) in healthy older p.R47H carriers. This was driven by under 65s for the putamen (P<0.01) and total brain volume (p<0.01). Lower putamen volume (P=0.04) was found in p.D87N carriers. Lower memory scores were found in p.T96K carriers (p<0.01).



Conclusion: TREM2 p.R47H is a risk factor for AD but is not associated with younger age of onset or with PD. Lack of association between p.T96K, p.R62H or p.D87N and AD may relate to smaller effect sizes and cohort age (median 69 years). We found nominal brain volume reductions in healthy carriers of p.R47H and p.D87N. Therefore, TREM2 may influence brain structure prior to neurodegeneration onset.

Disclosure: Nothing to disclose.

OPR-028

DIAGNOSTIC VALIDITY OF CSF ALPHA-SYNUCLEIN TO PREDICT PSYCHOSIS IN PRODROMAL ALZHEIMER'S DISEASE

J. Monge-Agrilés¹, J. Sáez-Valero^{2,3,4}, J. Sánchez-Payá^{2,6}, R. Gasparini-Berenguer^{1,2}, M. Cortés-Gómez^{1,2}, M.S. García-Ayllón^{3,4,5}

¹ Servicio de Neurología, Hospital General Universitario de Alicante, Alicante, Spain ² Instituto de Investigación Sanitaria y Biomédica de Alicante (ISABIAL), Alicante, Spain, ³ Unidad de Investigación. Hospital General Universitario de Elche. FISABIO, Spain, ⁴ Instituto de Neurociencias de Alicante, Universidad Miguel Hernández-CSIC. San Joan d'Alacant, Alicante, Spain, ⁵ Centro de investigación Biomédica en Red sobre enfermedades Neurodegenerativas (CIBERNED), San Joan d'Alacant, Spain ⁶ Servicio de Medicina Preventiva. Hospital General Universitario de Alicante, Alicante, Spain

Background and aims: The emergence of psychotic symptoms (PS) in Alzheimer's disease (AD) involves a poor prognosis of the illness. To study the diagnostic validity of alpha-synuclein (AS) in CSF, to predict the emergence of PS in prodromal AD patients.

Methods: Mild cognitive impairment patients (according to Petersen 2006) from the out-patient consultation of Alicante University General Hospital (Spain) were recruited between 2010–2018. All the patients followed NIA-AA 2018 criteria for AD biomarkers. At inclusion, all of them had MMSE higher than 22, Neuropsychiatric Inventory lower than 10 and a follow-up higher than 2 years. The Pittsburgh sleep quality index and the Cummings criteria for psychosis (2020) were applied. Core AD biomarkers and AS were measured in CSF obtained in the prodromal phase of the illness.

Results: 130 prodromal AD were included. 50 of them (38.4%) accomplished the PS criteria into the 8 years follow-up. In every comparison made between groups and subgroups, AS was the best CSF biomarker to differentiate psychotic versus non psychotic groups. The level of AS 1.257 pg/mL reached at least 80% of sensitivity to differentiate between both groups. A negative predictive value of 80% was found to differentiate between groups.

Conclusion: The measurement of AS in CSF is the most valid biomarker used in this study to predict the emergence of PS during the 8 years after the prodromal phase of AD. In our knowledge, is the first time that a CSF biomarker shows a diagnostic validity to predict PS in prodromal AD.

Disclosure: Funded by ISABIAL.

OPR-029

Belgian Carriers of Rare ABCA7 Mutations Present with Pronounced Cerebral Amyloid Angiopathy and Alzheimer's Disease

E. Hendrickx Van de Craen¹, L. Bossaerts¹, A. Sieben², C. Loos³, L. Yperzeele³, S. Engelborghs⁴, P. De Deyn⁵, P. Cras³, C. Van Broeckhoven¹

¹ Neurodegenerative Brain Diseases Group, Center for Molecular Neurology, VIB, Antwerp, ² Department of Pathology, University Hospital Antwerp, Edegem, Belgium, ³ Department of Neurology, University Hospital Antwerp, Edegem, Belgium, ⁴ Department of Neurology, University Hospital Brussels and University Center for Neurosciences, VUB, Brussels, Belgium, ⁵ Department of Neurology and Memory Clinic, Hospital Network Antwerp, Antwerp, Belgium

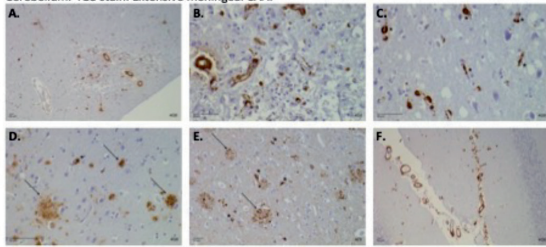
Background and aims: ABCA7 is a major risk gene for Alzheimer's disease (AD), and rare premature termination codon (PTC) and missense mutations are enriched in AD patients. In preliminary studies, we obtained that ABCA7 PTC and missense mutation carriers present with a classical AD phenotype, but severe levels of cerebral amyloid angiopathy (CAA) were also observed at neuropathological examination. We aim to delineate the clinicopathological phenotype of rare ABCA7 mutation carriers in Belgian CAA patients.

Methods: Genetic screening of ABCA7 in Belgian CAA cohort (n=83), with genotype-phenotype comparison of the ABCA7 carriers using demographic and clinicopathology data.

Results: In 20.5% of CAA patients a rare ABCA7 mutation was identified. Six patients carried a PTC mutation, 10 a missense mutation and in one patient we found a deletion. Mean onset age was 66.4±12.8 (range 47-84) years, while mean age at death was 68.0±10.3 (range 48-92) years. Cognitive decline was present in 52.9% (9/17). Nine patients were diagnosed as probable CAA, and four as possible CAA. In six patients postmortem examination showed moderate-to-severe levels of CAA in all but one patient (83.3%, 5/6) and AD neuropathological hallmarks (100%, 6/6). Extensive levels of CAA were present in both the meningeal and capillary blood vessels, and moderate to high levels of CAA in the parenchymal blood vessels.

Figure 1. Neuropathology of ABCA7 PTC mutation carrier

A. Frontal cortex. 4G stain. Cortical micro infarction. In the region of infarction, there is abundant CAA. B. Frontal cortex. 4G stain. Capillary CAA. C. Frontal cortex. 4G stain. Focus on capillary CAA(*). D. Hippocampus. 4G8 stain. Presence of diffuse plaques and capillary amyloid angiopathy (*). E. Hippocampus. AT8 stain. Presence of neurofibrillary tangles (*) and dystrophic neurites (arrow). F. Cerebellum. 4G8 stain. Extensive meningeal CAA.



Conclusion: Our data suggest that rare ABCA7 mutations are frequently present in CAA patients. Carriers show signs of severe levels of CAA, as well as AD neuropathological hallmarks. The findings of this study have important implications for future research and clinical practice.

Disclosure: Nothing to disclose.

OPR-030

Huntingtin as a presymptomatic regulator of Alzheimer's disease

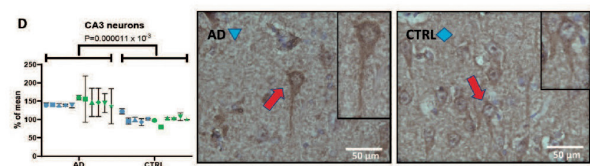
M. Axenhus, S. Schedin-Weiss, P. Nilsson,
B. Winblad, L. Tjernberg

Division of Neurogeriatrics, Department of Neurobiology,
Care Sciences and Society, Karolinska Institutet, Solna,
Sweden

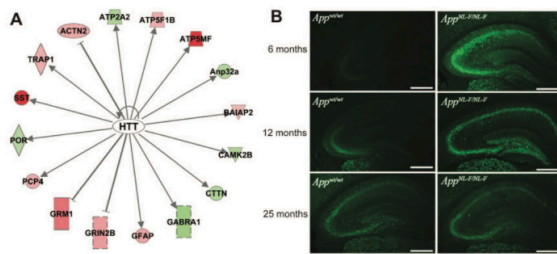
Background and aims: The identification of pathological elements that regulate disease progression, so called regulators, are essential when studying progressive diseases. When Alzheimer disease (AD) presents with symptoms, irreversible nerve damage has already occurred. Targetable intervention and therapy need to address presymptomatic processes and regulators of disease progression. Due to the multi-factorial pathology of AD, a multi-modal approach is needed in order to identify disease regulators.

Methods: Proteomics and subsequent ingenuity pathway analysis was performed on human and the App NL-F/NL-F mouse model brain. The App NL-F/NL-F mouse is a knock-in model, which specifically produces increased levels of highly neurotoxic A β 42, making it suitable for the study of A β 42-driven pathology. The levels of huntingtin in human and mice brain were quantified using immunohistochemistry and the location was determined by fluorescence-microscopy.

Results: Huntingtin was identified as a presymptomatic regulator of disease progression in AD. Microscopic studies showed increased levels of huntingtin in pyramidal neurons in the hippocampus and frontal cortex of AD patients compared to nondemented controls. In contrast to Huntington's disease, huntingtin did not colocalize with reactive astrocytes in AD brain. Huntingtin increased in a time-dependent manner and preceded amyloid deposition in App NL-F/NL-F mice.



Huntingtin levels in Alzheimer's disease brain (red arrows) show increased accumulation in pyramidal neurons. Huntingtin were found in particularly high levels in hippocampal subareas such as CA3.



Ingenuity pathway analysis (A) show huntingtin as a regulator of disease progression. APP NL-F/NL-F mice brain show a time-dependent increase in huntingtin (B) which predates accumulation of other pathological elements typical of Alzheimer's disease.

Conclusion: Huntingtin accumulates in the AD brain and is distinct from the huntingtin accumulation seen in Huntington's disease. These findings implicate huntingtin in the pathology of AD and warrant further studies. Huntingtin could possibly be a target for therapeutical intervention. Mechanistic studies in neuronal cell cultures will shed light on the relationship between huntingtin and AD pathogenesis.

Disclosure: Nothing to disclose.

OPR-031

Huntingtin intermediate alleles influence the progression from Subjective Cognitive Decline to Mild Cognitive Impairment

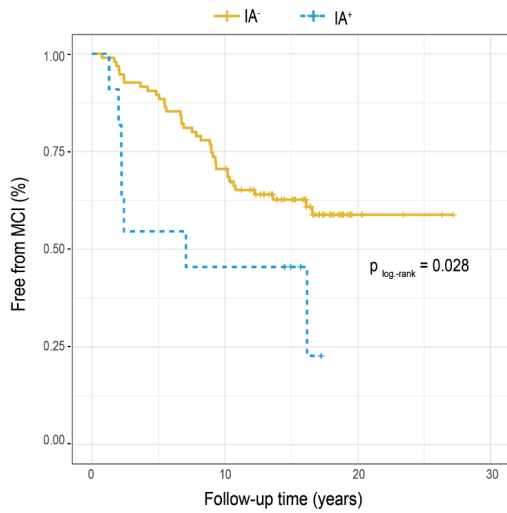
S. Mazzeo¹, F. Emiliani¹, S. Bagnoli¹, S. Padiglioni², V. Conti¹, A. Ingannato¹, G. Giacomucci¹, J. Balestrini¹, C. Ferrari¹, S. Sorbi³, B. Nacmias¹, V. Bessi¹

¹ Department of Neuroscience, Psychology, Drug Research and Child Health, University of Florence, Azienda Ospedaliera-Universitaria Careggi, Florence, Italy, ² Unit Clinic of Organizations Careggi University Hospital, Florence, Italy, ³ IRCCS Fondazione Don Carlo Gnocchi, Florence, Italy

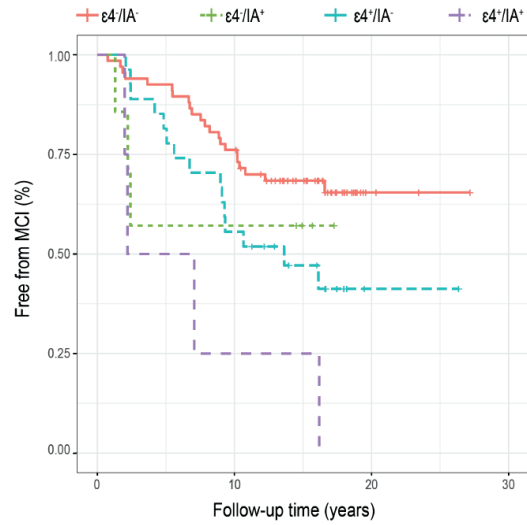
Background and aims: Huntingtin (HTT) is a gene containing a key region of CAG repeats. HTT alleles containing from 27 to 35 CAG repeats are termed as intermediate alleles (IAs). We aim to assess the effect of IAs on progression of cognitive impairment in patients with subjective cognitive decline (SCD).

Methods: We included 106 patients with SCD. All the patients underwent neuropsychological assessments and blood sample collections at baseline. Patients were followed-up for a median time of 13.75 (IQR=8.17). We genotyped APOE and HTT at the end of the follow-up.

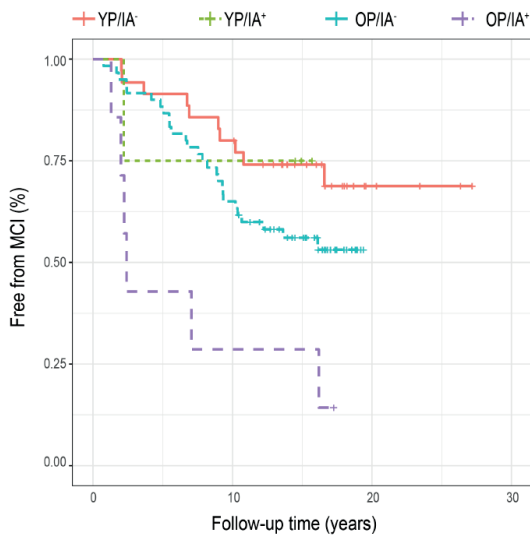
Results: Eleven out of 106 patients (10.38% [95% CI=4.57–16.18]) were carriers of IA (IA+). During the follow-up, 44 patients (41.51% [95% CI=32.13–50.89]) progressed to MCI (p-SCD), while 62 patients (58.49% [95% CI=49.11–67.87]) did not (np-SCD). Rate of progression to MCI was associated with IAs (Fig.1), age at baseline, and APOE ϵ 4. We dichotomized age at baseline (<60 = younger patients [YP], >60 = older patients [OP]) and classified patients into four groups: YP/IAS-, YP/IAS+, OP/IAS- and OP/IAS+. OP/IAS+ had a higher proportion of progression from SCD to MCI (85.71% [95% C.I.=59.79–100]) as compared to YP/IAS- (28.57% [95% C.I.=13.60–43.54], $\chi^2=15.25$, $p<0.001$) and OP/IAS- (45.00% [95% C.I.=32.41–57.59], $\chi^2=7.903$, $p=0.005$) (Fig.2). We classified patients according to APOE and IA as: ϵ 4-/IA-, ϵ 4-/IA+, ϵ 4+/IA-, ϵ 4+/IA+. Proportion of progression in ϵ 4+/IA+ group (100%) was higher as compared to ϵ 4-/IA- (33.33% [95% C.I.=21.96–44.71], $\chi^2=14.43$, $p<0.001$) and ϵ 4+/IA- (55.56% [95% C.I.=36.81–74.30], $\chi^2=4.60$, $p=0.032$) (Fig.3).



Kaplan-Meier survival analysis for comparison of distributions of progression from SCD to MCI between IA- (n=95) and IA+ (n=1).



Kaplan-Meier survival analysis for comparisons of distributions of progression from SCD to MCI among groups defined according to APOE status and IA: $\epsilon 4-/IA-$ (n = 67), $\epsilon 4-/IA+$ (n = 7), $\epsilon 4+/IA-$ (n = 27) and $\epsilon 4+/IA+$ (n = 4).



Kaplan-Meier survival analysis for comparisons of distributions of progression from SCD to MCI among groups classified according to age at baseline and IA: YP/IA- (n=35), YP/IA+ (n=4), OP/IA- (=60) and OP/IA+ (n=7).

Conclusion: IAs interact with age and APOE $\epsilon 4$ increasing the risk of progression to MCI in SCD patients.

Disclosure: No authors report any conflicts of interest for this study.

COVID-19

OPR-032

Persistent olfactory dysfunction in COVID-19: a seed-based resting-state fMRI study

L. Muccioli¹, G. Sighinolfi¹, M. Mitolo², L. Ferri¹, M. Rochat², U. Pensato¹, L. Taruffi¹, P. Cortelli¹, C. Testa², M. Masullo¹, R. Liguori¹, R. Lodi¹, C. Tonon¹, F. Bisulli¹

¹ Department of Biomedical and Neuromotor Sciences, University of Bologna, Bologna, Italy; ² IRCCS Istituto delle Scienze Neurologiche di Bologna, Bologna, Italy

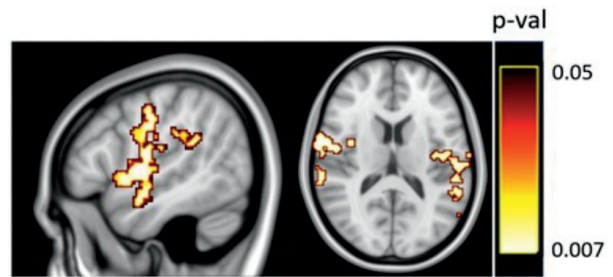
Background and aims: Olfactory dysfunction (OD) is a frequent manifestation of COVID-19 and, in a minority of patients, may persist for several months. The pathogenesis is still debated and may involve disruption of the olfactory system at different levels. We aimed to explore the integrity of the olfactory network in a cohort of patients with COVID-19-related persistent OD, through resting-state functional magnetic resonance imaging (rs-fMRI).

Methods: We included 23 patients (mean age 37±14 years, 12 females) with persistent (11±5 months) COVID-19-related OD confirmed by Sniffin' Sticks Test (mean score 24±5/48, hyposmia cut-off: 30) and 28 sex- and age-matched healthy controls. Participants underwent a neuropsychological assessment and a standardized brain MR acquisition protocol (3 T), including rs-fMRI. Seed-based correlation analysis was performed on pre-processed rs-fMRI data to localize each subject's olfactory network, using spherical seeds in the bilateral anterior insula, piriform cortex and orbitofrontal cortex (Figure 1). Whole-brain functional connectivity (FC) with the seeds was compared between patients and controls (statistical significance: p-value<0.05).



Location of the ROI used as seeds for the seed-based correlation analysis

Results: The olfactory network was successfully identified in seven patients, and significantly lower FC was found, compared to healthy controls, between the right anterior insula and a wide spread area of the bilateral superior temporal, middle frontal and inferior parietal areas (Figure 2). Additionally, the FC between the left piriform cortex and the right frontal pole was significantly higher in the patients' group compared to controls.



Clusters of altered functional connectivity with the right superior insula

Conclusion: Patients with persistent COVID-19-related OD showed altered olfactory network connectivity (i.e. anterior insula and the piriform cortex).

Disclosure: Nothing to disclose.

OPR-033

The risk of neurological diseases after COVID-19, influenza A/B or community-acquired pneumonia infection

P. Zarifkar¹, C. Peinkhofer¹, M. Benros², D. Kondziella¹

¹ Department of Neurology, Copenhagen University Hospital, Rigshospitalet, Copenhagen, Denmark,

² Copenhagen Research Centre for Mental Health - Mental Health Centre Copenhagen, Copenhagen University, Hellerup, Denmark and Department of Immunology and Microbiology, Faculty of Health and Medical Sciences, Copenhagen University, Copenhagen, Denmark

Background and aims: Two years after onset of the pandemic, the precise nature and temporal evolution of the effects of COVID-19 on neurologic disorders remain uncharacterized. Studies have established an association with neurological syndromes, including anosmia, encephalopathy, and ischemic stroke, but it is unknown whether COVID-19 also influences the incidence of specific neurologic diseases and whether it differs from other respiratory infections.

Methods: Using population-based electronic health records we investigated the association between COVID-19 and specific central and peripheral neurologic diseases. We compared patients with COVID-19 to individuals without, and to patients with influenza A/B and community-acquired bacterial pneumonia. We assessed the incidence of neurologic disease one, three, six, and twelve months after positive test results.

Results: We identified 42,535 people with COVID-19, 8,329 with influenza, 1,566 with pneumonia, and 2,392,400 without COVID-19. Compared to individuals without COVID-19, patients with COVID-19 had increased relative risk (RR) of developing Guillain Barré syndrome (RR=3.1; 95% CI=1.5–6.7), multiple sclerosis (RR=1.4; 95% CI=1.2–1.7), narcolepsy (RR=3.2; 95% CI=1.6–6.2), Parkinson's disease (RR=2.8; 95% CI=2.4–3.2), Alzheimer's disease (RR=4.9; 95% CI=4.0–6.0), dementia of any type (RR=5.2; 95% CI=4.5–6.1), and ischemic stroke (RR=2.3; 95% CI=2.1–2.5). However, compared to patients hospitalized with influenza, patients hospitalized with COVID-19 only had an increased risk of ischemic stroke at one (RR=1.9; 95% CI=1.3–2.8), three (RR=1.8; 95% CI=1.3–2.5) and six months (RR=1.9, 95% CI=1.3–2.7). Compared to patients hospitalized with pneumonia, the risk of neurologic diseases was not increased.

Conclusion: COVID-19 increases the risk of a broad range of neurological disorders. However, except for ischemic stroke, there is no excess risk compared to influenza A/B and community-acquired pneumonia.

Disclosure: The authors have none to declare.

OPR-034

Neuronal and glial damage during acute COVID infection in absence of clinical neurological manifestations

D. Plantone, S. Locci, L. Bergantini, C. Manco,

R. Cortese, E. Bargagli, N. De Stefano

Department of Medicine, Surgery and Neuroscience, University of Siena, Siena, Italy

Background and aims: SARS-Cov 2 has a particular tropism for the nervous system and can infect neurons and glia. Serum neurofilament light chain (sNfL) and serum glial fibrillary acidic protein (sGFAP) represent two promising markers of neuronal and glial degeneration. The aim of this study is to evaluate sNfL and sGFAP levels in COVID hospitalized patients without neurological symptoms and previous neurological co-morbidities.

Methods: 68 COVID patients, 72 healthy subjects (HSs) and 21 non-COVID patients with interstitial pneumonia were enrolled in the study. Blood samples were collected within 24–48 h of hospitalization and sNfL and sGFAP levels were assessed in each serum sample of patients and controls. We used the commercially available immunoassay kits for GFAP and NfL run on the ultrasensitive SR-X™ Biomarker Detection System (Quanterix) following manufacturer instructions. Non parametric statistical analysis was performed to assess difference between the three groups.

Results: In this ongoing study, COVID patients showed higher levels of sNfL (COVID: 38.02+57.87 pg/mL) than in non-COVID pneumonia (13.63+6.82, p 0.02) and HSs (6.65+2.85 pg/mL, p<0.0001). COVID patients showed also higher levels of sGFAP (COVID: 232.98+223.06 pg/mL) in comparison to non-COVID pneumonia (145.32+77.26, p=0.05) and HSs (84.12+33.70 pg/mL, p=0.006). No significant differences were found between non-COVID patients and HSs for both biomarkers. In COVID patients, no significant correlation was found between blood levels of sNfL or sGFAP and disease severity.

Conclusion: The preliminary results of this ongoing study suggest inflammatory-related neuronal and glial degeneration in patients with COVID infection independently of presence of clinical neurological manifestations.

Disclosure: R. Cortese was awarded a MAGNIMS-ECTRIMS fellowship in 2019. N. De Stefano received honoraria from Biogen-Idec, Bristol Myers Squibb, Celgene, Genzyme, Immunic, Merck Serono, Novartis, Roche and Teva.

OPR-035

Does gender influences outcome of stroke in COVID+ and COVID- patients: a large collaborative study in Northern Italy

F. Martinelli Boneschi¹, D. Sangalli², M. Versino³, I. Colombo⁴, A. Ciccone⁵, S. Beretta⁶, V. Patisso¹, S. Marcheselli⁷, M. Roncoroni⁸, S. Beretta⁹, L. Lorusso¹⁰, A. Cavallini¹¹, A. Prella¹², D. Guidetti¹³, S. La Gioia¹⁴, S. Canella¹⁵, C. Zanferrari¹⁶, G. Grampa¹⁷, E. D'Adda¹⁸, L. Peverelli¹⁹, A. Salmaggi², A. Colombo²⁰

¹ IRCCS Fondazione Ca' Granda Ospedale Maggiore Policlinico, Neurology Unit, Milan, Italy, ² Neurological Department, Alessandro Manzoni Hospital, ASST Lecco, Italy, ³ Neurology and Stroke Unit, ASST SetteLaghi, Ospedale di Circolo, Varese, Italy, ⁴ Neurology and Stroke Unit, Ospedale di Desio, ASST Monza, MB, Italy, ⁵ Department of Neurosciences, Carlo Poma Hospital, ASST di Mantova, Mantua, Italy, ⁶ Department of Neurology, San Gerardo Hospital, ASST Monza, University of Milano Bicocca, Monza, Italy, ⁷ Neurologia d'urgenza e Stroke Unit, Humanitas Clinical and Research Center – IRCCS, Rozzano, Milan, Italy, ⁸ Neurology and Stroke Unit, P.O. Saronno, ASST Valle Olona, Varese, Italy, ⁹ Neurology, Vimercate Hospital, ASST Vimercate, Vimercate, MB, Italy, ¹⁰ Neurological Department, San Leopoldo Mandic Hospital, ASST Lecco, Merate, Italy, ¹¹ Neurologia d'Urgenza e Stroke Unit, IRCCS Fondazione Mondino, Pavia, Italy, ¹² Neurology, ASST Ovest Milanese, Legnano, Italy, ¹³ Neurology Unit, Guglielmo da Saliceto Hospital, Piacenza Italy, ¹⁴ Department of neurology, Papa Giovanni XXIII Hospital, Bergamo, Italy, ¹⁵ Neurology and Stroke Unit, San Giuseppe-Multimedica Hospital, Milan, Italy, ¹⁶ Neurology and Stroke Unit, PO Vizzolo Predabissi, ASST Melegnano Martesana, Milan, Italy, ¹⁷ Neurology Unit, S. Anna Hospital, Como, Italy, ¹⁸ Neurology Unit, Ospedale Maggiore di Crema, ASST Crema, Crema, Italy, ¹⁹ Neurology, Ospedale Maggiore di Lodi, ASST Lodi, Italy, ²⁰ Polo Neurologico Brianteo, Seregno, MB, Italy

Background and aims: The impact of the COVID-19 pandemic during the first wave in Italy caused a decrease of hospital admissions, delays in reperfusion treatments and an overall worse outcome in COVID+ patients with stroke. However, few data are available on outcome of stroke stratified by gender.

Methods: A multi-center observational study on neurological complications in COVID-19 patients was conducted in 19 Neurology Units by the Italian society of Hospital Neuroscience (SNO). Adult patients admitted to Neurological units between March–April 2020 with ischaemic stroke were recruited. Demographic, clinical, treatment and outcome data were compared in patients with (COVID19+) and without COVID-19 (COVID19-), as well as in male and female patients.

Results: 812 patients with ischemic stroke were enrolled (682 COVID-, 129 COVID+); males were 54.1% and 52.7%. Intra-hospital mortality was 31.9% in COVID+ patients (38.6% in male and 27.8% in female) and 7.2% in COVID- (8.4% in males and 6% in females). Male patients

with COVID+ were more likely to have cPAP (30.9% vs 14.8%; $p=0.03$) or being intubated (14.9% vs 3.3%; $p=0.02$) than females. Reperfusion treatment was administered more frequently in women if COVID- (34.5% vs 29.8%), while less frequently if COVID+ (11.5% vs 29.4%; $p=0.01$). COVID+ patients had a higher frequency of ESUS than COVID- (31.8% vs 22.3%; $p=0.02$), with a higher frequency in COVID+ females compared to males (36.1% vs 27.9%).

Conclusion: Our study detected some differences due to gender in ischaemic stroke with and without COVID-19. Multivariate analyses is ongoing to define predictors of mortality across gender categories.

Disclosure: Nothing to disclose.

OPR-036

The COVID-19 pandemic has caused large disruptions to dementia mortality, care, and diagnosis in Sweden during 2020

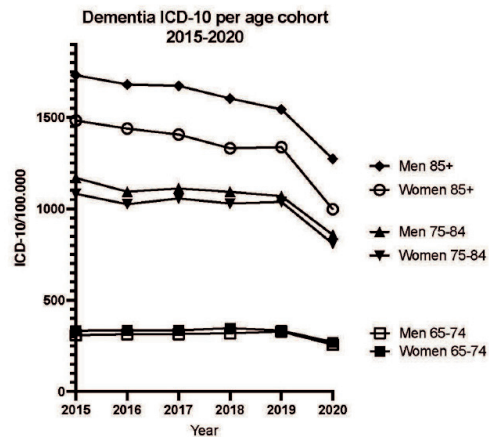
B. Winblad¹, S. Schedin-Weiss¹, L. Tjernberg¹, A. Wimo¹, G. Bucht², M. Eriksson³, M. Axénhus¹

¹ Division of Neurogeriatrics, Department of Neurobiology, Care Sciences and Society, Karolinska Institute, Sweden, ² Department of Community medicine and Rehabilitation, Umeå University, Umeå, Sweden, ³ Division of Clinical geriatrics, Department of Neurobiology, Care Sciences and Society, Karolinska Institute, Sweden

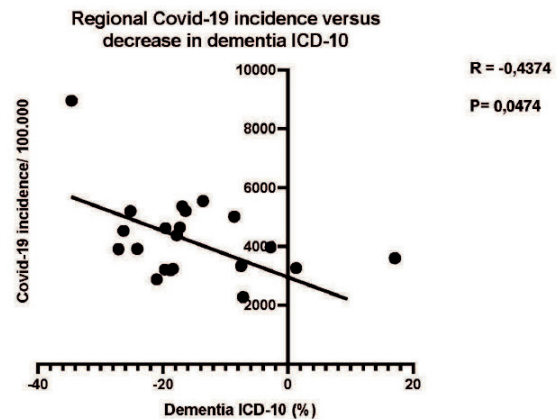
Background and aims: Covid-19 might cause indirect deaths and reduction in diagnoses amongst vulnerable patient populations such as dementia patients. Quantifying the effect of Covid-19 on dementia patient population in the form of deaths and diagnosis amongst the group is essential to understand the full scope of the pandemic impact and formulate future response.

Methods: Registry based national data from 2015–2019 was collected in the form of periodic mortality, years of potential life lost, dementia diagnosis coding, and Covid-19 incidence in Sweden and its 21 regions. Multivariable regression analysis and moving averages was used to predict values for each parameter during 2020. Pearson correlation analysis was used to confirm correlation between Covid-19 incidence and mortality, years of potential life lost, or dementia diagnosis coding.

Results: During 2020, Covid-19 caused a seasonal increase in mortality amongst dementia patients that coincided with pandemic waves. Dementia diagnosis coding was severely impacted in all regions and correlated to Covid-19 incidence but not mortality. All dementia diagnoses decreased significantly. Elderly women were particularly affected. Unspecified dementia was found to be increased. Preliminary data from first half of 2021 showed similar results.



Dementia associated ICD-10 coding of age cohorts in Sweden during 2015–2020 showing a marked decrease in dementia coding during 2020.



Dementia ICD-10 associated coding correlate to Covid-19 incidence in the 21 regions of Sweden.

Conclusion: Covid-19 is linked to increase in mortality amongst dementia patients. Covid-19 has also caused large impacts to dementia diagnosis and care. These findings might have severe long-term consequences in the form of underdiagnosis and undertreatment of dementia, particularly amongst elderly women. Increased percentage of unspecified dementia making up dementia diagnoses might be indicative of decreased quality in dementia diagnosis. Healthcare reforms are necessary to address these shortcomings.

Disclosure: Nothing to disclose.

OPR-037

Safety of vaccines against SARS-CoV-2 among patients with multiple sclerosis treated with disease modifying therapies

J. Kulikowska¹, K. Kapica-Topczewska¹, A. Czarnowska¹, J. Tarasiuk¹, J. Kochanowicz¹, W. Broła², A. Kalinowska-Łyszczarz³, M. Adamczyk-Sowa⁴, M. Stasiołek⁵, E. Krzystanek⁶, K. Rejdak⁷, A. Słowik⁸, S. Budrewicz⁹, H. Bartosik-Psujek¹⁰, A. Kułakowska¹

¹ Department of Neurology, Medical University of Białystok, Białystok, Poland, ² Collegium Medicum, Jan Kochanowski University, Kielce, Poland, ³ Poznan University of Medical Science, Poznań, Poland,

⁴ Department of Neurology, Medical University of Silesia, Zabrze, Poland, ⁵ Medical University of Lodz, Lodz, Poland,

⁶ Department of Neurology, Faculty of Health Science, Katowice, Poland, ⁷ Medical University of Lublin, Lublin, Poland, ⁸ Jagiellonian University, Medical College, Kraków, Poland, ⁹ Medical University of Wrocław, Wrocław, Poland,

¹⁰ Department of Neurology, Institute of Medical Science, University of Rzeszów, Rzeszów, Poland

Background and aims: The aim of the study was to report side effects after vaccination against coronavirus disease 2019 (COVID-19) among individuals with multiple sclerosis (MS) treated with disease-modifying therapies (DMTs) in Poland.

Methods: The study included 2,203 patients with MS treated with DMTs and vaccinated against COVID-19 in 17 Polish MS centers. The data was collected through 15 December 2021. The information included demographics, specific MS characteristics, current DMTs, type of vaccine, side effects after vaccination, time of side effect symptoms onset and resolution, applied treatment, relapse occurrence, and incidence of COVID-19 after vaccination. The results were obtained using maximum likelihood estimates for the odds ratio and logistic regression.

Results: The majority (1,782/2,203; 80.89%) of included patients were vaccinated with nucleoside-modified messenger RNA (mRNA) vaccines. Mild symptoms after immunization, more often after the first dose, were reported by 70.04% of individuals. Most common were: arm pain (47.34% after the first and 34.59% after the second dose), fever (18.11% after the first and 19.38% after the second dose), and fatigue (10.67% after the first and 10.94% after the second dose). Only one individual presented severe side effects (pro-thrombotic complications). None of the DMTs predisposed to the development of particular side effects. Relapse after vaccination occurred in 99 individuals, in 16 ones less than 21 days after the first or second dose of immunization. 7 patients had confirmed SARS-CoV-2 infection despite vaccination

Conclusion: Serious side effects after vaccination against COVID-19 in patients with MS are very rare and are not related to particular DMT.

Disclosure: Authors have nothing to disclose.

Cerebrovascular diseases: Small vessel disease and ICH

OPR-038

Clinical characteristics of Cortical Superficial Siderosis – a 10 years (2009-2021) single centre experience

A. Toma¹, S. Pikija¹, M. Koepf², A. Rohrer¹, G. Kuchukhidze³, M. McCoy³, E. Trinka³

¹ Department of Neurology, Christian-Doppler-University Hospital, Member of the European Reference Network EpiCARE, and Centre for Cognitive Neuroscience, Paracelsus Medical University, Salzburg, Austria,

² Department of Clinical and Experimental Epilepsy, UCL Institute of Neurology; University College London; National Hospital for Neurology and Neurosurgery, London, United Kingdom; Chalfont Centre for Epilepsy, Chalfont St Peter, Gerrards Cross, London, United Kingdom, ³ Department of Neurology, Christian-Doppler-University Hospital, Member of the European Reference Network EpiCARE, and Neuroscience Institute, Centre for Cognitive Neuroscience, Paracelsus Medical University, Salzburg, Austria

Background and aims: Cortical Superficial Siderosis (cSS) is caused by supratentorial hemosiderin deposits limited to the cortical sulci, supposedly due to acute non-traumatic convexity subarachnoid haemorrhage (cSAH) in subarachnoid space. cSS is a neuroimaging biomarker for cerebral amyloid angiopathy (CAA) and a common cause of transient focal neurological deficits (TFNEs).

Methods: This is a descriptive retrospective study of symptomatic patients with cSS and TFNEs who presented in the Christian-Doppler-University Hospital, between 2009 and 2021. We analysed demographic, semiological, and MRI data of 37 patients older than 55 years, with cSS/cSAH and neuroimaging features of probable/possible CAA in conformity with the Boston-Criteria.

Results: We identified 37 patients (35% male) with probable (n=24; 65%) or possible (n=13; 35%) CAA with a median age of 70 years (IQR 68–77). 65% (n=26) of them showed cardiovascular risk factors, and 56% were presented in our clinic with at least one transient focal neurological episode, mostly in the form of non-motor sensory symptoms (n=19) with a median duration of symptoms up to 15 minutes (IQR 10–30). The patients with only TFNEs were significantly older (median 81 vs. 70 years of age, p=0.005) than patients with symptoms due to stroke (infarction or haemorrhagic) ±TFNEs. In the MRI, the most frequent localization of cSS was in the frontal (n=54) followed by parietal (n=38) and occipital (n=28) region.

Conclusion: In the population with established cSS, those presenting only with TFNEs tend to be older than their counterparts presenting with additional stroke symptoms.

Disclosure: Nothing to disclose.

OPR-039

MRI small vessel disease classification of intracerebral haemorrhage and risk of recurrent cerebrovascular events

M. Goeldlin¹, M. Mueller¹, B. Siepen¹, A. Hakim², D. Strambo³, T. Fischer⁴, F. Medlin⁵, N. Peters⁶, E. Carrera⁷, G. Karwacki⁸, C. Cereda⁹, J. Niederhaeuser¹⁰, A. Mueller¹¹, S. Wegener¹¹, S. Sartoretti-Schefer¹², A. Polymeris¹³, R. Sturzenegger¹⁴, M. Psychogios¹⁵, W. Z'Graggen¹⁶, D. Bervini¹⁷, L. Bonati¹³, M. Arnold¹, U. Fischer¹³, D. Seiffge¹

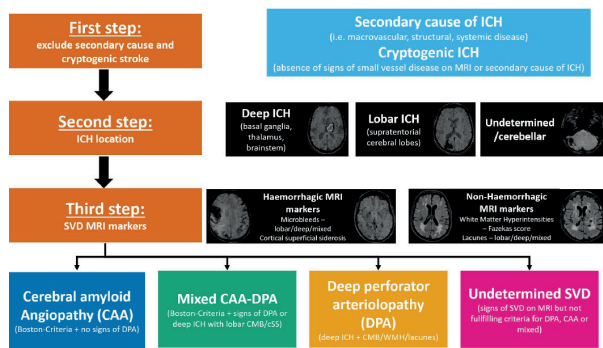
¹ Department of Neurology, Inselspital Bern University Hospital and University of Bern, Bern, Switzerland,

² University Institute for Diagnostic and Interventional Neuroradiology, Inselspital Bern University Hospital and University of Bern, Bern, Switzerland, ³ Service of Neurology, Department of Clinical Neurosciences, Lausanne University Hospital and University of Lausanne, Lausanne, Switzerland, ⁴ Department of Radiology, Cantonal Hospital, St. Gallen, Switzerland, ⁵ Stroke Unit and Division of Neurology, HFR Fribourg – Cantonal Hospital, Villars-sur-Glâne, Switzerland, ⁶ Stroke Center Hirslanden, Klinik Hirslanden Zurich, Zurich, Switzerland, ⁷ Stroke Research Group, Department of Clinical Neurosciences, University Hospital and Faculty of Medicine, Geneva, Switzerland, ⁸ Department of Radiology and Nuclear Medicine, Luzerner Kantonsspital, Luzern, Switzerland,

⁹ Stroke Center EOC, Neurocenter of Southern Switzerland, Lugano, Switzerland, ¹⁰ Stroke unit, GHOL, Hôpital de zone de Nyon, Nyon, Switzerland, ¹¹ Department of Neurology, University Hospital and University of Zurich, Switzerland, ¹² Department of Radiology and Nuclear Medicine, Kantonsspital Winterthur, Switzerland, ¹³ Department of Neurology, University Hospital Basel, Basel, Switzerland, ¹⁴ Department of Neurology, Kantonsspital Graubünden, Chur, Switzerland, ¹⁵ Diagnostic and Interventional Neuroradiology, Department of Radiology and Nuclear Medicine, University Hospital Basel, Basel, Switzerland, ¹⁶ Department of Neurology, Bueggerspital Solothurn, Solothurn, Switzerland, ¹⁷ 8 Departments of Neurology and Neurosurgery, Inselspital Bern University Hospital and University of Bern, Bern, Switzerland

Background and aims: We present a novel MRI-based small vessel disease (SVD)-phenotype classification of intracerebral haemorrhage (ICH) and investigate associations with outcomes.

Methods: We included all consecutive patients with non-traumatic, small vessel disease-related ICH from the multicenter, prospective Swiss Stroke Registry who underwent MRI. Patients were classified according to a novel MRI-based classification using haemorrhagic (microbleeds, cortical siderosis) and non-haemorrhagic (white matter hyperintensities, lacunes) markers and haematoma location as cerebral amyloid angiopathy (CAA), deep perforator arteriopathy (DPA), mixed SVD or undetermined SVD. Primary outcome was recurrent ICH or ischaemic strokes within 3 months.



MRI-based small vessel disease phenotypic classification: Flowchart

Results: We enrolled 858 patients (median age 73 years, IQR 62–79; 44.4% female, admission NIHSS 8). The distribution of MRI-phenotypes was 22.6% DPA (194 patients), 10.8% CAA (93 patients), 51.0% mixed SVD (438 patients) and 15.5% undetermined SVD (133 patients). During follow-up, 8.4% (58 patients) suffered ≥ 1 recurrent event (27 ischaemic strokes, 32 ICH). Rates of recurrent ICH and ischaemic stroke were 3.1%/3.1% respectively in patients with DPA, 3.9%/0% in CAA, 4.6%/6.1% in mixed SVD and 7.9%/1.0% in patients with undetermined SVD. After adjusting for confounders (incl. atrial fibrillation for ischaemic stroke and history of ICH for recurrent ICH), we did not observe a significant association of events with MRI phenotype.

Conclusion: This new MRI-based SVD-ICH phenotype classification is feasible and reproducible. Larger studies with longer follow-up are needed to determine distinct risk profiles for recurrent ICH and ischaemic stroke beyond established risk factors.

Disclosure: Dr. Goeldlin: Grants from Swiss Academy of Medical Sciences/Bangerter-Rhyner-Foundation (for the submitted work), Mittelbauvereinigung der Universität Bern and Pfizer congress grant (outside the submitted work).

OPR-040

Tranexamic Acid Administration for Patients with Aneurysmal Subarachnoid Hemorrhage

M. Diah Gabra¹, H.S. Ghaith², M. Ahmed Ebada³, O. Ezekiel Dada⁴, H. Al-Shami⁵, E.I. Bahbah⁶, U. Sidney Kanmounye⁷, I.N. Esene⁸, A. Negida⁹

¹ Faculty of medicine, South Valley University, Qena, Egypt,

² Faculty of Medicine, Al-Azhar University, Cairo, Egypt,

³ Faculty of Medicine, Zagazig University, Zagazig, Egypt,

⁴ College of Medicine, University of Ibadan, Ibadan,

Nigeria, ⁵ Department of Neurosurgery, National Bank Hospital, Nasr City, Egypt, ⁶ Faculty of Medicine, Al Azhar University, New Damietta, Egypt, ⁷ Research Department,

Association of Future African Neurosurgeons, Yaounde,

Cameroon, ⁸ Neurosurgery Division, Faculty of Health

Sciences, University of Bamenda, Bamili, Cameroon,

⁹ Global Neurosurgery Initiative, Harvard Medical School,

Boston, MA, United States of America

Background and aims: Antifibrinolytics as ϵ -aminocaproic acid and tranexamic acid (TXA), have been widely used for decades to reduce the risks of rebleeding. Here, we aim to synthesize evidence from published clinical trials on the efficacy and safety of the administration of tranexamic acid (TXA) in patients with aneurysmal subarachnoid hemorrhage (aSAH).

Methods: We followed the standard methods of Cochrane Handbook of Systematic Reviews for interventions and the PRISMA statement guidelines 2020 when conducting and reporting this study. A computer literature search of PubMed, Scopus, Web of Science, and Cochrane Central Register of Controlled Trials was conducted from inception until 1 January 2022. We selected observational studies and clinical trials comparing TXA versus no TXA in aSAH patients. Data of all outcomes were pooled as the risk ratio (RR) with the corresponding 95% confidence intervals in the meta-analysis models.

Results: 13 studies with a total of 2,991 patients were included in the analysis. TXA could significantly cut the risk of rebleeding (RR 0.56, 95% CI 0.44 to 0.72) and mortality from rebleeding (RR 0.60, 95% CI 0.39 to 0.92, $p=0.02$). However, TXA did not significantly improve the overall mortality, neurological outcome, delayed cerebral ischemia, or hydrocephalus (all $p>0.05$). In terms of safety, no significant adverse events were reported. No statistical heterogeneity or publication bias were found in all outcomes.

Conclusion: In patients with aSAH, TXA significantly reduces the incidence of rebleeding and mortality from rebleeding. However, current evidence does not support any benefits in overall mortality, neurological outcome, delayed cerebral ischemia, or hydrocephalus.

Disclosure: Nothing to disclose.

OPR-041

Inter-method reliability and validity of the modified Rankin Scale in patients with aneurysmal subarachnoid hemorrhage

E. Nobels-Janssen¹, E. Postma², I. Abma⁸, M. Van Dijk³, R. Haeren⁴, H. Schenck⁴, W. Moojen⁵, H. Den Hertog⁶, D. Nanda⁶, A. Potgieser³, B. Coert², W. Verhagen⁷, R. Bartels¹, P. Van der Wees⁸, D. Verbaan², J. Boogaarts¹
¹ Neurosurgery, Radboud University Medical Center, Nijmegen, The Netherlands, ² Neurosurgery, Amsterdam University Medical Center, Amsterdam, The Netherlands, ³ Neurosurgery, University Medical Center Groningen, Groningen, The Netherlands, ⁴ Neurosurgery, Maastricht University Medical Center, Maastricht, The Netherlands, ⁵ Neurosurgery, Medical Center Haaglanden, The Hague, The Netherlands, ⁶ Neurosurgery & Neurology, Isala Hospital, Zwolle, The Netherlands, ⁷ Neurology, Canisius Wilhelmina Hospital, Nijmegen, The Netherlands, ⁸ IQ healthcare, Radboud University Medical Center, Nijmegen, The Netherlands

Background and aims: The aims of this study are to assess: 1) inter-method reliability of different assessment methods of the mRS 2) convergent validity and 3) responsiveness of the mRS; and 4) the distribution of mRS scores across patient reported outcome measures (PROMs).

Methods: This is a prospective, randomized, multicenter study. Patients were seen by a physician who assigned an mRS score, followed depending on randomization by either the structured interview or the self-assessment. All patients completed different PROMs. Inter-method reliability was assessed with the quadratic weighted kappa score and percentage of agreement. Convergent validity and responsiveness were assessed by testing hypotheses.

Results: The quadratic weighted kappa was 0.60 between the assessment of the physician and structured interview and 0.56 between assessment of the physician and self-assessment. Percentage agreement was respectively 50.8% and 19.6%. The assessment of the mRS through a structured interview and self-assessment resulted in systematically higher mRS scores than by the physician. The correlation of the mRS with PROMs was moderate. Three out of four hypotheses for convergent validity were met. Improvement on GPE was indicated by 83% of patients; the mean change score on the mRS was -0.08 (SD 0.915). None of the hypotheses for responsiveness were met.

Conclusion: The mRS scores obtained with different assessment methods differ significantly. The agreement between the scores is low, although the reliability between the assessment methods is good. The mRS generally correlates with other instruments as expected, but it lacks responsiveness.

Disclosure: Nothing to disclose.

OPR-042

Clinical manifestations of deep perforator small vessel disease in intracerebral haemorrhages versus lacunar stroke

M. Goeldlin¹, J. Vynckier², M. Mueller¹, B. Siepen¹, A. Hakim³, J. Kaesmacher³, M. Jesse⁴, M. Mueller⁴, T. Meinel¹, M. Beyeler¹, L. Clénin⁵, B. Maamari⁵, J. Gralla³, W. Z'Graggen⁶, D. Bervini⁴, M. Arnold⁵, U. Fischer⁷, D. Seiffge⁵

¹ Department of Neurology, Inselspital Bern University Hospital and Graduate School for Health Sciences, University of Bern, Bern, Switzerland, ² Department of Neurology, Onze-Lieve-Vrouwziekenhuis Campus Aalst: Aalst, Oost-Vlaanderen, Belgium, ³ University Institute for Diagnostic and Interventional Neuroradiology, Inselspital Bern University Hospital and University of Bern, Bern, Switzerland, ⁴ Department of Neurosurgery, Inselspital Bern University Hospital and University of Bern, Bern, Switzerland, ⁵ Department of Neurology, Inselspital Bern University Hospital and University of Bern, Bern, Switzerland, ⁶ Departments of Neurology and Neurosurgery, Inselspital Bern University Hospital and University of Bern, Bern, Switzerland, ⁷ Department of Neurology, University Hospital Basel, Basel, Switzerland

Background and aims: Deep perforator arteriopathy is the leading etiology of intracerebral haemorrhage (ICH) and lacunar strokes (LS) located in deep, non-lobar brain regions. We compared clinical and MRI characteristics and outcomes in patients with deep ICH and LS.

Methods: We included patients with MRI-confirmed LS or ICH in the basal ganglia, thalamus, internal capsule or brainstem from the Bernese Stroke Registry (2013–2019). We assessed MRI markers of small vessel disease (SVD), calculating overall burden. Co-primary outcomes were modified Rankin Scale (mRS) and new ischaemic stroke or ICH at 3-months.

Results: We included 711 patients, 112 patients (15.8%) with deep ICH (mean age (SD) 65 (±15.1) years, 36.8% female) and 599 patients (84.2%) with LS (mean age (SD) 69.7 (±13.6) years, 39.9% female). Deep ICH was independently associated with higher SVD burden score (aOR 3.2, 95% CI 2.2–4.7). At 3 months, deep ICH was associated with higher mRS (ordinal shift: aOR 2.2, 95% CI 1.2–4.0). Risk of ischaemic strokes was numerically higher in deep ICH (8.6%) compared to LS (2.9%; p=0.046), but attenuated after adjustment for confounders (e.g. atrial fibrillation; aOR 2.9, 95% CI 0.96–8.7). Recurrent ICH within 3 months occurred in only two patients with ICH, but none with LS.

Conclusion: Deep perforator arteriopathy manifesting as ICH is less frequent but characterized by more severe disease burden on MRI and worse outcome compared to LS. The risk of subsequent ischaemic stroke seems at least as high in deep ICH as in LS, advocating for shared pathomechanisms with potential consequences for future secondary prevention strategies.

Disclosure: Disclosures Dr. Goeldlin: Grants from Swiss Academy of Medical Sciences/Bangerter-Rhyner-Foundation (for the submitted work), Mittelbauvereinigung der Universität Bern and Pfizer congress grant (outside the submitted work).

OPR-043

Cerebral white matter hyperintensities indicate severity and progression of coronary artery calcification

M. Kneihsl¹, R. Zweicker², E. Hofer¹, S. Fandler-Höfler¹, M. Haidegger¹, S. Perl², C. Enzinger¹, R. Schmidt¹, T. Gatteringer¹

¹ Department of Neurology, Medical University of Graz, Graz, Austria, ² Division of Cardiology, Department of Internal Medicine, Medical University of Graz, Graz, Austria

Background and aims: Cerebral white matter hyperintensities (WMH) are an important brain imaging feature of cerebral small vessel disease and have been associated with subclinical atherosclerosis including coronary artery calcification (CAC). However, previous studies on this association are limited by only cross-sectional analysis. We here aimed to explore the relationship between WMH and CAC in elderly individuals both cross-sectionally and longitudinally.

Methods: The study population consisted of elderly participants without stroke and dementia from the community-based Austrian Stroke Prevention Family Study (ASPS-Fam). Baseline and follow-up assessment comprised brain MRI, coronary artery computed tomography and clinical/laboratory examination of vascular risk factors. WMH load (via semi-automated volumetric assessment) and CAC levels (via the Agatston Score) were analyzed quantitatively at baseline and after a median follow-up period of 6 years.

Results: Of 331 study participants (mean age: 65.1±10.5 years; female: 59.8%), 105 underwent follow-up. Baseline WMH load (mean: 7.9±13.7cm³) correlated with baseline CAC levels (mean Agatston Score: 149±329) in univariable ($r=0.253$, $p=0.007$) and multivariable analysis (adjusted for age, sex and hypertension; $p<0.001$). While baseline CAC levels were not predictive for WMH progression (mean: 1.1±2.6cm³, $p>0.1$), baseline WMH load was associated with increase of CAC (mean: 149±289) during the follow-up period in multivariable analysis ($\beta=0.321$, $p<0.001$).

Conclusion: In this community-based cohort of elderly individuals, WMH were associated with CAC at baseline and predictive of its progression over a 6-year follow-up after adjustment for important co-variables.

Disclosure: Nothing to disclose.

Neuroimaging 1

OPR-044

Normative charts for brain volume development: Use and interpretation

J. Simarro ^{1,2}, T. Phan ¹, D. Sima ¹, T. Billiet ¹, E. Ortibus ^{2,3,4}

¹ Research and Development, icometrix, Leuven, Belgium, ² Department of Development and Regeneration, KU Leuven, Leuven, Belgium, ³ Centre For Developmental Disabilities, Leuven, Belgium, ⁴ Campus Pellenberg, Cerebral Palsy Reference Centre, University Hospital Leuven, Leuven, Belgium

Background and aims: Child growth standards (e.g. height, weight) defined by the World Health Organization are used worldwide. However, brain volume charts (i.e. quantitative models of brain development) are rarely used and occasionally misinterpreted as abnormal even though within normal limits. In this study, we investigate the reliability of percentiles provided by normative charts for pediatric MRI data and propose a suitable interpretation. **Methods:** In 2,114 healthy subjects aged 5 to 96, gray matter (GM) and white matter (WM) volumes scaled for head size were computed using the automatic software icobrain. Afterwards, volumetric percentile trajectories were modeled as a function of age. An independent multicenter test-retest pediatric MRI dataset composed of 211 subjects aged 6 to 20 was then employed to evaluate the reproducibility of percentiles on these normative brain volume charts.

Results: Percentile variability was higher for test-retest means close to the percentile 50 (see Figure 1). As most of the controls were distributed around this value, slight volumetric differences led to high differences in percentile values (see Figure 2). On the contrary, test-retest errors were smaller when the test-retest mean was below percentile 10 or above percentile 90, providing higher confidence about the atypical volumes.

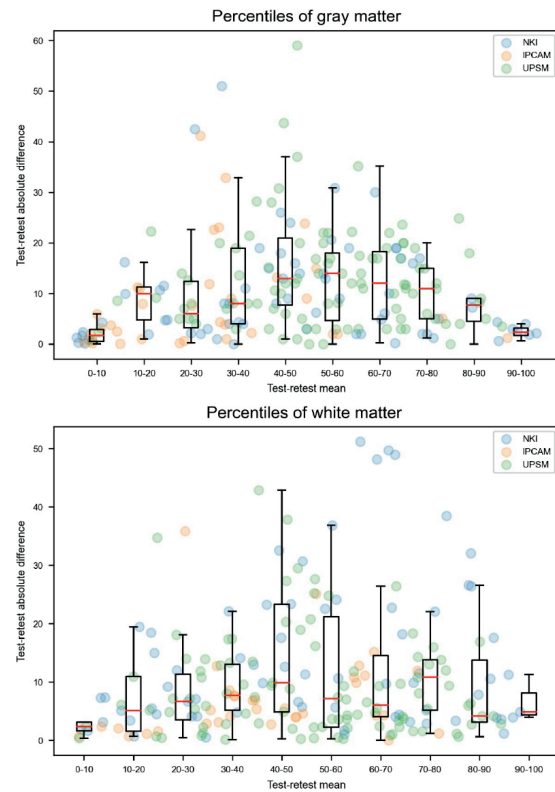


Fig 1: Absolute version of Bland-Altman plot of the test-retest percentiles of gray matter (top) and white matter (bottom). In these box plots, each independent dataset is color-coded.

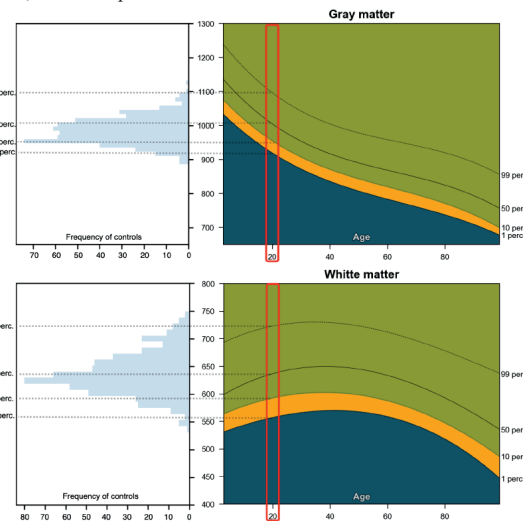


Fig 2: Control subjects distribution and quantitative models of brain development for gray matter (top) and white matter (bottom). The distribution represents the controls subjects used to compute the percentiles for 20 years old.

Conclusion: Given the high variability of percentiles close to the percentile 50, individual changes in a patient’s brain volume should be assessed as within or out of the normal range. In contrast, abnormal brain development can reliably be assessed by extreme percentiles.

Disclosure: This project has received funding from the European Union H2020-MSCA-ITN program (PARENT, 956394).

OPR-045

Brain age estimation by machine learning outperforms brain parenchymal fraction as imaging marker in multiple sclerosis

E. Høgestøl¹, T. Kaufmann², A. De Lange³, T. Moridi⁴, L. Stawiarz⁵, R. Ouellette⁶, B. Ineichen⁶, D. Beck⁷, D. Ferreira⁸, S. Muehlboeck⁸, S. Brune⁹, G. Nygaard¹⁰, P. Berg-Hansen¹⁰, M. Beyer¹⁰, P. Sowa¹¹, A. Manouchehrinia⁵, E. Westman¹³, T. Olsson⁵, E. Celius⁹, J. Hillert⁵, I. Kockum⁵, H. Harbo⁹, F. Piehl⁴, T. Granberg⁶, L. Westlye¹⁴

¹ Department of Psychology, University of Oslo, Institute of Clinical Medicine, University of Oslo, Department of Neurology, Oslo University Hospital, Oslo, Norway, ² NORMENT, Division of Mental Health and Addiction, Oslo University Hospital, Oslo, Norway. Tübingen Center for Mental Health, Department of Psychiatry and Psychotherapy, University of Tübingen, Tübingen, Germany, ³ Department of Psychology, University of Oslo, Oslo, Norway, LREN, Centre for Research in Neurosciences – Department of Clinical Neurosciences, CHUV and University of Lausanne, Lausanne, Switzerland. Department of Psychiatry, University of Oxford, Oxford, United Kingdom, ⁴ Department of Clinical Neuroscience, Karolinska Institutet, Stockholm, Sweden. Center of Neurology, Academic Specialist Center, Stockholm Health Services, Stockholm, Sweden, ⁵ Department of Clinical Neuroscience, Karolinska Institutet, Stockholm, Sweden, ⁶ Department of Clinical Neuroscience, Karolinska Institutet, Stockholm, Sweden, ⁷ Department of Psychology, University of Oslo, Oslo, Norway, NORMENT, Division of Mental Health and Addiction, Oslo University Hospital, Oslo, Norway. Department of Psychiatric Research, Diakonhjemmet Hospital, Oslo, Norway, ⁸ Division of Clinical Geriatrics, Department of Neurobiology, Care Sciences and Society, Karolinska Institutet, Stockholm, Sweden, ⁹ Institute of Clinical Medicine, University of Oslo, Oslo, Norway; Department of Neurology, Oslo University Hospital, Oslo, Norway, ¹⁰ Department of Neurology, Oslo University Hospital, Oslo, Norway, ¹¹ Division of Radiology and Nuclear Medicine, Oslo University Hospital, Oslo, Norway, ¹³ Division of Clinical Geriatrics, Department of Neurobiology, Care Sciences and Society, Karolinska Institutet, Stockholm, Sweden. Department of Neuroimaging, King's College London, London, United Kingdom, ¹⁴ Department of Psychology, University of Oslo, Oslo, Norway. Institute of Clinical Medicine, University of Oslo, Oslo, Norway. K.G. Jebsen Center for Neurodevelopmental disorders, University of Oslo, Oslo, Norway

Background and aims: The brain age paradigm applies patterns of normal aging from large brain imaging data repositories, allowing us to estimate an individual's brain age. Our objectives were to apply an established brain age estimation model on longitudinal brain magnetic resonance imaging (MRI) data from people with multiple sclerosis (pwMS) and healthy controls (HC) and to compare clinical and demographic associations with brain age and brain parenchymal fraction (BPF).

Methods: PwMS (n=1.515, mean age 38.9 years) and HC (n=876, mean age 45.9 years) were included from Oslo and Karolinska University Hospitals. Structural 3D T1-weighted MRI data were processed using a harmonized pipeline to extract 1.118 cerebellar, cortical and subcortical features per subject. We estimated brain age using our published training set (n=35,474, age 3–89 years), residualizing for age, age², sex and scanner. We used linear mixed models to test for clinical and demographic associations with brain age and BPF, respectively.

Results: The average estimated brain age of pwMS was 6.5 years older than HC (CI=5.4–7.5, p=2.6x10⁻³⁴). PwMS had an accelerated annual increase in brain age of 22% (CI=0.15–0.29, p=8.0x10⁻¹¹), not evident for HC. Brain age performed better than BPF for clinical associations (expanded disability status scale; t=4.5, p=7.0x10⁻⁶ vs. t=2.6, p=0.01 and disease duration; t=4.3, p=2.5x10⁻⁵ vs. t=1.8, p=0.07).

Table 1 Overview of the demographic and clinical features of the multiple sclerosis cohort at the first scan

	All	Karolinska	Oslo
(a) Demographic characteristics			
n	1515	1187	328
Female, % (n)	72 % (1098)	73 % (861)	72 % (237)
Age, mean years (SD, range)	38.9 (11.6, 11-75)	39.0 (11.9, 11-75)	38.7 (10.3, 18-49)
Disease duration, mean years (SD, range)	5.6 (7.2, 0-50.4)	5.7 (7.4, 0-50.4)	5.1 (6.5, 0-36.9)
Total scans, n	4983	3838	746
Follow-up, % (n)	72 (1007)	77 (912)	53 (175)
Follow-up time, mean years (SD, range)	3.6 (3.8, 0-14.3)	4.1 (3.9, 0-14.3)	1.7 (2.2, 0-7.0)
(b) Clinical evaluation			
Multiple sclerosis classification			
RRMS % (n)	78 (1180)	73 (869)	95 (311)
SPMS % (n)	8 (123)	10 (113)	3 (10)
PPMS % (n)	5 (68)	5 (62)	2 (6)
PPMS with activity % (n)	1 (16)	1 (10)	0 (0)
Unknown % (n)	8 (128)	11 (127)	0 (0)
Neurological disability			
Baseline EDSS, median (SD, interquartile range, n)	2.0 (1.4, 1.0-3.0, n=1399)	2.0 (1.7, 1.0-3.0, n=881)	2.0 (1.3, 1.0-2.5, n=338)
Most recent EDSS, median (SD, interquartile range, n)	2.0 (1.8, 1.0-3.5, n=1252)	2.0 (1.9, 1.0-3.5, n=881)	2.0 (1.4, 1.0-2.5, n=328)

Abbreviations: EDSS, expanded disability status scale; MS, multiple sclerosis; PPMS, primary-progressive MS; RRMS, relapsing-remitting MS; SD, standard deviation; SPMS, secondary-progressive MS

Table 1. Overview of the demographic and clinical features of the multiple sclerosis cohort at the first scan

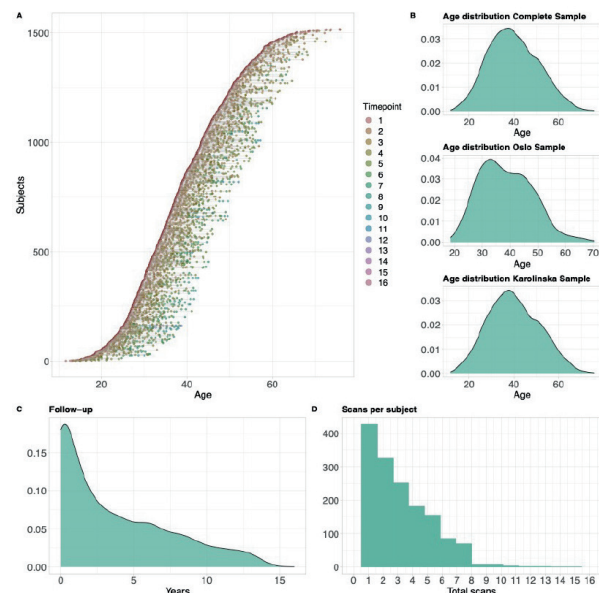


Figure 1 An overview of the multiple sclerosis cohort. Visualized in A we depicted every multiple sclerosis subject in ascending order based on age at the first scan, with chronological age on the x-axis, and the follow-up period as an individual horizontal line. The colour of the circles indicates the number of total MRI scans included for that specific subject. In B the chronological age distribution of the complete sample is shown in the top figure, while the samples from Oslo and Karolinska are shown below. In C we show the distribution of the follow-up time between the first and the last MRI scan across the multiple sclerosis sample with proportion on the x-axis, while in D we list the maximum number of scans per subject with number of patients on the x-axis.

Figure 1. An overview of the multiple sclerosis cohort.

Conclusion: In our large-scale study, pwMS displayed older brain age and accelerated brain aging compared to HC. The brain age paradigm outperformed standard BPF analyses in terms of mapping clinical associations and can potentially serve as an individual global imaging marker of neurodegeneration in MS.

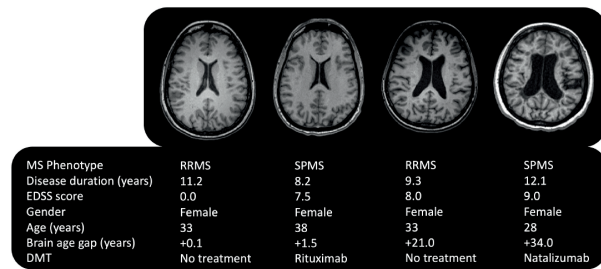


Figure 2 A visualization of four people with multiple sclerosis. All people in the same age group, but with different disability, brain age, treatment, and disease duration.

Disclosure: EAH, SB, PBH, MKB, PS, AM, TO, EGC, JH, HFH, FP and TG received honoraria from different pharmaceutical companies and grants. All other authors report no relevant disclosures.

OPR-046

The subcortical and neurochemical organisation of the ventral and dorsal attention networks

P. Alves¹, M. Thiebaut de Schotten²

¹ Department of Neurosciences and Mental Health, Neurology, Hospital de Santa Maria, CHULN, Lisbon, Portugal, ² Brain Connectivity and Behaviour Laboratory, Sorbonne University, Paris, France

Background and aims: The cortical mapping of attentional systems identified two segregated networks that mediate stimulus-driven and goal-driven processes, the Ventral and the Dorsal Attention Networks. Deep brain electrophysiological recordings, behavioural data from phylogenetic distant species and observations from human brain pathologies suggest that purely corticocentric models might not fully express the neural background of attention. Here, we aimed to map the subcortical architecture of attention networks, using advanced methods of functional alignment applied to resting-state functional connectivity.

Methods: First, we seeded functional network maps of the Ventral and the Dorsal Attention Networks from 110 7T resting-state functional MRIs. Network maps were functionally aligned in a functional space through iterative diffeomorphic transformations. Then, we examined the structural, functional and graph centrality properties of the identified subcortical structures. Finally, we computed the spatial correlation between the projections of the brainstem nuclei and the distribution maps of the neurotransmitter systems.

Results: Functionally aligned maps of both networks overlapped the pulvinar, the superior colliculi, the head of caudate nuclei, and a cluster of brainstem nuclei (Fig. 1). Structurally, these nuclei were densely connected network hubs, integrating projection fibers, namely fronto-pulvinar, parieto-pulvinar and tecto-pulvinar tracts. The structural projections of the brainstem nuclei were spatially correlated with the distribution of the nicotinic acetylcholine receptors and the dopamine transporters (Fig. 2).

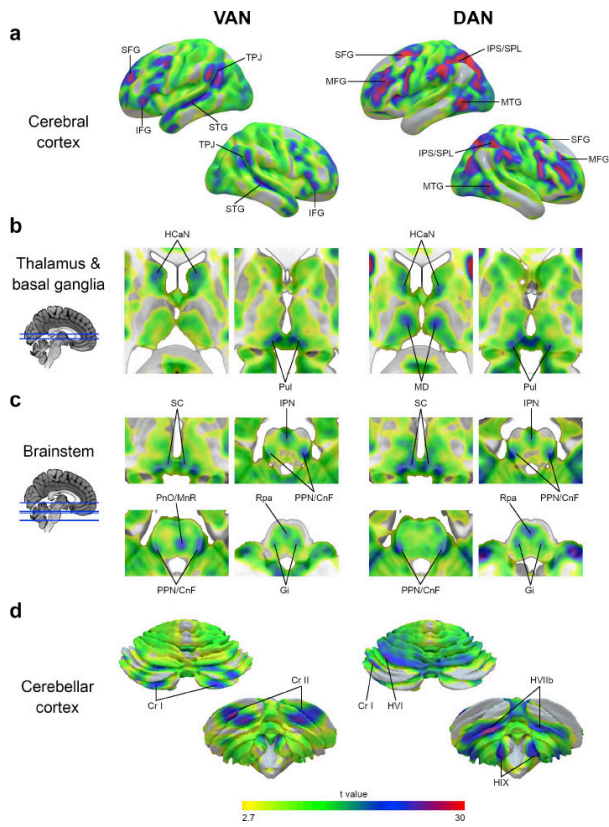


Figure 1: VAN (left) and DAN (right) maps after functional alignment, at different anatomical levels, namely cerebral cortical surface (a), thalamus and basal ganglia (b), brainstem (c) and cerebellar cortical surface (d).

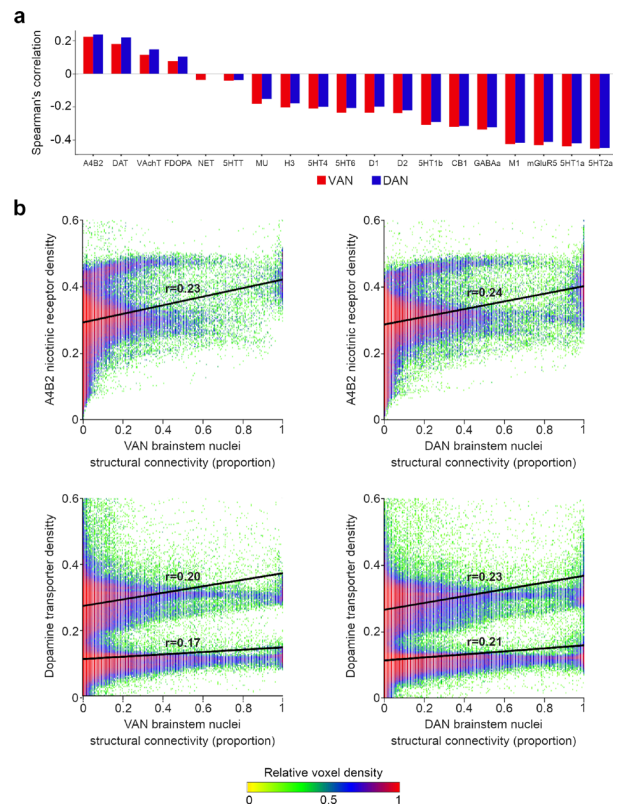


Figure 2: Correlation between the structural projections of the brainstem nuclei and the neurotransmitter systems. (a) Spearman's correlation with the maps of receptors and transporters; (b) Graphical representation of the highest correlations.

Conclusion: The convergence of functional, structural and neurochemical evidence provides a novel framework to comprehensively understand the neural basis of attention across different species and the pathophysiology of attention disorders that may arise from lesions of deep brain nuclei, such as subcortical neglect.

Disclosure: Nothing to disclose.

OPR-047

Brain network centrality abnormalities associated with multiple sclerosis disease course

A. Carotenuto¹, P. Valsasina¹, M. Schoonheim², J. Geurts², F. Barkhof³, A. Gallo⁴, G. Tedeschi⁴, N. Petsas⁵, P. Pantano⁵, M. Filippi⁶, M. Rocca⁶

¹ Neuroimaging Research Unit, Division of Neuroscience, IRCCS San Raffaele Scientific Institute, Milan, Italy,

² Department of Anatomy and Neurosciences, MS Center Amsterdam, Amsterdam Neuroscience, Amsterdam UMC, Vrije Universiteit Amsterdam, Amsterdam, The Netherlands,

³ Radiology and Nuclear Medicine, MS Center Amsterdam, Amsterdam Neuroscience, Amsterdam UMC, Vrije Universiteit Amsterdam, Amsterdam, The Netherlands,

⁴ Division of Neurology and 3T MRI Research Center, Department of Advanced Medical and Surgical Sciences, University of Campania "Luigi Vanvitelli", Naples, Italy,

⁵ Department of Human Neurosciences, Sapienza University, Rome, Italy; and Department of Radiology, IRCCS

NEUROMED, Pozzilli, Italy, ⁶ Neuroimaging Research Unit, Division of Neuroscience, and Neurology Unit, IRCCS San Raffaele Scientific Institute, and Vita-Salute San Raffaele University, Milan, Italy

Background and aims: Voxel-wise degree centrality (DC) captures brain network topography from resting-state functional MRI (RS fMRI). We aimed at assessing DC abnormalities in multiple sclerosis (MS) patients and to evaluate their association with disease course.

Methods: 971 MS patients (47 clinically isolated syndrome [CIS]; 704 relapsing-remitting MS [RRMS]; 145 secondary progressive MS [SPMS] and 75 primary progressive MS [PPMS]) and 330 healthy controls (HCs) performed RS fMRI and clinical assessment. SPM12 age-, sex-, centre- and gray matter volume adjusted ANOVA and multivariable regressions were employed. All p were <0.05 family wise error corrected.

Results: MS patients showed reduced DC in the bilateral insula and somatosensory areas and increased DC in the bilateral precuneus and middle occipital gyri vs HCs. These DC abnormalities were mostly observed in RRMS and SPMS. We reported on increased DC in frontal and temporal regions in RRMS vs CIS, which became more widespread in PPMS vs CIS and also involved the precuneus and the hippocampus in SPMS vs RRMS patients. Cognitively impaired patients showed reduced DC in somatosensory areas and increased DC in the default mode network (DMN) vs both HCs and cognitively preserved patients. Finally, in MS, more severe disability correlated with increased DC in the right precuneus.

Conclusion: MS patients showed progressive DC reduction in the salience and primary sensory networks and a DC increase in the DMN over the disease course mirroring disability accrual. MS pathology may produce a sensorimotor network collapse, with a possible attempt of the DMN to counteract for this damage.

Disclosure: Antonio Carotenuto was supported by a MAGNIMS/ECTRIMS research fellowship.

Headache

OPR-048

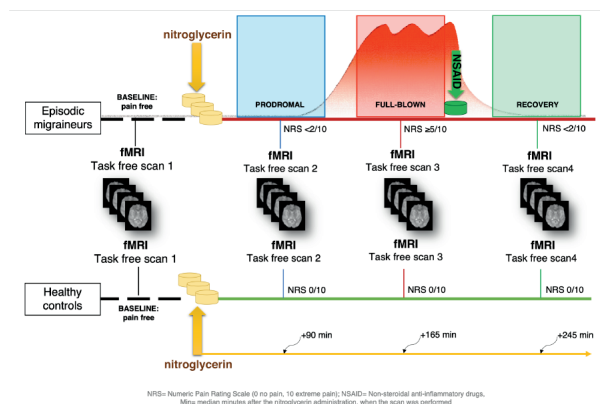
Resting state fMRI to assess the Pain Connectome integrity during nitroglycerin-induced migraine attacks

D. Martinelli ¹, G. Castellazzi ², M. Pocora ¹, R. De Icco ¹, A. Bacila ³, M. Allena ⁴, E. Guaschino ⁴, G. Sances ⁴, A. Pichiecchio ⁵, C. Tassorelli ¹

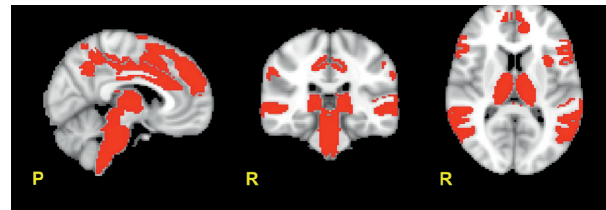
¹ Headache Science and Rehabilitation Center, IRCCS C. Mondino Foundation, Pavia, Italy/ Department of Brain and Behavioural Sciences, University of Pavia, Pavia, Italy, ² Headache Science and Rehabilitation Center, IRCCS C. Mondino Foundation, Pavia, Italy/ NMR Research Unit, Queen Square MS Centre, Department of Neuroinflammation, UCL Queen Square Institute of Neurology, Faculty of Brain Sciences, London, United Kingdom, Department, ³ Neuroradiology Unit, IRCCS C. Mondino Foundation, Pavia, Italy, ⁴ Headache Science and Rehabilitation Center, IRCCS C. Mondino Foundation, Pavia, Italy, ⁵ Neuroradiology Unit, IRCCS C. Mondino Foundation, Pavia, Italy / Department of Brain and Behavioural Sciences, University of Pavia, Pavia, Italy

Background and aims: Resting state functional MRI (rs-fMRI) has been widely used to study the brain functional connectivity (FC) changes occurring in migraine, to better understand the underlying cyclical mechanisms. In this pilot study, we focused on the pain connectome (PC) and we used rs-fMRI to address its functional integrity during a nitroglycerin-induced migraine-like attack.

Methods: Ten episodic migraineurs (EM, 4 female, 29.4 yo, 4 MMD) underwent 3T MRI examination consisting in four rs-fMRI repetitions during the subsequent phases of a nitroglycerin-induced migraine attack (baseline, prodrome, full-blown attack, recovery, Fig.1). Nine healthy controls (HC, 3 female, 26.7 yo) were enrolled for reference. Subjects' scans were processed to identify the PC (Fig. 2). A non-parametric permutation test was run to detect significant FC changes inside PC between EM and HC subjects in the different attack phases.

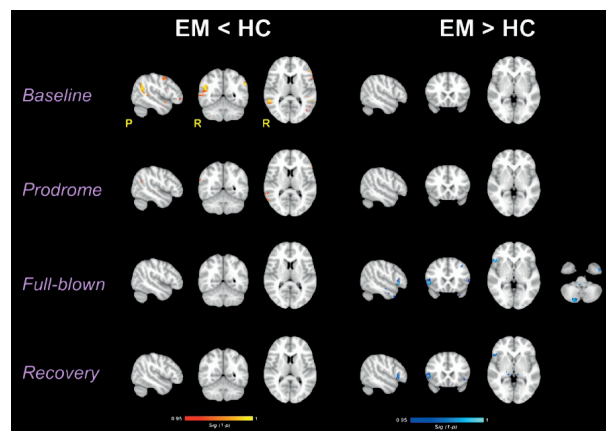


All subjects underwent four rs-fMRI scans temporally-matched with a nitroglycerin-induced migraine attack: pain-free baseline, prodromal, full-blown attack, recovery. None of the HCs developed a migraine attack following the nitroglycerin challenge.



Brain areas of the pain connectome (PC) used for the present study. The PC mainly includes: inferior, middle and superior Frontal gyri, bilateral insula, inferior, middle and superior Temporal gyri, precuneus, bilateral thalami, pons and posterior cerebellum.

Results: At baseline EM subjects showed a significantly reduced FC within PC in right temporal lobe and superior frontal gyrus when compared to HCs. This difference was progressively lost during the full-blown phase and the recovery. During the full-blown phase, EM subjects showed increased FC in prefrontal cortex and cerebellar crus of the PC, which persisted over the recovery (Fig. 3).



Altered areas of FC within the pain connectome in EM subjects compared to HCs. On the left: in red-yellow, areas of reduced FC in EM vs HC (EM < HC). On the right: in blue-light blue, areas of increased FC in EM (EM > HC).

Conclusion: The findings observed suggest a baseline alteration in descending modulation pain processing in migraine. Migraine-like pain induction caused a profound PC alteration, which persisted over recovery. Our findings also point to the involvement of the cerebellum - a multiple effector system integrator and a ruler of pain perception modulation - possibly in the resolution of pain.

Disclosure: RDI has received speaker honoraria for oral presentations from Eli-Lilly. CT has received fees for advisory boards or scientific lecturing from Allergan/AbbVie, Eli Lilly, Lundbeck, Novartis, and TEVA; and institutional payments for clinical trials from Allergan/AbbVie, Eli Lilly, Novartis Lundbeck, and TEVA. SG received honoraria for the participation in advisory board or for oral presentation from: Eli-Lilly and Novartis. MA SG received honoraria for the participation in advisory board or for oral presentation from: Eli-Lilly and Teva. All other Authors have no conflicts of interest to declare.

OPR-049

CGRP plasma levels in migraine patients before and after CGRP monoclonal antibodies therapy

N. Vashchenko¹, A. Uzhakhov², M. Bogorodskaya³,
D. Korobkova², J. Azimova², K. Skorobogatykh²

¹ Sechenov University, Moscow, Russian Federation,

² University Headache Clinic, Moscow, Russian Federation,

³ Research Clinical Centre for Neuropsychiatry, Moscow, Russian Federation

Background and aims: Monoclonal antibodies against calcitonin gene-related peptide (CGRP) or its receptor are the first targeted preventive migraine treatment. Erenumab - one of these medications - is well studied in clinical trials; however, the data on its use in real-world practice are still insufficient. To date, there is no knowledge of whether it has any effect on plasma CGRP levels.

Methods: We included 58 patients (50 women, average age 44,6±11,4) with migraine on the preventive therapy with CGRP monoclonal antibody erenumab. We evaluated previous prophylactic medications, headache days per month, adverse events. To assess CGRP levels, we obtained blood samples from the antecubital vein outside a migraine attack before and after 6 months of therapy. CGRP levels were measured by enzyme-linked immunosorbent assay (ELISA).

Results: 49 patients had chronic migraine, 15 patients had resistant migraine and 2 patients – refractory migraine. During the study, two patients dropped out due to adverse events (constipation). 42 patients continued taking erenumab 70 mg for at least six months. The average number of headache days per month before treatment was 21.6, decreasing to 6.8 after therapy. In the preliminary analysis, we assessed plasma samples from 18 patients. Before treatment, the mean plasma CGRP level was 23.1±26.5 pg/ml and 59.1±29.6 pg/ml after treatment. Thus, plasma CGRP level in peripheral blood after 6 months of therapy with erenumab increased on average more than twice the baseline level.

Conclusion: CGRP levels increase significantly after the therapy. Further studies with more participants are needed to confirm these data.

Disclosure: Nothing to disclose.

OPR-050

Late response to anti-CGRP (calcitonin gene-related peptide) monoclonal antibodies: implication for clinical practice

C. Aurilia¹, G. Egeo¹, G. Fiorentini¹, S. Cevoli²,
R. Messina³, A. Salerno⁴, P. Torelli⁵, M. Albanese⁶,
A. Carnevale⁷, F. Bono⁸, D. D'Amico⁹, C. Altamura¹⁰,
B. Colombo³, F. Frediani¹¹, B. Mercuri⁴, F. D'Onofrio¹²,
L. Grazzi⁹, M. Aguggia¹³, C. Finocchi¹⁴, P. Di Fiore¹¹,
M. Zucco¹⁵, M. Trimboli¹⁶, S. Bonassi¹⁷, F. Vernieri¹⁰,
P. Barbanti¹

¹ Headache and Pain Unit, IRCCS San Raffaele Roma, Rome, Italy, ² IRCCS - Institute of Neurological Sciences – Bologna, Bologna, Italy, ³ Neurology Unit, Neurorehabilitation Unit, and Neurophysiology Unit, Vita-Salute San Raffaele University and San Raffaele Scientific Institute, Milan, Italy, ⁴ San Giovanni Addolorata Hospital, Rome, Italy, ⁵ Unit of Neurology, Department of Medicine and Surgery, Headache Center, University of Parma, Parma, Italy, ⁶ Neurology Unit, Headache Center, University Hospital of Rome “Tor Vergata”, Rome, Italy, ⁷ San Filippo Neri Hospital, Rome, Italy, ⁸ Center for Headache and Intracranial Pressure Disorders, Neurology Unit, A.O.U. Mater Domini, Catanzaro, Italy, ⁹ Neurology Unit, Headache Center Fondazione IRCCS Istituto Neurologico “Carlo Besta”, Milan, Italy, ¹⁰ Headache and Neurosonology Unit Policlinico Universitario Campus Bio-Medico, Rome, Italy, ¹¹ UOC Neurologia and Stroke Unit, Headache Center - ASST Santi Paolo Carlo – Milan, Italy ¹ ² Headache Center, AOSG Moscati, Avellino, Italy, ¹³ Cardinal Massaia Hospital, Headache Center, Asti, Italy, ¹⁴ IRCCS Ospedale Policlinico San Martino, Headache Center, Genova, Italy, ¹⁵ San Camillo Hospital, Headache Center, Rome, Italy ¹⁶ Institute of Neurology, Department of Medical and Surgical Sciences, University Magna Graecia of Catanzaro, Italy, ¹⁷ Clinical and Molecular Epidemiology, Department of Human Sciences and Quality of Life Promotion IRCCS San Raffaele Roma, Rome, Italy

Background and aims: Monoclonal antibodies (mAbs) targeting the Calcitonin Gene-Related Peptide (CGRP) are characterized by an early onset of efficacy, but late response (>12 weeks) may occur in some patients. Aims: To assess the prevalence of late responders (≥50% response after >12 weeks) to antiCGRP mAbs in patients affected by high-frequency episodic (HFEM: 8-14 days/month) or chronic migraine (CM).

Methods: In this multicenter (n=16), cohort, real life study, we evaluated the ≥50% response rate in all consecutive patients affected HFEM or CM treated with erenumab, galcanezumab or fremanezumab for ≥12 months from 20/12/2018 to 01/12/2021. Primary endpoint was the proportion of late-responders (≥50% response >12 weeks); the secondary endpoint was the estimation of median week of response in these patients.

Results: 912 migraine patients (HFEM/CM: 222/690) were treated with mAbs (erenumab: 789 pts; fremanezumab: 65 pts; galcanezumab: 58 pts) for at least 12 months. Overall, 352 patients (38.6%) were non-responders at week 12 (erenumab: 344, 43.6%; fremanezumab: 14, 21.5%; galcanezumab: 14, 24.1%). Among non-responders, 128 patients (36.4%) were indeed late responders (erenumab: 114, 33.1%; fremanezumab: 5, 35.7%; galcanezumab: 9, 64.2%), showing on average a $\geq 50\%$ response after median 20 (IQR 4–24) weeks of treatment (erenumab median weeks: 20, IQR 16–24; fremanezumab: 16, IQR 16–24; galcanezumab: 20, IQR 16–21).

Conclusion: Late response to antiCGRP mAbs may occur in more than one third of migraine patients considered not responders at 12 weeks. Our findings suggest extending the efficacy treatment evaluation for antiCGRP mAbs to 6 months, also in terms of reimbursement policies.

Disclosure: Nothing to disclose.

OPR-051

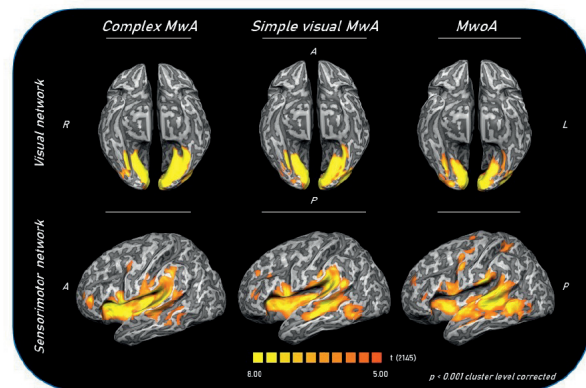
Functional connectivity changes in complex migraine aura: beyond the visual network

A. Russo, M. Silvestro, A. Tessitore,
F. Scotto di Clemente, F. Esposito, G. Tedeschi
*Department of Advanced Medical and Surgical Sciences,
University of Campania “Luigi Vanvitelli”, Caserta, Italy*

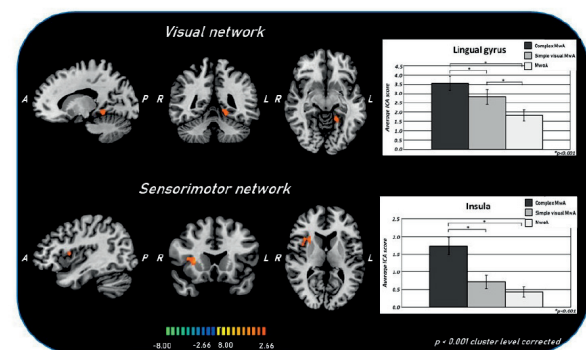
Background and aims: Although the majority of migraine with aura (MwA) patients experiences simple visual aura, a discrete percentage also reports somatosensory, dysphasic or motor symptoms (the so-called complex auras). The wide aura clinical spectrum led to investigate whether the heterogeneity of aura phenomenon could be subtended by different neural correlates, suggesting an increased visual cortical excitability in complex MwA. We aimed to explore whether complex MwA patients are characterized by more pronounced connectivity changes of the visual network and whether functional abnormalities may extend beyond the visual network encompassing also the sensorimotor network in complex MwA patients when compared to simple visual MwA patients.

Methods: By using a resting state-fMRI approach, we compared the resting state functional connectivity (RS-Fc) of both visual and sensorimotor networks in 20 complex MwA patients in comparison with 20 simple visual MwA patients and 20 migraine without aura (MwoA) patients.

Results: Complex MwA patients showed a significantly higher RS-Fc of the left lingual gyrus, within the visual network, and of the right anterior insula, within the sensorimotor network, when compared to both simple visual MwA and MwoA patients ($p < 0.001$). The abnormal right anterior insula RS-Fc was able to discriminate complex MwA patients from simple aura MwA patients as demonstrated by logistic regression analysis (AUC: 0.83).



Group-level (main effects) functional connectivity of visual and sensorimotor networks in complex MwA, simple visual MwA and MwoA patients



T-map of statistically significant differences within the visual and sensorimotor networks between complex MwA and simple visual MwA

Conclusion: Our findings suggest that higher extrastriate RS-Fc might promote the CSD onset representing the neural correlate of simple visual aura that can propagate to sensorimotor regions, if an increased insula RS-Fc coexists, leading to complex aura phenotypes.

Disclosure: Nothing to disclose.

Motor neurone diseases

OPR-052

Electrodiagnostic Findings in Facial Onset Sensory Motor Neuronopathy (FOSMN)

H. Oliveira¹, M. Silsby², S. Jaiser¹, M. Lai³, N. Pavey², M. Kiernan², T. Williams⁴, S. Vucic², M. Baker¹
¹ Institute of Translational and Clinical Research, University of Newcastle, Newcastle upon Tyne, United Kingdom,
² Brain and Nerve Research Centre, Concord Clinical School, Sydney Medical School, The University of Sydney, Sydney, Australia, ³ Department of Neurophysiology, Royal Victoria Infirmary, Newcastle upon Tyne, United Kingdom,
⁴ Department of Neurology, Royal Victoria Infirmary, Newcastle upon Tyne, United Kingdom

Background and aims: FOSMN is a rare clinical syndrome initially described in a seminal case series of five patients who presented with facial sensory deficits, followed by motor deficits, evolving rostro-caudally. Clinical, genetic and neuropathological data strongly suggest that FOSMN is a rare phenotype of amyotrophic lateral sclerosis (ALS). Herein, we review the published electrodiagnostic data for FOSMN and report detailed electrophysiological data from two cohorts (n=10) with this syndrome, proposing a specific approach to electrodiagnostic testing in patients who present with facial sensory symptoms.

Methods: Blink Reflexes, Electromyography, Nerve Conduction Studies, Somatosensory Evoked Potentials, Threshold Tracking Transcranial Magnetic Stimulation.

Results: Findings on standard electrophysiological assessment were in broad agreement with those published: blink reflexes were abnormal in all but one patient (Figure 1); SNAPs were reduced but CMAPs preserved; mixed acute and chronic neurogenic change was identified on needle EMG in bulbar and cervicothoracic muscles in approximately 50% of patients. In addition, upper limb SEP central conduction times were increased (n=4) and progressed on repeat testing (n=3) (Figure 2), and upper motor neuron dysfunction was revealed by several measures [ipsilateral MEPs (n=1); reduced short interval intra-cortical inhibition on threshold-tracking TMS (n=2); absent beta-band intermuscular coherence (n=3)].

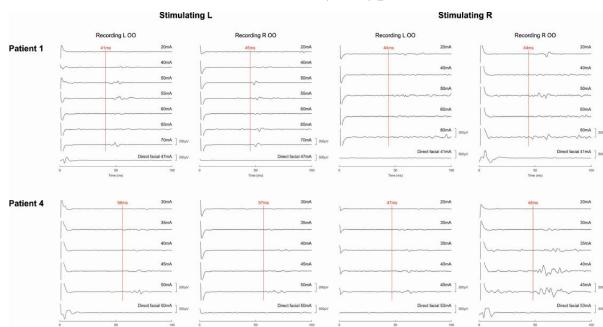


Figure 1. Blink reflexes. Illustrative examples of blink reflex responses acquired from patients 1 and 4. Responses were recorded from left (L) and right (R) orbicularis oculi (OO) following stimulation of the supraorbital nerve at a range of intensities.

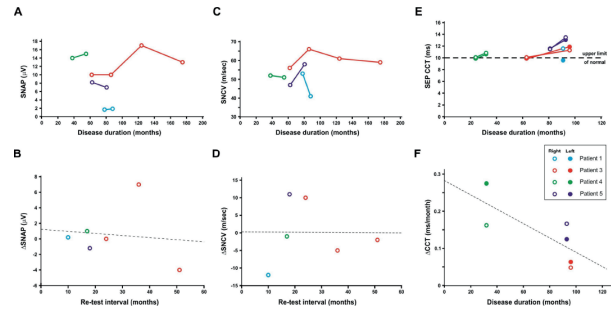


Figure 2. Changes in SNAP amplitudes, SNCVs and upper limb SEPs. In a subset of FOSMN patients (n=4) nerve conduction studies were repeated more than once. Only median digit III SNAP/SNCV data are presented (NB. There was no evidence of carpal tunnel syndrome).

Electrodiagnostic findings in FOSMN

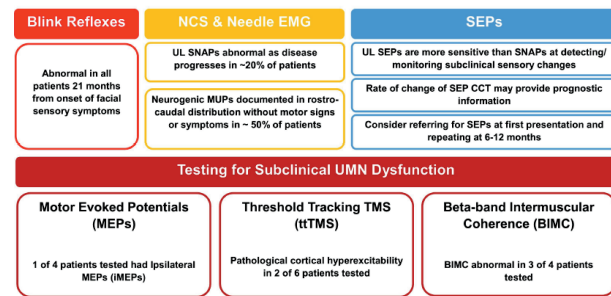


Figure 3. Summary of electrodiagnostic findings in FOSMN. The neurophysiological examination is useful in identifying pathognomonic signs of FOSMN such as abnormal blink reflexes, in addition to identifying subclinical lower and upper motor neurons.

Conclusion: Electrodiagnostic investigation of FOSMN should include blink reflex testing, SEPs and tests of upper motor neuron function (Figure 3). The combination of progressive lower motor neuron disease and upper motor neuron disease on neurophysiological investigation provides further support for the contention that FOSMN is a rare phenotypic variant of ALS.

Disclosure: Nothing to disclose.

OPR-053

Directionality of disease spread is associated with clinical phenotype in amyotrophic lateral sclerosis

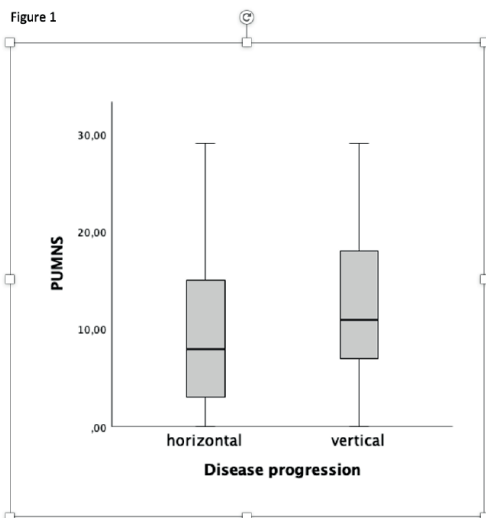
A. Maranzano¹, E. Colombo¹, B. Poletti¹, S. Torre¹, F. Verde², C. Morelli¹, V. Silani², N. Ticozzi²

¹ Department of Neurology, Istituto Auxologico Italiano IRCCS, Milan, Italy, ² Department of Pathophysiology and Transplantation, "Dino Ferrari" Center, Università degli Studi di Milano, Milan, Italy

Background and aims: increasing evidence shows that disease spread in amyotrophic lateral sclerosis (ALS) follows a preferential pattern rather than a random model with more frequent involvement of contiguous regions from the site of symptoms onset. Aim of our study is to assess if specific pattern of disease progression may influence the clinical phenotype.

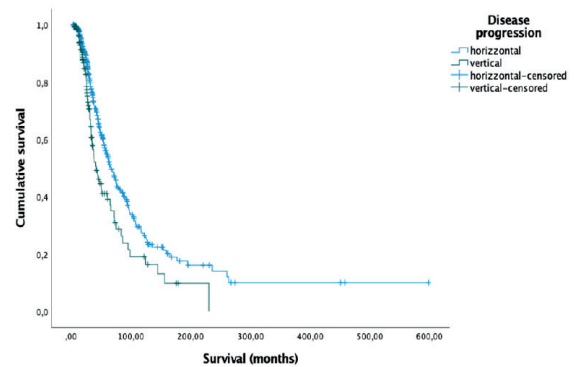
Methods: A single center retrospective cohort of 854 Italian ALS patients has been evaluated to assess correlations between directionality of the disease process after symptoms onset and motor/neuropsychological phenotype. Order of affected regions was established from medical history. Penn Upper Motor Neuron Score (PUMNS) and MRC scale for muscle strength were used to assess motor phenotype. The Italian version of the Edinburgh Cognitive and Behavioural ALS Screen (ECAS) was administered to evaluate cognitive and behavioural profiles.

Results: The most frequent directionality of initial spread included adjacent horizontal regions (41%) and it was observed in patients with lower MRC ($p=0.049$) while vertical diffusion (17%) was associated with higher PUMNS ($p<0.0001$) and with reduced survival ($p=0.001$). Noncontiguous disease spread was more frequently observed in older individuals with the same motor profile of patients with vertical diffusion and with impairment of ALS specific and non-specific domains at ECAS.



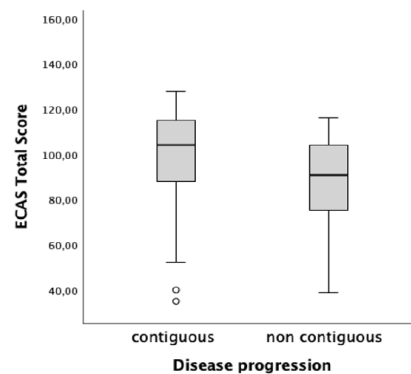
Distribution of UMN involvement using the Penn Upper Motor Neuron Score (PUMNS) in ALS patients with horizontal and vertical disease spread. Kruskal-Wallis test for independent samples.

Figure 2



Kaplan-Meier plots of survival probabilities: patients with horizontal disease progression (green line) had significantly prolonged survival when compared to patients with vertical spread (light blue line) (Log Rank: $\chi^2=10,438$; $p=0,001$)

Figure 3



Distribution of ECAS Total score in ALS patients with contiguous and noncontiguous disease spread. Kruskal-Wallis test for independent samples.

Conclusion: our study supports the hypothesis of a preferential pattern of disease spread according to prevalent involvement of upper or lower motor neuron. Furthermore, our results indicate that disease extension from site of onset may influence the clinical phenotype.

Disclosure: Nothing to disclose.

OPR-054

Motor, cognitive and behavioral features of C9ORF72-associated amyotrophic lateral sclerosis

E. Colombo ¹, B. Poletti ¹, A. Maranzano ¹, S. Torre ¹, F. Verde ², F. Solca ¹, R. Bonetti ¹, L. Carelli ¹, C. Morelli ¹, A. Ratti ³, V. Silani ², N. Ticozzi ²

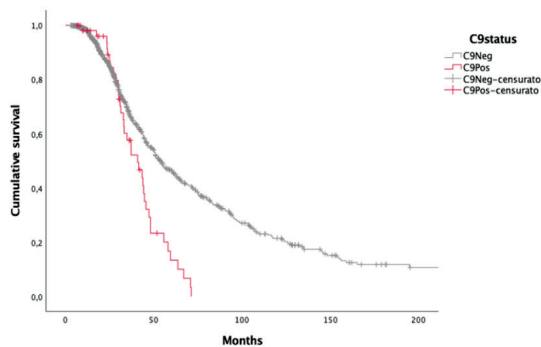
¹ Department of Neurology, Istituto Auxologico Italiano IRCCS, Milan, Italy, ² Department of Pathophysiology and Transplantation, University of Milan, Milan, Italy,

³ Department of Neurology and Laboratory of Neuroscience, IRCCS Istituto Auxologico Italiano, Milano, Italy

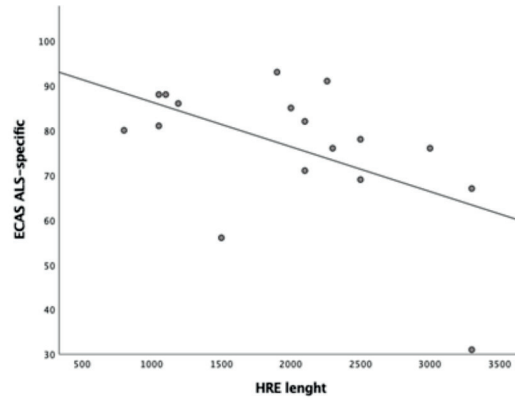
Background and aims: In several reports, ALS individuals carrying the hexanucleotide repeat expansion (HRE) in the c9orf72 gene (C9Pos) have been described as presenting distinct features compared to the general population (C9Neg). Here we aim to identify the phenotypic traits more closely associated with the HRE and analyze the role of the repeat length as a modifier factor.

Methods: We studied a cohort of 960 ALS patients. Motor phenotype was determined using the MRC scale, the lower motor neuron score (LMNS) and the Penn upper motor neuron score (PUMNS). Neuropsychological profile was studied using the Italian version of the Edinburgh Cognitive and Behavioral ALS Screen (ECAS), the Frontal Behavioral Inventory (FBI), the Beck Depression Inventory-II (BDI-II) and the State-Trait Anxiety Inventory (STAI). A two-step PCR protocol and a Southern blotting were performed to determine respectively the presence and the size of HRE.

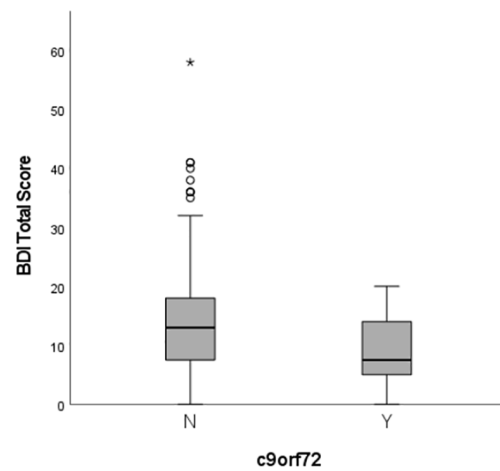
Results: HRE was detected in 55/960 (5.7%) patients. C9pos patients showed a younger onset, higher odds of bulbar onset, increased burden of UMN signs and, reduced survival, and higher frequency of concurrent dementia. Concerning cognitive phenotype, we found an inverse correlation between the HRE length and the performance at ECAS ALS-specific tasks (p=0.031). C9pos patients also showed higher burden of behavioral disinhibition (p=1.6x10⁻⁴) and lower degrees of depression (p=0.015) and anxiety (p=0.008) when compared to C9Neg cases.



Kaplan-Meier plots of survival probabilities: the patients carrying the pathogenic C9orf72 repeat expansion (C9Pos, red line) display shorter survival time than the patients without genetic mutations (C9Neg, grey line); +: censored cases.



Simple dispersion with adjustment curve of hexanucleotide repeat expansion (HRE) length for for Edinburgh Cognitive and Behavioural ALS Screen (ECAS) ALS-specific



Distribution of BDI -II total scores in C9Pos and C9Neg patients. Kruskal-Wallis for independent samples.

Conclusion: Our study provides an extensive characterization of motor, cognitive and behavioral features of c9orf72-associated ALS. Furthermore, our results indicate that the c9orf72 HRE size may represent a modifier of cognitive phenotype along the ALS-FTD spectrum.

Disclosure: Nothing to disclose.

OPR-055

The heterogeneity of respiratory failure occurrence in Amyotrophic Lateral Sclerosis: a two-step cluster analysis.

M. Torrieri¹, U. Manera¹, A. Mattei², A. Canosa¹, C. Moglia¹, F. Palumbo¹, F. Casale¹, N. Launaro³, M. Bellocchia², F. Ribolla², R. Vasta¹, G. Mora⁴, A. Calvo¹, A. Chiò¹

¹Rita Levi Montalcini¹ Department of Neuroscience, University of Turin, Turin, Italy, ²S.C. Pneumologia U, Azienda Ospedaliero-Universitaria Città della Salute e della Scienza, Turin, Italy, ³Respiratory Intensive Care Unit - Presidio Ospedaliero di Saluzzo, Saluzzo, Italy, ⁴Neurorehabilitation Department, ICS Maugeri IRCCS, Institute of Milan, Milan, Italy

Background and aims: Recognizing early respiratory impairment in Amyotrophic Lateral Sclerosis (ALS) can be demanding. We aimed at identifying ALS patients' clusters, based on clinical features, pulmonary function tests, and arterial blood gas analysis (ABG) parameters, to improve patients' prognostic stratification and respiratory management.

Methods: We included 488 ALS patients. A two-step cluster analysis was performed by using the following model variables: respiratory symptoms derived from ALSFRS-r scale, disease progression rate (Δ ALSFRS), severe bulbar involvement, FVC, pCO₂ and HCO₃- arterial blood levels. We compared the survival analysing the differences among clusters. Regression analysis was used to identify the variables that better predict the occurrence of respiratory symptoms.

Results: Five clusters were identified: Cluster 1, patients without respiratory failure ("normal" patients, NP); Cluster 2, patients with nocturnal hypoventilation (NH); Cluster 3, fast progressors (FP); Cluster 4, patients with severe bulbar impairment (SB); Cluster 5, patients with respiratory failure (RF). NH, FP, SB and RF clusters showed a shorter survival when compared to NP (21.6 months, 95% CI 19.7–23.4, $p < 0.001$), without any significant difference among them ($p > 0.05$ for all comparisons). After NIV adaptation FP had the longest prolongation of survival (about 10 months, $p < 0.001$), while SB patients did not show any benefit ($p = 0.675$). Respiratory symptoms can be predicted by a combination of variables (FVC%, pCO₂, ALSFRS-r score, Δ ALSFRS), showing only a moderate correlation to them ($R = 0.490$, $p < 0.001$).

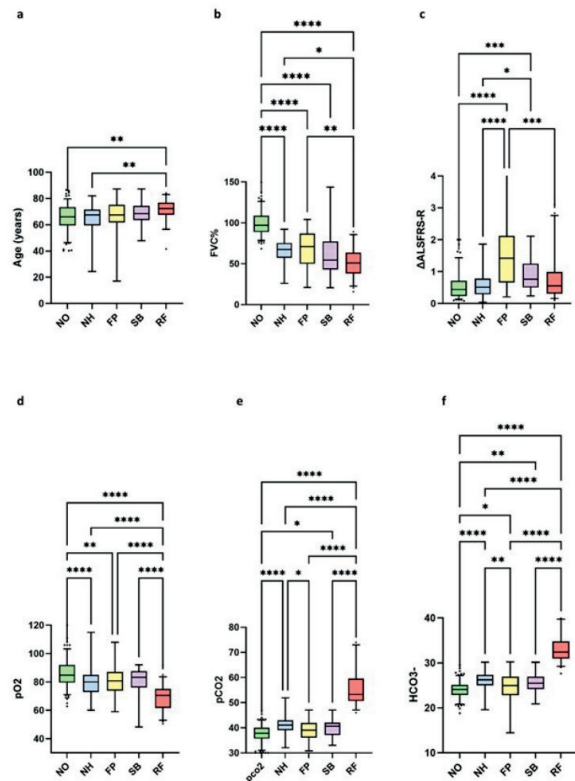


Figure 1. Box-plots: significant differences among clusters.

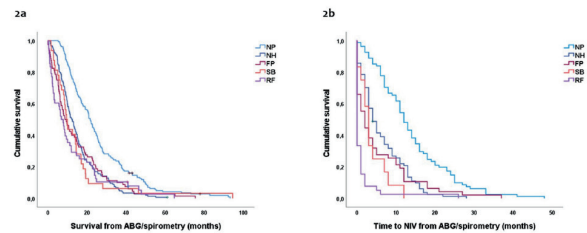


Figure 2. Kaplan-Meier curves. Fig. 2a: Survival from ABG/spirometry in all clusters. Fig. 2b: time from ABG/PFT to NIV initiation in all clusters.

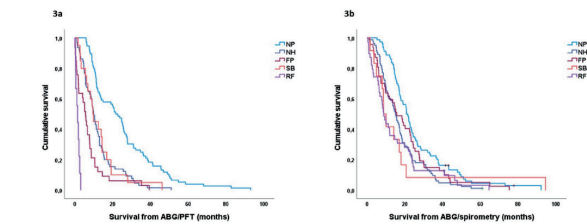


Figure 3. Kaplan-Meier curves: survival from ABG/spirometry in all clusters depending on NIV adaptation (Fig 3a patients who did not undergo NIV; Fig 3b patients who underwent NIV).

Conclusion: ALS patients show different pulmonary dysfunction presentations, independently from respiratory symptoms, that can be grouped in homogeneous clusters, to predict prognosis and plan respiratory management properly.

Disclosure: Dr Torrieri, Dr Manera, Dr Mattei, Dr Canosa, Dr Moglia, Dr Palumbo, Dr Casale, Dr Launaro, Dr Ribolla, Dr Bellocchia, Dr Vasta and Dr Mora report no conflicts of interest. Prof Calvo has received research grant from Cytokinetics. Prof Chiò serves on scientific advisory boards for Mitsubishi Tanabe, Roche, Biogen, Denali Pharma, AC Immune, Biogen, Lilly, and Cytokinetics. The sponsor organizations had no role in data collections and analysis and did not participate to writing and approving the manuscript. The information reported in the manuscript has never been reported elsewhere.

OPR-056

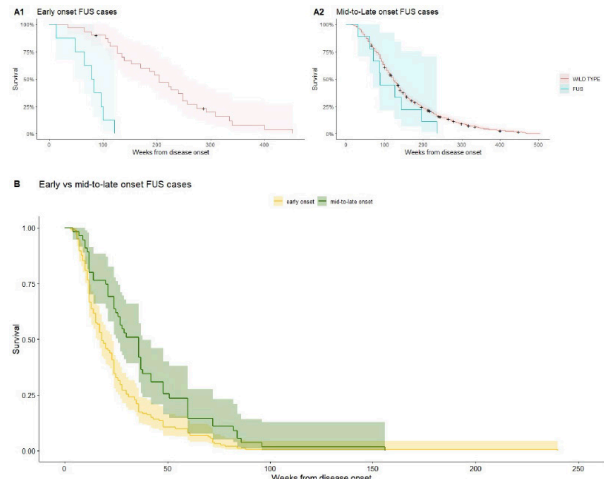
Phenotype analysis of FUS mutations in ALS

M. Grassano¹, C. Moglia¹, G. Brodini¹, U. Manera¹, R. Vasta¹, A. Canosa¹, A. Calvo¹, B. Traynor², A. Chiò¹
¹ ALS Centre, "Rita Levi Montalcini" Department of Neuroscience, University of Turin, Italy, ² Neuromuscular Diseases Research Section, Laboratory of Neurogenetics, National Institute on Aging, NIH, Bethesda, MD, United States of America

Background and aims: Mutations in Fused in Sarcoma (FUS) are among the most common genetic causes of ALS worldwide. They are supposedly characterized by a homogeneous pure motor phenotype with early-onset and short disease duration. However, a few FUS-mutated cases with a very late disease onset and slow progression have been reported. Therefore, here we analyzed genotype-phenotype correlations and identify the prognostic factors in FUS-ALS cases.

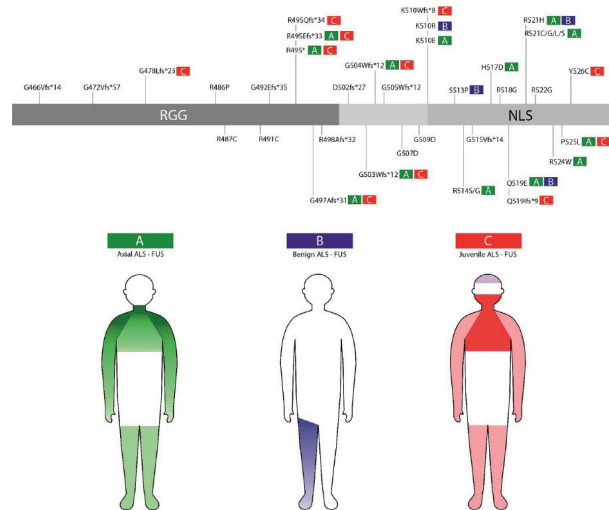
Methods: We identified and cross-sectionally analyzed 22 FUS-ALS patient histories from a single-center cohort of 2615 genetically tested patients and reviewed 289 previously published FUS-ALS cases.

Results: Survival of FUS-ALS is age-dependent: in our cohort only, early-onset FUS ALS patients had a rapid disease progression and short survival ($p=0.000003$). Meta-analysis of literature data confirmed this trend ($p=0.00003$). This survival pattern is not observed in other ALS-related genes in our series. We clustered FUS-ALS patients in three phenotypes: (a) axial ALS, with upper cervical and dropped-head onset in mid-to-late adulthood; (b) benign ALS, usually with a late-onset and slow disease progression, (c) juvenile ALS, often with bulbar onset and preceded by learning disability or mild mental retardation. Those phenotypes arise from different mutations.



(A) Survival analysis of early onset FUS carriers (age at onset < 46 ys, A1) and mid-to-late onset FUS (> 46 ys, A2) vs non-mutated ALS cases. (B) Survival analysis of early onset FUS carriers (age at onset < 46 ys) vs mid-to-late onset FUS (> 46 ys)

Conclusion: We observed specific genotype-phenotype correlations of FUS-ALS and identified age at onset as the most critical prognostic factor. Our results demonstrated that FUS mutations underlie a specific subtype of ALS and enable a careful stratification of newly diagnosed FUS-ALS cases in terms of clinical course and potential therapeutic windows. This will be crucial in the light of incoming gene-specific therapy.



Patterns of motor and non-motor involvement in FUS-ALS and genotype-phenotype correlation of FUS mutations

Disclosure: All authors report no disclosures relevant to the study.

Sunday, June 26, 2022

Movement disorders 1

OPR-057

3D visualization of Lewy Bodies: Insight into Parkinsonian's substantia nigra using Synchrotron Phase-Contrast Imaging

E. Sole Cruz¹, M. Fournier², E. De Schlichting³, A. Rabier⁴, J. Perriere⁴, E. Brun⁵, A. Bellier⁴, A. Pacureanu⁶

¹ Movement Disorders Department, Neurology/CHU Grenoble Alpes, Grenoble, France, ² General Neurology Department, Neurology/Centre Hospitalier du Pays d'Aix, Aix-en-Provence, France, ³ General Neurosurgery Department, Neurosurgery/CHU Grenoble Alpes, Grenoble, France, ⁴ Laboratoire d'Anatomie des Alpes Françaises/ Université Grenoble Alpes, Grenoble, France, ⁵ UA7 STROBE, Inserm/Université Grenoble Alpes, Grenoble, France, ⁶ ID16a/European Synchrotron Radiation Facility, Grenoble, France

Background and aims: Parkinson disease (PD) is histologically characterized by alpha-synuclein aggregates forming the Lewy Bodies (LB), mostly found in the substantia nigra (SN). Conventional imaging techniques such as MRI or TDM lack of spatial resolution. Histology and electronic microscopy do not allow 3D analysis, require staining and are limited in the size of sample (μm). Synchrotron Phase contrast X-ray imaging (S-PCI) is an emerging modality that exploits the differing refractive indices of materials to create additional contrast, especially in soft tissues. The aim of this study was to assess the ability of multiscale S-PCI to visualize the morphologic abnormalities present in human SN affected by PD.

Methods: Five samples of SN from four deceased-donors affected by PD and one age-matched control were imaged at the European Synchrotron Radiation Facility (ESRF, Grenoble, France). The whole SN was acquired at a resolution of 3 and 0.6 microns. Then, targeted regions were imaged at a resolution of 50 nanometers. No contrast agent was used in this study.

Results: Targeting of neuromelanin neurons was easy, and few artefacts were observed. Neuromelanin neurons, were individualizable in the SN (Fig. 1). Some Parkinsonian neuromelanin neurons contained dense spheric structures repelling the neuromelanine granulations, recognized as LB (Fig. 2 and Fig. 3). Pale bodies were identified too.

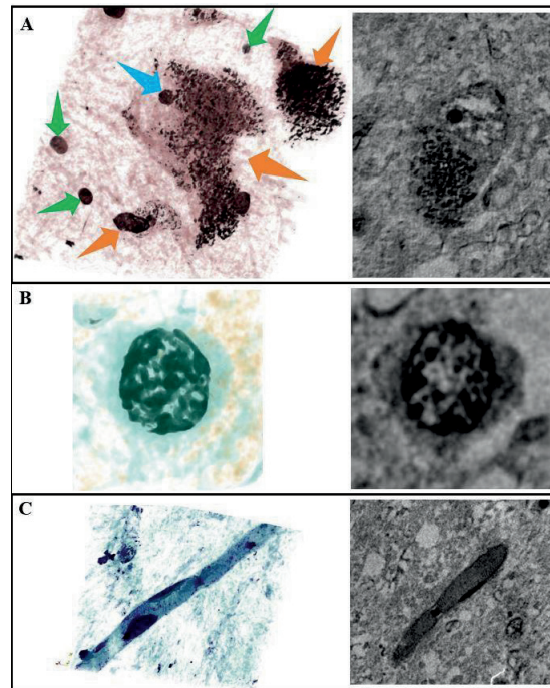


Figure 1. SN components at 50nm resolution: A. Neuromelanin neurons (purple = Neuromelanin; Green = Glial cells; Blue = nucleus; Orange = neurons); B. Glial cell; C. Blood vessel.

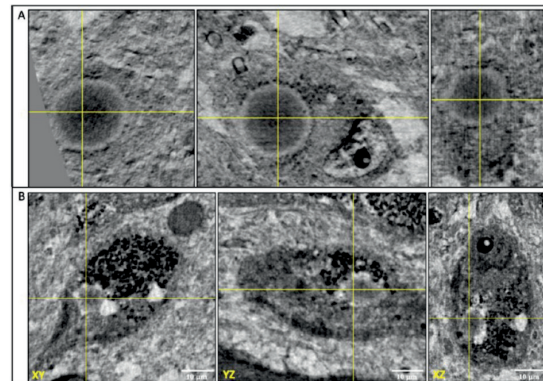


Figure 2. Lewy Body in SN in of two different donnors (A and B) at 50nm resolution. Yellow crosses indicate the position of the LB in the different views and planes (XY, YZ, XZ)

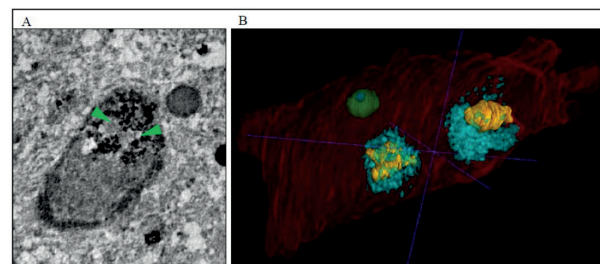


Figure 3. (A) 2D representation of a cell containing two misshapen LB at 50nm (Green arrows = LB). (B) matching 3D representation (Red = Cell membrane; Green = nucleolus; Yellow = LB; blue = Neuromelanin)

Conclusion: In this study we proved non-inferiority of multiscale S-PCI for visualizing LB in PD compared with conventional histological technique, and the capacity to study them in 3D for the first time. A deeper understanding of LB 3D structure with the S-PCI technology could allow new therapeutic targets.

Disclosure: The authors declare that they have no relevant or material financial interests that relate to the research described in this manuscript.

OPR-058

Neuroimaging evidence for a body schema disorder in Pisa syndrome of Parkinson's disease

E. Biassoni¹, W. Kreshpa¹, P. Mattioli¹, D. Arnaldi¹, M. Pardini¹, B. Orso¹, F. Massa¹, A. Donniaquio¹, S. Raffa², M. Bauckneht², S. Morbelli², F. Nobili¹

¹ Dept of Neuroscience, Neurorehabilitation, Ophthalmology, Genetics, and Mother and Child Health (DiNOGMI), University of Genoa, Genoa, Italy, ² Dept. of Health Sciences (DiSSAL), University of Genoa, Genoa, Italy

Background and aims: The pathogenesis of Pisa syndrome (PS) in Parkinson's disease (PD) is still uncertain and both 'central' and 'peripheral' mechanisms have been claimed. We explored nigrostriatal function and grey matter metabolism to unveil possible central dysregulation.

Methods: We retrospectively selected 34 mostly de novo PD patients (18 females, mean age:69+/-8) undergoing Dopamine Transporter (DaT)-SPECT (30 pts) and/or FDG-PET (22 pts) and who developed PS 56+/-53 months later. We divided both DaT (right 14 pts, left 16 pts) and FDG-PET (right 9 pts, left 13 pts) groups according to body leaning side. 'Right' and 'left' subgroups were compared each other with both techniques. Then, 30 DaT-SPECT PS patients were compared with 60 de novo PD patients without PS, and 22 FDG-PET PS patients were compared with 42 healthy controls. 'Right' and 'left' subgroups were also compared with controls in both modalities.

Results: There were no significant DaT-SPECT or FDG-PET differences between 'right' and 'left' subgroups, and in DaT-SPECT between PS patients and PD controls. Conversely, PS patients as a whole (Fig. 1) but also the 'left' and the 'right' subgroups showed significant relative hypometabolism in a right hemispheric cluster (Brodmann area 39).

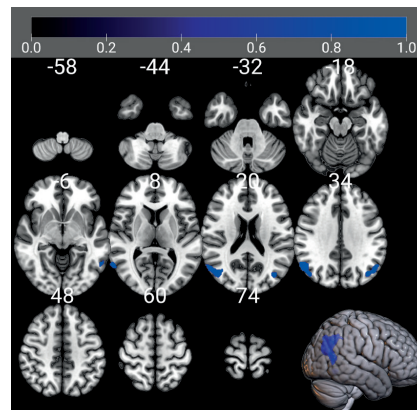


Figure 1 shows clusters of relative hypometabolism (FWE-corrected p

Conclusion: We showed that right angular gyrus metabolism is impaired since the time of diagnosis in PD patients who will later develop PS, irrespective of body leaning side. This finding suggests that a disorder of body schema representation is involved in the PS pathogenesis.

Disclosure: The authors do not have disclosures related to this manuscript.

OPR-059

Intestinal histomorphological and molecular alterations in patients with Parkinson's disease: results from a pilot study

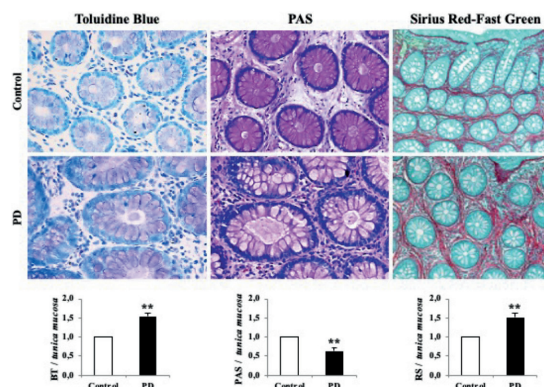
G. Bellini¹, D. Frosini², L. Benvenuti³, C. Ippolito⁴, C. Segnani⁴, G. Palermo¹, E. Del Prete², C. Pellegrini⁴, G. Siciliano¹, N. Bernardini⁴, M. Bellini⁵, M. Fornai³, R. Ceravolo¹

¹ Neurology Unit, Department of Clinical and Experimental Medicine, University of Pisa, Italy, ² Department of Medical Specialties, Neurology Unit, AOUP, Pisa, Italy, ³ Unit of Pharmacology and Pharmacovigilance, Department of Clinical and Experimental Medicine, University of Pisa, Pisa, Italy, ⁴ Section of Histology, Department of Clinical and Experimental Medicine, University of Pisa, Pisa, Italy, ⁵ Gastrointestinal Unit, Department of Translational Research and New Technologies in Medicine and Surgery, University of Pisa, Pisa, Italy

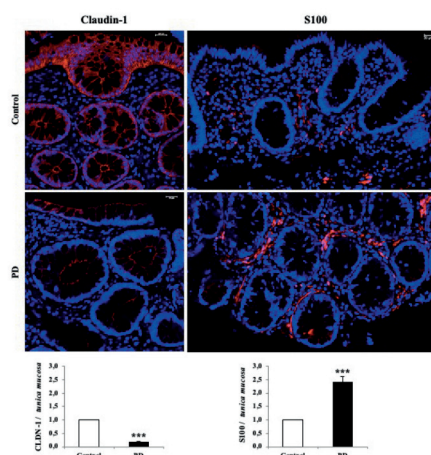
Background and aims: Parkinson's disease (PD) is characterized by alpha-synuclein accumulation, changes in gut microbiota composition, impairment of intestinal epithelial barrier (IEB) and enteric neurogenic/immune/inflammatory responses, which could all play a role in the pathogenesis of the disease. The aim of the study was to investigate in PD patients 1) changes of inflammatory markers in plasma and stool, 2) morpho-functional alterations of colonic mucosal barrier and 3) changes in faecal microbiota composition.

Methods: 19 PD patients and 19 healthy controls were enrolled. Plasma lipopolysaccharide binding protein (LBP; marker of altered intestinal permeability) and interleukin-1 beta (IL-1beta), as well as stool IL-1beta and tumour necrosis factor (TNF) were assessed. Gut microbiota analysis was also performed. Colonic biopsies collected during colonoscopy were processed for the evaluation of epithelial mucins, collagen fibres, Claudin-1 and S-100 positive glial cells.

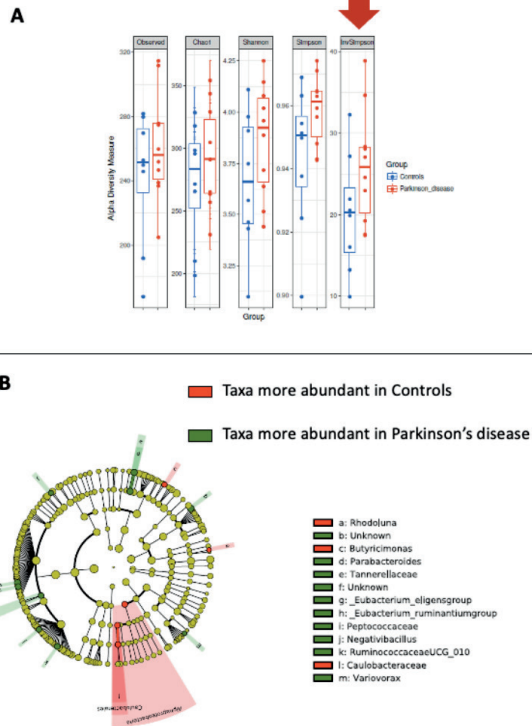
Results: Compared with controls, PD patients showed a significant increase in plasma LBP, faecal TNF and IL-1beta levels. Histological analysis of tissues from PD patients identified elevated expression of acidic mucins, collagen fibres and S-100 positive glial cells, and a decrease in neutral mucins and Claudin-1 expression, compared with controls. Faecal microbiota analysis revealed a significant difference in the alpha-diversity between PD patients and controls, whereas no differences were found in the beta-diversity.



Representative photomicrographs of toluidine blue (BT)-stained acidic mucins, PAS-stained neutral mucins, Sirius Red (SR)-stained collagen fibres and Fast Green (FG)-stained non-collagen proteins in colonic mucosal biopsies from controls and PD patients.



Representative photomicrographs of claudin-1 and S100 immunostaining in colonic mucosal biopsies from controls or PD patients. Original magnification 40 \times and 63 \times , respectively. Column graphs display the fold changes of the respective immunostaining \pm SEM.



(A) Significant difference in the alpha-diversity in PD patients in comparison with control subjects; (B) Significant difference in Bacterial Taxa abundance between PD patients in comparison with control subjects.

Conclusion: PD patients exhibited increased permeability of the gut barrier and colonic mucosal barrier remodelling, associated with changes in gut microbiota composition. Further studies are needed to establish whether such alterations are relevant in PD pathogenesis or represent only a consequence of the disease.

Disclosure: The authors declare that there are no additional disclosures to report.

OPR-060 MRI and genetic correlates of apathy and impulsive-compulsive behavior in Parkinson's disease

H. Theis¹, G. Bischof², J. Hammes², M. Hoenig², M. Tittgemeyer³, L. Timmermann⁴, G. Fink¹, A. Drzezga², C. Eggers⁴, T. Van Eimeren²

¹ University of Cologne, Department of Neurology, Cologne, Germany ² University of Cologne, Department of Nuclear medicine, Cologne, Germany ³ Max Planck Institute for Metabolism Research, Munich, Germany ⁴ University of Marburg, Department of Neurology, Marburg, Germany

Background and aims: Many Parkinson's disease (PD) patients concomitantly suffer from impulsive-compulsive behavior (ICB) and apathy. We investigated whether ICB and apathy share similar neural underpinnings in form of functional connectivity and structural brain alterations and evaluated the influence of D2/D3 receptors status in a group of PD patients.

Methods: 54 PD patients underwent resting-state fMRI and T1-weighted MRI. They completed the QUIP-RS (ICB quantification) and the AES (Apathy Evaluation Scale). Taq1A (D2) and Ser9Gly nucleotide (D3) polymorphism were determined. We examined resting-state connectivity patterns and structural volume. SPM12 was used for voxel-wise correlation analyses (ICB, Apathy).

Results: ICB and Apathy were positively correlated ($R=0.51$, $p<0.001$). D3 polymorphism was associated with more ICB. An interaction analysis revealed that ICB severity was influenced by apathy and D3 receptor status (Figure 1). Apathy was associated with smaller anterior cingulate cortex volume (Figure 2A). When controlling for ICB, we found a negative correlation between Apathy and volume of the ventral striatum and putamen ($p<0.001$ uncorrected) (Figure 2B). The connectivity analysis with a seed in the left putamen led to a connectivity network similar to the salience network (Figure 3). In apathetic PD, connectivity between putamen and superior frontal gyrus was stronger than in non-apathetic ($p<0.05$ FWE-corrected).

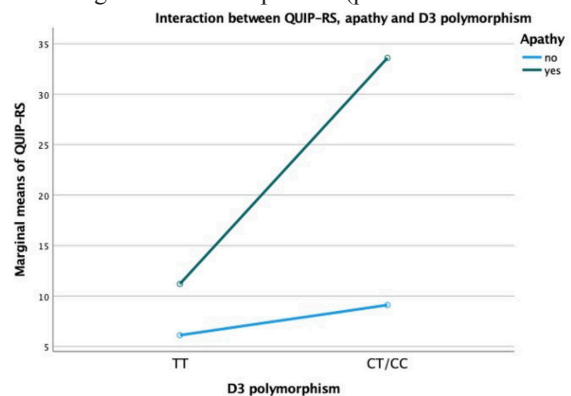


Figure 1: Univariate two-way ANOVA with bootstrap. D3, $F=10.882$, $p<0.002$. Apathy, $F=14.770$, $p<0.001$. D3*Apathy, $F=6.365$, $p=0.015$

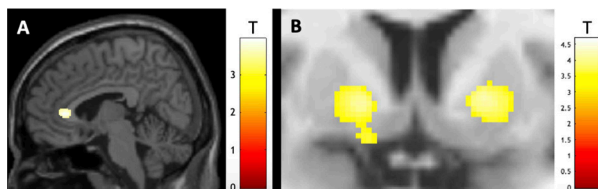


Figure 2: A Significant negative correlation between AES and volume of the anterior cingulate cortex. B Significant negative correlation between AES and volume of the striatum controlled for QUIP-RS. (Illustratory threshold $p < 0.001$ uncorrected.)

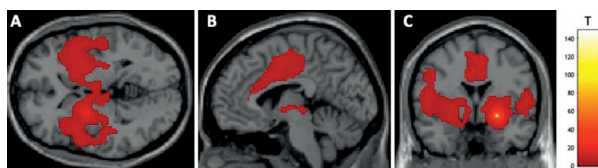


Figure 3: A (axial view), B (sagittal view), C (coronal view): Average functional connectivity map with seed in the left putamen. (Illustratory threshold: $p < 0.05$ FWE-corrected.)

Conclusion: Apathy and ICB were strongly correlated, but underlying neural underpinnings were different, since apathy was associated with atrophy and connectivity changes in the salience network. Interestingly, there were no imaging changes associated with ICB. Together, apathy in combination with D3 status elevates the risk for ICB severity in PD.

Disclosure: Nothing to disclose.

OPR-061

Visual Sequencing Search Strategy in Parkinson's Disease

E. Ștefănescu¹, G. D'inverno³, S. Brunetti³, M. Sampoli⁴, A. Bargagli⁴, D. Zanca⁴, M. Bianchini³, D. Muresanu², A. Rufa⁴

¹ RoNeuro Institute for Neurological Research and Diagnostic, Cluj-Napoca, Romania, ² Department of Neuroscience, Iuliu Hatieganu University of Medicine and Pharmacy, Cluj-Napoca, Romania, ³ Dipartimento di Ingegneria dell'Informazione e Scienze Matematiche, Università degli Studi di Siena, Siena, Italy,

⁴ Neurosense-Evalab-Eyeteck; Dipartimento di Scienze Mediche Chirurgiche e Neuroscienze Università di Siena, Siena, Italy

Background and aims: Patients with Parkinson's disease (PD) have prominent visual and oculomotor dysfunctions. In early stages, disturbances in visual acuity, pupil reactivity, saccadic and pursuit eye movements, motion perception, peripheral visual fields and visual processing speeds are reported. It has been demonstrated that patients with Parkinson's disease have greater difficulty discriminating details of peripheral images and perceive these images less strongly than healthy volunteers.

Methods: To further investigate the pattern of visual exploration in PD patients, we examined the distribution of fixation during the execution of a high cognitive demanding task of visual sequential search (TOP-DOWN Search) in 46 PD patients compared to controls. In the Visual Sequential Search Test (VSST) the subjects are asked to connect by gaze a logical sequence of numbers and letters. Visual search can be quantified in terms of the analysis of the scan-path, which is a sequence of saccades and fixations.

Results: The distribution of fixation in PD patients was lower in the peripheral ROIs, being centered mostly over central ROIs. Overall, these results might indicate the need for resampling the element's position because of a deficit in spatial map, working memory or attention or difficulties in encoding the sequential string of letters and numbers. Moreover, the profile of fixation distribution may indicate a neglected attraction to peripheral target or deficit in peripheral vision.

Conclusion: We detected a score of Visual Search Strategy (VSS) performance that was significantly lower in PD patients than controls, indicating a significant deficit of sequencing ability in PD patients.

Disclosure: All authors declare no conflict of interest.

OPR-062

Abstract withdrawn

Epilepsy 1

OPR-063

Analysing clinical text from electronic health records to diagnose anti-NMDAR encephalitis, a proof-of-concept study

H. Ariño¹, R. Stewart²

¹ Institut d'Investigacions Biomèdiques August Pi i Sunyer (IDIBAPS), Barcelona, Spain, ² Maudsley NIHR Biomedical Research Centre, London, United Kingdom

Background and aims: Anti-NMDAR encephalitis typically presents with psychiatric symptoms resembling a primary psychiatric disorder, which can lead to delays in diagnosis and treatment. We aim to investigate whether the clinical notes in electronic health records (EHR) could serve to discriminate between diseases.

Methods: We analysed all patients diagnosed with anti-NMDAR encephalitis (n=35) and compared it with other psychosis (n=70), from a large mental health provider from the NHS (UK). Text analysed comprised clinician-recalled quoted speech (QS) and the mental state examination (MSE). We used a bag of word representation, latent dirichlet allocation for topic modelling, and support vector machines -SVM-, multinomial naive bayes and logistic regression for binary classification. Performance was measured in the test set with accuracy and F1 scores by 5-fold cross-validation.

Results: We obtained two raw corpora of 5.898 or 275 instances (14% or 8% for encephalitis) in 105 or 44/105 patients for QS or MSE corpus respectively. Topic modelling found a different distribution in QS corpus (chi2 p-value=0.03); features like “paediatric”, “bladder”, “shakes” only appeared in encephalitis. The best accuracy, F1-encephalitis metrics were respectively 88%, 23% for QS corpus, and 95%, 44% for the MSE corpus, with a precision of 100% for encephalitis in MSE corpus using SVM.

Conclusion: Textual features in EHR could serve as diagnostic biomarkers in autoimmune encephalitis. Although a distinct psychopathological pattern is not evident, prediction of encephalitis with machine learning using the mental state examination corpus can reach a precision (or positive predictive value) of 100%.

Disclosure: HA receipts the BITRECS fellowship, funded by EU’s Horizon 2020 program and “La Caixa” Foundation.

OPR-064

Abnormal sensorimotor cortex and thalamo-cortical networks in FAME2: pathophysiology and diagnostic implications

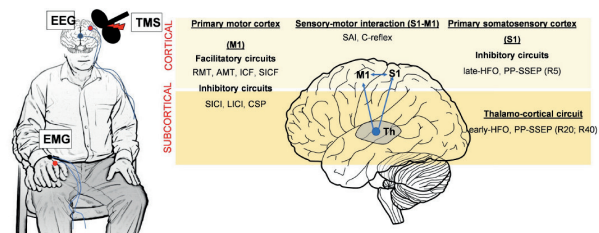
R. Dubbioso¹, P. Striano², A. Coppola¹

¹ Department of Neuroscience, Odontostomatology and Reproductive Sciences, Federico II University, Naples, Italy,

² Department of Neurosciences, Rehabilitation, Ophthalmology, Genetics, Maternal and Child Health (DiNOGMI), University of Genoa, Genoa, Italy

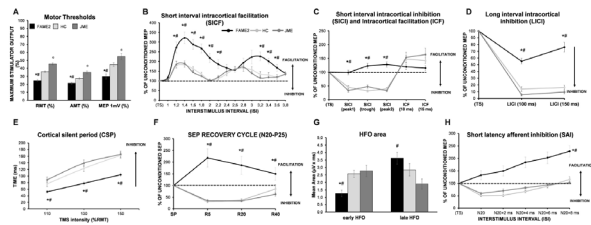
Background and aims: To systematically study with an extensive electrophysiological battery the sensory-motor hyperexcitability in Familial Adult Myoclonic Epilepsy type2 (FAME2) patients and to establish reliable neurophysiological biomarkers for the diagnosis.

Methods: We evaluated the facilitatory and inhibitory circuits within the primary motor cortex (M1) using single and paired-pulse transcranial magnetic stimulation (TMS) paradigms. We also probed the excitability of the somatosensory (S1) cortex as well as the thalamo-S1 connection by using ad hoc somatosensory evoked potential (SEP) protocols in a cohort of genetically confirmed Italian FAME2 patients, a group of patients with Juvenile Myoclonic Epilepsy (JME) and a subset of healthy control subjects. The sensitivity, and specificity of TMS and SEP metrics were derived from receiver operating curve analysis.

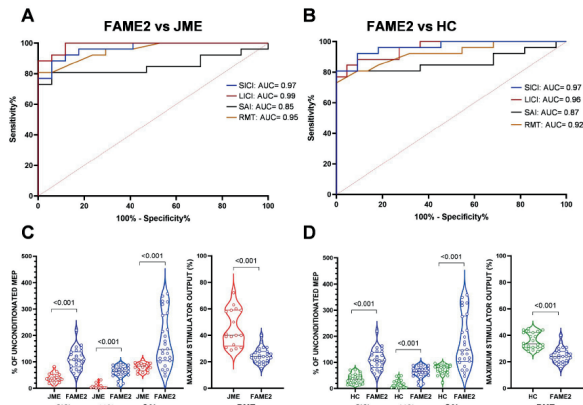


Overview of Neurophysiological protocols to evaluate cortical and subcortical circuits. During the experiment patients and healthy controls underwent an extensive neurophysiological battery aimed to evaluate the excitability of cortical circuits.

Results: 26 FAME2 subjects, 17 JME patients and 22 healthy controls (HC), were evaluated. Overall, FAME2 patients displayed increased facilitation and decreased inhibition within the sensory-motor cortex compared with JME patients (all p<0.05) and HC (all p<0.05). SEP protocols also displayed a significant reduction of early high-frequency oscillations and less inhibition at paired-pulse protocol, suggesting a concomitant failure of thalamo-S1 circuits. Disease duration, age and myoclonus severity, and surface EMG did not correlate with sensory-motor hyperexcitability (all p>0.05). Finally, FAME2 condition was reliably diagnosed using TMS, demonstrating its superiority as a diagnostic factor compared to SEP measures.



Assessment of facilitatory and inhibitory circuits in the primary motor cortex (M1), in the somatosensory cortex (S1) and evaluation of thalamo-cortical connectivity. Group average of stimulation intensity to produce motor thresholds (RMT, AMT).



Diagnostic accuracy of TMS measures Receiver operating characteristic (ROC) and area under the curve (AUC) values for TMS parameters, namely RMT, SICI, LICI and SAI in differentiating patients with FAME2 from those with JME (A) and HC (B).

Conclusion: Sensory-motor cortical and thalamo-cortical circuits are involved in the pathophysiology of FAME2. In addition, TMS displays an overall higher accuracy than SEP to reliably distinguish FAME2 from JME and HC.

Disclosure: Nothing to disclose.

OPR-065

GAD-antibody associated temporal lobe epilepsy: T cells kill neurons, plasma cells and antibodies are bystanders

C. Bien¹, A. Tröscher², K. Mair², L. Verdú de Juan², A. Becker³, I. Blümcke⁴, M. Finzel⁵, C. Geis⁶, R. Höftberger⁷, C. Mawrin⁸, T. Von Oertzen⁹, R. Surges¹⁰, B. Voges¹¹, S. Weis¹², M. Winklehner⁷, J. Bauer²

¹ Department of Epileptology (Krankenhaus Mara), Medical School, Campus Bielefeld-Bethel, Bielefeld University, Bielefeld, Germany, ² Department of Neuroimmunology, Center for Brain Research, Medical University of Vienna, Vienna, Austria, ³ Department of Neuropathology, University Hospital Bonn, Bonn, Germany, ⁴ Department of Neuropathology, University Hospital Erlangen, Erlangen, Germany, ⁵ Epilepsy Center Kleinwachau, Radeberg, Germany, ⁶ Department of Neurology, University Hospital Jena, Jena, Germany, ⁷ Division of Neuropathology and Neurochemistry, Department of Neurology, Medical University of Vienna, Vienna, Austria, ⁸ Department of Neuropathology, University Hospital Magdeburg, Magdeburg, Germany, ⁹ Department of Neurology I, Neuromed Campus, Kepler University Hospital Linz, Linz, Austria, ¹⁰ Department of Epileptology, University Hospital Bonn, Bonn, Germany, ¹¹ Hamburg Epilepsy Center, Protestant Hospital Alsterdorf, Department of Neurology and Epileptology, Hamburg, Germany, ¹² Division of Neuropathology, Department of Pathology and Molecular Pathology, Neuromed Campus, Kepler University Hospital Linz, Linz, Austria

Background and aims: GAD-antibody associated temporal lobe epilepsy is a chronic condition. Response to immunotherapy is mostly unsatisfying. A better understanding of the pathophysiology may help improving the timing of immunotherapy.

Methods: We collected formalin-fixed paraffin-embedded mediotemporal brain samples of 15 patients and compared them to a control cohort (n=8) by performing histopathology and whole-genome transcriptomics. We assessed MRI courses and CSF-serum pairs.

Results: After shorter disease duration, CD3+CD8+GranzymeB+ cytotoxic T-cells were elevated in the brain parenchyma. T cell numbers decreased with longer disease duration. Transcriptomics showed upregulated T cell genes in patients with high T cell counts. In such cases, also B cell- and complement-associated pathways were overrepresented. This was paralleled by high numbers of plasma cells in the perivascular space of blood-vessels as well as in the parenchyma. These cases, however, showed no neural IgG deposition or complement activation. In cases with short disease duration, loss of hippocampal neurons and APP+ axonal bulbs indicated acute neural damage. Patients showed mediotemporal volume and signal increase on MRI and intrathecal IgG- or GAD antibody-synthesis in temporal proximity to active brain inflammation. This resulted in hippocampal sclerosis.

Conclusion: Early in the disease course, cytotoxic T cells damage neurons. Subsequently, plasma cells enter the brain but there are no signs of antibody-mediated pathology. This early encephalitic period can be recognized by MRI scans showing mediotemporal swelling with signal increase and CSF studies revealing intrathecal antibody synthesis. The early irreversible neural destruction may explain incomplete responses to delayed immunosuppressive therapy and calls for early immunotherapy.

Disclosure: Nothing to disclose.

OPR-066

DNA methylation profiling of cfDNA in epilepsy patients demonstrates potential cerebral origin

R. Martins Ferreira¹, B. Leal³, J. Chaves⁴, L. Ciudad¹, R. Samões⁴, A. Martins da Silva⁵, P. Pinho Costa², E. Ballestar¹

¹ Epigenetics and Immune Disease Group, Josep Carreras Research Institute (IJC), Badalona, Barcelona, Spain, ² Immunogenetics Lab, Molecular Pathology and Immunology Instituto de Ciências Biomédicas Abel Salazar – Universidade do Porto (ICBAS-UPorto), Rua Jorge Viterbo Ferreira, Porto, Portugal, ³ Autoimmunity and neuroscience group. Unit for Multidisciplinary Research in Biomedicine (UMIB), ICBAS-UPorto, Rua Jorge Viterbo Ferreira, Porto, Portugal, ⁴ Hospital de Santo António - Centro Hospitalar Universitário do Porto (HSA-CHUP), Neurology Service, Porto, Portugal, ⁵ HSA-CHUP, Neurophysiology Service, Porto, Portugal

Background and aims: Cell-free DNA (cfDNA) consist of highly degraded DNA fragments shed into peripheral blood circulation. Its origin is predominantly associated with cell death. DNA methylation patterns are strongly preserved in specific tissues and cell types. Screening of cfDNA methylation has been used to track cell type-specific cell-death. Mesial Temporal Lobe Epilepsy with Hippocampal Sclerosis (MTLE-HS) is characterized by severe neuronal death in the mesial regions.

Methods: We performed cfDNA methylation profiling, using EPIC BeachChips, in serum of 12 MTLE-HS patients (2M, 9F; 44.8±11.4 years of age) and 11 non-epileptic controls (4M, 8F; 38.9±8.4 years of age). Cell-of-origin deconvolution was performed with the `meth_atlas` algorithm. Differential methylation was performed with the `minfi` and `limma` R packages.

Results: No significant differences in the proportion of “cortical neuron”-derived cfDNA was observed between MTLE-HS patients and controls. We identified 235 differentially methylated CpG positions between patients and controls. Gene ontology analysis of the hypomethylated cluster (151 CpGs) revealed enrichment of terms associated with cerebral function, such as chemical synaptic transmission, positive regulation of oligodendrocyte progenitor proliferation and glutamate receptor activity.

Conclusion: The use of a deconvolution tool could not detect significant differences in the proportions of neuron-derived cfDNA in MTLE-HS. However, direct differential comparison of methylation between patients and controls demonstrated enrichment of pathways associated with CNS function. We consider relevant to enhance the detection of brain-derived cfDNA through more precise deconvolution tools. The detection of brain-derived cfDNA in serum of MTLE-HS patients may constitute a promising new biomarker for early detection of occurring neuronal death.

Disclosure: No conflicts of interest disclosed.

Sleep-wake disorders

OPR-067

Derivation and validation of a conversion pattern in idiopathic REM sleep Behavior Disorder

P. Mattioli¹, B. Orso¹, C. Liguori², F. Famà¹, L. Giorgetti³, A. Donniaquio¹, A. Giberti¹, D. Vallez Garcia⁴, S. Meles⁵, K. Leenders⁵, R. Renken⁶, F. Placidi², M. Spanetta², A. Chiaravallotti⁷, R. Camedda⁷, O. Schillaci⁷, F. Izzi⁸, N. Mercuri², M. Pardini¹, M. Bauckneht⁹, S. Morbelli⁹, F. Nobili¹, D. Arnaldi¹

¹ Department of Neuroscience, Rehabilitation, Ophthalmology, Genetics, Maternal and Child Health (DINO GMI), University of Genoa, Genoa, Italy, ² Department of Systems Medicine, University of Rome "Tor Vergata", Rome, Italy, ³ IRCCS Ospedale Policlinico S. Martino, Genoa, Italy, ⁴ Department of Radiology and Nuclear Medicine, Amsterdam UMC, Location VuMC, Amsterdam Neuroscience, Amsterdam, The Netherlands, ⁵ Department of Neurology, University of Groningen, University Medical Center Groningen, Groningen, The Netherlands, ⁶ Neuroimaging Center, Department of Neuroscience, University of Groningen, Groningen, The Netherlands, ⁷ Department of Biomedicine and Prevention, University of Rome "Tor Vergata", Rome, Italy, ⁸ Sleep Medicine Center, Neurology Unit, University Hospital "Tor Vergata", Rome, Italy, ⁹ Department of Health Science (DISSAL), University of Genoa, Genoa, Italy

Background and aims: Idiopathic REM-Sleep Behaviour disorder (iRBD) is considered an early-stage alpha-synucleinopathy. We aimed to identify an iRBD brain glucose metabolism phenoconversion-related pattern (RBDconvRP), which could potentially be used to predict phenoconversion of iRBD patients to Parkinson's disease (PD) or Dementia with Lewy bodies (DLB).

Methods: 76 (70±6 years, 15 females) iRBD patients were enrolled in Genoa and Rome and prospectively evaluated for 28±18 months. 30 patients (Table 1) phenoconverted to overt alpha-synucleinopathy (14 PD and 16 DLB). Patients underwent baseline brain 18F-FDG-PET. A RBDconvRP was identified using Scaled-Subprofile-Model Principal-Component-Analysis (SSM-PCA), and cross-validated by a leave-one-out procedure. Survival-analysis and Cox-regression were used to explore prediction power, using age, site, and sex as covariates.

Table 1: Demographic and clinical characteristics of RBD patients. Values are shown as mean ± standard deviation.

	RBD converted patients	RBD non converted patients	p value
	n = 30	n = 46	
Age (yr)	73±6; 72 [61-84]	69±6; 70 [56-82]	0.02
Education (yr)	10±4; 8 [5-18]	11±4; 8 [5-18]	0.85
Sex (females)	7	8	0.53
MMSE score	28±2; 28 [22-30]	29±1; 29 [24-30]	0.06
MCI (presence)	19	15	<0.01
MDS-UPDRS-III score	3±1; 3 [0-8]	1±2; 0 [0-7]	0.02
Phenoconversion			
Survival Time (months)	21±14; 18 [3-55]	33±19; 29 [7-137]	<0.01
PD	14	/	
DLB	16	/	
MSA	0	/	

Legend: DLB = Dementia with Lewy Bodies; MDS-UPDRS-III = Movement Disorders Society-sponsored revision of the Unified Parkinson's Disease Rating Scale, motor section; MMSE = Mini Mental State Examination; PD = Parkinson's Disease; RBD = REM sleep behavior disorder; REM = Rapid eye movements. Values are expressed as means ± standard deviation, median [minimum-maximum] for continuous variables, as absolute numbers for categorical variables.

Table 1: Demographic and clinical characteristics of RBD patients. Values are shown as mean ± standard deviation, median [minimum-maximum] for continuous variables, as absolute numbers for categorical variables.

Results: SSM-PCA was first applied in a derivation set (Genoa patients) of 16 converter and 27 non-converter patients. The pattern was applied to a validation set (Roma) of 14 converter and 19 non-converter patients. Another SSM-PCA was performed using Roma patients to derive a pattern and Genoa patients as the validation set. The two patterns were comparable, thus SSM-PCA was applied to the whole set, identifying the RBDconvRP (figure 1). Receiver operating characteristic analysis showed an area under the curve of 0.87 (sensitivity 80%, specificity 78%) in differentiating converters from non-converters. At Cox-regression analysis, RBDconvRP showed high prediction power in identifying converters patients, surviving adjustment for site, age, and sex (figure 2, HR: 9.87, CI 95%: 3.8–25.9).

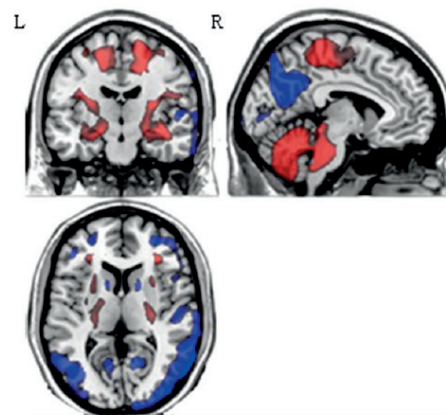


Figure 1: Results of the SSM-PCA. Stable voxels of the RBDconvRP, determined after bootstrap resampling 95% confidence interval not straddling zero are shown. Red indicates positive voxel weights and blue indicates negative voxel weights.

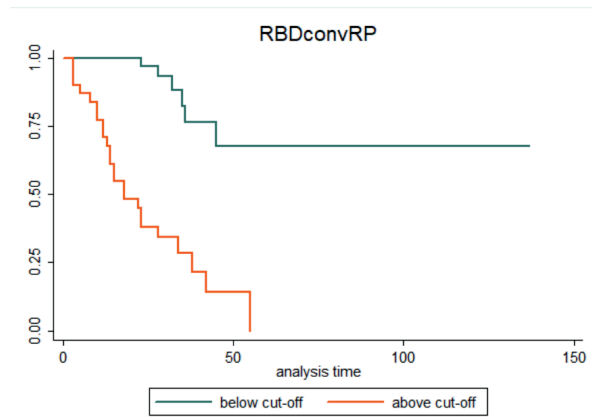


Figure 2. Survival analysis of RBDconvRP expression. On the x axis, survival time is reported in months, on the y axis percentage of patients. The green line represents patients expressing RBDconvRP below the empirical optimal cut-point (1.05 ds)

Conclusion: We identified and validated a stable RBDconvRP, able to discriminate converter from non-converter iRBD patients and possibly useful in future studies to predict phenoconversion.

Disclosure: I have nothing to disclose.

OPR-068

Unsupervised clustering of central hypersomnolence disorders enables data-driven phenotyping

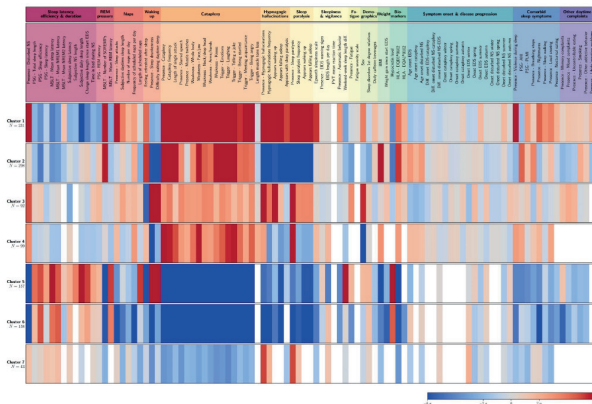
J. Gool¹, Z. Zhang², M. Oei³, S. Mathias⁴, R. Fronczek⁵, R. Khatami⁶, G. Lammers⁵, On behalf of the European Narcolepsy Network members⁷

¹ Sleep Wake Center SEIN Heemstede, Heemstede, The Netherlands. Dep. of Neurology and Clinical Neurophysiology, Leiden University Medical Center, Leiden, The Netherlands. Dep. of Anatomy and Neurosciences, Amsterdam UMC (Location VUmc), Amsterdam, The Netherlands, ² Center for Sleep Medicine, Sleep Research and Epileptology, Klinik Barmelweid AG, Barmelweid, Switzerland, ³ Leiden Observatory, Leiden University, Leiden, The Netherlands, ⁴ Department of Anatomy and Neurosciences, Amsterdam UMC (Location VUmc), Amsterdam, The Netherlands, ⁵ Sleep Wake Center SEIN Heemstede, Heemstede, The Netherlands. Dep. of Neurology and Clinical Neurophysiology, Leiden University Medical Center, Leiden, The Netherlands, ⁶ Center for Sleep Medicine, Sleep Research and Epileptology, Klinik Barmelweid AG, Barmelweid, Switzerland. Department of Neurology, Inselspital, Bern University Hospital, University of Bern, Bern, Switzerland

Background and aims: Recent studies fueled doubts as to whether the currently defined central disorders of hypersomnolence are stable entities, especially narcolepsy type 2 (NT2) and idiopathic hypersomnia (IH). The main aim of this data-driven observational study on neurological sleep disorders was to see if data-driven algorithms would segregate narcolepsy type 1 (NT1), and identify more reliable subgrouping of individuals without cataplexy.

Methods: We used the newly developed agglomerative hierarchical clustering package Bowerbird, an unsupervised machine learning algorithm, to identify distinct hypersomnolence clusters in the large-scale European Narcolepsy Network database. We included 1,078 unmedicated patients and 97 variables, covering all aspects of central hypersomnolence disorders (e.g. symptoms, demographics, sleep measures, laboratory biomarkers).

Results: Seven clusters were identified, of which clusters 1–4 included predominantly individuals with cataplexy (Figure 1). The two most distinct clusters (5 and 6) were dominated by those without cataplexy and, amongst other variables, significantly differed in presence of sleep drunkenness, subjective difficulty awakening and weekend-week sleep length difference. Patients formally diagnosed as NT2 and IH were evenly mixed in these two clusters.



Each column represents 1 variable and each row represents 1 of 7 clusters. The difference between the mean value of the individual cluster with the entire EU-NN database is displayed for each variable in standard deviations in blue-to-red (lower-higher).

Conclusion: In the largest study on central disorders of hypersomnolence to date, we identified distinct data-driven subgroups within the central disorders of hypersomnolence population. Our results confirm NT1 diagnosis with multiple subtypes, contest inclusion of sleep-onset rapid eye moment periods (SOREMPs) in diagnostic criteria for people without cataplexy, and provide promising new variables for reliable diagnostic categories. Data-driven classification will result in a more solid hypersomnolence classification system with less vulnerability to single, instable features.

Disclosure: The EU-NN database is internally financed, but financial support from UCB Pharma Brussels was provided for database development.

OPR-069

Sleep disordered breathing and atrial fibrillation in acute stroke and their impact on long-term outcome

X. Yang, M. Dekkers, J. Lippert, S. Baillieux, S. Duss, M. Schmidt, C. Bassetti
Sleep-Wake-Epilepsy Center, Department of Neurology, University Hospital Bern, University of Bern, Bern, Switzerland

Background and aims: Despite the evidence of a complex and bidirectional relationship between sleep disordered breathing (SDB) and atrial fibrillation (AF) on cerebro-cardiovascular events, studies investigating the long-term effects of this association in stroke patients are still rare.

Methods: We prospectively studied 353 patients with acute ischemic stroke with a follow-up of three years. The apnea-hypopnea index (AHI) was determined acutely after stroke with respiratory polygraphy. 7-days long-term electrocardiograms (7d-ECG) were performed up to three times during the first year.

Results: During the acute phase after stroke, 89 patients (25%) had moderate-severe SDB ($AHI \geq 20/h$). AF was diagnosed in 56 patients (16%) and 23 patients (7%) had both AF and SDB ($AHI \geq 20/h$). Over the follow-up period, 95 new cerebro- cardiovascular events were recorded, including 17 fatal casualties. Patients with comorbid SDB ($AHI \geq 20/h$) and AF have a significantly increased risk (Hazard Ratio, 2.30) of an incident cerebro- cardiovascular or fatal event compared with either AF (Hazard Ratio, 1.77) or SDB (Hazard Ratio, 1.39) after adjusting for age, sex, body mass index, hypertension, diabetes mellitus and dyslipidemia. Moreover, stroke patients with comorbid SDB and AF are more likely to have cardioembolism.

Table 1: Baseline Characteristics according to AF

	No (N=297)	AF (N=56)	Total (N=353)	P value
Age, Mean (SD)	63.659 (13.155)	70.327 (9.896)	64.717 (12.914)	< 0.0011
Sex				0.0452
Male	181 (60.9%)	42 (75.0%)	223 (63.2%)	
Female	116 (39.1%)	14 (25.0%)	130 (36.8%)	
AHI	13.534 (15.902)	18.614 (16.064)	14.340 (16.013)	0.0291
SDB severity				0.0032
AHI < 20	231 (77.8%)	33 (58.9%)	264 (74.8%)	
AHI ≥ 20	66 (22.2%)	23 (41.1%)	89 (25.2%)	
NIHSS at admission	3.192 (3.814)	4.446 (6.093)	3.391 (4.271)	0.0441
NIHSS at discharge	1.347 (2.214)	0.839 (1.233)	1.266 (2.096)	0.0971
TOAST				< 0.0012
CE	81 (27.3%)	31 (55.4%)	112 (31.7%)	
LAA	77 (25.9%)	10 (17.9%)	87 (24.6%)	
Other	20 (6.7%)	0 (0.0%)	20 (5.7%)	
SVO	22 (7.4%)	5 (8.9%)	27 (7.6%)	
Unknown	97 (32.7%)	10 (17.9%)	107 (30.3%)	
Hypertension				0.0472
Yes	170 (57.2%)	40 (71.4%)	210 (59.5%)	
No and undiagnosed	127 (42.8%)	16 (28.6%)	143 (40.5%)	
Diabetes mellitus				0.5662
Yes	46 (15.5%)	7 (12.5%)	53 (15.0%)	
No and undiagnosed	251 (84.5%)	49 (87.5%)	300 (85.0%)	
Dyslipidemia				0.2522
Yes	161 (54.2%)	35 (62.5%)	196 (55.5%)	
No and undiagnosed	136 (45.8%)	21 (37.5%)	157 (44.5%)	

*Abbreviations: CE, Cardioembolic; SVO, Small vessel occlusion; LAA, Large artery atherosclerosis; NIHSS, National Institutes of Health Stroke Scale

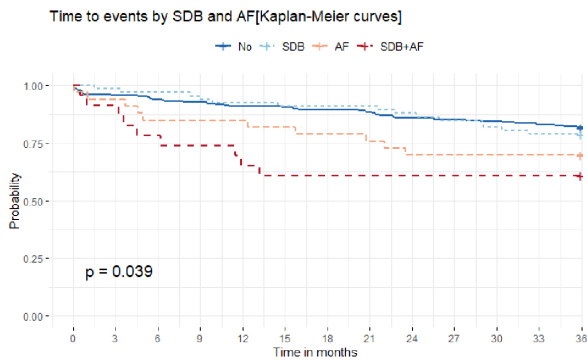


Figure 1. Time to events probability in No, SDB, AF, and SDB+AF groups. No: No AF with AHI=20; AF: AF with AHI=20.

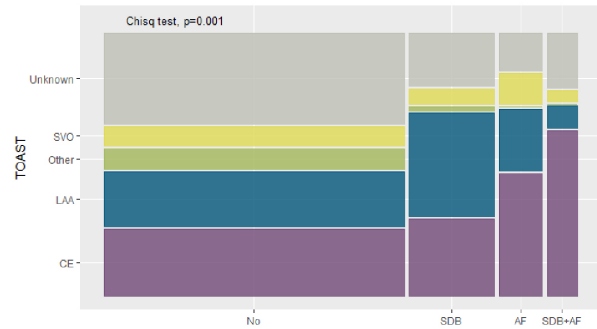


Figure 2. Distribution of TOAST stroke subtype classification in No, SDB, AF, and SDB+AF groups.

Conclusion: Stroke patients with both SDB and AF have a significantly higher risk of long-term cardiovascular morbidity and mortality compared to SDB or AF alone. Further studies are needed to clarify the pathomechanisms underlying this observation and lead to specific diagnostic and treatment recommendations.

Disclosure: This work was supported by a grant from Swiss National Science Foundation (SNFS; #320030_149752), and a PhD fellowship from China Scholarship Council. All authors declare no conflict of interest related to the current work.

OPR-070
Abstract withdrawn

Peripheral nerve disorders

OPR-071

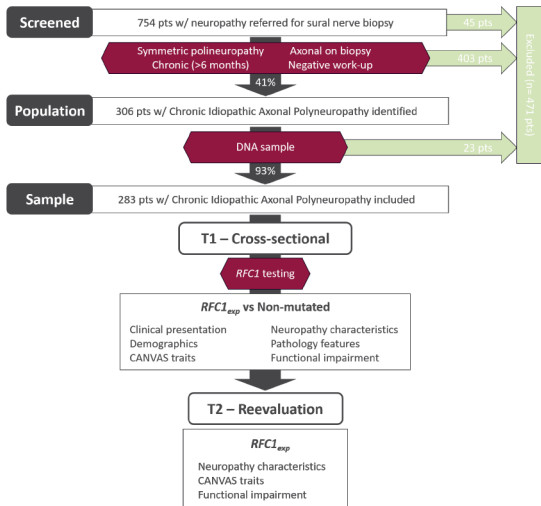
RFC1-neuropathy cases frequently convert to full-blown CANVAS: a cohort-sequential study

M. Tagliapietra ¹, N. Mesiano ², D. Cardellini ³, M. Ferrarini ¹, S. Testi ¹, S. Ferrari ¹, S. Monaco ¹, T. Cavallaro ¹, G. Fabrizi ¹

¹ Department of Neurosciences, Biomedicine, and Movement Sciences, University of Verona, Verona, Italy, ² Otolaryngology Unit, Hospital of Verona, Verona, Italy, ³ Neurology Unit, Hospital of Treviso, Treviso, Italy

Background and aims: Cerebellar Ataxia with Neuropathy and Vestibular Areflexia Syndrome (CANVAS), a multisystem neurological disease often characterized by sensory disturbances at onset, has recently been associated to a biallelic Replication Factor C subunit 1 AAGGG intronic repeat expansion mutation (RFC1exp). Penetrance of the full phenotype and predictors of clinical progression are currently unknown. We investigated RFC1exp in a Chronic Idiopathic Axonal Polyneuropathy (CIAP) population to assess its prevalence, characteristics and long-term disease progression.

Methods: We identified 286 CIAP cases among patients referred to our Center for sural nerve biopsy. We reported clinical features at the time of biopsy (T1) and pathology results. RFC1exp patients were longitudinally reevaluated (T2) to assess disease progression.

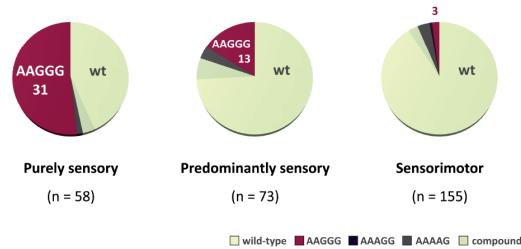


Study flowchart

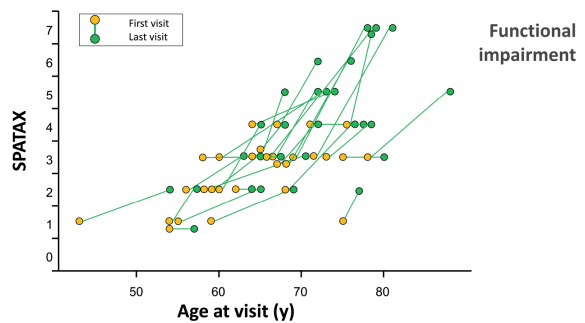
Results: RFC1exp cases were common in pure sensory (31/58, 53%) and predominantly sensory neuropathies (13/73, 18%) compared to sensorimotor cases (3/155, 2%) and characterized by frank signs of sensory ataxia and mild autonomic disturbances. Apart from retention of deep tendon reflexes, other peculiar CANVAS features at T1 were exceptional. Pathology revealed a severe involvement

of all nerve fibers but scant regenerative changes. At T2 (median disease duration 13 years IQR 9–16) most patients exhibited at least mild features of cerebellar (19/23, 83%) and vestibular involvement (16/22, 73%). Chronic cough was universally reported. Intriguingly, age at visit was a stronger predictor of overall functional impairment than disease duration.

Prevalence of biallelic RFC1 expansions



Prevalence of RFC1 expansion mutations according to clinical presentation



Grade of functional impairment according to SPATAX scale and age at first (yellow) and last (green) visit in RFC1-neuropathy

Conclusion: Emergence of the full-blown CANVAS phenotype is a frequent but late event in RFC1exp patients presenting with an isolate sensory neuropathy. Aging but not age at onset is a major determinant of disease progression.

Disclosure: Nothing to disclose.

OPR-072

Kinesin-5 inhibition enhances functional recovery in experimental autoimmune neuritis

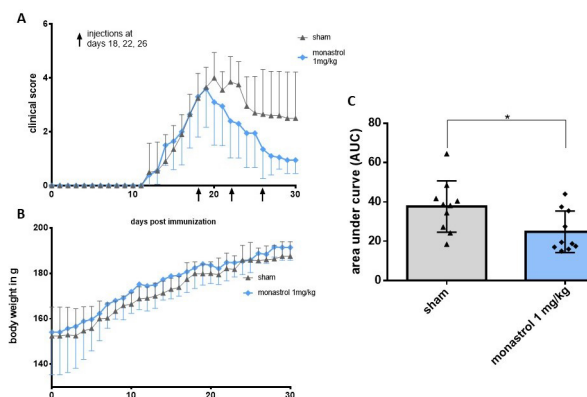
F. Kohle, R. Ackfeld, I. Klein, M. Svacina, G. Fink, H. Lehmann

Department of Neurology, Faculty of Medicine, University of Cologne and University Hospital Cologne, Cologne, Germany

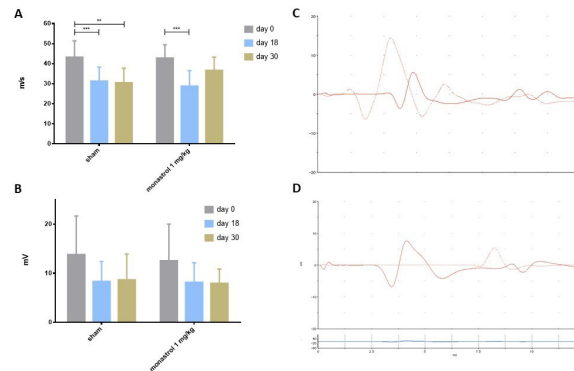
Background and aims: Kinesin-5 is a motor protein that interacts with microtubules and is highly expressed in postmitotic neurons. Inhibition of kinesin-5 accelerates the growth rates of cultured neurons. We examined the influence of kinesin-5 inhibition on functional recovery in experimental autoimmune neuritis (EAN) in female Lewis rats.

Methods: EAN was induced using myelin 53-78 P2 protein. The clinical disease severity score was assessed daily until day 30 post-immunization (p.i.). At the peak of EAN, at days 18, 22, and 26 p.i., rats were treated with either sham or 1 mg/kg body weight of the kinesin-5 inhibitor monastrol intraperitoneally. Nerve conduction studies and histological analysis of the sciatic nerve and the tibialis anterior muscle were performed. Non-parametric Mann-Whitney t-test was used for statistical analysis.

Results: Treatment with 1 mg/kg body weight monastrol ameliorated significantly clinical signs in the recovery phase of EAN (p-value for the area under curve: 0.0288). Motor nerve conduction velocity (mNCV) reached near pre-immunization values (p-value for days 0 and 30: 0.1819). Immunohistochemical analysis of the macrophage marker Iba1 showed no differences (p-value: 0.0564), while a significant reduction of CD3+ T-cells was observed (p-value: 0.0012). An increase of partially or fully innervated neuromuscular junctions (NMJs) was observed (76.49% to 65.05%).

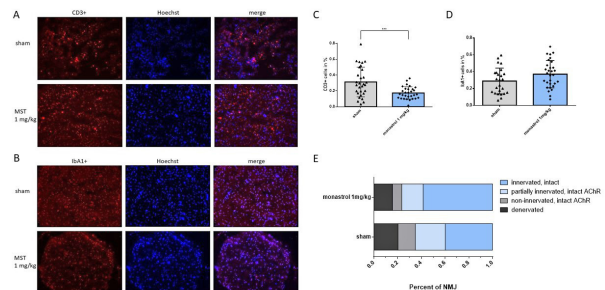


Treatment with 1 mg/kg of the kinesin-5 inhibitor monastrol enhances functional recovery after EAN.



Kinesin-5 inhibition accelerates mNCV recovery.

Conclusion: Kinesin-5 inhibition accelerates functional and histological recovery in EAN. Our preliminary results suggest an effect on infiltratory T-cells and reinnervation of disrupted NMJs. Further studies are warranted to investigate the potential of kinesin-5 inhibition in patients suffering from autoimmune neuropathy.



Immunohistochemical analysis of the sciatic nerve shows a significant reduction of CD3+ T-cell infiltration and enhanced recovery of NMJ-innervation.

Disclosure: F. Kohle and R. Ackfeld are supported by the Koeln Fortune Program/Faculty of Medicine, University of Cologne. I. Klein, M.K.R. Svacina, G. R. Fink, and H.C. Lehmann reported no disclosures related to this study.

OPR-073

A software platform to identify diagnostic and prognostic parameters in neuromuscular diseases towards trials readiness

F. Torri ¹, G. Ricci ¹, A. Tonacci ², G. Aringhieri ³, F. Sansone ², A. Rubegni ⁴, G. Astrea ⁴, G. Siciliano ¹, F. Santorelli ⁴, R. Conte ²

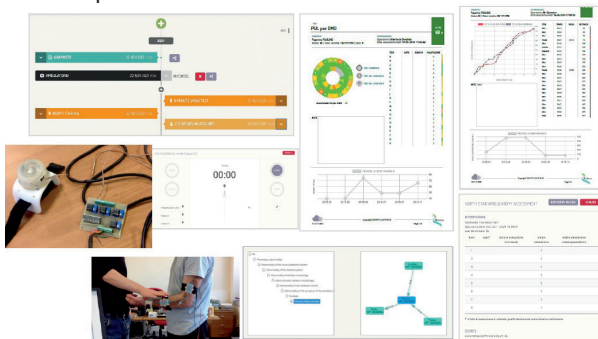
¹ Department of Clinical and Experimental Medicine, University of Pisa, Pisa, Italy, ² Clinical Physiology Institute, National Research Council of Italy (IFC-CNR), Pisa, Italy, ³ Diagnostic and Interventional Radiology, Department of Translational Research, University of Pisa, Pisa, Italy, ⁴ Molecular Medicine, IRCCS, Fondazione Stella Maris, Pisa, Italy

Background and aims: We are working on an integrated, multiparametric approach in diagnosis and management of neuromuscular diseases (NMDs) by using a single support software platform, potentially useful in implementing diagnosis and taking care towards trials readiness. Promising preliminary results have been obtained to date with the Health360 platform under the umbrella of the InGene 2.0 project.



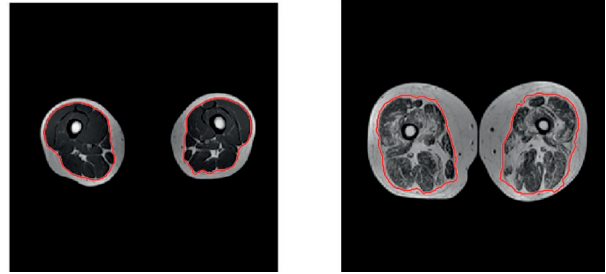
Participants and aims of the InGene2.0 Project

Methods: Health360, a platform developed under the Software-as-a-Service (SaaS) principles, merges all that, with sections dedicated to the collection of personal data (under the premises of the EU 2016/679 GDPR Regulation), as well as modules devoted to biomedical images storage and interpretation.



Modules of the software platform and integration with wearable devices

Results: In particular, further modules, including neurological examination and functional motor tests, mta, muscle biopsies, are under development and optimization.



Development of and AI algorithm for muscle MRI analysis

Conclusion: The possibility to upload such images in a common, user-friendly software platform, where data and image storage, as well as the analysis of images and loops can be performed in an intelligent manner, would be of extreme aid to the clinician. If confirmed on larger cohorts and with robust statistical approach, such results could drive the present tool to be used for diagnostic aims, phenotypic characterization and clinical follow-up.

Disclosure: The project is funded by the Progetto Toscana Salute 2018.

OPR-074

Cancer-related neuropathic pain in Europe: differences in diagnosis and treatment in 13 countries-patient's perspective

M. Rakusa¹, D. Dupouiron², C. Eeltink³, B. Barragán⁴, D. Bell⁵, G. Petersen⁶, M. Eerdekens⁶, D. Ryan⁷, S. Brill⁸

¹ Department of Neurological Diseases, University Medical Centre Maribor, Maribor, Slovenia, ² Institut de Cancérologie de l'ouest, Département Anesthésie, Douleur, Cedex, France, ³ Amsterdam UMC, location VUmc, department of Hematology, Amsterdam, The Netherlands, ⁴ Grupo Español de Pacientes con Cancer (GEPAC), Madrid, Spain, ⁵ Macmillan Cancer Support, Strategy Development, London, United Kingdom, ⁶ Grunenthal GmbH, Aachen, Germany, ⁷ Pain Alliance Europe, Brussels, Belgium, ⁸ European Pain Federation EFIC, Brussels, Belgium; Pain Institute, Tel Aviv Medical Center, Israel

Background and aims: With effective treatments available, people with cancer live longer but often with sequelae such as neuropathic pain. Cancer patients from 13 European countries shared their experiences with the diagnosis and management of CRNP.

Methods: An online survey, prepared, conducted and analysed with a team of experts including physicians, nurses and patients, was completed in June 2021. Adults consenting to participate and diagnosed with cancer were screened for symptoms of CRNP. Respondents who met three or more of the DN4 (Douleur Neuropathique 4) criteria were enrolled and provided detailed information about diagnosis and management of their pain.

Results: 549 persons living with CRNP participated in the survey (24–103 respondents per country). Of those recruited, 32% experienced severe pain daily (21–49%). Although neuropathic pain symptoms were present, only 60% of respondents received a formal diagnosis of CRNP varying from 40% in France to 87% in Switzerland. Pharmaceutical treatment by a healthcare professional (HCP) varied from 32% in Norway to 79% in Switzerland where also the highest treatment satisfaction was reported with 91% of responses. On average 60% of patients have been warned by a HCP to develop CRNP (thereof 45% by their oncologist) with the highest rate in Switzerland (83%) and the lowest in the UK (42%).

Conclusion: Major differences have been identified between European countries regarding diagnosis and treatment of CRNP. Highest patient satisfaction was reported in countries where HCPs spent enough time with their patients, which demonstrates the relevance of HCP-patient communication in CRNP care.

Disclosure: Grünenthal GmbH has financially supported this survey.

OPR-075

The diagnostic value of the rise slope of the compound sensory nerve action potential in human nerves

S. Xirou, S. Aristeidou, P. Koutsoudaki, P. Kokotis, N. Karandreas, T. Zambelis, E. Anagnostou
Department of Neurology, University of Athens, Eginition Hospital, Athens, Greece

Background and aims: The average rise slope of the sensory nerve action potential (SNAP) appreciates the steepness of the initial negative deflection of the waveform, which might be a useful metric for the first part of the potential.

Methods: Sural nerve sensory neurography was performed in patients with various axonal neuropathies and median nerve sensory studies were carried out in patients suffering from carpal tunnel syndrome. Age matched healthy individuals served as controls. The rise slope was compared to conventional SNAP parameters such as conduction velocity, latency, duration and rise time.

Results: 537 sensory studies were prospectively analyzed. The rise slope of the sural SNAP demonstrated superior classification performance in terms of sensitivity (92.5%), specificity (97%) and area under the receiver operating characteristic curve (0.986), as compared to conventional SNAP parameters. Its diagnostic power was similarly excellent in median nerve studies, whereas here a slightly better classification performance was obtained by SNAP latency and conduction velocity.

Conclusion: The average rise slope appears to do justice to the tight interplay between amplitude and rise time of the initial negative spike deflection, outperforming many conventional measures. This composite metric proved high diagnostic potency in particular with regard to axonal sensory nerve dysfunction.

Disclosure: None of the authors has any conflict of interest to disclose.

OPR-076

Super-resolution imaging provides new insights into nerve pathologies in patients with peripheral neuropathies

J. Linke¹, L. Appeltshauer², H. Heil¹, C. Karus¹, J. Schenk¹, C. Sommer², K. Doppler², K. Heinze¹

¹ *Rudolf Virchow Center for Experimental Biomedicine, University of Würzburg, Würzburg, Germany,* ² *Department of Neurology, University of Würzburg, Würzburg, Germany*

Background and aims: With today's super-resolution fluorescence microscopy methods, it is possible to study the molecular organization of the Node of Ranvier. Previous studies have revealed a 190nm periodic arrangement of nodal, paranodal and internodal structural proteins of murine myelinated axons. However, the ultrastructural anatomy of the paranodal region of peripheral human myelinated axons under physiological and pathophysiological conditions has not been explored yet.

Methods: We use dual color dStorm microscopy and high content confocal imaging in combination with colocalization analysis to examine the structure of the paranodal complex and its cytoskeletal anchor molecules in nerve biopsies of n=16 patients with peripheral neuropathies.

Results: We show an increase in the periodic distance of the proteins of the paranodal axoglial complex of Neurofascin-155 and Caspr-1 in patients with polyneuropathy. Double immunofluorescence colocalization analysis shows that both proteins are not detached even if the periodic arrangement is pathologically altered. However, colocalization of Caspr-1 to its anchor protein β 2-Spectrin is disrupted in patients with axonal neuropathy. In comparison to chronic axonal (n=5) and demyelinating (n=5) forms, patients with acute axonal polyneuropathies (n=6) show a paranodal elongation and a significant reduction of nodes per tissue volume in teased fiber preparations correlating to the cross-sectional fiber density.

Conclusion: Our data provide new insights into the histopathologic changes in polyneuropathy and objectively quantify alterations between different forms of neuropathy. In the future, dStorm and high content confocal microscopy could serve as sophisticated tools for a better understanding and discrimination of subtypes and stages of polyneuropathies.

Disclosure: The authors declare no competing financial interests.

Epilepsy 2

OPR-077

Cenobamate: preliminary results of efficacy and safety in a real-life setting

G. Falcicchio¹, S. Lattanzi², E. Russo³, G. Boero⁴, A. Alicino¹, T. Francavilla¹, M. Trojano¹, A. La Neve¹
¹ Department of Basic Medical Sciences, Neurosciences and Sense Organs, University of Bari, Bari, Italy, ² Department of Experimental and Clinical Medicine, Neurological Clinic, Marche Polytechnic University, Ancona, Italy, ³ Science of Health Department, School of Medicine, University Magna Graecia, Catanzaro, Italy, ⁴ Complex Structure of Neurology, SS Annunziata Hospital, Taranto, Italy

Background and aims: The percentage of patients with drug-resistant epilepsy has not changed despite the increasing available anti-seizure medications (ASMs). Cenobamate (CNB) has been recently approved as adjunctive treatment of uncontrolled focal-onset seizures (FOS). So far, evidence about CNB use in clinical practice is limited.

Methods: Starting from December 2020, 20 patients aged ≥ 18 years, diagnosed with uncontrolled FOS and without other potential treatment alternatives, were enrolled in an Italian Expanded Access Program (EAP). Clinical data to assess CNB efficacy and safety were collected at 3, 6, and 12 months after CNB administration, along with plasma concentrations of concomitant ASMs. Therapeutic adjustment of concomitant ASMs was allowed. Primary efficacy outcomes were median percentage change in monthly seizure frequency compared to baseline and responder rate (patients with $\geq 50\%$ monthly seizure frequency reduction from baseline). Adverse events (AEs) were reported considering their severity and duration.

Results: Patients taking CNB reported significant reductions in monthly seizure frequency compared to baseline at 3 months (-63%) with 11/20 (58%) presenting $\geq 50\%$ seizure frequency reduction. Sustained decrease in seizure frequency was registered at 6 and 12 months. 16/20 (80%) patients experienced AEs, which were mainly mild and transient and generally disappeared after reducing the posology of concomitant ASMs.

Conclusion: Despite the small number of patients and the short follow-up, to our knowledge, this is one of the first real-world study on CNB use in clinical practice.

Disclosure: Nothing to disclose.

OPR-078

Seizure forecasting with non-invasive and minimally-invasive mobile devices – Epilepsy Foundation My Seizure Gauge study

P. Viana¹, M. Nasser², E. Nurse³, P. Karoly³, T. Pal Attia², N. Gregg², B. Joseph², C. Grzeskowiak⁵, M. Dümpelmann⁶, M. Cook³, G. Worrell², A. Schulze-Bonhage⁶, D. Freestone⁴, M. Richardson¹, B. Brinkmann²
¹ Institute of Psychiatry, Psychology and Neuroscience, King's College London, London, United Kingdom, ² Dept. of Neurology, Mayo Foundation, Rochester MN, United States of America, ³ Seer Medical, Melbourne VIC Australia; University of Melbourne, Depts of Biomedical Engineering and Medicine, Melbourne VIC Australia, ⁴ Seer Medical, Melbourne VIC Australia, ⁵ Epilepsy Foundation of America, ⁶ Department of Neurosurgery, Epilepsy Center, Medical Center – University of Freiburg, Faculty of Medicine, University of Freiburg, Germany

Background and aims: Seizure forecasting has been established using continuous intracranial EEG, however invasive devices are not appropriate for all patients. Non-invasive and minimally invasive devices may facilitate seizure forecasting, and they may provide accurate seizure records to support clinical decision making.

Methods: Patients with drug-resistant epilepsy were enrolled for ultra long-term (>8 months) monitoring with an electronic diary, a wearable device (Empatica E4, Fitbit Charge 4/HR, or Fitbit Inspire) and ambulatory EEG monitoring (UNEEG SubQ, EpiMinder Subscalp, NeuroPace RNS) at three sites. Recorded data were analyzed to identify circadian and multi-day seizure cycles which, together with machine learning methods, were used to forecast seizures.

Results: 40 enrolled subjects have recorded over 11,400 days (31.2 years) of ambulatory data, including over 1,600 seizures. Nine patients left the study prematurely due to device malfunctions, complications, poor adherence, poor data quality or unanticipated seizure freedom. 20 patients continue recording data and eleven have completed the study. Analyses in this cohort has established the following:

- Heart rate circadian and multi-day cycles are significantly phase-locked with self-reported seizure likelihood
- Electrodermal activity, heart rate, and actigraphy were significantly correlated with electrographic seizures in 11 patients
- Seizure forecasting significantly better than chance in 5 of 6 patients using a wrist-worn device and long-short term memory (LSTM) neural networks
- Circadian and multi-day seizure cycles are detectable in subcutaneous EEG recordings
- Seizure forecasting significantly greater than chance in 5 of 6 patients using subcutaneous EEG

Conclusion: This project has established the feasibility of forecasting seizures using seizure cycles, wearable devices and subcutaneous EEG.

Disclosure: This work is supported by the Epilepsy Foundation of America.

OPR-079

Epilepsy in School-aged Children and academic performance in standardized tests: A Danish nation-wide cohort study

J. Dreier¹, B. Trabjerg¹, O. Plana-Ripoll¹, N. Skipper¹, E. Agerbo¹, C. Cotsapas², A. Berg³, J. Christensen⁴
¹ Department of Economics and Business Economics, Aarhus University, Aarhus, Denmark, ² Department of Neurology, Yale, New Haven, United States of America, ³ Department of Neurology, Northwestern University – Feinberg School of Medicine, Chicago, United States of America, ⁴ Department of Neurology, Aarhus University Hospital, Aarhus, Denmark

Background and aims: We evaluated whether epilepsy is associated with performance in standardized tests among Danish school-aged children.

Methods: We performed a register-based, nation-wide, matched cohort study of children born in Denmark during 1997–2009 who participated in the Danish National School Test Program between 2010–2019. Population and health registers were used to identify CWE along with randomly sampled sex- and age-matched reference children without epilepsy (ratio 1:10). Academic performance was assessed in language (2nd, 4th, 6th, 8th grade) and mathematics (3rd, 6th, 8th grade). Differences in mean standardized scores (scale, 1–100) between children with and without epilepsy were estimated using linear regression models while adjusting for relevant confounders.

Results: Of 582,475 eligible children, we studied 4,322 (0.74%) CWE and sampled 43,220 matched reference children. The median (IQR) age at epilepsy onset was 6.9 (3.5–10.2) years. Having epilepsy was significantly associated with poorer performance in language (mean score CWE=48.8 and reference=56.4; adjusted difference=-6.0, 95% CI: -6.8 to -5.2), and mathematics (mean score CWE=47.7 and reference=57.3; adjusted difference=-7.7, 95% CI: -8.6 to -6.8). Worse performance was found in all epilepsy subgroups, including in the 3,015 CWE considered neurotypical (i.e. with no pre-existing neurologic or intellectual disabilities or an identified underlying cause for the epilepsy), (adjusted difference=-6.0, 95% CI: -6.8 to -5.1).

Conclusion: CWE are at increased risk of poor academic outcomes, with average score differences of -10.6% in language and -13.4% in mathematics. Our findings highlight the need for educational support of CWE, even among those who are otherwise neurotypical.

Disclosure: This work was supported by the Independent Research Fund Denmark, the Novo Nordisk Foundation (NNF16OC0019126), the Central Denmark Region, and the Danish Epilepsy Association. Dr. Christensen reports personal fees from Eisai AB, personal fees from UCB Nordic, during the conduct of the study. The other authors report no conflicts of interests.

OPR-080

The European Study on the Burden and Care of Epilepsy

J. Christensen¹, C. Linehan², T. Tomson³, A. Marson⁴
¹ Department of Neurology, Aarhus University Hospital, Aarhus, Denmark, ² UCD Centre for Disability Studies, University College Dublin, Dublin, Ireland, ³ Department of Clinical Neuroscience, Karolinska Institutet, Stockholm, Sweden, ⁴ Institute of Translational Medicine, University of Liverpool, Liverpool, United Kingdom

Background and aims: The European Study on the Burden and Care of Epilepsy (ESBACE) provides data on the burden and care of epilepsy in Europe.

Methods: This study had three main goals: 1) to estimate prevalence of epilepsy in four European countries based on information from medical record, 2) to use a “top-down,” register-based approach in more than 5 million people in Denmark to study prevalence and cost of epilepsy, and 3) to study stigma and quality of life in persons with epilepsy.

Results: The retrospective chart review found a prevalence of 0.67% (0.61–0.72), but a precise prevalence estimate could not be generated because of limited information and access to hospital records. In the “top-down” study, the prevalence of epilepsy was 0.67% (0.69% males; 0.65% females), (Figure 1), and the cost of epilepsy was €30,683/person/year. Epilepsy was associated with stigma and lower quality of life compared to matched controls.

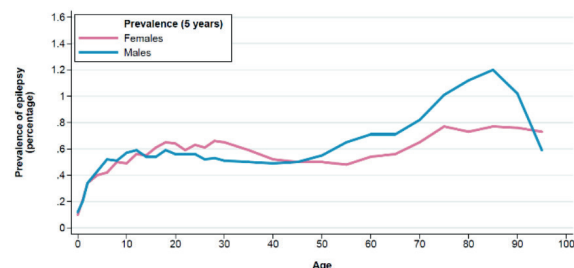


Figure 1. Age- and sex-specific prevalence of epilepsy in Denmark on December 31, 2016

Conclusion: This European study provides important insight into burden and care in persons with epilepsy:

- Chart review faced a number of challenges largely due to data protection legislation, and poor documentation of epilepsy diagnoses in medical records.
- It was possible to use a “top-down” approach to estimate epilepsy prevalence, and establish the very high costs associated with epilepsy.
- A significant proportion of people with epilepsy are still affected by the stigma and report lower quality of lives compared with those without the condition – a circumstance that has not improved in recent decades.

Disclosure: The European Union (no. 2014//199564).

OPR-081

The Scottish Epilepsy Deaths Study Score (SEDS Score): a risk prediction model for epilepsy-related deaths

G. Mbizvo ¹, C. Schnier ², C. Simpson ³, S. Duncan ¹, R. Chin ¹

¹ *Muir Maxwell Epilepsy Centre, Centre for Clinical Brain Sciences, University of Edinburgh, Edinburgh, United Kingdom*, ² *Usher Institute, University of Edinburgh, Edinburgh, United Kingdom*, ³ *School of Health, Wellington Faculty of Health, Victoria University of Wellington, Wellington, New Zealand*

Background and aims: This study uses routine clinical information to develop a risk-prediction model for epilepsy-related deaths.

Methods: In this age/sex-matched case-control study, we compared adults (aged ≥ 16 years) suffering epilepsy-related death between 2009–2016 to living adults with epilepsy in Scotland. Cases were captured from national mortality records, and controls from a research database or epilepsy clinics. Medical record data were used in univariable and multivariable conditional logistic regression to develop a risk prediction model consisting of four variables chosen a priori. A sum of the factors present was taken to create a risk index – the SEDS Score. Odds ratios (OR) with 95% CIs were estimated.

Results: 224 cases and 224 controls were compared (mean age 48 years). Univariables predicting epilepsy-related death were recent epilepsy-related A&E attendance (OR 5.1, CI 3.2–8.3), living in deprived areas (OR 2.5, CI 1.6–4.0), developmental epilepsy (OR 3.1, CI 1.7–5.7), alcohol abuse (OR 4.4, CI 2.2–9.2), absent recent neurology review (OR 3.8, CI 2.4–6.1), generalised epilepsy (OR 1.9, CI 1.2–3.0), and mental health problems (OR 1.6, CI 1.0–2.6). SEDS Score model variables consisted of the first three listed above, alongside the number of comorbidities (adjusting variable). Compared to having a SEDS Score of 0, those with a SEDS Score of 1, 2, and 3, had 3.6x (CI 1.9–6.8), 17.2x (CI 7.4–39.6), and 19.8x (CI 5.1–76.6) increased odds of death, respectively.

Conclusion: SEDS Scoring may help predict epilepsy-related death and requires external validation. Figure 1 illustrates a prototype SEDS Scoring card for clinical use.

SIGNALLING QUESTIONS	RESPONSE	NUMBER OF POINTS AWARDED
DOES THE PATIENT LIVE IN ONE OF THE TWO MOST DEPRIVED SIMD QUINTILES?	No	0
	Yes	1
HAS THE PATIENT EXPERIENCED AT LEAST ONE A&E ATTENDANCE OR HOSPITAL ADMISSION BECAUSE OF A SEIZURE OR RELATED TO THEIR EPILEPSY WITHIN THE LAST 12 MONTHS?	No	0
	Yes	1
DOES THE PATIENT HAVE AN INHERITED OR CONGENITAL AETIOLOGY/RISK FACTOR FOR THEIR EPILEPSY?	No	0
	Yes	1
HOW MANY COMORBIDITIES DOES THE PATIENT HAVE ALONGSIDE THEIR EPILEPSY?	None	0
	1 condition	0
	≥ 2 conditions	0
TOTAL NUMBER OF POINTS		
INTERPRETATION OF TOTAL NUMBER OF POINTS:		
0 POINTS = reference category		
1 POINT = patient has ~4x increased risk of premature epilepsy-related death within seven years		
2 POINTS = patient has ~17x increased risk of premature epilepsy-related death within seven years		
3 POINTS = patient has ~20x increased risk of premature epilepsy-related death within seven years		
URGENT REFERRAL TO EPILEPSY CLINIC FOR PATIENTS WITH A SCORE OF 1 OR MORE		

Figure 1: Prototype SEDS Scoring card

Disclosure: Nothing to disclose.

OPR-082

Short term efficacy and safety of adjunctive cenobamate in patients with super-refractory focal epilepsy

A. Gifreu¹, M. Machío Castelló², M. Quintana¹, M. Toledo¹, E. Santamarina¹, E. Fonseca¹, L. Abreira¹, D. Campos¹, E. Conde³, M. Centeno³, M. Carreño³, B. Giráldez², J. Serratosa²

¹ Vall d'Hebrón University Hospital, Epilepsy Unit, Neurology Department, Barcelona, Spain, ² Fundación Jiménez Díaz, Epilepsy Unit, Madrid, Spain, ³ Hospital Clínic, Epilepsy Unit, Neurology Department, Barcelona, Spain

Background and aims: To assess safety and efficacy of cenobamate (CNB) as adjunctive therapy in adult patients with focal onset seizures participating in an early access program.

Methods: We performed a multicenter prospective longitudinal study including adult patients with drug-resistant focal epilepsy who were treated with at least a single dose of CNB as adjunctive therapy in the early access program. We analyzed adverse effects (AE) at 3 and 6 months and responder, seizure free and retention rates at 6 months. Baseline seizure frequency was measured during a 3-month period prior to CNB initiation.

Results: 58 patients were included (mean age 40, range: 19–70; 53.4% women). Median number of previous and concomitant antiseizure medications (ASM) were 9 and 3, respectively. Median dose at 6 months was 200 mg/day (range: 75–400 mg/day). Median seizure frequency per month decreased significantly at 6 months (4 vs 8; $p < 0.001$). 67.5% of patients (25/37) were responders (reduction of >50% seizure frequency) and 8.1% (3/37) were seizure-free at 6 months. Retention rate at 6 months was 85% (34/40). 36/58 patients experienced AE during the titration period at 3 months, and 21/39 at 6 months, the most common being somnolence, unsteadiness and dizziness. 8/58 patients discontinued CNB (3 due to AE, 2 due to lack of efficacy and 3 due to both).

Conclusion: In our series, cenobamate showed a high efficacy as adjunctive therapy in patients with super-refractory focal epilepsy. AE were the typical of other ASM and led to CNB withdrawal in 10% of the patients.

Disclosure: Nothing to disclose.

Movement disorders 2

OPR-083

Scoring Algorithm-Based Genomic Testing in Dystonia: real-life data from the outpatient clinic

E. Indelicato¹, M. Zech², W. Nachbauer¹, A. Eigentler¹, M. Amprosi¹, R. Granata¹, A. Hussl¹, S. Boesch¹

¹ Center for Rare Movement Disorders, Department of Neurology, Medical University of Innsbruck, Innsbruck, Austria, ² Institute of Neurogenetics, Helmholtz Zentrum München, Munich, Germany

Background and aims: A recent multicentric study defined a scoring algorithm to guide the choice of whole exome sequencing (WES) in patients with dystonia. Positive predictors consisted of an age at onset <20 (2 points), segmental/generalized involvement (1 point) and presence of further neurological symptoms (1–2 points). This scoring algorithm has been validated in a second prospectively recruited multicentric cohort. Real-life data from dystonia outpatient clinics are lacking.

Methods: We screened the patients regularly attending the dystonia outpatient clinic of the Innsbruck Medical University, excluding acquired forms (e.g. history of trauma, neuroleptic intakes) and secondary dystonia forms (e.g. oromandibular dystonia or blepharospasms due to atypical parkinsonism). WES studies were performed within a cooperation with the Technical University and the Helmholtz Center, Munich.

Results: We regularly follow 372 patients with primary dystonia. WES was performed in 4/4 patients with score=5, 27/29 patients with score=3–4 and 140/338 patients with score ≤2 (total=171). WES yielded a genetic diagnosis in 3 out of 4 patients with a score of 5 (75%), in 16 out of 27 patients with a score=3–4 (59%) and in 12 out of 140 patients with a score ≤2 (9%).

Conclusion: The diagnostic yield of WES in our dystonia cohort correlated with a higher predictive score. Furthermore, our positivity rates were overall higher than previously described in a unselected prospective cohort (51%, 25% and 2% with a score of 5, 3 to 4 and ≤2 respectively). Our real-life data outline the even greater diagnostic rate of WES in the setting of a clinically well-defined dystonia population.

Disclosure: No disclosures related to the present abstract.

OPR-084

Abstract withdrawn

OPR-085

Survival in monogenic forms of Parkinson's disease: results of a large retrospective study

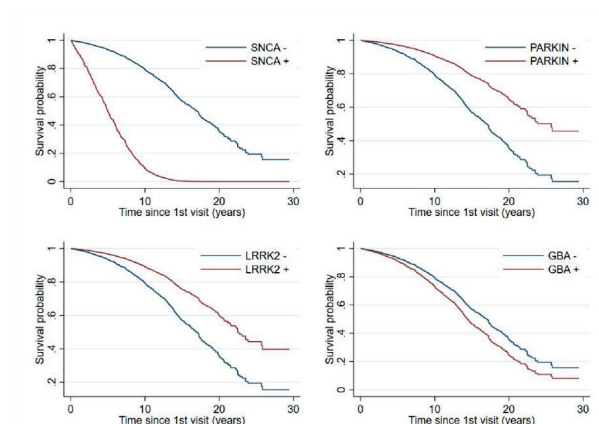
A. Lanore¹, F. Casse², C. Tesson², S. Lesage², L. Mariani¹, G. Mangone¹, S. Sambin¹, P. Menon¹, T. Courtin³, A. Brice³, A. Elbaz⁴, J. Corvol¹

¹ Sorbonne Université, Institut du Cerveau – Paris Brain Institute – ICM, Inserm, CNRS, Paris, France, ² Assistance Publique Hôpitaux de Paris, Department of Neurology, CIC Neurosciences, Hôpital Pitié-Salpêtrière, Paris, France, ³ Assistance Publique Hôpitaux de Paris, Department of genetics, Hôpital Pitié-Salpêtrière, Paris, France, ⁴ Paris-Saclay University, Paris-South University, UVSQ, Center for Research in Epidemiology and Population Health, INSERM, Villejuif, France

Background and aims: Parkinson's Disease (PD) is a neurodegenerative disorder with environmental and genetic determinants. The most common mutations causing PD are in the SNCA, LRRK2, and PRKN genes, while variants in GBA are considered as risk factors. This is the first study comparing mortality in PD patients carrying SNCA, LRRK2, PRKN, or GBA variants.

Methods: Data were retrieved from a large multicentric cohort of PD patients. Multivariable Cox proportional hazards model with time since first visit as the time scale were adjusted for age, sex, time from symptom onset to first visit, and included a random effect to account for intra-familial correlations (shared frailty). Patients were censored at time of death or end of study. The reference group were PD patients without any mutation.

Results: A total of 2,037 patients were included in this analysis, of whom had 890 died during follow up. In the multivariable model, patients with LRRK2 (Hazard ratio of death [HR]=0.5, p=0.028) or PRKN (HR=0.42 p=0.001) mutations had a longer survival than PD patients without mutations, while those with SNCA (HR=10.20, p <0.001) or GBA (HR=1.36, p=0.048) mutations had a shorter survival.



Survival predicted by Cox models according to mutation

Conclusion: Survival from the first visit is increased in LRRK2 and PRKN mutated patients while it is decreased in SNCA and GBA mutated patients compared to PD patients without mutations. The later mortality of LRRK2- and PRKN-mutated patients may be related to slower progression, while the earlier mortality of SNCA- and GBA-mutated patients could be due to faster progression and early development of cognitive impairment.

Disclosure: Nothing to disclose.

OPR-086

Differentiation of Essential and Parkinson's Disease Tremor using time series feature extraction and machine learning

V. Häring¹, V. Selzam¹, R. Peach¹, J. Martin-Rodriguez², P. Schwingenschuh³, G. Tamas⁴, G. Deuschl⁵,

P. Mir Rivera², K. Bhatia⁶, J. Volkmann¹, S. Schreglmann¹

¹ Klinik und Poliklinik Neurologie, Universitätsklinikum Würzburg, Würzburg, Germany, ² Unidad de Trastornos del Movimiento, Servicio de Neurología y Neurofisiología Clínica, Instituto de Biomedicina de Sevilla, Hospital Universitario Virgen del Rocío / CSIC / Universidad de Sevilla, Seville, Spain, ³ Department of Neurology, Medical University of Graz, Graz, Austria, ⁴ Department of Neurology, Semmelweis University, Budapest, Hungary, ⁵ Department of Neurology, Christian Albrechts University, Kiel, Germany, ⁶ Department of Clinical and Movement Neurosciences, Institute of Neurology, UCL, London, United Kingdom

Background and aims: Tremor is a frequent symptom, causing a relevant disease burden in individual patients. In the absence of a bio-marker, diagnostic differentiation between even the most prevalent tremor disorders Essential Tremor (ET) and Parkinson's Disease (PD) is non-trivial. Massive time series feature extraction and machine learning approaches are novel tools to analyse oscillating biological signals. This study aims to explore the utility of combining these two methods to facilitate tremor disorder diagnosis.

Methods: Accelerometer recordings from n=340 patients suffering from ET and PD from four centres have been collated in a single data set. Clinical diagnosis was based on current, recognized diagnostic criteria. After quality control and pre-processing, massive higher-order feature extraction is applied to same length segments of recordings from the more affected hand. Supervised learning is performed using different machine learning algorithms according to clinical diagnosis in order to identify disease-specific features.

Results: Based on the combination of recordings taken at rest and posture, statistical learning based on >7000 extracted features correctly classified up to 86.2% of patients correctly, depending on centre and number of features combined. We evaluate the effects of different machine learning algorithms to further optimize stratification.

Conclusion: This study provides evidence for the usefulness of unbiased tremor signal analysis to differentiate ET and PD tremor. Feature-based tremor analysis has the potential to improve patient care beyond differential diagnostic accuracy, e.g. as a tool to predict treatment response or guide therapeutic interventions.

Disclosure: Authors report no conflict of interest.

OPR-087

Neural correlates of motor and non-motor manifestations in cervical dystonia, revealed by fixel-based analysis

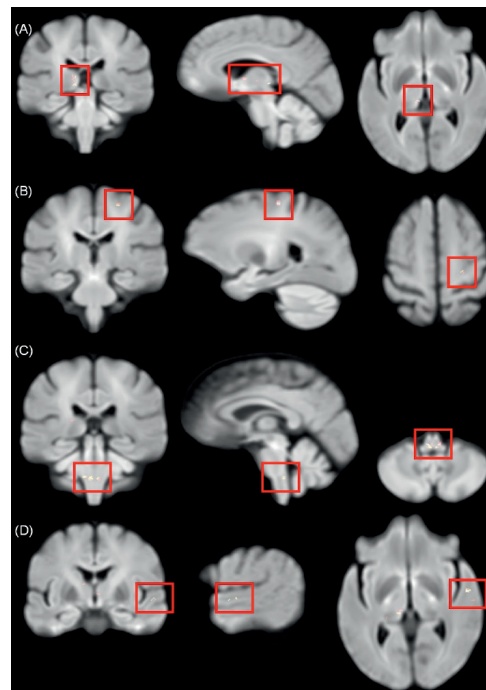
G. Zito ¹, R. Valabregue ², M. Vidailhet ³, C. Gallea ³, E. Roze ³, Y. Worbe ³

¹ Department of Health Sciences and Technology, ETH Zurich, Zurich, CH, ² Center for NeuroImaging Research (CENIR), Paris Brain Institute, Sorbonne University, UPMC Univ Paris 06, Inserm U1127, CNRS UMR 7225, Paris, France, ³ Sorbonne University, Inserm U1127, CNRS UMR7225, UM75, Paris Brain Institute, Movement Investigation and Therapeutics Team, Paris, France,

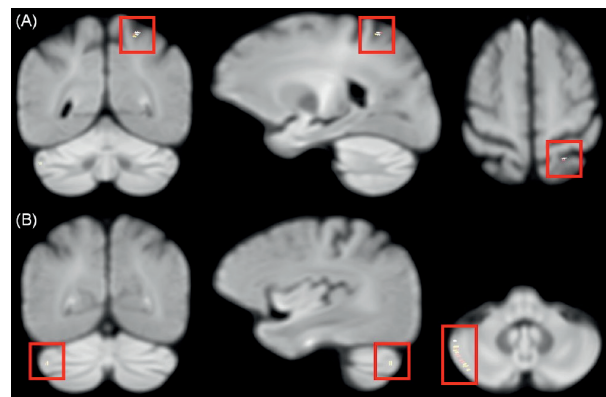
Background and aims: Cervical dystonia (CD) is a form of isolated focal dystonia, characterized by abnormal head posture. It is often accompanied by psychiatric symptoms, such as depression, and its pathophysiology has been linked to large-scale brain networks abnormalities. However, the specific neural correlates of motor and psychiatric manifestations, respectively, are still unknown. We analyzed patterns of white matter fibers in CD, and investigated the brain networks associated with abnormal head posture and psychiatric symptoms.

Methods: 18 CD patients and 21 healthy controls had diffusion weighted imaging (DWI). We applied fixel-based analysis, a novel method able to extract multiple populations of fibers within the same voxel, and thus account for fiber orientation across voxels. We compared white matter fibers between CD patients and controls, and correlated them with the severity of dystonia (Toronto Western Spasmodic Torticollis Rating Scale - TWSTRS), and depression (Beck Depression Inventory - BDI), respectively, in patients.

Results: Compared to controls, patients showed decreased white matter fibers in the basal ganglia and sensorimotor areas, as well as in the superior temporal regions and the brainstem (Figure1). TWSTRS scores negatively correlated with white matter in the superior parietal lobule, whereas BDI showed positive correlation with associative cerebellar areas, such as the crus 1 (Figure2).



Significant clusters of decreased white matter fibers in CD patients in: (A) the basal ganglia, (B) the sensorimotor regions, (C) the brainstem, and (D) and temporal areas.



Significant clusters of white matter fibers in CD patients showing: (A) positive correlation with BDI scores, and (B) negative correlation with TWSTRS.

Conclusion: We identified distinct patterns of neural correlates associated with motor and non-motor manifestations of CD. A loss of inhibitory output from the basal ganglia may propagate to several functional networks beyond the motor system. This may result in a progressive maladaptive plasticity, and culminate in overt symptoms of dystonia.

Disclosure: The authors declare no conflict of interest.

OPR-088

Personality and Early Parkinson's disease phenotypes

B. Meira¹, E. Lhommée¹, E. Schmit², H. Klinger³, A. Bichon², P. Péliissier¹, M. Anheim⁴, C. Tranchant⁴, V. Fraix², S. Meoni², F. Durif⁵, J. Houet⁶, J. Azulay⁷, E. Moro², S. Thobois³, P. Krack⁸, A. Castrioto²

¹ Movement disorders Center, Neurology, CHU Grenoble Alpes, Grenoble, France, ² Université Grenoble Alpes, Inserm, U1216, CHU Grenoble Alpes, Grenoble Institut Neurosciences, 38000 Grenoble, France, ³ Hospices Civils de Lyon, Hôpital Neurologique Pierre Wertheimer, Neurologie C, Centre Expert Parkinson, Lyon, France, ⁴ Département de neurologie, Hôpital de Haute-pierre, Hôpitaux Universitaires de Strasbourg, Strasbourg, France, ⁵ Université Clermont Auvergne, EA7280 NPsy-Sydo, Clermont-Ferrand University Hospital, Neurology Department, Clermont-Ferrand, France, ⁶ Service de Neurologie, Centre Expert Parkinson, CHU de Limoges, UMR1094 INSERM, Université de Limoges, Limoges, France, ⁷ Neurology and Pathology Department of the Movement, University Hospital of Marseille, Timone Hospital, Marseille, France, ⁸ Department of Neurology, Inselspital, University Hospital Bern, CH-3010, Bern, Switzerland

Background and aims: Although there is a previous description of a parkinsonian personality characterized as rigid, introverted, and cautious, little is known about personality traits in de novo Parkinson's disease (PD) patients and their relationships with motor and neuropsychiatric symptoms. We intend to investigate these two questions.

Methods: The personality of 193 de novo PD patients was assessed using Cloninger's biosocial model and motor and non-motor symptoms using several clinical scales. We conducted correlations and cluster analysis to investigate the relationship between personality traits, motor, and non-motor symptoms.

Results: PD patients have low novelty seeking, high harm avoidance, and normal reward dependence and persistence scores. Harm avoidance was positively correlated with depression, anxiety, and apathy ($r_s = [0.435, 0.676]$, $p < 0.001$) and negatively correlated with quality of life ($r_s = -0.492$, $p < 0.001$). Novelty seeking, reward dependence, and persistence were negatively correlated with apathy ($r_s = [-0.274, -0.375]$, $p < 0.001$). Cluster analysis revealed 3 distinct clusters: i) neuropsychiatric phenotype (with high harm avoidance, low novelty seeking, and hypodopaminergic neuropsychiatric symptoms), ii) motor phenotype (with low novelty seeking and higher motor severity), iii) benign phenotype (low harm avoidance and high novelty seeking, reward dependence, and persistence traits clustered with lower symptoms severity and low impulsivity).

Conclusion: Personality in de novo PD seems to play a role in the presence of different clinical phenotypes with harm avoidance and novelty seeking traits having a higher impact on susceptibility to mood disorders. Identification of different PD subgroups may help to investigate if some personality features might influence disease evolution and treatment.

Disclosure: All authors declare absence of commercial or financial relationships that could be construed as potential conflicts of interest.

Neuroimaging 2

OPR-089

Longitudinal whole-brain metabolic network changes following acute unilateral vestibulopathy

A. Zwergal¹, M. Grosch¹, H. Buchholz², S. Ziegler³, T. Brandt¹, M. Dieterich¹, S. Becker-Bense¹

¹ German Center for Vertigo and Balance Disorders, LMU Munich, Germany ² Department of Nuclear Medicine, University of Mainz, Germany ³ Department of Nuclear Medicine, LMU Munich, Germany

Background and aims: Symptoms of acute unilateral vestibulopathy (AUV) partially recover due to adaptive brain plasticity. In this study, we analysed whole-brain metabolic connectivity changes after AUV by longitudinal 18F-FDG-PET imaging.

Methods: 22 patients with AUV underwent resting state 18F-FDG-PET scans in the acute phase (mean: 6d) and after partial behavioural compensation (mean: 6m). PET data were compared to 22 matched controls. Images were flipped reconstructed, registered, filtered, normalized, and segmented (AAL2/3 atlas). Pearson's correlations between all segmented brain regions were performed ($r > 0.5$ / $p < 0.001$). Functional metabolic connections between/ within hemispheres, and in vestibular/multisensory/motor/ cognitive were calculated.

Results: Patients had severe vestibular asymmetry in the acute stage (mean horizontal slow-phase velocity (SPV): 9.9°/sec, subjective visual vertical (SVV): 7.6°), which recovered until 6m after AUV (SPV: 0.7°/sec, SVV: 1.7°). As compared to controls, whole-brain metabolic network analysis indicated a significant drop in the total number of connections, in interhemispheric projections between homotopic regions and especially in vestibular and multisensory cortical networks in the acute stage. In the chronic stage, the asymmetry in interhemispheric connections of homotopic regions persisted. Multisensory network connectivity relatively increased in the ipsilesional hemisphere compared to the early stage. Patients with a persistent caloric vestibular deficit had a higher asymmetry index compared to those with reconstituted peripheral function.

Conclusion: AUV disrupts the symmetry of multisensory metabolic networks between hemispheres persistently and mostly in patients with a chronic peripheral vestibular deficit. These data may be important for the understanding of higher sensory network dysfunction and conversion risk to functional dizziness after AUV.

Disclosure: Nothing to disclose.

OPR-090

A Deep-Learning Approach to Predicting Disease Progression in Multiple Sclerosis Using Magnetic Resonance Imaging

L. Storelli¹, M. Azzimonti¹, M. Gueye¹, C. Vizzino¹, P. Preziosa¹, G. Tedeschi², N. De Stefano³, P. Pantano⁴, M. Filippi⁵, M. Rocca⁵

¹ Neuroimaging Research Unit, Division of Neuroscience, IRCCS San Raffaele Scientific Institute, Milan, Italy;

² Department of Advanced Medical and Surgical Sciences, and 3T MRI-Center, University of Campania "Luigi Vanvitelli", Naples, Italy; ³ Department of Medicine, Surgery and Neuroscience, University of Siena, Siena, Italy;

⁴ Department of Human Neurosciences, Sapienza University of Rome, Rome, Italy; and IRCCS NEUROMED, Pozzilli, Italy;

⁵ Neuroimaging Research Unit, Division of Neuroscience, and Neurology Unit, IRCCS San Raffaele Scientific Institute, and Vita-Salute San Raffaele University, Milan, Italy

Background and aims: In this study, we developed an artificial intelligence deep-learning algorithm on a large multicenter cohort of MS patients collected from the Italian Neuroimaging Network Initiative (INNI) to predict disease evolution (based on clinical disability and cognitive impairment) at two-years of follow-up from their baseline MRI features. The performance of the algorithm was then evaluated on an independent test-set and compared to that of two expert physicians.

Methods: For 373 patients, baseline T2-weighted and T1-weighted brain MRI, as well as baseline and two-year clinical and cognitive assessments were collected from the INNI repository. A deep-learning architecture based on convolutional neural networks was implemented (Fig. 1) to predict: (1) clinical worsening (Expanded Disability Status Scale [EDSS]-based model), (2) cognitive deterioration (Symbol Digit Modalities Test [SDMT]-based model), or (3) both (EDSS+SDMT-based model). The method was tested on an independent dataset and compared to the performance of two expert physicians.

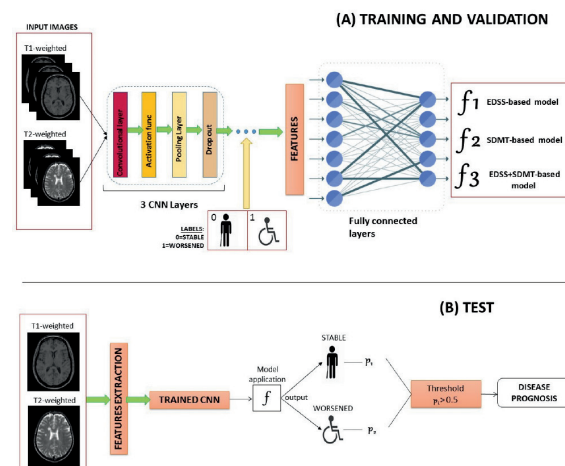


Fig. 1: A schematic overview of the deep-learning network architecture implemented to train and optimize the model (in A), and to finally test it on an independent dataset (in B).

Results: For the independent test-set, the model showed high predictive accuracy for clinical (83.3%) and cognitive (67.7%) worsening, although the highest accuracy was reached when training the algorithm using both EDSS and SDMT information (85.7%). Artificial intelligence classification performance exceeded that of two expert physicians (70% of accuracy for the human raters).

Conclusion: We developed a robust and accurate model for predicting clinical and cognitive worsening of MS patients after two years, based on conventional brain T2-weighted and T1-weighted baseline MRI. This algorithm may be valuable for supporting physicians in their clinical practice for the earlier identification of MS patients at risk of disease worsening.

Disclosure: This study was partially supported by Fondazione Italiana Sclerosi Multipla with a research fellowship (FISM 2019/BR/009) and research grants (FISM2018/R/16; FISM2018/S/3), and financed or co-financed with the '5 per mille' public funding.

OPR-091

Functional brain connectome in ventral and dorsal variants of posterior cortical atrophy

E. Canu¹, F. Agosta², M. Magno¹, S. Basaia¹, C. Cividini², F. Caso¹, G. Magnani¹, M. Montembeault³, R. Levy⁴, R. Migliaccio⁴, M. Filippi²

¹ IRCCS San Raffaele Scientific Institute, Milan, Italy,

² IRCCS San Raffaele Scientific Institute, and Vita-Salute San Raffaele University, Milan, Italy, ³ University of California in San Francisco, San Francisco, United States of America, ⁴ Sorbonne Université, and Hôpital de la Pitié Salpêtrière, Paris, France

Background and aims: The study aims at investigating the functional brain connectome architecture in patients with ventral (vPCA) and dorsal (dPCA) variant of posterior cortical atrophy (PCA).

Methods: 36 PCA patients and 69 healthy controls underwent neurologic and cognitive examinations, and a brain MRI. Patients were categorized in vPCA (N=19) and dPCA (N=17) variants based on the symptoms prevalence, and were matched for age, sex, education, MMSE and disease duration. Topological brain network properties and regional functional connectivity (FC) were compared between groups using graph analysis and connectomics.

Results: Relative to controls, only vPCA patients showed global functional network alterations. Lobar network analysis showed common alterations of nodal strength within the occipital area in all PCA patients compared with controls, while vPCA showed additional involvement of temporal, parietal and occipital areas. No differences were observed between PCA variants. At the regional level, compared to controls, each PCA variant showed diffuse FC breakdown. Compared to dPCA, vPCA patients showed further FC breakdown within the occipital and parietal lobe, and between frontal, sensorimotor nodes and basal ganglia.

Conclusion: Our findings suggest the potentially high sensitivity of graph-analysis and connectomic in capturing signs of neurodegeneration in PCA variants. With sociodemographic and clinical features being equal, the vPCA group showed a more severe pattern of FC breakdown. Longitudinal investigations are needed to understand whether patterns associated with each PCA variant are able to predict distinct disease trajectories.

Disclosure: Supported by: Italian Ministry of Health (#GR-2010-2303035; #GR-2011-02351217), Philippe Chatrier and France Alzheimer Foundations, Fondation pour la Recherche sur Alzheimer.

OPR-092

Association of the Frailty Index with structural brain volumes in The Irish Longitudinal Study on Ageing (TILDA)

R. Gutierrez Zuñiga ¹, J. Davis ², C. De Looze ², D. Carey ², J. Meany ³, A. O'Halloran ², R. Kenny ², R. Romero Ortuño ², S. Knight ²

¹ Global Brain Health Institute (GBHI), Trinity College Dublin, Ireland, ² The Irish Longitudinal Study on Ageing (TILDA), School of Medicine, Trinity College Dublin, the University of Dublin, Dublin, Ireland, ³ The National Centre for Advanced Medical Imaging (CAMI), St. James's Hospital, Dublin, Ireland

Background and aims: Frailty is a recognised state of vulnerability in older adults. The Frailty Index (FI) measures frailty according to 32 deficits across multiple domains (Table 1) that accumulate with age and could have an impact in brain health. Our aim was to study brain volume signatures of a FI in The Irish Longitudinal Study on Ageing (TILDA).

Methods: We included TILDA wave 3 participants aged 65+ years who took part in a 3T MRI sub-study. Using Freesurfer we measured total cortical grey matter (GM) volume and regional GM volumes according to the Desikan-Killiany atlas. We performed partial correlation analyses with FI and Desikan GM regions volumes adjusted by age, sex and total brain volume; and performed a partial correlation tests to compare total cortical GM volume with each FI item adjusted by age and sex.

Results: In 407 participants, the volumes of regions related with prefrontal cortex and temporal cortex were negatively correlated with the FI and positive correlated with left precuneus (Figure 1). Only FI deficits related with functional impairments, osteoporosis and polypharmacy were associated with total cortex volume (Table 1).

FI item	R	p	FI item	R	p
Difficulty walking 100 m	-0.116	0.020	Cataracts	-0.088	0.079
Poor self rated physical health	-0.098	0.050	Arthritis	-0.014	0.785
Poor self rated vision	-0.110	0.028	Osteoporosis	-0.015	0.764
Poor self rated hearing	-0.107	0.031	Cancer	-0.003	0.946
Daytime sleepiness	-0.068	0.170	Varicose ulcer	-0.007	0.885
Polypharmacy	-0.103	0.038	Difficulty climbing one flight of stairs	-0.029	0.562
Knee pain	-0.114	0.022	Glaucoma/Age related macular degeneration	-0.057	0.256
Urinary incontinence	0.020	0.696	Self rated day-to-day memory	-0.006	0.911
Hypertension	0.008	0.865	Difficulty following a conversation with four people	-0.109	0.028
Angina	0.014	0.775	Difficulty stooping, kneeling or crouching	-0.075	0.131
Heart attack	-	-	Difficulty reaching above shoulder height	-0.088	0.078
Difficulty rising from a chair	-0.022	0.664	Difficulty pushing/pulling large objects	-0.052	0.301
Diabetes	-0.085	0.087	Difficulty lifting/carrying weights >=10lb	-0.042	0.405
High cholesterol	0.032	0.518	Difficulty picking up coin from table	-0.007	0.887
Irregular heart rhythm	0.035	0.479	Feeling lonely	0.026	0.605
Other CVD	-0.043	0.393	Stroke or TIA	-	-

Table 1. Differences in global cortex volume for each item within FI.

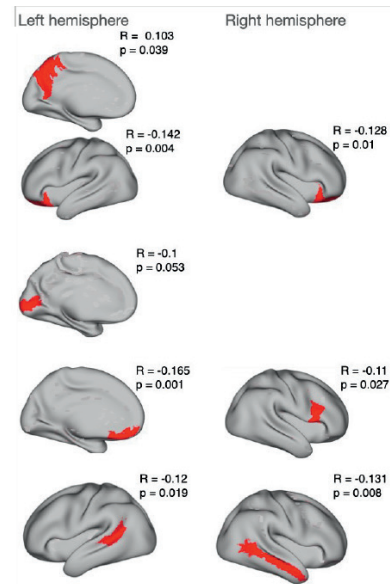


Figure 1. Significant partial correlation coefficient for brain volume by region and FI, adjusted by age, sex and total brain volume.

Conclusion: From a volumetric perspective, results suggest that frailty as captured by a FI may primarily involve the visual-executive-planification coordination systems. Further studies are necessary to replicate this finding with other FIs; compare associations with other frailty measurement tools; complement analyses with connectivity studies. A better understanding of the neuro correlates underlying frailty in older adults is needed for better prevention and treatment of age-related disability.

Disclosure: Nothing to disclose.

OPR-093

White matter microstructural changes in healthy aging: a DTI and NODDI study

S. Basaia¹, C. Cividini², F. Guarnaccia³, E. Spinelli², M. Filippi², F. Agosta²

¹ IRCCS San Raffaele Scientific Institute, Milan, Italy,

² IRCCS San Raffaele Scientific Institute, and Vita-Salute San Raffaele University, Milan, Italy, ³ IRCCS San Raffaele Scientific Institute, Milan, Italy

Background and aims: The goal of this study was to assess white matter (WM) integrity changes associated with aging using different diffusion metrics in a cohort of young and older adults.

Methods: 48 young (YC), aged 20–31 years, and 65 old controls (OC), aged 40–85 years, were enrolled and underwent multi-shell diffusion MRI. Fractional anisotropy (FA) and mean diffusivity (MD) maps were computed. Furthermore, Intra-cellular Volume Fraction (ICVF), Orientation Dispersion Index (ODI) and Isotropic Volume Fraction (ISO) maps were estimated using the NODDI model. Tract-Based Spatial Statistic analysis assessed significant metrics variability between the two groups ($p < 0.05$, family-wise error corrected, 5,000 permutations).

Results: A widespread age-related reduction of FA was detected in supratentorial regions in OC relative to YC. A focal decrease of ICVF was found in OC relative to YC in the WM frontal fibers, specifically in the anterior sub-regions of corpus callosum, anterior corona radiata, frontal fibers of the superior longitudinal fasciculus, inferior fronto-occipital fasciculus and uncinate fasciculus. A widespread increase of MD and ISO was observed in OC relative to YC replicating the widespread WM alteration pattern obtained by FA results. Furthermore, an increased ODI of the WM fibers in OC relative to YC was identified, involving not only the supratentorial regions but also the cerebellar architecture.

Conclusion: The information provided by multi-shell diffusion MRI acquisition and multi-model reconstruction allowed us to quantify the extent of WM architecture deterioration with aging. Multiple diffusion metrics may lead to a reliable profiling of the healthy brain aging.

Disclosure: Supported by European Research Council (StG-2016_714388_NeuroTRACK).

Neurotraumatology

OPR-094

tDCS in patients with disorders of consciousness: a multicentre randomized double-blind sham-controlled clinical trial

A. Thibaut¹, G. Martens¹, A. Estraneo², S. Fiorenza², E. Noe³, R. Llorens³, R. Formissano⁴, G. Morone⁴, A. Bender⁵, M. Rosenfelder⁵, G. Lamberti⁶, E. Kodratyeva⁷, L. Legostaeva⁸, C. Krewer⁹, F. Müller⁹, N. Lejeune¹⁰

¹ Coma Science Group, GIGA-Consciousness & Centre du Cerveau2, University & University Hospital of Liège, Belgium, ² Don Carlo Gnocchi Foundation, Scientific Institute for Research and Health Care, Neurorehabilitation Dept, Florence, Sant'Angelo dei Lombardi, Italy, ³ Neurology Unit, Santa Maria della Pietà General Hospital, Nola, Italy, ⁴ Santa Lucia Foundation, Neurorehabilitation and Scientific Institute for Research and, Rome, Italy, ⁵ Therapiezentrum Burgau, Burgau, Germany, ⁶ Neurorehabilitation and Vegetative State Unit E. Viglietta, Cuneo, Italy, ⁷ Almazov National Medical Research Center, Saint-Petersburg, Russian Federation, ⁸ Research Center of Neurology, Moscow, Russian Federation, ⁹ Schoen Clinic Bad Aibling, Bad Aibling, Germany, ¹⁰ Centre Hospitalier Neurologique William Lennox, Ottignies-Louvain-la-Neuve, Belgium

Background and aims: Left dorsolateral prefrontal cortex (LDLPFC) transcranial direct current stimulation (tDCS) has shown to transiently improve the level of consciousness of severely brain-injured patients with disorders of consciousness (DOC). However, no large-sample multicenter study confirmed its efficacy.

Methods: In this sham-controlled double-blind randomized trial, we investigated whether 4 weeks of tDCS improves consciousness/responsiveness in patients in prolonged DOC during rehabilitation stay. LDLPFC-tDCS was applied for 20 days (five days per week). We used the Coma Recovery Scale-Revised (CRS-R) weekly and up to 3-months follow-up. We used a mixed general linear model to evaluate behavioral changes (4-week and 3-month) between active and sham groups. Differences between baseline and week-4 and month-3 were analyzed with a Mann-Whitney test.

Results: 62 patients (18 women, 30 MCS, 39 non-TBI, 260±171 days post-injury, 33 active-tDCS) were treated without any serious adverse events. At the group level, no treatment effect was found. Subgroup analyses revealed a significant improvement for the active compared to the sham group for MCS ($p=0.015$) and TBI ($p=0.023$). No other comparisons were significant.

Conclusion: Our results suggest that at the group level, tDCS applied during rehabilitation does not significantly enhance patients' signs of consciousness. On the other hand, at 3-month follow-up, the subgroups of MCS and TBI patients demonstrated a better recovery in the treated compared to the sham groups. tDCS should be specifically applied in this subgroups of patients to promote their recovery.

Disclosure: Nothing to disclose.

OPR-095

Early post-traumatic seizures in hospitalized patients with traumatic brain injury

H. Sødal¹, G. Storvig², C. Tverdal¹, H. Robinson³, E. Helseth⁴, E. Taubøll⁵

¹ Institute of Clinical Medicine, Faculty of Medicine, University of Oslo, Oslo, Norway, ² Department of Psychology, Faculty of Social and Educational Sciences, Norwegian University of Science and Technology, Trondheim, Norway, ³ Institute of Health and Society, Faculty of Medicine, University of Oslo, Oslo, Norway, ⁴ Department of Neurosurgery, Oslo University Hospital, Oslo, Norway, ⁵ Department of Neurology, Oslo University Hospital, Oslo, Norway

Background and aims: Early post-traumatic seizures (EPTS) are a well-known complication of traumatic brain injury (TBI). EPTS increase the risk of secondary brain injury and are associated with worse outcomes. Use of seizure prophylaxis medication to prevent EPTS is controversial and not routine in many countries, including Norway. The purpose of this study was to expand the understanding of EPTS by examining incidence and risk factors in hospitalized TBI-patients.

Methods: Adult patients with TBI and neuroradiological evidence of intracranial injury admitted to Oslo University Hospital between 2015 and 2019 were identified from the Oslo TBI Registry – Neurosurgery. Demographic and clinical data including occurrence of seizures were retrieved from the registry. Univariate and multivariable logistic regression analyses were used to investigate risk factors associated with EPTS.

Results: 103 of 1.827 patients (5.6%) had new-onset seizures within the first week after TBI. Alcohol abuse [odds ratio 3.6 (95% confidence interval: 2.3–5.7), $p<0.001$], moderate and severe brain injury [2.2 (1.3–3.8), $p=0.004$ and 2.1 (1.2–3.6), $p=0.012$], brain contusion [1.6 (1.0–2.4), $p=0.046$] and subdural hematoma [1.6 (1.0–2.6), $p=0.052$] were associated with EPTS in the multivariable model.

Conclusion: In our material, EPTS occurred in 5.6% of hospital-admitted patients with TBI. Chronic alcohol abuse was the most significant independent risk factor, followed by moderate and severe brain injury. The results contribute to the discussion about preventive treatment of EPTS in certain risk groups.

Disclosure: None of the authors has any conflict of interest to disclose.

OPR-096

Autonomic dysfunction after moderate-severe traumatic brain injury: symptom spectrum and clinical testing outcomes

L. Li¹, E. Vichayanrat², M. Del Giovane³, H. Lai³, V. Iodice²

¹ Division of Brain Sciences, Imperial College London, United Kingdom, ² National Hospital of Neurology and Neurosurgery/UCL, London, United Kingdom, ³ UK DRI Centre for Care Research & Technology, Imperial College London, United Kingdom

Background and aims: Survivors of moderate-severe traumatic brain injury (msTBI) frequently experience troublesome unexplained somatic symptoms. Autonomic dysfunction may contribute to these symptoms. We aimed to provide a clinical description of subjective and objective autonomic dysfunction in msTBI.

Methods: We conducted two cohort studies. Cohort 1 comprises msTBI patients (with a control group) prospectively recruited from a regional referral TBI outpatient clinic, in whom we assessed burden of autonomic symptoms using the Composite Autonomic Symptom Score (COMPASS31) questionnaire. Cohort 2 comprises msTBI patients who had standard clinical autonomic function testing, retrospectively identified from referrals to a national referral autonomies unit.

Results: Cohort 1 comprises 39 msTBI patients (10F:20M, median age 40 years, range 19-76), with median time since injury 19 months (range 6–299), and 44 controls (22F:22M, median age 45, range 25–71). Patients had significantly higher mean scores than controls in the weighted total COMPASS-31 score ($p < 0.001$) (Figure 1), and also gastrointestinal, orthostatic and secretomotor subscores (corrected $p < 0.05$) (Figure 2). Total COMPASS31 score inversely correlated with subjective rating of general health ($p < 0.001$, $r_s = -0.84$). Cohort 2 comprises 18 msTBI patients (7F:11M, median age 44 years, range 21-64), with median time between injury and testing 57.5 months (range 2-416). Clinical autonomic function testing revealed a broad spectrum of autonomic dysfunction in 13/18 patients (Figure 3).

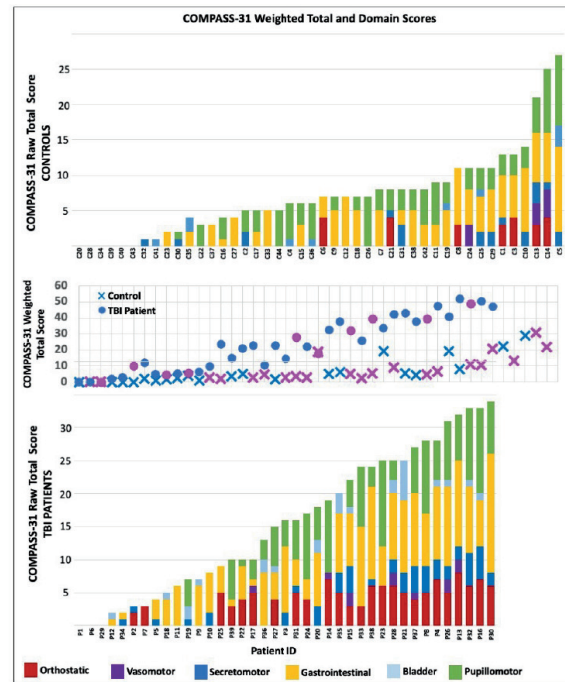


Fig. 1: Symptom burden, with weighted total COMPASS31 score for each patient (middle panel: circles=controls, crosses=TBI & pink=female, blue=male) and corresponding domain subscore distribution (top panel controls, bottom panel TBI).

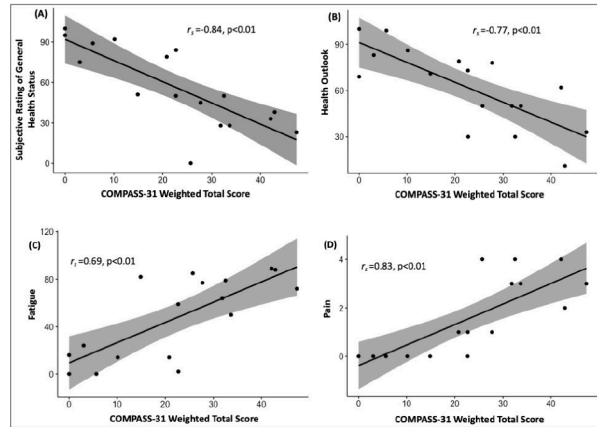


Fig. 2: Relationship between the COMPASS-31 weighted total score and (A) subjective rating of general health status, (B) Health Outlook, (C) Fatigue and (D) Pain.

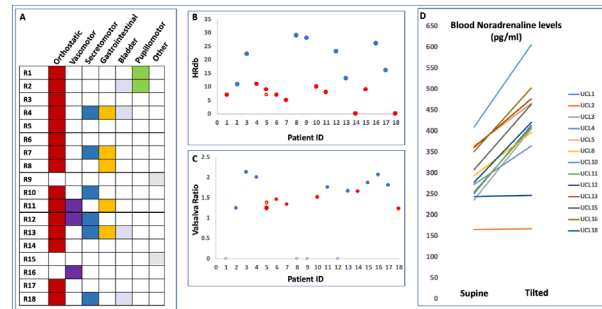


Fig. 3: For each patient (A) reported symptom types, (B) HRDB, measuring respiratory sinus arrhythmia. (C) Valsalva ratio. (D) Supine and tilted blood noradrenaline levels, where available. Red denotes abnormal for age.

Conclusion: Our results provide evidence for clinically relevant autonomic dysfunction after moderate-severe TBI, even at the chronic stage. We advocate for routine enquiry about potential autonomic symptoms, and demonstrate the utility of formal autonomic testing in providing diagnoses.
Disclosure: Nothing to disclose.

OPR-097

CT scans in acute traumatic brain injury: high interrater agreement in the emergency settings and during follow-up

I. Komoltsev¹, M. Sinkin⁷, A. Timokhova³, M. Makhmudov⁵, F. Rider³, S. Burkitbaev¹, I. Samotaeva¹, N. Semenovykh³, R. Luzin³, L. Khamidova², A. Yakovlev¹, A. Talygov², W.A. Hauser⁴, N. Gulyaeva¹, A. Guekht⁵, V. Krylov⁶

¹ Moscow Research and Clinical Center for Neuropsychiatry, Moscow, Russia and Institute of Higher Nervous Activity and Neurophysiology, Moscow, Russian Federation,

² Sklifosovsky Research Institute of Emergency Care, Moscow, Russian Federation, ³ Moscow Research and Clinical Center for Neuropsychiatry, Moscow, Russian Federation, ⁴ Gertrude H. Sergievsky Center, College of Physicians and Surgeons, Columbia University, New York, NY, USA, ⁵ Moscow Research and Clinical Center for Neuropsychiatry, Moscow, Russia and Pirogov Russian National Research Medical University, Moscow, Russian Federation, ⁶ Moscow State University of Medicine and Dentistry, Moscow, Russian Federation, ⁷ Sklifosovsky Research Institute of Emergency Care, Moscow, Russia and Moscow State University of Medicine and Dentistry, Moscow, Russian Federation

Background and aims: Proper evaluation of computer tomography (CT) scans is crucial for prognosis of traumatic brain injury (TBI) outcome and treatment strategy choice; however, in the acute settings it should be done within a limited time period. We evaluated interrater agreement (IRA) of CT findings between interpretation of radiologists in emergency department at time of injury and compared to subsequent readings by radiologists free of time constraints.
Methods: We retrospectively evaluated brain CT scans of 53 patients with acute TBI, performed a non-reference interrater variability test and calculated Cohen's kappa score to compare scan analysis in emergency settings ("A" team) and in the follow up ("R" team).

Results: We found no statistically significant differences in the proportion of positive and negative findings between "A" and "R" team either by type of pathology or its combinations, or by time of day when acute assessment was performed. The highest IRA reaching 100% was observed for depressed skull fracture, epidural hematoma, and intraventricular hemorrhage (Fig. 1). For a linear skull fracture, subdural hematoma, and SAH we also found good IRA: Cohen's Kappa (k) was 0.89, 0.88 and 0.81 respectively. Moderate IRA rate was observed for brain concussions (k=0.58). In most cases, missing findings could be explained by small size and specific location of lesions.

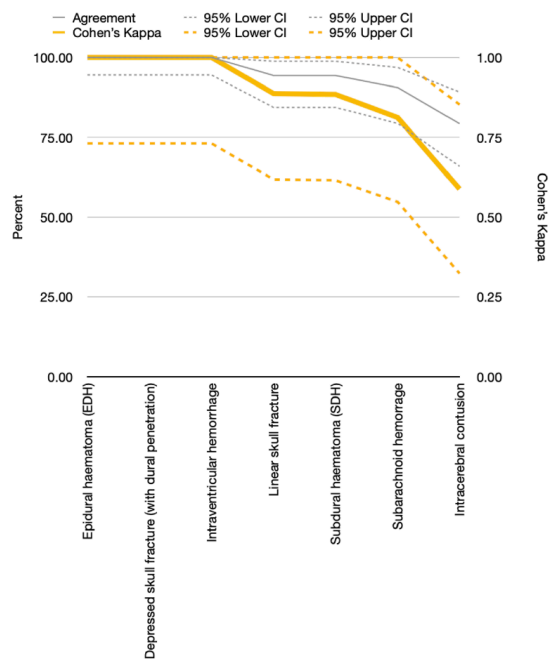


Figure 1. Cohen's Kappa for different type of pathology, analyzed in emergency settings and in the follow-up.

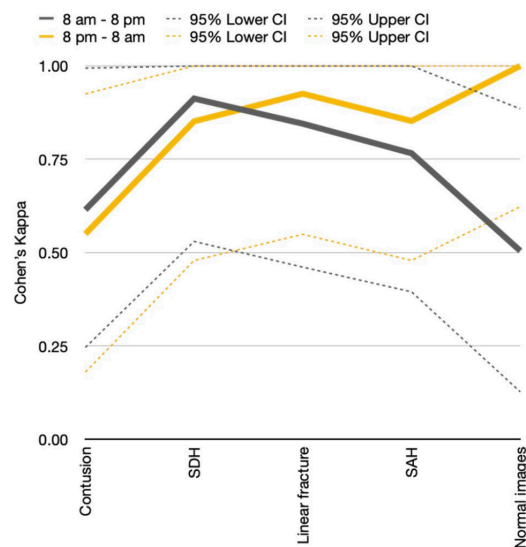


Figure 2. Cohen's Kappa for different type of pathology, analyzed in emergency settings by time of day when acute assessment was performed, and in the follow-up.

Conclusion: The interrater agreement demonstrated that despite time constraints, evaluation of TBI CT scans in emergency settings allows to correctly identify most lesions.
Disclosure: Nothing to disclose.

OPR-098

Risk of traumatic brain haemorrhage in patients on direct oral anticoagulant drugs (DOAC) or vitamin K antagonists (VKA)

K. Laufer¹, K. Petek¹, S. Rakusa², A. Cretnik³,
M. Rakusa²

¹ Faculty of Medicine, University of Maribor, Maribor, Slovenia, ² Department of Neurological Diseases, University Medical Centre Maribor, Maribor, Slovenia, ³ Department of Traumatology, University Medical Centre Maribor, Maribor, Slovenia

Background and aims: Patients on DOAC or VKA may have an increased risk for Intracranial haemorrhage (ICH) and poor clinical outcomes after mild traumatic brain injury (mTBI). Our aim was to evaluate the risk, incidence and clinical characteristics of ICH in patients who sustained mTBI.

Methods: We collected demographic data and clinical characteristics from the medical records of the 420 consecutive patients and compared them between patients with and without haemorrhage. In the end, we calculated risks and odd-ratio for haemorrhage and DOAC/VKA.

Results: In total, 35 received anticoagulant therapy, and 55 had traumatic haemorrhage (46 had no treatment, 4 VKA, 5 DOAC). Patients with haemorrhages were older (66.1 SD 19.6 vs 56.8 SD 24.5 years), stayed in the hospital longer (12.6 SD 14.7 vs 7.2 SD 11.5 days), had higher initial blood sugar (7.7 SD 7.6 vs 6.8 SD 2.3 mmol/L), lower GCS (14.0 SD 2.7 vs 14.7 SD 0.9) and higher mRS at the admission (0.5 SD 1.4 vs 0.2 SD 0.7) and the discharge (1.9 SD 1.9 vs 1.2 SD 1.5). The absolute risk for haemorrhage for DOAC was 9.1%, and for VKA 7.3%, the relative risk was 0.6 and 0.3, and odds-ratio 1.82 (95% CI 0.65 to 5.10) and 2.45 respectively (95% CI 1.08 to 5.53).

Conclusion: The overall risk and incidence for intracranial haemorrhage after mild traumatic brain injury was low. Although the odds ratio for ICH was lower for patients on DOAC than for those on VKA, the difference was insignificant.

Disclosure: Nothing to disclose.

Monday, June 27, 2022

Neurocritical care

OPR-099

Consciousness in Neurocritical Care Cohort Study Using fMRI and EEG (CONNECT-ME): Level of consciousness in ICU

M. Amiri¹, P. Fisher², A. Sidaros³, M. Cacic Hribljan³, I. Zibrandtsen³, M. Othman¹, E. Waldemar Jakobsen¹, S.S. Albrechtsen¹, M. Harboe Olsen⁴, V. Nersesjan⁵, V. Andrée Larsen⁶, J. Lilja S. Højgaard¹, M. Nolic³, J. Hauerberg⁷, C. Hassager⁸, J. Møller⁸, C. Sølling⁴, H. Ravnholt Jensen⁴, F. Raimondo⁹, J.D. Sitt⁹, M. Ejler Fabricius³, G. Moos Knudsen², J. Kjærgaard⁸, K. Møller⁴, D. Kondziella¹

¹ Department of Neurology, Rigshospitalet, Copenhagen, Denmark, ² Neurobiology Research Unit, Rigshospitalet, Copenhagen, Denmark, ³ Department of Neurophysiology, Rigshospitalet, Copenhagen, Denmark, ⁴ Department of Neuroanesthesiology, Rigshospitalet, Copenhagen, Denmark, ⁵ Biological and precision psychiatry at the Copenhagen research center for mental health, Copenhagen University Hospital, Denmark, ⁶ Department of Radiology, Rigshospitalet, Copenhagen, Denmark, ⁷ Department of Neurosurgery, Rigshospitalet, Copenhagen, Denmark, ⁸ Department of Cardiology, Rigshospitalet, Copenhagen, Denmark, ⁹ Institut du Cerveau et de la Moelle Epinière, Paris, France

Background and aims: Functional MRI (fMRI) and EEG in clinically unresponsive patients may reveal signs of covert consciousness. Research in so-called cognitive motor dissociation is primarily based on data from patients with chronic disorders of consciousness (DoC). CONNECT-ME aims to explore and facilitate individualized multimodal assessment for signs of residual consciousness in patients with acute and subacute DoC, using fMRI and EEG in the intensive care unit (ICU).

Methods: We assessed 87 acutely brain-injured adult patients for residual consciousness by clinical evaluation, fMRI (resting-state) and EEG (resting-state and passive stimulations), between 2016–2020. EEG and fMRI data were used as features in a cross-validated machine learning (ML) framework to predict level of consciousness (LoC) during ICU admission. Area under the curve (AUC) of ROC curves was used for comparison of prediction performance.

Results: Of 87 patients (50.0±18 years, 43% women), 51 (59%) were clinically in coma/unresponsive wakefulness (UWS) and 36 (41%) in minimally consciousness state (MCS) or better. During ICU-admission, 31 (36%) patients died, of whom 29 (94%) were in coma/UWS with main cause of death being withdrawal of life-sustaining-therapy due to poor prognosis (n=28). EEG was available for 86 patients, and fMRI for 64 patients. EEG visual, spectral and ML-derived characteristics predicted LoC (coma/UWS vs. ≥MCS) with AUC 0.78±0.06 (p<0.05), while fMRI mean connectivity measures (N=62) predicted LoC with AUC 0.75±0.06 (p<0.01). Combining EEG and fMRI (N=50) resulted in AUC 0.80±0.08; p<0.01).

Conclusion: In patients with acute/subacute DoC, EEG- and fMRI-measures predicted consciousness levels during ICU admission, both alone and in combination.

Disclosure: Nothing to disclose.

OPR-100

The impact of non-convulsive seizures and ictal-interictal continuum on the recovery of patients with a DoC

A. Comanducci¹, A. Viganò¹, C. Derchi¹, A. Mazza¹, S. Casarotto², P. Trimarchi¹, M. Rosanova², J. Navarro Solano¹, M. Massimini¹

¹ IRCCS Fondazione Don Carlo Gnocchi ONLUS, Milan, Italy, ² Department of Biomedical and Clinical Sciences “L. Sacco”, University of Milan, Milan, Italy

Background and aims: Non-convulsive seizures (NCS) represent a confounding clinical factor that may hamper the assessment of consciousness and contribute to the high misdiagnosis rate. Recently, the American Clinical Neurophysiology Society provided definitions for NCS and for an intermediate pattern – the ictal-interictal continuum (IIC) – which cannot be qualified neither as non-convulsive ictal nor as interictal. These patterns with absent or only minimal clinical correlates occur with relative high frequency and are independently associated with a worse outcome in comatose patients. In this study, we investigated the prevalence of NCS/ICC and whether these patterns have a role in recovery of patients with a prolonged disorder of consciousness (DoC).

Methods: We recorded clinical EEG in 137 patients with a prolonged DoC. Patients were diagnosed as unresponsive wakefulness syndrome (UWS) or minimally conscious state (MCS) according to standardized behavioral criteria. The 6-months clinical outcome was dichotomously defined as an improvement in diagnosis (i.e. a MCS who emerged or a UWS who regained at least MCS) versus the absence of improvement. The presence of interictal epileptiform abnormalities or NCS/ICC was evaluated by two blinded board-certified neurophysiologists.

Results: Epileptiform abnormalities were identified in 38% of DoC patients and specifically the NCS/ICC pattern was found in 14.6%. The presence/absence of NCS/ICC was not related to etiology, diagnosis or antiepileptic therapy. Using logistic regression, we found that the presence of NCS/ICC was a significant predictor of lack of clinical improvement (OR 9.95).

Conclusion: The occurrence of NCS/IIC patterns should be carefully investigated to identify treatable causes of unresponsiveness.

Disclosure: This work was supported by ERA PerMed JTC2019 “PerBrain”.

OPR-101

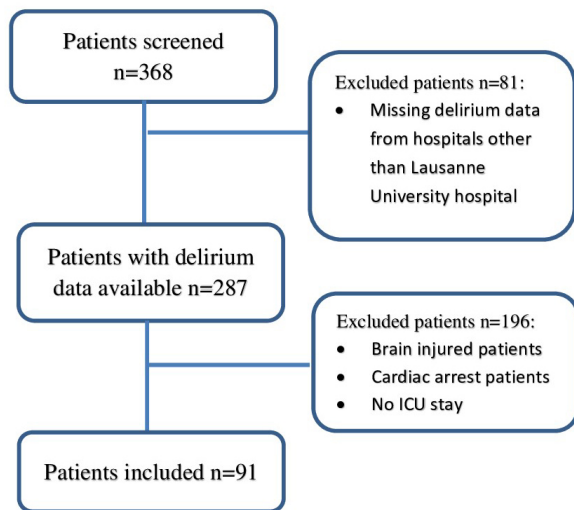
Electroencephalography of mechanically ventilated patients at high risk of delirium

E. Eskioglu¹, I. Carolina², V. Alvarez³, S. Rüegg⁴, K. Schindler⁵, A. Rossetti⁶, M. Oddo¹

¹ Department of Intensive Care Medicine, University Hospital (CHUV) and University of Lausanne, Lausanne, Switzerland, ² School of Medicine and Surgery, University of Milan, Monza, Italy, ³ Department of Neurology, Hôpital du Valais, Sion, Switzerland, ⁴ Department of Neurology, University Hospital Basel and University of Basel, Basel, Switzerland, ⁵ Sleep-Wake-Epilepsy-Center, Department of Neurology, Inselspital, Bern University Hospital, University of Bern, Bern, Switzerland, ⁶ Department of Clinical Neuroscience, University Hospital (CHUV) and University of Lausanne, Lausanne, Switzerland

Background and aims: Neurophysiological exploration of ICU delirium is limited. Here, we examined EEG characteristics of medical-surgical critically ill patients with new onset altered consciousness state at high risk for ICU delirium.

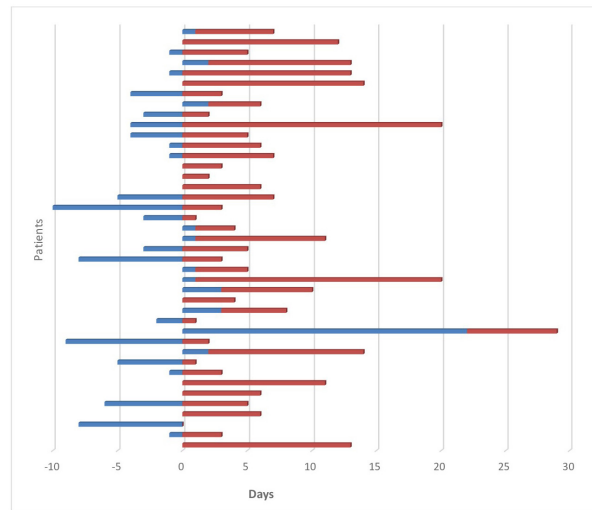
Methods: Pre-planned analysis of non-neurological mechanically ventilated medical-surgical ICU subjects, who underwent a prospective multicenter randomized, controlled EEG study (NCT03129438, April 2017–November 2018). EEG characteristics, according to the 2012 ACNS nomenclature, included background activity, rhythmic periodic patterns/epileptic activity, amplitude, frequency, stimulus-induced discharges, triphasic waves, reactivity and NREM sleep. We explored EEG findings in delirious vs. non-delirious patients, specifically focusing on presence of burst-suppression and rhythmic periodic patterns (ictal-interictal continuum), and ictal activity.



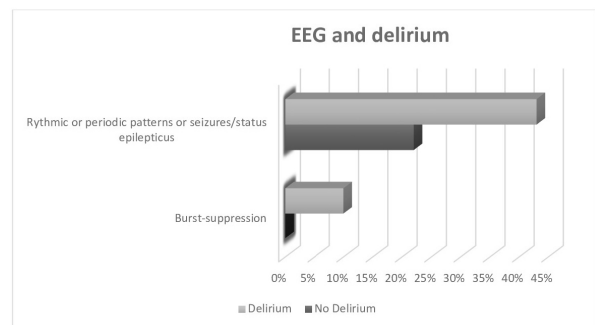
Flowchart of patient's inclusion

Study flow chart

Results: We analyzed 91 patients (median age, 66 years) who underwent EEG because of new onset altered consciousness state at a median 5 days from admission; 42 patients developed delirium (46%). Burst-suppression (10 vs. 0%, $p=0.02$), rhythmic/periodic patterns (43% vs. 22%, $p=0.03$) and epileptiform activity (7 vs. 0%, $p=0.05$) were more frequent in delirious vs. non-delirious patients. The presence of at least one of these abnormal EEG findings (32/91 patients; 35%) was associated with a significant increase in the likelihood of delirium (42 vs. 15%, $p=0.006$). Cumulative dose of sedatives and analgesics, as well as all other EEG characteristics, did not differ significantly between the two groups.



EEG chronologic relationship between delirium duration. In blue: number of days with delirium before EEG; in orange, number of days with delirium after EEG.



EEG characteristics between two groups

Conclusion: In mechanically ventilated non-neurological critically ill patients with new onset alteration of consciousness, EEG showing burst-suppression, rhythmic or periodic patterns, or seizures/status epilepticus indicate an increased risk of ICU delirium.

Disclosure: Swiss National Science Foundation (SNSF).

OPR-102

Consciousness in Neurocritical Care Cohort Study Using fMRI and EEG (CONNECT-ME): Clinical outcome at 3- and 12-month

M. Amiri¹, P.M. Fisher², A. Sidaros³, M. Cacic Hribljan³, I. Zibrandtsen³, M. Othman¹, E. Waldemar Jakobsen¹, S.S. Albrechtsen¹, M. Harboe Olsen⁴, V. Nersesjan⁵, V. Andrée Larsen⁶, J. Lilja S. Højgaard¹, M. Nicolici³, J. Hauerberg⁷, C. Hassager⁸, J. Møller⁸, C. Sølling⁴, H. Ravnholt Jensen⁴, F. Raimondo⁹, J.D. Sitt⁹, M. Ejler Fabricius³, G. Moos Knudsen², J. Kjærgaard⁸, K. Møller⁴, D. Kondziella¹

¹ Department of Neurology, Rigshospitalet, Copenhagen, Denmark, ² Neurobiology Research Unit, Rigshospitalet, Copenhagen, Denmark, ³ Department of Neurophysiology, Rigshospitalet, Copenhagen, Denmark, ⁴ Department of Neuroanesthesiology, Rigshospitalet, Copenhagen, Denmark, ⁵ Biological and precision psychiatry at the Copenhagen research center for mental health, Copenhagen University Hospital, Copenhagen, Denmark, ⁶ Department of Radiology, Rigshospitalet, Copenhagen, Denmark, ⁷ Department of Neurosurgery, Rigshospitalet, Copenhagen, Denmark, ⁸ Department of Cardiology, Rigshospitalet, Copenhagen, Denmark, ⁹ Institut du Cerveau et de la Moelle Epinière, Paris, France

Background and aims: Clinical prognosis in unresponsive patients following brain-injury may be improved with functional MRI (fMRI) and EEG. We investigated prediction of 3- and 12-month outcome in patients with acute/subacute disorders of consciousness (DoC) using fMRI and EEG.

Methods: We assessed 87 acutely brain-injured adult patients in the intensive care unit with clinical and multimodal brain assessment including fMRI (resting state) and EEG (resting state and passive stimulations) between 2016–2020. EEG and fMRI data were used as features in a cross-validated machine-learning framework to predict 3- and 12-month clinical outcome (dichotomized at GOS-E>3). Area under the curve (AUC) of ROC-curves was used for comparison of prediction performance.

Results: Follow-up data was available for 85 patients (97.7%). At 3- and 12-months, 37 (42.5%) and 40 (47.1%) had died, respectively. Prediction performance of 3-month outcome was AUC-ROC: 0.70±0.06 (p=0.07; n=70), 0.57±0.09 (p=0.24; n=62), and 0.65±0.05 (p=0.24; n=50) for EEG, fMRI, and EEG and fMRI combined, respectively. Corresponding prediction performance of 12-month outcome was AUC-ROC: 0.78±0.06 (p<0.01), 0.68±0.05 (p=0.07) and 0.70±0.07 (p<0.05). Unfavorable outcome at 3- and 12-months was significantly associated with age>60 years (OR 3.43, 95% CI 1.0–16.5, p<0.05; OR 8.06 (2.4–38.4), p<0.001), and coma/unresponsive wakefulness at time of EEG/fMRI (OR 3.0 (1.1–8.9), p<0.05; OR 7.38, (2.8–20.8), p<0.001) and at discharge (OR 20.8, (3.9–518), p<0.001; OR 16.1, 95% CI 4.9–77.1, p<0.001), respectively.

Conclusion: We observed evidence that clinical status at 3- and 12-months was predicted by EEG and fMRI, with significantly above chance performance at 12-months. Age and consciousness during admission was also predictive of future clinical outcome.

Disclosure: Nothing to disclose.

OPR-103

Reliable prediction of poor outcome in postanoxic coma using EEG in a four-electrode frontotemporal montage

M. Admiraal¹, M. Van Merkerk¹, J. Hofmeijer², C. Hoedemaekers³, M. Van Putten⁴, J. Horn⁵, A. Van Rootselaar¹

¹ Department of Neurology / Clinical Neurophysiology, Amsterdam UMC, location AMC, Amsterdam, The Netherlands, ² Department of Neurology, Rijnstate hospital, Arnhem, The Netherlands, ³ Department of Intensive care, Radboud UMC, Nijmegen, The Netherlands, ⁴ Department of Neurology/ Clinical Neurophysiology, Medisch Spectrum Twente, Enschede, The Netherlands, ⁵ Department of Intensive care, Amsterdam UMC, location AMC, Amsterdam, The Netherlands

Background and aims: EEG background patterns in the first 24h after cardiac arrest (CA) are highly valuable for prognostication in postanoxic coma. However, limited resources in many hospitals hamper widespread implementation of continuous EEG monitoring. In the present study, the reliability of EEG in a four-electrode frontotemporal montage for prediction of poor outcome was investigated.

Methods: Continuous EEG registrations of 154 consecutive cardiac arrest patients were available from a multicenter prospective cohort study. Five-minute EEG epochs at 12 and 24h after CA were reviewed by three blinded experts in both a 9-channel bipolar (standard) montage and a four-channel frontotemporal (FT) montage (T3-Fp1, Fp1-Fp2, Fp2-T4, T3-T4). EEG background patterns were scored according to the American Clinical Neurophysiology Society nomenclature. Poor outcome was defined as a best Cerebral Performance Category score of 3–5 at six months after CA. Interrater agreement was determined using the intraclass correlation coefficient (ICC).

Results: 152 Patients had EEG available at 24h after CA, of which 74 (49%) had poor outcome. Suppression, burst-suppression with identical bursts, or low voltage EEG was present in 25 patients and predicted poor outcome at 24h with 100% specificity (95% CI 95–100%) in both montages. Sensitivity was 34% (95% CI 23–46%) for the standard montage and 31% (95% CI 21–43%) for the FT montage. ICC for scoring EEG background pattern was 0.94 for both montages.

Conclusion: EEG with only four electrodes in a frontotemporal montage seems reliable for prognostication after cardiac arrest. These results suggest the possibility to reduce the number of EEG electrodes without compromising accuracy of prognostication after cardiac arrest.

Disclosure: Nothing to disclose.

OPR-104

Strengths and limits of robotic-guided continuous Transcranial Color Doppler

C. Kulyk¹, A. Fattorello Salimbeni², A. Pieroni², F. Viaro², F. Favruzzo², T. Von Oertzen¹, M. Vosko¹, C. Baracchini²

¹ Stroke Unit and Neurosonology Laboratory, Department of Neurology, Johannes Kepler University Hospital GmbH, Johannes Kepler University Linz, Linz, Austria, ² Stroke Unit and Neurosonology Laboratory, Department of Neuroscience, University of Padua School of Medicine, Padua, Italy

Background and aims: Transcranial Color Doppler (TCD) can be used to monitor cerebral blood flow in intensive and operative settings; however, its applicability has been limited because of the need of specialized manpower during the whole examination. We evaluated the strengths and limits of artificial intelligence assisted robotic TCD (AI-TCD) for prolonged monitoring in different clinical settings.

Methods: Instructed sonographers at our two large university centers used AI-TCD (NovaGuide™ Intelligent Ultrasound, NovaSignal Corp, USA) to find the middle cerebral artery flow and automatically track the signal in case of head movements. Patients were investigated in different settings (outpatient clinic, stroke unit, neuro-intensive care unit (ICU), anesthesiology ICU, neuroradiological and cardiological interventional suites and operation theater for carotid endarterectomy). Examinations characteristics including duration, technical aspects and adverse effects were collected.

Results: We performed 47 monitorings on 38 patients (27 in Linz and 11 in Padova). AI-TCD examinations were safe in all patients. Yet, the examination was feasible in 5 of 7 settings. It was not possible during carotid endarterectomy, since the device was interfering with the surgical field, and during endovascular intracranial procedure as the system was not radiotransparent and did not allow radiological intra-procedural control.

Conclusion: AI-TCD allowed excellent and practical continuous data acquisition in most intensive, interventional and acute clinical settings. Further developments are needed to extend the range of settings in which this new technology might be applied.

Disclosure: Nothing to disclose.

Autonomic nervous system diseases

OPR-105

EAN-EFAS Survey on cardiovascular ANS disturbances following a SARS-CoV2 infection or COVID-19 vaccination

A. Fanciulli¹, D. Reis Carneiro², F. Leys¹, G. Calandra Buonauro³, J. Camaradou⁴, G. Chiaro⁵, P. Cortelli³, C. Falup Pecurariu⁶, R. Granata¹, P. Guaraldi³, R. Helbok¹, M. Hilz⁷, V. Iodice⁸, J. Jordan⁹, E. Kaal¹⁰, A. Kamondi¹¹, A. Pavy Le Traon¹², I. Rocha¹³, J. Sellner¹⁴, A. Terkelsen¹⁵, G. Wenning¹, M. Krbot Skorić¹⁶, R. Thijs¹⁷, W. Struhal¹⁸, M. Habek¹⁹

¹ Department of Neurology, Medical University of Innsbruck, Innsbruck, Austria, ² Department of Neurology, Faculty of Medicine, University of Coimbra, Coimbra, Portugal, ³ IRCCS Istituto delle Scienze Neurologiche di Bologna, Bologna, Italy, ⁴ Patient partner of the EAN Scientific Panel for Autonomic Nervous System Disorders, London, United Kingdom, ⁵ Neurocenter of Southern Switzerland, Ospedale Civico, Lugano, Switzerland, ⁶ Department of Neurology, Faculty of Medicine, Transilvania University, Brasov, Romania, ⁷ Icahn School of Medicine at Mount Sinai, New York, United States of America & University Erlangen-Nuremberg, Germany, ⁸ Autonomic Unit, National Hospital for Neurology and Neurosurgery, Queen Square, London, UK & UCL Queen Square Institute of Neurology, Faculty of Brain Sciences, University College London, London, United Kingdom, ⁹ German Aerospace Center, Cologne, Germany, ¹⁰ Department of Neurology, Maasstad Ziekenhuis, Rotterdam, The Netherlands, ¹¹ Department of Neurology, National Institute of Mental Health, Neurology and Neurosurgery, Budapest, Hungary, ¹² Department of Neurology, Centre Hospitalier Universitaire de Toulouse, Toulouse, France, ¹³ Institute of Physiology, Faculty of Medicine, University of Lisbon, Lisbon, Portugal, ¹⁴ Landesklinikum Mistlbach-Gänserndorf, Mistelbach, Austria & Christian Doppler Medical Center, Paracelsus Medical University, Salzburg, Austria, ¹⁵ Department of Neurology, Aarhus University Hospital and Danish Pain Research Center, Aarhus University, Aarhus, Denmark, ¹⁶ Faculty of Electrical Engineering and Computing, University of Zagreb, Zagreb, Croatia & Department of Neurology, University Hospital Centre, Zagreb, Croatia, ¹⁷ Department of Neurology, Leiden University Medical Centre, Leiden, The Netherlands, ¹⁸ Karl Landsteiner University of Health Sciences, Department of Neurology, University Hospital Tulln, Tulln, Austria, ¹⁹ Department of Neurology, University Hospital Centre, Zagreb, Croatia

Background and aims: To run a survey among European neurological and interdisciplinary autonomic nervous system (ANS) laboratories on newly-diagnosed or significantly deteriorated cardiovascular ANS disorders following a SARS-CoV2 infection or COVID-19 vaccination.

Methods: We invited 83 laboratories in 22 European countries to answer a web-based survey.

Results: 45 laboratories completed the survey (54%). Postural orthostatic tachycardia syndrome was the most frequently reported newly-diagnosed or deteriorated cardiovascular ANS disorder following a SARS-CoV2 infection or COVID-19 vaccination (Figure 1). 47% of the survey participants reported on persons with orthostatic complaints but negative tilt-table findings after a SARS-CoV2 infection, 16% on patients with new onset of psychogenic pseudosyncope following the infection. Newly-diagnosed ANS disorders were deemed likely associated with the SARS-CoV2 infection or COVID-19 vaccination by 53% and 31% of the responders. Deterioration of previously-diagnosed ANS disorders was deemed likely associated with the infection by 79% of the responders, with the vaccination by 22% thereof. A follow-up was available in 54% of cases. 69% of patients with newly-diagnosed cardiovascular ANS disorders following a SARS-CoV2 infection and 78% of those after a COVID-19 vaccination improved at follow-up. In patients with previously-diagnosed ANS disorders who had worsened after a SARS-CoV2 infection or COVID-19 vaccination, recovery was observed by 50% and 65% of the survey participants.

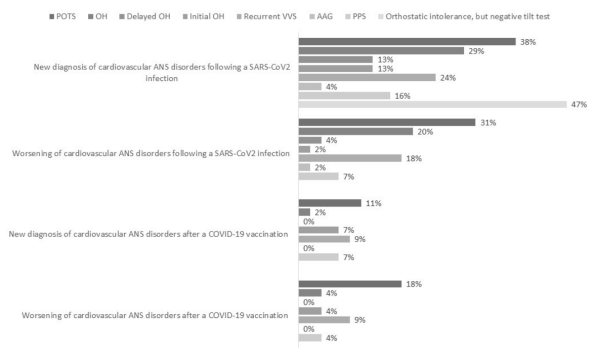


Figure 1: Percentage of European ANS laboratories reporting new diagnosis or significant deterioration of cardiovascular ANS disorders following a SARS-CoV2 infection or COVID-19 vaccination. ANS, autonomic nervous system; POTS, Postural orthostatic tachycardia syndrome.

Conclusion: Cardiovascular ANS disorders may develop or worsen following a SARS-CoV2 infection, while the association with a COVID-19 vaccination remains controversial. A specialized diagnostic work-up helps exclude autonomic disorders in persons with unspecific orthostatic complaints or syncope lookalikes following a SARS-CoV2 infection.

Disclosure: The authors declare no conflicts of interest. This project was approved by the EAN Scientific Committee and by the Board of the European Federation of Autonomic Society. We received administrative support from the EAN Head Office.

OPR-106

Pelvic autonomic dysfunction is common in patients with Pure Autonomic Failure

E. Vichayanrat¹, C. Hentzen³, S. Simeoni¹, M. Pakzad¹, V. Iodice², J. Panicker¹

¹ Department of Uro Neurology, National Hospital for Neurology and Neurosurgery, Queen Square, London, United Kingdom, ² Autonomic Unit, National Hospital for Neurology and Neurosurgery, Queen Square, London, United Kingdom, ³ Sorbonne Universite, GRC 01, GREEN Groupe de Recherche Clinique en Neuro-Urologie, AP-HP, Hopital Tenon, Paris, France

Background and aims: Cardiovascular autonomic failure is the hallmark finding in Pure autonomic failure (PAF) however other autonomic functions are likely to be affected. This study aims to characterise genitourinary dysfunction in PAF patients and explore their relationship with cardiovascular autonomic dysfunction.

Methods: In this cross-sectional observational study, PAF patients who underwent cardiovascular autonomic testing completed self-administered questionnaires evaluating urinary and sexual symptoms and a 3-day bladder diary measuring fluid intake and urine output. Demographic, clinical features, disease duration and related medical comorbidities were assessed.

Results: 25 PAF patients (10 males) were included (mean age 71+8 years; disease duration 13+8 years). Lower urinary tract symptoms were reported by 96% (24/25) using the Urinary Symptom Profile and sexual dysfunction was present in 84% using the Arizona Sexual Experience Scale. Overactive bladder symptoms (n=23; 92%; median overactive subscore 8 (IQR 3–11)) were more frequently reported than voiding symptoms (n=19; 76%; median low stream subscore 2 (IQR 1–3)). Four (16%) patients required catheterisation. 22 patients completed a bladder diary and 19 (86%) had nocturnal polyuria (NP), defined as NP index > 0.3 (nocturnal urine volume/24-hour urine volume), mean NP index 0.45 (range, 0.20–0.73). There were no significant correlations between age, disease duration and cardiovascular parameters (orthostatic BP drop, supine hypertension, respiratory sinus arrhythmia, Valsalva ratio) with urogenital parameters including need for catheterisation and degree of NP (p>0.05).

Conclusion: NP and genitourinary symptoms are common in PAF. The pathophysiology of NP in PAF is likely to be multifactorial and may not only be explained by cardiovascular autonomic failure.

Disclosure: JNP is supported in part by funding from the United Kingdom's Department of Health NIHR Biomedical Research Centres funding scheme. CH is supporting in part by scholar grants from the SIFUD-PP (the francophone society of urodynamics), from LILIAL-GREEN GRC-01 UPMC (Group of clinical REsearch in Neurourology), from the French Society of Physical and Rehabilitation Medicine (SOFMER) and from the endowment fund Renaître. Dr VI is supported by NIHR UCLH Biomedical Research Centre.

OPR-107

The European Network of Autonomic Nervous System laboratories: an EAN-EFAS survey

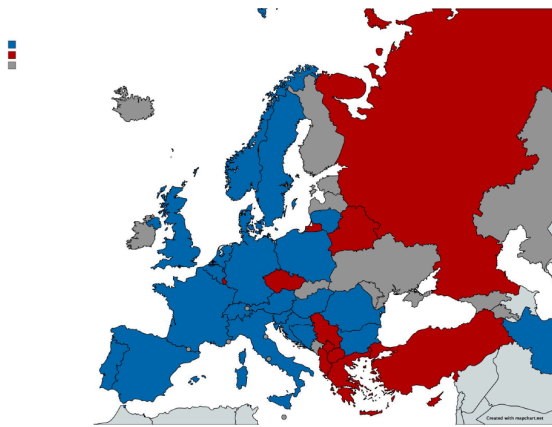
M. Habek¹, D. Reis Carneiro², F. Leys³, G. Calandra Buonauro⁴, J. Camaradou⁵, G. Chiaro⁶, P. Cortelli⁴, C. Falup Pecurariu⁷, R. Granata³, P. Guaraldi⁴, R. Helbok³, M. Hilz⁸, V. Iodice⁹, J. Jordan¹⁰, E. Kaal¹¹, A. Kamondi¹², A. Pavy Le Traon¹³, I. Rocha¹⁴, J. Sellner¹⁵, A. Terkelsen¹⁶, G. Wenning³, M. Krbot Skoric¹⁷, R. Thijs¹⁸, W. Struhal¹⁹, A. Fanciulli³

¹ Department of Neurology, University of Zagreb, School of Medicine, Zagreb, Croatia, ² Department of Neurology, Faculty of Medicine, University of Coimbra, Coimbra, Portugal, ³ Department of Neurology, Medical University of Innsbruck, Innsbruck, Austria, ⁴ IRCCS Istituto delle Scienze Neurologiche di Bologna, Bologna, Italy, ⁵ Patient partner of the EAN Scientific Panel for Autonomic Nervous System Disorders, London, United Kingdom, ⁶ Neurocenter of Southern Switzerland, Ospedale Civico, Lugano, Switzerland, ⁷ Department of Neurology, Faculty of Medicine, Transilvania University, Brasov, Romania, ⁸ Icahn School of Medicine at Mount Sinai, New York, United States of America & University Erlangen – Nuremberg, Germany, ⁹ Autonomic Unit, National Hospital for Neurology and Neurosurgery, Queen Square, London, UK & UCL Queen Square Institute of Neurology, Faculty of Brain Sciences, University College London, London, United Kingdom, ¹⁰ German Aerospace Center, Cologne, Germany, ¹¹ Department of Neurology, Maasstad Ziekenhuis – Rotterdam, The Netherlands, ¹² Department of Neurology, National Institute of Mental Health, Neurology and Neurosurgery, Budapest, Hungary, ¹³ Department of Neurology, Centre Hospitalier Universitaire de Toulouse, Toulouse, France, ¹⁴ Institute of Physiology, Faculty of Medicine, University of Lisbon, Lisbon, Portugal, ¹⁵ Landesklinikum Mistelbach-Gänserndorf, Mistelbach, Austria & Christian Doppler Medical Center, Paracelsus Medical University, Salzburg, Austria, ¹⁶ Department of Neurology, Aarhus University Hospital and Danish Pain Research Center, Aarhus University, Aarhus, Denmark, ¹⁷ Faculty of Electrical Engineering and Computing, University of Zagreb, Zagreb, Croatia, ¹⁸ Department of Neurology, Leiden University Medical Centre, Leiden, The Netherlands, ¹⁹ Karl Landsteiner University of Health Sciences, Department of Neurology, University Hospital Tulln, Tulln, Austria

Background and aims: The aim of this EAN-EFAS survey was to identify neurology-driven or interdisciplinary autonomic nervous system (ANS) laboratories in Europe, to describe their personnel, equipment and patient characteristics and to explore differences between European regions.

Methods: We contacted national neurological societies of 51 European countries to identify ANS laboratories in each country. Each identified laboratory, answered a specifically designed survey evaluating personnel, equipment and patient characteristics of the laboratory.

Results: 38 national societies provided information about their country (65%), altogether identifying 83 ANS laboratories in 22 countries, 45 thereof (54%) answered the survey (Figure 1). All laboratories perform cardiovascular and 84% perform sudomotor evaluation. Blood testing for catecholamines and antibodies are performed in 64% and 56%, respectively. 62% of the laboratories perform epidermal nerve fiber density analysis. Each laboratory has a median of 2 consultants (0–10), 1 resident (0–10), 1 technician (0–8), and 1 nurse (0–5). The median number of tilt-up table tests/laboratory/year is 100 (0–4.000). An ANS outpatient clinic is available in 34 (76%) centers with a median of 200 (6–5.544) outpatient visits/year. Inpatient admissions are available in 41 (91%) centers with a median of 20 (0–300) inpatient visits/year. There is a significant difference in available ANS services between different European regions (11/21 countries from south/east/wider Europe vs 11/12 countries from north/west Europe, $p=0.021$).



Distribution of laboratories for testing of the autonomic nervous system across Europe (Blue indicates county with at least one laboratory, red indicates country with no laboratory, and dark grey indicates country from which no response was obtained).

Conclusion: This survey highlights significant differences in the availability of care for people with ANS disorders, stressing the need to improve access to diagnostic and treatment facilities across Europe.

Disclosure: The authors declare no conflicts of interest. This project was approved by the EAN Scientific Committee and by the Board of the European Federation of Autonomic Society. We received administrative support from the EAN Head Office.

OPR-108

A clinico-genetic study based on the Innsbruck MSA Registry (IMSA-R)

F. Leys¹, S. Eschlboeck¹, N. Campese², M. Peball¹, P. Mahlknecht¹, V. Sidoroff¹, R. Granata¹, V. Bonifati³, J. Zschocke⁴, S. Kiechl¹, W. Poewe¹, K. Seppi¹, G. Wenning¹, A. Fanciulli¹

¹ Department of Neurology, Medical University of Innsbruck, Innsbruck, Austria, ² Neurology Unit, Department of Clinical and Experimental Medicine, University of Pisa, Pisa, Italy, ³ Department of Clinical Genetics, Erasmus Medical Center, Rotterdam, The Netherlands, ⁴ Institute of Human Genetics, Medical University of Innsbruck, Innsbruck, Austria

Background and aims: While genetic factors may contribute to the pathogenesis of Parkinson’s disease (PD), multiple system atrophy (MSA) is generally considered a sporadic disease. However, neuropathologically confirmed cases of MSA with positive family history (FH) for MSA and other neurodegenerative disorders have been described. **Methods:** Here we screened the Innsbruck MSA (n=255) and Parkinson Registry (n=368) for patients with MSA or PD providing informative FH for neurodegenerative disorders among 1st to 3rd degree relatives and compared their prevalence with those from published population-based studies.

Results: Forty percent of MSA and 54% of PD cases ($p=0.023$) had a positive FH for neurodegenerative disorders, with parkinsonism being most prevalent [18.3% vs. 25.6%; $p=0.108$]. Familial clustering (≥ 2 affected relatives) occurred in 9.5% of MSA and 17.3% of PD cases ($p=0.065$). Median age at onset was comparable between FH-positive MSA and PD cases [55 vs. 56 years; $p=0.712$], but differed in FH-negative ones [58 vs. 63 years; $p=0.036$]. Both in PD and in MSA, we observed no differences in the initial clinical presentation between FH-positive and negative cases. The prevalence of first-degree FH for parkinsonism was comparable between the MSA and PD cohort [10.4% (95% CI 6.3–16.6) vs. 17.1% (95% CI 12.6–22.7); $p=0.079$], whereas both exceeded previously reported prevalence rates in population-based elderly controls [5.6% (95% CI 5.1–6.1); vs. MSA $p=0.012$; vs. PD $p<0.001$].

Conclusion: The higher prevalence of positive FH for parkinsonism observed in patients with MSA compared to the general population suggests that genetic, yet unidentified, factors may play a role in the pathogenesis of the disease.

Disclosure: Academic work without external funding. Dr Leys is supported by the US MSA Coalition and the Dr. Johannes & Hertha Tuba Foundation, outside of the submitted work.

OPR-109

Hemodynamic determinants of supine hypertension in neurogenic orthostatic hypotension

R. Thijs¹, A. Van der Stam², J. Van Dijk¹

¹ Department of Neurology, Leiden University Medical Centre, Leiden, The Netherlands, ² Department of Neurology, Radboud University Medical Centre, Nijmegen, The Netherlands

Background and aims: Patients with neurogenic orthostatic hypotension (nOH) often exhibit supine hypertension. The mechanisms underlying supine hypertension are poorly understood.

Methods: We performed a retrospective analysis of continuous blood pressure (BP) patterns in 65 nOH patients who underwent a tilt table test and compared the means of the periods -180 to -20 seconds before, and 170–190 seconds after the head-up tilt. Mean arterial pressure (MAP) and its constituents heart rate (HR), stroke volume (SV) and total peripheral resistance (TPR) were analysed. The measures were compared between two groups, which were split based on the median systolic supine BP.

Results: Patients with nOH and a high supine BP had a higher supine TPR than those with low supine BP. HR and SV in a supine position did not differ between groups. Three minutes after tilt only the MAP differed between the two groups, and HR, SV and TPR did not. Notably, in those with nOH and high supine BP, TPR did not change upon tilting. The differences between the supine values and the values three minutes after tilt indicate a smaller SV fall, smaller TPR increase, and a larger BP decrease in the high supine BP group (Figure 1).

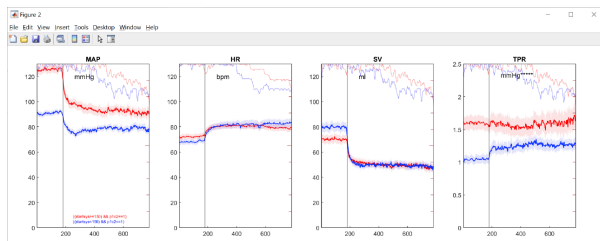


Figure 1

Conclusion: Supine hypertension in nOH is primarily driven by a high TPR in supine position and associated with a larger BP fall upon standing.

Disclosure: The authors declare that there is no competing interest related to this work.

Cerebrovascular diseases: Clinical presentation and cognition

OPR-110

Novel patterns of stroke neural damage link endovascular thrombectomy to the occurrence of spatial delusions

P. Alves, A. Fonseca, T. Pinho-e-Melo, I. Martins
Department of Neurosciences and Mental Health, Neurology, Hospital de Santa Maria, CHULN, Lisbon, Portugal

Background and aims: Behavioural changes are disturbing consequences of stroke, whose occurrence depends on strategic patterns of lesion and disconnection. Spatial delusions are right hemisphere disconnection syndromes characterized by the firm belief of place reduplication, transformation or mislocation. Endovascular thrombectomy may modify the classical anatomical distribution of brain infarcts. We aimed to determine whether endovascular thrombectomy is associated with a higher incidence of spatial delusions and what are the anatomical determinants of this putative association.

Methods: We performed a prospective, cumulative, case-control study, from December/2016 to June/2021. Acute right hemisphere ischemic strokes patients were consecutively included. The main outcome was the occurrence of spatial delusions. Stroke lesions were delimited and structural disconnection maps were inferred based on the tract-wise analysis of 7 Tesla tractographies.

Results: In a sample composed by 78 cases and 212 stroke controls, endovascular thrombectomy was significantly associated with the occurrence of spatial delusions (multivariate linear regression model including age, clinical severity, vascular territory, inter-hospital transfer and endovenous thrombolysis: OR 2.46, 95% CI 1.18 to 5.16, $p=0.017$). The structural disruption proportion and the beta coefficient maps associated with endovascular thrombectomy had a significantly higher spatial correlation with the structural disruption maps of cases than controls ($p<0.001$; Fig.1).

Endovascular thrombectomy was found to share with spatial delusions significant clusters of lesion and structural disconnection ($p<0.05$) overlapping thalamo-orbitofrontal fibers and anterior temporal regions (Fig.2).

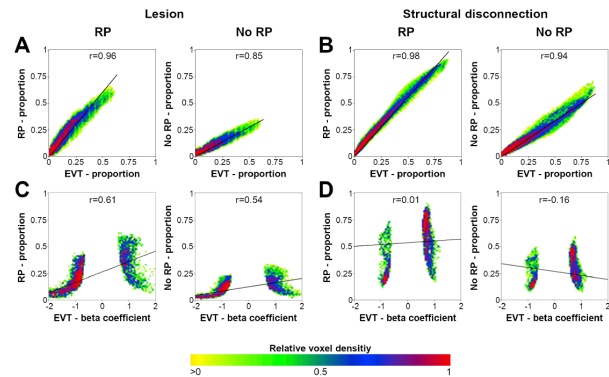


Figure 1: Spatial correlations between: proportion map of endovascular thrombectomy (EVT) and voxel lesion/disconnection (A/B); beta coefficient map of endovascular thrombectomy and voxel lesion/disconnection (C/D). RP, reduplicative paramnesia.

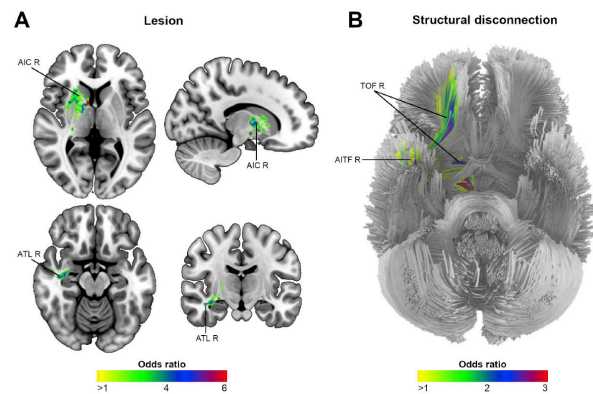


Figure 2: Statistically significant clusters of the conjunction analysis between the structural disconnectome map of reduplicative paramnesia and the endovascular thrombectomy associated lesion/disconnection maps (A/B), regressing for confounders.

Conclusion: This study suggests that endovascular thrombectomy is an independent predictor of the occurrence of spatial delusions after right hemisphere stroke, by novel patterns of lesion and structural disconnection.

Disclosure: Nothing to disclose.

OPR-111

Remember that? Previous stroke as independent recurrence risk factor for global transient amnesia

P. Ferreira, C. Duque

Department of Neurology, Hospital Pedro Hispano, Matosinhos, Portugal

Background and aims: Transient global amnesia (TGA) is generally described as a sole and benign event. Recurrence varies between 2,9–26,3% and risk factors (RF) are poorly defined. Our aim was to describe a population of patients diagnosed with TGA in the emergency department (ED) and evaluate possible RF for recurrence and development of dementia.

Methods: Retrospective study of data from patients discharged from the ED with the diagnosis of TGA between 2010–2020 with descriptive and comparative analysis for identification of recurrence RF.

Results: 124 patients were included, 84 were female (68%) and mean age was 63 years (SD±8). Most episodes lasted between 3 and 6 hours (23%). One possible trigger was identified in 49 patients (41%). 12 patients had, at least, another episode (10%), most of which occurred after 1 year. Gender, age, episode duration, reported trigger, headache, vascular RF, blood glucose, hemoglobin A1C, MRI and EEG alterations weren't associated with recurrence. Previous stroke history was associated with a new episode [OR: 9, (CI 95% 1.2–77.5), p=0,036]. In the follow-up, 22 patients had an alternative diagnosis (13%). The most frequent were functional disorder (n=6) and epileptic transient amnesia (n=8). In our population, only 1 patient had a diagnosis of dementia within 5 years follow-up.

Conclusion: We present a relatively large population with long follow-up and TGA diagnosis. Recurrence was similar to those reported in the literature and the episode's intrinsic characteristics did not predict recurrence. Notably, the presence of a previous stroke was associated significantly with new episodes, which, to our knowledge, is not described in the existing literature.

Disclosure: Nothing to disclose.

OPR-112

Masseter area is associated with cognitive and motor performance but not with white matter hyperintensity volume

J. Pitkänen¹, A. Arola², L. Enqvist³, H. Laakso⁴, M. Ahlström¹, J. Lempiäinen¹, J. Koikkalainen⁵, J. Lötjönen⁵, A. Korvenoja³, T. Strandberg⁸, N. Oksala⁹, T. Erkinjuntti¹, H. Jokinen², S. Melkas¹

¹ Department of Neurology, Helsinki University Hospital and University of Helsinki, Helsinki, Finland, ² Department of Psychology and Logopedics, Faculty of Medicine, University of Helsinki, Helsinki, Finland, ³ HUS Diagnostic Center, Radiology, Helsinki University Hospital and University of Helsinki, Helsinki, Finland, ⁴ HUS Neurocenter, Division of Neuropsychology, Helsinki University Hospital and University of Helsinki, Helsinki, Finland, ⁵ Combinostics Ltd, Tampere, Finland, ⁸ HUS Internal Medicine and Rehabilitation, Helsinki University Hospital and University of Helsinki, Helsinki, Finland, ⁹ Faculty of Medicine and Health Technology, Tampere University, Tampere, Finland

Background and aims: Masseter sarcopenia is an indicator of physical frailty, which in turn is associated with vascular aging. Vascular aging is associated with cognitive impairment and functional decline. However, documentation on the relation between masseter sarcopenia and cognitive impairment, and the relation to cerebral small vessel disease findings in brain imaging is lacking. We aimed to identify potential correlation between masseter area, cognitive and motor performance, and white matter hyperintensities (WMH).

Methods: The Helsinki Small Vessel Disease study comprised 152 patients (age 65–75 years) who underwent brain magnetic resonance imaging (MRI) and comprehensive neuropsychological and clinical evaluation. WMH volume was obtained with automated segmentation. Masseter muscle area was evaluated visually according to previously set standards.

Results: Analysed with linear regression models adjusted for age, sex, and education, masseter area was significantly associated with global cognition (stand.β 0.28, p=0.001), processing speed (β 0.28, p=0.001), and executive functioning (β 0.21, p=0.013) but not with memory (β 0.16, p=0.055). Masseter area was also associated with Timed Up and Go test (β -0.26, p=0.004) and walking speed (β 0.27, p=0.003), but not with grip strength (β 0.12, p=0.057) after adjustments. No association was found between masseter area and WMH volume (β 0.03, p=0.771). Additional controlling for missing teeth had no effect on the results.

Conclusion: We found that masseter area is associated with both cognitive and motor performance. However, WMH volume did not correlate with masseter area, so according to our study WMH volume does not seem to be the link between sarcopenia and cognitive impairment.

Disclosure: JK and JL are shareholders at Combinostics Oy. JL has received lecture fees from Merck and Sanofi (paid to the employer). The other authors report no competing of interests.

OPR-113

The effect of neuropsychological findings of stroke on the risk of recurrent stroke

F. Çetin, E Kumral

Department of Neurology, Ac badem Bursa Hospital, Bursa, Turkey

Background and aims: In patients characterized by executive dysfunction, vascular depression has been clinically termed as “depression-executive dysfunction syndrome”. Despite enthusiasm for this approach, few studies have examined the predictive utility of cognitive functions in understanding the course and outcome of post-stroke depression (PSD).

Methods: The current study involved the patients with ischemic stroke who were admitted during the time period from April 2017 to December 2018. Data were obtained from the evaluations performed by the research staff involved in the clinical research study. All participants were provided a large battery of neuropsychological tests that covered cognitive domains relevant to the understanding of depression. To determine which factors were independently associated with stroke recurrence and cardiovascular event, a multiple logistic regression method was performed using variables found to be significant ($p < 0.05$) in the univariate analyses.

Results: The study included 440 patients who had depression. After 52 weeks of follow-up, 371 patients (84%) completed the study. Among vascular risk factors age, hypertension, large-artery disease and atrial fibrillation were significantly higher in patients with stroke recurrence. In addition, executive function disorder ($p = 0.001$), reduced processing speed ($p = 0.01$), episodic memory disorder ($p = 0.005$) and language processing disorder ($p = 0.001$) were significantly associated with stroke recurrence.

Conclusion: The current study supports the importance of executive dysfunctions in predicting recurrent strokes. This result warrants further studies to demonstrate the effects of depression treatment on stroke recurrence.

Disclosure: Nothing to disclose.

OPR-114

EEG for post-stroke delirium monitoringE. Vandervorst¹, M. Vanderstraeten², T. De Winne³, E. Van Dellen⁴, A. Slooter⁵, S. De Raedt¹

¹ *Department of Neurology, Universitair Ziekenhuis Brussel, Center for Neurosciences, VUB, Brussels, Belgium,* ² *Faculty of Medicine and Pharmacy, Family Medicine and Chronic Care, VUB, Brussels, Belgium,* ³ *Faculty of Medicine and Pharmacy, VUB, Brussels, Belgium,* ⁴ *Department of Psychiatry, Brain Center, University Medical Center Utrecht, Utrecht, The Netherlands,* ⁵ *Department of Intensive Care Medicine, Brain Center, University Medical Center Utrecht, Utrecht, The Netherlands*

Background and aims: Establishing the diagnosis of post-stroke delirium (PSD) remains challenging, especially in patients with dysphasia. The EEG parameter relative delta power (RDP) has been associated with the presence of postoperative delirium; however, it remains unclear whether these results can be extrapolated to patients with PSD. The aim of this study was to explore whether RDP may differentiate between patients with and without delirium after left middle cerebral artery (MCA) infarction.

Methods: In a dataset of 514 patients with acute ischemic stroke (AIS), we used a retrospective chart review based on DSM-5 criteria to diagnose PSD within the first week after stroke onset. A subset of 20 patients was randomly selected, all with left MCA infarction: 10 with and 10 without PSD. For each patient, the first 8 artifact-free epochs of 8 seconds were selected and RDP (0.5–4Hz) was computed using a fast Fourier transformation and averaged over all channels and epochs. Fp1 and Fp2 were excluded. RDP was compared using a Mann-Whitney-U-test.

Results: Median RDP among all channels and epochs, was significant higher in patients with PSD (0.587; IQR 0.241) compared to patients without PSD (0.408; IQR 0.183) (p -value=0.043). When studying difference in RDP between patients with and without PSD among all derivations (channel against average reference), RDP in P3 was associated with the lowest p -value (0.009).

Conclusion: Preliminary results suggest that RDP differs between patients with and without PSD after left MCA infarction, implicating a potential role of this EEG parameter for objective PSD monitoring.

Disclosure: Nothing to disclose.

OPR-115

Crossed cerebellar diaschisis worsens the clinical presentation in large vessel occlusion acute ischemic stroke

A. Abderrakib¹, N. Torcida¹, N. Sadeghi², N. Ligot¹, G. Naeije¹

¹ Neurology Department, Université Libre de Bruxelles - Cliniques Universitaires de Bruxelles - Hôpital Erasme, Bruxelles, Belgium, ² Radiology Department, Université Libre de Bruxelles - Cliniques Universitaires de Bruxelles - Hôpital Erasme, Bruxelles, Belgium

Background and aims: The cerebellum modulates both motor function and higher cortical processes through cortico-cerebellar loops. Crossed cerebellar diaschisis (CCD) refers to the association between a local supratentorial brain lesion and a decrease of contralateral cerebellar blood flow and metabolic activity. The aim of this study is to determine the prevalence of CCD by whole brain perfusion CT (PCT) realized in acute ischemic stroke due to anterior circulation large vessel occlusion (LVO) and the clinical and radiologic factors that affect the occurrence of crossed cerebellar diaschisis.

Methods: Patients with anterior LVO who benefited from both PCT and mechanical thrombectomy were retrospectively identified from our stroke alert registry (January 2017 to July 2021). CCD was defined as lower blood volume and flow in the cerebellum contralateral to stroke on PCT. Clinical and radiological factors were compared between patient with and without CCD.

Results: Out of the 296 thrombectomy considered, 131 patients met inclusion criteria. CCD was present in 89 patients (68%). NIHSS at admission was significantly higher when CCD was present (11.5 ± 8.3 vs 18.0 ± 6.1 , $p < 0.001$). CCD was also associated with higher volume of ischemic core ($13.5 \text{ml} \pm 26.1$ vs $32 \text{ml} \pm 35.8$, $p = 0.001$) and hypoperfusion ($68.9 \text{ml} \pm 50.9$ vs $119 \text{ml} \pm 60.2$, $p < 0.001$).

Conclusion: CCD occurs in 68% of patients with anterior LVO and is associated with higher NIHSS on admission and with higher ischemic penumbra and core volumes. These results suggest that part of the LVO initial clinical deficit may be related to superimposed cerebellar dysfunction.

Disclosure: Nothing to disclose.

Neurogenetics 1

OPR-116

Characterisation of the St. Gallen von Hippel-Lindau disease-Cohort: confirmatory and surprising results

J. Zimmermann¹, C. Rothermundt², T. Hundsberger³

¹ Medical student, Joint medical master University of Zürich and Cantonal hospital St. Gallen, Switzerland, ² Department of medical Oncology and hematology, Cantonal St. Gallen, St. Gallen, Switzerland, ³ Department of Neurology, Cantonal hospital St. Gallen, St. Gallen, Switzerland

Background and aims: The von Hippel-Lindau (VHL) disease is a rare autosomal dominant tumour predisposition syndrome. Penetrance is greater than 90% by the age of 65 years. VHL disease is caused by genetic aberration of the short arm of chromosome 3 (3p25-p26), 50% of germline mutations arise spontaneously (non-familial). Retinal capillary hemangioblastoma, cystadenoma of the epididymis or the broad ligament and endolymphatic sac tumours were the earliest tumours that developed. CNS and/or spinal hemangioblastomas, pheochromocytomas and pancreatic cysts appeared somewhat later. Clear cell renal cell carcinomas and pancreatic neuroendocrine tumours were the last to be diagnosed.

Methods: To evaluate the genotype and phenotype of the St. Gallen VHL cohort and to disclose novel tumour manifestations and comorbidities.

Results: The cohort comprised 31 patients from 16 different families. The age of all patients ranged from 24 to 73 years. The median age is 43 years. Three of the 31 patients had already died. The most common organ lesions were renal cysts (87%), pancreatic cysts (87%), spinal hemangioblastomas (74%), infratentorial hemangioblastomas (71%) and retinal angiomas (61%). Rare tumours were hemangioblastomas of peripheral nerves (13%), cystadenoma of the epididymis (13%), supratentorial hemangioblastomas (10%) and pancreatic neuroendocrine tumours (7%).

Conclusion: We here provide a comprehensive genotype/phenotype characterisation of a large cohort of the von-Hippel Lindau disease in Switzerland. Formally unknown comorbidities, unusual manifestation sites of supratentorial hemangioblastomas, trigeminal neuralgia, hemangioblastomas of the peripheral nerves among other findings will be reported. Intra-familial heterogeneity is obvious, but may be related to pre-symptomatic testing in familial cases

Disclosure: Nothing to disclose.

OPR-117

Clinico-genetic spectrum of limb-girdle muscular weakness in Austria: a multi-centre cohort study

M. Krenn¹, M. Wagner², G. Zulehner¹, R. Weng¹, J. Rath¹, G. Bsteh¹, O. Keritam¹, I. Colonna³, C. Paternostro¹, F. Jäger¹, E. Lindeck-Pozza⁴, S. Iglseider⁵, S. Grinzing⁶, M. Schönfelder⁷, C. Hohenwarter⁸, M. Freimüller⁸, N. Embacher⁹, J. Wanschitz¹⁰, R. Topakian¹¹, A. Töpf¹², V. Straub¹², S. Quastoff³, F. Zimprich¹, W. Löscher¹⁰, H. Cetin¹

¹ Department of Neurology, Medical University of Vienna, Vienna, Austria, ² Institute of Human Genetics, Technical University Munich, Munich, Germany, ³ Department of Neurology, Medical University of Graz, Graz, Austria, ⁴ Department of Neurology, Klinik Favoriten, Vienna, Austria, ⁵ Department of Neurology, KH der Barmherzigen Brüder, Linz, Austria, ⁶ Department of Neurology, Paracelsus Medical University of Salzburg, Salzburg, Austria, ⁷ Department of Neurology, Klinikum Klagenfurt am Wörthersee, Klagenfurt, Austria, ⁸ Department of Neurorehabilitation, Gaital-Klinik, Hermagor, Austria, ⁹ Department of Neurology, University Hospital St. Pölten, St. Pölten, Austria, ¹⁰ Department of Neurology, Medical University of Innsbruck, Innsbruck, Austria, ¹¹ Department of Neurology, Klinikum Wels-Grieskirchen, Wels, Austria, ¹² John Walton Muscular Dystrophy Research Centre, Translational and Clinical Research Institute, Newcastle University and Newcastle Hospitals NHS Foundation Trust, Newcastle upon Tyne, United Kingdom

Background and aims: Molecular diagnosis of hereditary myopathies with limb-girdle muscular weakness (LGW), a genetically heterogeneous group of diseases, remains challenging to this date. In our study, we aimed to present clinical data of a large cohort of patients, unravelling the genetic nature of LGW.

Methods: Patients with LGW and a suspected association with hereditary myopathies were included in this nationwide cohort study. Demographic and clinical parameters associated with genetic aetiologies were evaluated. Furthermore, we assessed the predictive value of these parameters for the identification of causative variants in genetic analyses.

Results: Molecular diagnoses were identified in 62% (75/121) of the study cohort. Next-generation sequencing (NGS) identified a higher proportion of solved cases than single gene testing (77.3% vs. 22.3%). The median time from symptom onset to genetic diagnosis was 8.9 years (IQR 3.7–19.9) for single gene testing and 17.8 years (IQR 7.9–27.8) for NGS. Variants in the genes for CAPN3 (n=9), FKRP (n=9), ANO5 (n=8), DYSF (n=8) and SGCA (n=5) were the five most common molecular diagnoses, together accounting for 32.2%. Causative variants were significantly associated with a younger age at symptom onset (p=0.043), elevated CK activity levels (p=0.024) and myopathic changes on electromyography (p=0.007), but inversely associated with isolated upper limb weakness at onset.

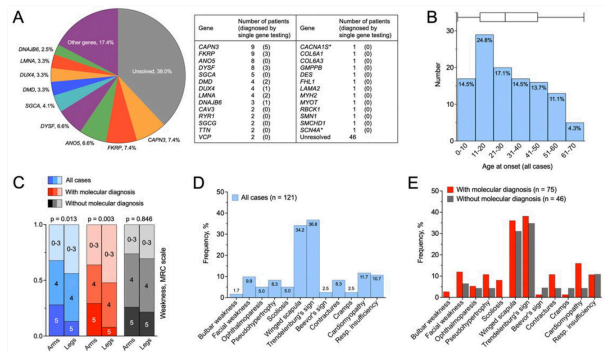


Fig. 1 Genetic spectrum and clinical characteristics of patients with LGW. (A) Causative variants. (B) Age at onset. (C) Affected muscle groups. Frequency of clinical symptoms in total cohort (D) and in patients with or without molecular diagnosis.

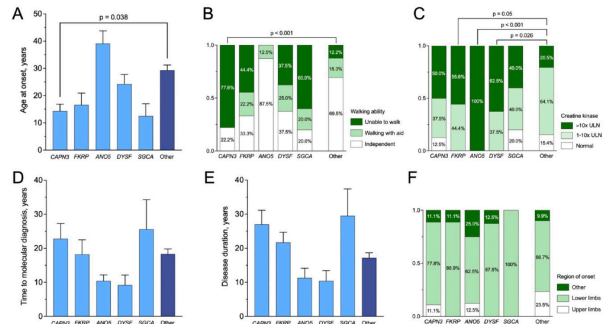


Fig. 2 Demographic and clinical characterisation of common genetic aetiologies in patients with LGW. (A) Disease onset. (B) Waling ability. (C) Creatine kinase levels. (D) Time to molecular diagnosis. (E) disease duration. (F) region of onset.

Conclusion: We suggest early application of NGS in patients with LGW to avoid diagnostic delays. In addition, clinical factors predictive of specific molecular diagnosis may help in the selection of patients for genetic analyses, especially in centres with limited access to sequencing.
Disclosure: The study was financially supported by Sanofi Genzyme.

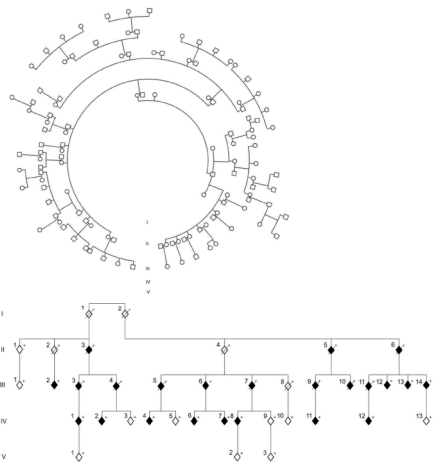
OPR-118 MAPT p.R406W carriers present with a nonconforming clinical phenotype

H. Gossye^{1,2,3}, S. Van Mossevelde^{1,2,3,4}, A. Sieben^{4,5}, M. Bjerke⁶, E. Hendrickx Van de Craen^{1,2,3}, J. Van der Zee^{1,3}, S. Engelborghs^{4,6}, P.P. De Deyn^{4,7}, J. De Bleecker⁸, J. Versijpt⁶, J. Van den Ende⁹, O. Deryck¹⁰, P. Bourgeois¹¹, J. Bier¹², M. Goethals¹², C. Van Broeckhoven^{1,3}, on behalf of the BELNEU consortium

¹ Neurodegenerative Brain Diseases, VIB Center for Molecular Neurology, Antwerp, Belgium, ² Department of Neurology, University Hospital Antwerp, Edegem, Belgium, ³ Department of Biomedical Sciences, University of Antwerp, Antwerp, Belgium, ⁴ Institute Born-Bunge, Antwerp, Belgium, ⁵ Department of Anatomopathology, University Hospital Antwerp, Edegem, Belgium, ⁶ Department of Neurology, University Hospital Brussel and Center for Neurosciences, Vrije Universiteit Brussel, Brussel, Belgium, ⁷ Department of Neurology and Memory Clinics, Hospital Network Antwerp, Antwerp, Belgium, ⁸ Department of Neurology, University Hospital Ghent, Gent, Belgium, ⁹ Department of Medical Genetics, University Hospital Antwerp, Edegem, Belgium, ¹⁰ Department of Neurology, General Hospital Sint-Jan, Brugge, Belgium, ¹¹ Department of Neurology, General Hospital Groeninge, Kortrijk, Belgium, ¹² Department of Neurology, Erasmus Hospital, University Clinics of Brussels, Brussel, Belgium, ¹³ Department of Neurology, General Hospital Delta, Roeselare, Belgium

Background and aims: MAPT p.R406W is an autosomal dominantly inherited missense mutation associated with FTLN with an amestic, AD-like phenotype. Our group first described a carrier pedigree (labeled ADG) in 2003, with 47 relatives. We aim to delineate phenotypic and genetic characteristics of MAPT p.R406W carriers through 19-year follow-up, and to provide first data on mutation frequency in FTD and AD.

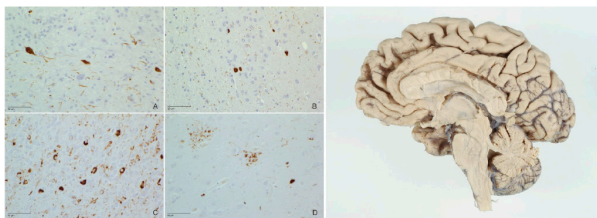
Methods: We extended the ADG pedigree, obtained data over 19 years on symptoms, biomarkers and neuropathology. Furthermore, we screened FTD (n=647) and AD (n=1100) patient cohorts for new carriers.



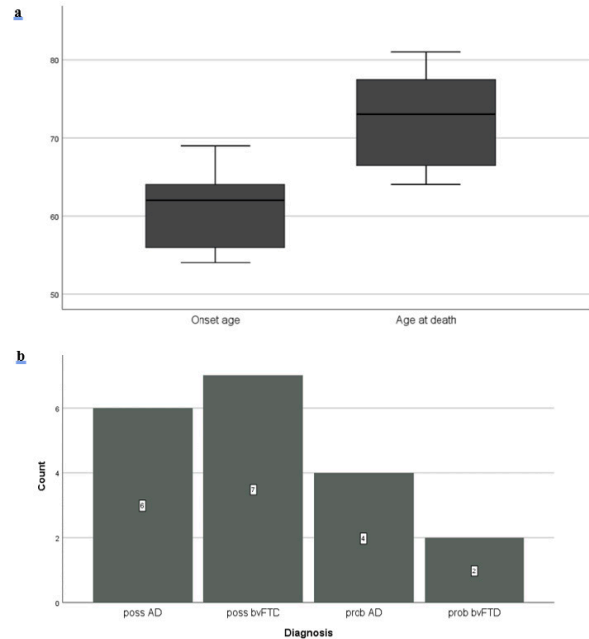
a. Full ADG pedigree in 2021. Pictured are different branches of families segregating p.R406W, traced back and found to all be part of the same large pedigree, named ADG. All family members sampled and screened for p.R406W are shown in this circular pedigree.
 b. ADG pedigree in 2021, showing only p.R406W carriers. Presented are all p.R406W carriers identified in the branches of the ADG pedigree. An autosomal dominant pattern of inheritance may be recognized. Exceptions exist, as clinical data may have been lacking or patients died young. Obligate carriers are marked with "o". Carriers with colored-in symbols were likely affected by disease. Crossed-off carriers are deceased.

Full ADG pedigree. A pattern of autosomal dominant inheritance may be discerned.

Results: The ADG family now counts 38 mutation carriers. 7 unrelated carriers were identified in AD and FTD cohorts. Inclusion of additional relatives procured 56 mutation carriers (39 affected). p.R406W mutation frequencies were 0.62% (FTD) and 0.27% (AD). All probands shared genetic kinship, suggesting a common ancestor. Average onset age and disease duration were 60.9 and 12.4 years (ranges 54–69, 5–25). Remarkably, two distinct phenotypes (clinical AD(n=10) or bvFTD(n=9)) emerged. bvFTD patients had significantly worse prognosis. Disinhibition/aggression were highly common (100% of bvFTD, 40% of AD patients). CSF amyloid-β1-42 was decreased in all 5 patients with CSF data, 2/5 with concomitant tau elevation. Neuropathology was FTLD-tau, notably showing only 3R-tau-isoforms.



Neuropathologic findings in patient with p.R406W-associated bvFTD.



Clinical profile of p.R406W mutation carriers. A wide spread in onset age and age at death can be seen, as well as variable clinical diagnoses. This figure illustrates the tremendous heterogeneity of the clinical phenotype.

Conclusion: We are first to report MAPT p.R406W mutation frequencies, unexpectedly high in FTD and AD. Contrary to previous reports, we observed a unique phenotypic shift in Belgian p.R406W carriers, with prominent behavioral symptoms, 47.4% with bvFTD. Surprisingly, CSF biomarkers showed decreased amyloid-β1-42, and neuropathology was FTLD-tau with isolated 3R-tau, highly unusual findings for this tauopathy.
Disclosure: Nothing to disclose.

OPR-119

Potential radiological biomarkers for the m.3243A>G-related MELAS syndrome

Y. Ng¹, C. Hossain¹, R. McFarland¹, J. Hall², A. Blamire³, G. Gorman¹

¹ Wellcome Centre for Mitochondrial Research, Translational and Clinical Research Institute, Newcastle University, Newcastle upon Tyne, United Kingdom, ² Directorate of Neurosciences, Royal Victoria Infirmary, Newcastle upon Tyne Hospital NHS Foundation Trust, Newcastle upon Tyne, United Kingdom, ³ Translational and Clinical Research Institute, Newcastle Magnetic Resonance Centre, Campus for Ageing and Vitality, Newcastle University, Newcastle upon Tyne, United Kingdom

Background and aims: The m.3243A>G variant is the most common cause of adult mitochondrial disease and has heterogeneous clinical manifestations, including mitochondrial encephalomyopathy, lactic acidosis and stroke-like episodes (MELAS) syndrome. Around 20% of patients with the m.3243A>G variant develop MELAS syndrome, and several clinical predictors including heteroplasmy, have been identified. This study sought to identify potential radiological biomarkers of MELAS syndrome.

Methods: 17 patients with the m.3243A>G variants were recruited; seven had MELAS syndrome, and 10 were without the syndrome. All patients were scanned on a Siemens 3T scanner using a 3D T1w anatomical protocol. 24 age- and gender-matched controls were included (Philips scanner).

Results: The mean (SD) age of patients were 40.3 years (12.6), and the mean age-corrected blood heteroplasmy was similar between the MELAS and non-MELAS groups (69% vs 68%, $p>0.05$). Patients with MELAS syndrome had a significantly smaller mean total intracranial volume (TICV) ($p<0.001$) (Figure 1), widespread cerebral and cerebellar volume loss ($p<0.001$) than non-MELAS and control groups. The cognition score of the Newcastle Mitochondrial Disease Rating Scale was strongly correlated with TICV ($r = -0.804$, $p<0.001$). Significant regional reductions in cortical thicknesses were observed in parts of the temporal lobe in MELAS and non-MELAS groups than in the control group ($p<0.05$).

Conclusion: TICV is emerging as a promising radiological biomarker that can predict individuals with the m.3243A>G variant at risk of developing MELAS syndrome. The clinical significance and underlying mechanisms of temporal lobe atrophy in non-MELAS patients warrant further investigation.

Disclosure: Nothing to disclose.

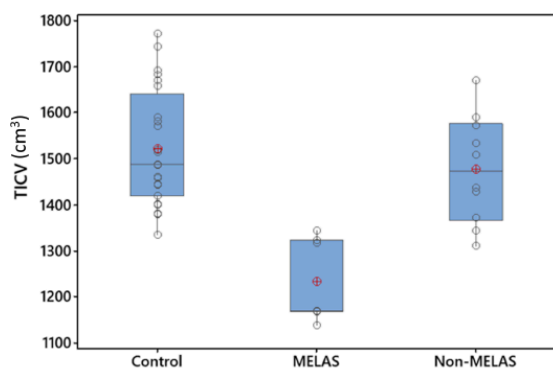


Figure 1. Boxplots of total intracranial volume. The circle with cross symbol denotes the mean value. MELAS= mitochondrial encephalomyopathy, lactic acidosis and stroke-like episodes.

MS and related disorders: Predictors for MS outcome

OPR-120

Does Cognitive Impairment Predict Physical Disability Progression? Evidence from EXPAND, a Phase 3 Long-Term SPMS Study

I. Penner¹, G. Giovannoni², T. Chitnis³, P. Vermersch⁴, S. Arnould⁵, S. Doerken⁶, S. Ansari⁵, J. Maca⁵, V. DeLasHeras⁵, G. Karlsson⁵, D. Piani-Meier⁵, L. Kappos*⁷, R. Benedict*⁸

¹ Department of Neurology, Heinrich Heine University, Germany and COGITO Center for Applied Neurocognition and Neuropsychological Research, Düsseldorf, Germany, ² Blizard Institute, Barts and The London School of Medicine and Dentistry, Queen Mary University of London, London, United Kingdom, ³ Department of Neurology, Brigham and Women's Hospital, Boston, MA, United States of America,, ⁴ University Lille, INSERM U1172, CHU Lille, FHU Precise, Lille, France, ⁵ Novartis Pharma AG, Basel, Switzerland, ⁶ DATAMAP GmbH, Freiburg, Germany, ⁷ Research Center for Clinical Neuroimmunology and Neuroscience Basel and MS Center, Departments of Head, Spine and Neuromedicine, Clinical Research, Biomedicine and Biomedical Engineering, University Hospital and University of Basel, Basel, Switzerland, ⁸ Department of Neurology, Jacobs School of Medicine, University at Buffalo, Buffalo, NY, United States of America, *Equal Contribution

Background and aims: Assess the predictive value of cognitive processing speed (CPS), using the Symbol Digit Modalities Test (SDMT) score, on the time-to-wheelchair (T2W) disability progression milestone in secondary progressive multiple sclerosis (SPMS) patients from the Phase 3 EXPAND study.

Methods: Patients from the core and core+extension parts (core+EP) of EXPAND were categorized into quartiles by baseline SDMT score and on-study (Month 0–24) SDMT change (worst-WQ [Q1], intermediate [Q2–Q3], best-BQ [Q4]). The predictive value of these baseline and on-study change categories for time-to-wheelchair (T2W: Expanded Disability Status Scale [EDSS] score ≥7) after up to 5-years of the core+EP was assessed for the total study population. The predictive value of on-study change was also assessed separately in the siponimod-group (patients received consistent treatment during the core and the subsequent EP).

Results: Risk of T2W was significantly higher in the WQ vs BQ by baseline SDMT (HRWQ/BQ=1.81, p=0.007). On-study SDMT change was predictive of subsequent T2W in both the total study population (HRWQ/BQ=1.73, p=0.046) and in the siponimod arm (HRWQ/BQ=1.93, p=0.047).

Table:	HRWQ/BQ (95% CI) for T2W (sustained till end of follow-up)
Baseline SDMT as a predictor of disability progression	
Total study population (n=1,628)	1.81 (1.17, 2.78), p=0.007
On-study SDMT change (M0–24) as a predictor of subsequent progression	
Total study population (n=1,119)	1.73 (1.01, 2.96), p=0.046
Siponimod group (n=761)	1.93 (1.01, 3.70), p=0.047
Model for baseline: Cox regression, adjusted for treatment, age, gender, baseline EDSS, baseline SDMT quartile, and treatment-by-baseline SDMT quartile interaction	
Model for on-study: Cox regression, adjusted for treatment, age, gender, baseline EDSS, baseline SDMT, on-study change in SDMT quartile	
Abbreviations: BQ, best quartile; EDSS, expanded disability status scale score =7; EP, extension part; SDMT, symbol digit modalities test; WQ, worst quartile	

Conclusion: In line with previous smaller studies, these findings from the EXPAND study confirm that CPS, considered an indirect measure of thalamic network efficiency and functional brain reserve, may have predictive value for long-term physical disability progression. Monitoring CPS in daily practice might therefore help identify patients at increased risk of progressing.

Disclosure: This study was funded by Novartis Pharma AG, Basel, Switzerland. The detailed author disclosures will be presented in the subsequent presentation.

OPR-121

Confirmed disability improvement and sustainability in secondary progressive multiple sclerosis placebo-arm patients

P. Xun¹, N. Sadetsky², K. Kresa-Reahl¹, S. Bogdanovich¹, A. Barlev², C. Watson²

¹ Atara Biotherapeutics, Thousand Oaks, CA, United States of America, ² Atara Biotherapeutics, South San Francisco, CA, United States of America

Background and aims: This study evaluates secondary progressive multiple sclerosis (SPMS) patients with a confirmed disability improvement (CDI) and its sustainability through 24 months in the Multiple Sclerosis Outcome Assessments Consortium (MSOAC) Placebo Database.

Methods: SPMS patients aged from 18 to 61 years with baseline Expanded Disability Status Scale (EDSS) scores between 3 and 6.5 in the MSOAC Placebo Database were identified. CDI was defined as ≥ 1.0 -point decrease from EDSS baseline score ≤ 5.0 or ≥ 0.5 -point decrease from EDSS baseline score ≥ 5.5 at 9-months confirmed at 12-months (cohort I) and at 12-months confirmed at 15-months (cohort II). Endpoints included mean duration of CDI (calculated from confirmation) and percentage of patients maintaining CDI status through 24 months.

Results: 553 SPMS patients were identified; 6.3% (28/444) and 7.0% (30/430) of eligible patients had CDI in cohorts I and II respectively. The majority were females; baseline EDSS scores were ≥ 5.5 for 75.0% of cohort I and 83.3% of cohort II (Table 1). Mean duration of CDI was 7.2 months in cohort I and 5.7 months in cohort II. Of the SPMS patients, 3.2% (cohort I) and 3.7% (cohort II) maintained CDI through 24 months (Table 2).

Table 1. Baseline characteristics of SPMS* improvers

Demographics	Cohort I 9 months confirmed at 12 months (n=28)	Cohort II 12 months confirmed at 15 months (n=30)
Age, years		
Mean (SD)	50 (6.1)	49.4 (6.7)
Median (min, max)	51 (36, 60)	51 (36, 60)
Sex, n (%)		
Female	20 (71.4)	22 (73.3)
Male	8 (28.6)	8 (26.7)
Baseline EDSS score, n (%)		
≤ 5	7 (25.0)	5 (16.7)
≥ 5.5	21 (75.0)	25 (83.3)

*SPMS includes both active and nonactive patients.

EDSS, Expanded Disability Status Scale; SD, standard deviation; SPMS, secondary progressive multiple sclerosis.

Table 1: Baseline characteristics of SPMS* improvers

Parameter	Overall ^a			Recently diagnosed ^b		
	Ofatumumab n=492	Teriflunomide n=468	p-value	Ofatumumab n=245	Teriflunomide n=238	p-value
Change in SDMT score from baseline to Month 24, mean (SE)	3.50 (0.358)	2.39 (0.365)	0.030	4.29 (0.489)	2.56 (0.492)	0.012
Percentage of patients with ≥ 4 -point sustained improvement on SDMT, % (n/N) ^c	25.0 (233/946)	19.6 (180/936)	0.005	26.9 (118/443)	20.2 (91/454)	0.018

^aMean age (SD): 38.2 (9.1) years.
^bMean age (SD): 35.9 (9.2) years.
^cCognitive status during the study was classified as improved, if 6mCCI was sustained until end of study (regardless whether 6mCCD status was met at an earlier visit-window). 6mCCD is defined as a decrease from baseline in SDMT score by ≥ 4 -point sustained for ≥ 6 months. 6mCCI is defined as an increase from baseline in SDMT by ≥ 4 points sustained for ≥ 6 months.
6mCCD, 6-month confirmed cognitive decline; 6mCCI, 6-month confirmed cognitive improvement; SDMT, Symbol Digit Modalities Test; SD, standard deviation; SE, standard error.

Table 2: Sustained improvement in patients with SPMS*

Conclusion: CDI was observed in ~6–7% of SPMS patients evaluated in clinical trial placebo arms, with ~3–4% maintaining CDI through 24 months. More transformational treatments are needed to improve disability in SPMS.

Disclosure: This study was funded by Atara Biotherapeutics. All authors are employees and shareholders of Atara Biotherapeutics. Medical writing assistance was provided by AMICULUM Ltd, funded by Atara Biotherapeutics.

OPR-122

Emergency medical care for multiple sclerosis: A five-year population study in the Campania Region (South Italy)

M. Moccia¹, G. Affinito², B. Ronga³, R. Giordana⁴, M. Fumo⁴, R. Lanzillo¹, M. Petracca⁵, A. Carotenuto¹, M. Triassi², V. Brescia Morra¹, R. Palladino²

¹ Department of Neuroscience, University of Naples "Federico II", Italy, ² Department of Public Health, University of Naples "Federico II", Italy, ³ Neurology and Stroke Unit, AORN Ospedale dei Colli, Naples, Italy, ⁴ Regional Healthcare Society (So.Re.Sa), Naples, Italy, ⁵ Department of Human Neurosciences, Sapienza University, Rome, Italy

Background and aims: Emergency hospital admissions are common in multiple sclerosis (MS), and can highlight unmet medical needs. We aim to evaluate burden, predictors and outcomes of MS emergency admissions.

Methods: This is a population-based study, conducted in the Campania Region (South Italy) from 2015 to 2019, using hospital discharge records, drug prescriptions, and outpatients. The risk of emergency hospital admissions and the likelihood of worse outcomes were evaluated using Cox-regression and multinomial logistic regression models, respectively, in relation to age, sex, disease modifying treatments (DMTs), comorbidities and adherence.

Results: We recorded 1.225 emergency admissions for 1.001 patients (out of 5765 prevalent MS patients), overall costing 4.143,764.67 EUR. The risk of emergency admissions increased with age (HR=1.02; 95%CI=1.01,1.03; p<0.01), and comorbidities (HR=1.62; p<0.01), and decreased in patients using DMTs (interferon beta/peg-interferon beta/glatiramer acetate HR=0.19; p<0.01; teriflunomide/dimethyl-fumarate/fingolimod HR=0.18; p<0.01; and alemtuzumab/cladribine/natalizumab/ocrelizumab HR=0.21; p<0.01), and with higher adherence (HR=0.18; 0.26; p<0.01). Following emergency admission, older age was associated with probability of death (n=63) (OR=1.06; p<0.01), and discharge to long-term facility (n=65) (OR=1.03; p=0.01).

Conclusion: With 17% people with MS requiring emergency medical care over 5 years, improved management of DMTs and comorbidities could potentially reduce their medical, social and financial burden.

Disclosure: Nothing to disclose.

OPR-123

Brain Age in Multiple Sclerosis: A comparison of traditional machine learning and deep learning methods

L. Skattebøl^{1,2}, M. Strømstad¹, E. Leonardsen^{3,4}, T. Kaufmann^{4,5}, T. Moridi^{6,7}, L. Stawiarz⁶, R. Ouellette^{6,8}, B. Ineichen^{6,8}, D. Ferreira⁹, S. Muehlboeck⁹, S. Brune^{1,2}, G. Nygaard¹, P. Berg-Hansen¹, P. Sowa¹⁰, A. Manouchehrinia⁶, E. Westman^{9,11}, T. Olsson⁶, E. Celius^{1,2}, J. Hillert⁶, I. Kockum⁶, H. Harbo^{1,2}, F. Piehl^{6,7}, T. Granberg^{6,8}, L. Westlye^{2,3,12}, E. Høgestøl^{1,2,3}

¹ Department of Neurology, Oslo University Hospital, Oslo, Norway, ² Institute of Clinical Medicine, University of Oslo, Oslo, Norway, ³ Department of Psychology, University of Oslo, Oslo, Norway, ⁴ NORMENT, Division of Mental Health and Addiction, Oslo University Hospital, Oslo, Norway, ⁵ Tübingen Center for Mental Health, Department of Psychiatry and Psychotherapy, University of Tübingen, Tübingen, Germany, ⁶ Department of Clinical Neuroscience, Karolinska Institutet, Stockholm, Sweden, ⁷ Center of Neurology, Academic Specialist Center, Stockholm Health Services, Stockholm, Sweden, ⁸ Department of Neuroradiology, Karolinska University Hospital, Stockholm, Sweden, ⁹ Division of Clinical Geriatrics, Department of Neurobiology, Care Sciences and Society, Karolinska Institutet, Stockholm, Sweden, ¹⁰ Division of Radiology and Nuclear Medicine, Oslo University Hospital, Oslo, Norway, ¹¹ Department of Neuroimaging, Centre for Neuroimaging Sciences, Institute of Psychiatry, Psychology and Neuroscience, King's College London, London, United Kingdom, ¹² K.G. Jebsen Center for Neurodevelopmental disorders, University of Oslo, Oslo, Norway

Background and aims: Brain age is a numerical predicted measure of biological age attained by combining magnetic resonance imaging (MRI) brain scans and artificial intelligence methods. Our main objective was to compare a deep learning (DL) simple fully convoluted neural network (SFCN) model with an established feature-based machine learning (ML) model for brain age estimation in a large longitudinal cohort of people with multiple sclerosis (PwMS).

Methods: PwMS with eligible MRI data were retrospectively analyzed (n=1.515). Clinical and demographic data are summarized in Table 1 and Figure 1. 3D T1-weighted MRIs from eight scanners were processed using in-house ML and DL models. Pearson's correlation and linear mixed effect (LME) models were used for associations between brain age, age and clinical variables.

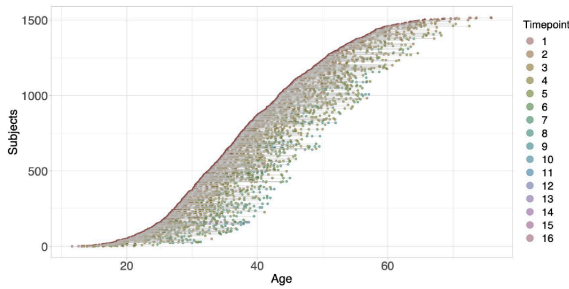


Figure 1 An overview of the multiple sclerosis cohort. We depicted every multiple sclerosis subject in ascending order based on age at the first scan, with chronological age on the x-axis, and the follow-up period as an individual horizontal line. The colour of the circles indicates the number of total MRI scans included for that specific subject

Table 1. Baseline Group Characteristics				
Clinical Values	MS (n = 1515)	EDSS ≤3.5 (n = 1064)	EDSS 4.0 - 6.0 (n = 110)	EDSS >6.0 (n = 35)
Sex, No. (%) females	1098 (72.5)	774 (72.7)	77 (70.0)	24 (68.6)
Age, mean (SD, range)	38.9 (11.6, 64.2)	37.5 (11.1, 64.2)	44.5 (11.8, 50.4)	46.1 (11.8, 45.5)
Disease Duration, mean (SD, range)	5.6 (7.2, 53.5)	5.0 (6.7, 51.2)	8.8 (7.8, 38.0)	13.9 (11.0, 41.4)
EDSS, median (IQR)	2.0 (2.0)	1.5 (1.0)	4.5 (1.5)	6.5 (0.5)
Age at diagnosis, mean (SD)	36.5 (11.0)	35.3 (10.6)	39.8 (11.3)	37.3 (12.7)
Year of MS, median	2010	2010	2004	2000
DMTs, No. (%)				
None	59.9	575 (54.0)	59 (53.6)	17 (48.6)
Effective	31.3	377 (35.4)	38 (34.5)	13 (37.1)
Highly effective	8.4	106 (10.0)	12 (10.9)	5 (14.3)
Other	7 (0.5)	6 (0.6)	1 (0.9)	N/A

MS: multiple sclerosis; EDSS: extended disability status scale; DMTs: disease-modifying therapies

Results: Correlations between the estimated brain age and chronological age were stronger for DL estimations (CI=0.89-0.90, $r=0.90$) than for ML estimations (CI=0.74-0.76, $r=0.75$), Figure 2. Using LME models, we observed increasing brain age to be significantly associated with higher Expanded Disability Status Scale (EDSS) for both the DL estimates ($t=5.3$, CI=0.17-0.37) and the ML estimates ($t=3.7$, CI=0.16-0.51) and longer disease duration ($t=5.8$, CI=0.08-0.15, and $t=6.5$, CI=0.15-0.28, respectively).

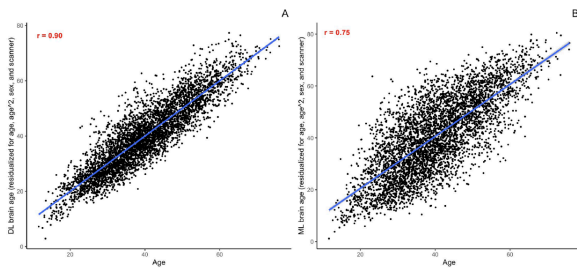


Figure 2. A visualization of the correlation between age and brain age estimations. Both DL (A) and ML (B) estimations were residualized for confounding factors of age, sex and scanner.

Conclusion: Both brain age models revealed significant associations with EDSS and disease duration. The DL model may be of higher clinical value due to a stronger association to EDSS than ML. However, further research is needed.

Disclosure: EAH, SB, PBH, MKB, PS, AM, TO, EGC, JH, HFH, FP and TG received honoraria from different pharmaceutical companies and grants. All other authors report no relevant disclosures.

Ageing and dementia 2

OPR-124

Visuospatial Navigation Strategies in Typical and Atypical Aging

M. Laczó¹, J. Kalinova¹, M. Vyhnalek¹, J. Hort¹, J. Wiener², J. Laczó¹

¹ Memory Clinic, Department of Neurology, Charles University, 2nd Faculty of Medicine and Motol University Hospital, Prague, Czech Republic, ² Department of Psychology, Ageing and Dementia Research Centre, Bournemouth University, Poole, United Kingdom

Background and aims: Spatial navigation and visuospatial function impairment are typical for early Alzheimer’s disease (AD). We used a realistic-looking virtual environment to analyse different aspects of visuospatial processing and spatial navigation performance in typical and atypical aging.

Methods: 219 participants: amnesic mild cognitive impairment (aMCI, n=75), mild AD dementia (n=66) and cognitively normal older adults (CN, n=78) underwent cognitive evaluation, MRI brain scan, biomarker assessment and spatial navigation testing in a virtual realistic-looking “Intersections” test. Test consisted of three tasks: i) egocentric “route repetition”, where participants repeated the route through a virtual city, ii) allocentric “route retracing”, where participants indicated their way back, and iii) allocentric “different approach direction” where participants indicated their positions from different perspectives at each intersection with two same and two unique houses. Participants were asked to report used navigation strategy (sequence-of-directions, stimulus-response, using specific or non-specific landmarks).

Results: aMCI and mild AD dementia groups performed worse compared to CN in all tasks (p<0.05). The most commonly used navigation strategy in both, route repetition and route retracing tasks, was Sequence-of-directions (≥68.6%) and looking at the specific landmarks in the different approach direction tasks (≥52.9%) in aMCI and CN groups. Non-specific strategies were most common in dementia group (p<0.05). Using non-specific strategies across all groups was associated with worse performance (p<0.05).

Conclusion: More effective visuospatial strategies were associated with better navigation performance. The results demonstrate that a realistic and ecologically valid spatial navigation test can differentiate between typical and atypical aging.

Disclosure: ENOCH no. CZ.02.1.01/0.0/0.0/16_019/0000 868; the Ministry of Health, University Hospital Motol, Prague grant no. 00064203; Institutional Support of Excellence 2. LF UK grant no. 6990332; Grant Agency of Charles University grant no. 327821

OPR-125

Abstract withdrawn

OPR-126

Dementia and antipsychotics are associated with significantly higher mortality in patients with COVID-19

J. Sečnčík¹, M. Eriksson¹, A. Rytarowski¹, M. Annetorp¹, K. Johnell⁴, S. Hägg⁴, D. Religa¹

¹ Center for Alzheimer Research, Division of Clinical Geriatrics, Department of Neurobiology, Care Sciences and Society, Karolinska Institutet, Huddinge, Sweden,

⁴ Department of Medical Epidemiology and Biostatistics, Karolinska Institutet, Stockholm, Sweden

Background and aims: Dementia and cognitive decline are discussed as risk factors for severe/lethal outcome of the coronavirus disease 2019 (COVID-19). We aimed to determine whether the presence of dementia is associated with higher in-hospital mortality in patients with COVID-19.

Methods: We conducted an open-cohort observational study based on electronic patient records from seven geriatric care clinics in Stockholm, Sweden between March 1st, 2020 and January 8th, 2021. In total, we identified 4,680 patients, out of which 480 (10.3%) patients had diagnosis of both COVID-19 and dementia, 2,361 (50.4%) had COVID-19 and were dementia-free and 1,839 (39.3%) had dementia without COVID-19. Patients’ age, sex, oxygen saturation, comorbidities, and medication prescription (cardiovascular and psychotropic medication) were registered at admission. The first and second wave of the COVID-19 pandemic were divided by the date August 31st, 2020. The hazard ratios (HRs) with 95% confidence intervals (CIs) of in-hospital mortality associated with dementia were obtained using proportional hazards regression with time since entry as time scale.

Results: Dementia was independently associated with 59% higher in-hospital mortality among COVID-19 patients compared to dementia-free patients at admission [HR 1.59 (1.26–2.01)]. In addition, the prescription of antipsychotic medication was associated with substantially higher mortality among patients without dementia [2.79 (2.05–3.80); vs dementia 1.32 (0.84–2.09)].

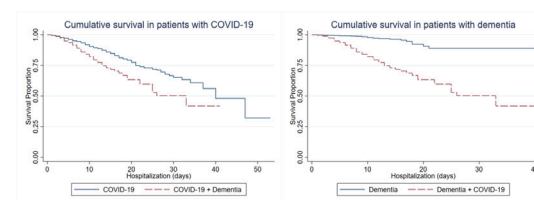


Figure 1. Kaplan-Meier cumulative survival curve during hospitalization by dementia and COVID-19 status.

Conclusion: Dementia is a risk factor for short-term mortality in geriatric patients hospitalized due to COVID-19. Antipsychotic medication seems to be a further risk factor among patients without dementia. Our results may help identify high-risk patients in need of more specialized care when infected with COVID-19.

Disclosure: Authors declare no conflict of interest.

OPR-127

Sleep disorders and incident dementia: a nationwide observational cohort study

L. Damsgaard¹, J. Janbek¹, T. Laursen², A. Erlangsen³, A. Spira⁴, G. Waldemar⁵

¹ Danish Dementia Research Centre, Department of Neurology, Copenhagen University Hospital - Rigshospitalet, Copenhagen, Denmark, ² National Centre for Register-based Research, Department of Economics and Business Economics, Aarhus BSS, Aarhus University, Aarhus, Denmark, ³ Danish Research Institute for Suicide Prevention, Mental Health Centre Copenhagen, Copenhagen, Denmark, Department of Mental Health, Johns Hopkins Bloomberg School of Public Health, Baltimore, United States of America, Center of Mental Health Research, Australian National University, ⁴ Department of Mental Health, Johns Hopkins Bloomberg School of Public Health, Baltimore, Maryland, United States of America, Department of Psychiatry and Behavioral Sciences, Johns Hopkins School of Medicine, Baltimore, Maryland, United States of America, ⁵ Danish Dementia Research Centre, Department of Neurology, Copenhagen University Hospital - Rigshospitalet, Copenhagen, Denmark. Department of Clinical Medicine, University of Copenhagen, Copenhagen, Denmark

Background and aims: Several studies have examined the role of sleep disturbances as a risk factor for dementia, however most of these studies involve smaller cohorts, short time intervals, and often rely on retrospective surveys and self-reported exposure data. Our aim was to examine the association between sleep disorders and late-onset dementia in an entire population.

Methods: In a nationwide cohort with 40-year follow-up we assessed associations between sleep disorder diagnoses and late-onset dementia using Danish register data. Incidence rate ratios (IRR) were calculated using Poisson regression.

Results: The cohort consisted of 1,491,276 people. Those with any sleep disorder had a 17% higher risk of dementia (IRR 1.17, 95% CI 1.11–1.24) compared to people with no sleep disorder after adjusting for age, sex, calendar year, education, and somatic and psychiatric comorbidities. IRR was significantly increased only for dementia within 5 years of sleep disorder diagnosis.

Conclusion: Our findings show a greater short-term risk of dementia following a sleep disorder diagnosis, while we found weaker evidence of a long-term risk. This could potentially point towards sleep disorders as an early symptom of dementia. Further research is needed to distinguish sleep disorders as an early symptom of dementia, a risk factor, or both.

Disclosure: Prof. Waldemar served as a consultant or speaker for Roche, Biogen, and Novo Nordisk (honorarium to department and without honorarium). Dr. Spira received honoraria for serving as a consultant to Merck and from Springer Nature Switzerland AG for guest editing special issues of Current Sleep Medicine Reports.

OPR-128

Life' Simple 7 and rate of cognitive decline in preclinical dementia: a population-based study

A. Speh^{1,2,3,4}, N. Payton⁵, M. Gregoric Kramberger^{3,4}, G. Grande¹, C. Qiu¹, B. Winblad^{2,6}, L. Fratiglioni^{1,7}, L. Bäckman¹, E. Jonsson Laukka^{1,7}

¹ Aging Research Center, Department of Neurobiology, Care Sciences and Society, Karolinska Institutet-Stockholm University, Stockholm, Sweden, ² Division of Neurogeriatrics, Department of Neurobiology, Care Sciences and Society, Karolinska Institutet, Stockholm, Sweden, ³ Department of Neurology, University Medical Center Ljubljana, Ljubljana, Slovenia, ⁴ Medical Faculty, University of Ljubljana, Ljubljana, Slovenia ⁵ Division of Clinical Geriatrics, Center for Alzheimer Research, Department of Neurobiology, Care Sciences and Society, Karolinska Institutet, Stockholm, Sweden, ⁶ Theme Inflammation and Aging, Karolinska University Hospital, Huddinge, Sweden, ⁷ Stockholm Gerontology Research Center, Stockholm, Sweden

Background and aims: We investigated whether vascular risk factors (VRFs) are associated with rate of cognitive decline in the preclinical dementia phase.

Methods: The population-based study included 1,449 participants aged ≥ 60 years ($M = 69.99$, $SD = 9.25$) from the Swedish National Study on Aging and Care-Kungsholmen, who underwent repeated neuropsychological testing (episodic memory, semantic memory, verbal fluency, and perceptual speed) across 12 years. VRFs were assessed with the Life's Simple 7 (LS7) score at baseline and included smoking, diet, physical activity, body mass index, plasma glucose, total serum cholesterol, and blood pressure. Participants were categorised as having poor or intermediate/optimal cardiovascular health. Level and change in cognitive performance as a function of LS7 categories and future dementia status (DSM-IV criteria) were estimated using linear mixed-effects models.

Results: Participants in a preclinical dementia phase were more likely to have a poorer LS7 score initially compared to those who remained dementia-free. For young-old individuals (< 72 years), poor diet was associated with an accelerated perceptual speed decline ($\beta = -0.05$, 95% CI -0.08 to -0.02) and a poor plasma glucose score was associated with faster rates of verbal fluency ($\beta = -0.019$, -0.09 to -0.01) and global cognitive ($\beta = -0.028$, -0.06 to 0.00) decline in the preclinical dementia group.

Conclusion: The association between VRFs and cognitive decline was most pronounced in young-old individuals in a preclinical phase of dementia and driven mostly by diet and glucose.

Disclosure: All authors have no conflict of interest to declare.

OPR-129

Sensitivity to early amyloid increases with higher education in individuals with subjective cognitive decline

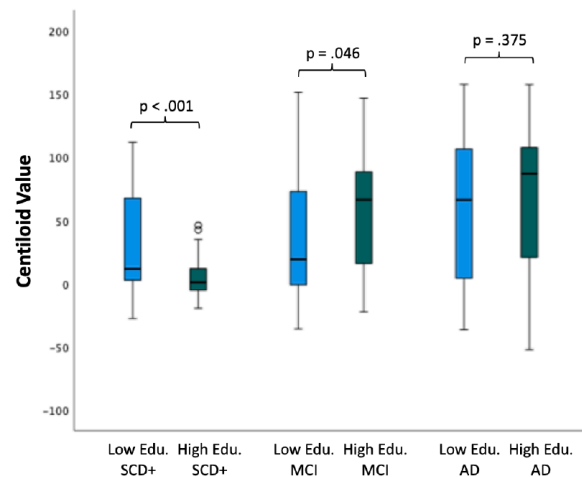
M. Höning¹⁰, C. Caprioglio¹, L. Collij², G. Frisoni¹, F. Barkhof², G. Farrar³, P. Scheltens², J. Delrieu⁴, J. Molinuevo⁵, O. Grau-Rivera⁵, Z. Walker⁶, A. Nordberg⁷, J. Demonet⁸, A. Stephens⁹, M. Battle³, C. Buckley³, J. Gisbert⁵, F. Jessen¹⁰, D. Altomare², A. Drzezga¹⁰

¹ University of Geneva, Geneva, Switzerland, ² Amsterdam UMC, VUmc, Amsterdam, The Netherlands, ³ GE Healthcare, Pharmaceutical Diagnostics, Amersham, United Kingdom, ⁴ Toulouse University Hospital, Toulouse, France, ⁵ Barcelonaβeta Brain Research Center (BBRC), Pasqual Maragall Foundation, Barcelona, Spain, ⁶ Division of Psychiatry, University College London, London, United Kingdom, ⁷ Karolinska University Hospital, Stockholm, Sweden, ⁸ Medical Informatics Platform, SP8, Human Brain Project, Lausanne, Switzerland, ⁹ Life Molecular Imaging, Berlin, Germany, ¹⁰ University Hospital Cologne, Cologne, Germany

Background and aims: Evidence suggests that higher educated patients with mild cognitive impairment (MCI) can tolerate more neuropathology than lower educated patients with similar clinical impairment. It is not known whether this observation also accounts for individuals with subjective cognitive decline plus (SCD+).

Methods: Data of 197 SCD+ individuals, 227 MCI and 157 AD patients were included, which were collected as part of the AMYPAD-DPMS cohort. First, median education in years was computed across the AD-spectrum groups for each of the 8 European sites. Next, using a median split, the AD-spectrum cohorts were separately categorized into a higher and lower educated group, excluding subjects with median education. Afterwards, the higher and lower educated AD-spectrum groups were matched for age, sex and cognitive function (MMSE) using propensity score matching in R, leading to the following sample (low/high education): 54/54 SCD+, 70/81 MCI and 56/65 AD patients. Global amyloid load was compared between education groups using Centiloid (CL) information derived from Flutemetamol and Florbetaben PET scans. Significance level was set to $p < 0.05$.

Results: Higher educated SCD+ subjects presented significantly ($p < 0.001$) lower CL values ($M(CL) = 16.48$) than lower educated SCD+ subjects ($M(CL) = 32.17$), whereas the opposite effect ($p < 0.046$) was observed in the MCI cohort and no difference was found in the AD group.



Group comparisons between the low and high educated SCD+, MCI and AD groups, respectively.

Conclusion: These results indicate that sensitivity to early amyloid accumulation may increase with higher education in stages of SCD, whereas higher education appears to support compensation to amyloid burden in early clinical stages of the disease.

Disclosure: Nothing to disclose.

MS and related disorders: Treatments and multiple sclerosis

OPR-130

Improvement in Cognitive Processing Speed with Ofatumumab in Patients with Relapsing Multiple Sclerosis

R.H.B. Benedict¹, I.-K. Penner², G. Cutter³, L. Kappos⁴, P.K. Coyle⁵, D. Piani-Meier⁶, A. Azmon⁶, I. Boer⁶, W. Su⁷, J. Cohen⁸

¹ Department of Neurology, University at Buffalo, Buffalo, NY, United States of America, ² Medical Faculty, Department of Neurology, Heinrich Heine University, COGITO Center for Applied Neurocognition and Neuropsychological Research, Düsseldorf, Germany, ³ UAB School of Public Health, Birmingham, AL, United States of America, ⁴ Research Center for Clinical Neuroimmunology and Neuroscience Basel and MS Center, Departments of Head, Spine and Neuromedicine, Clinical Research, Biomedicine and Biomedical Engineering, University Hospital and University of Basel, Basel, Switzerland, ⁵ Department of Neurology, Stony Brook University, Stony Brook, NY, United States of America, ⁶ Novartis Pharma AG, Basel, Switzerland, ⁷ Novartis Pharmaceuticals Corporation, East Hanover, NJ, United States of America, ⁸ Department of Neurology, Mellen MS Center, Neurological Institute, Cleveland Clinic, Cleveland, OH, United States of America

Background and aims: In the Phase 3 ASCLEPIOS I/II trials, ofatumumab significantly reduced inflammatory disease activity and relapses, and delayed disability worsening in patients with relapsing multiple sclerosis (RMS). Here, we report the effect of ofatumumab on cognitive processing speed (CPS).

Methods: We analysed the change in Symbol Digit Modalities Test (SDMT) score (baseline to Month 24; derived from a mixed model for repeated measures), proportion of patients with ≥ 4 -point sustained improvement on SDMT (by categorical analysis), and time-to-first 6-month confirmed cognitive improvement (6mCCI; ≥ 4 -point improvement on SDMT) in the overall population and in a subgroup of patients recently diagnosed (RD; within the last 3 years). Time-to-first 6mCCI was also analysed in a subgroup of patients with/without (SDMT score $\leq / > 43$) baseline cognitive impairment.

Results: Ofatumumab significantly improved SDMT scores from baseline to Month 24 in both the overall and RD populations; improvement was more pronounced in the RD subgroup (Table 1). More patients on ofatumumab had ≥ 4 -point sustained improvement on SDMT versus teriflunomide in both the overall and RD populations (Table 1). Ofatumumab numerically increased the probability of time-to-first 6mCCI (hazard ratio [95% confidence intervals]) in the overall population (1.14 [0.96, 1.36]), RD subgroup (1.19 [0.93, 1.52]) and patients without baseline cognitive impairment (1.23 [0.98, 1.56]).

Parameter	Overall ^a			Recently diagnosed ^b		
	Ofatumumab n=492	Teriflunomide n=468	p-value	Ofatumumab n=245	Teriflunomide n=238	p-value
Change in SDMT score from baseline to Month 24, mean (SE)	3.50 (0.358)	2.39 (0.365)	0.030	4.29 (0.489)	2.56 (0.492)	0.012
Percentage of patients with ≥ 4 -point sustained improvement on SDMT, % (n/N) ^c	25.0 (233/946)	19.6 (180/936)	0.005	26.9 (118/443)	20.2 (91/454)	0.018

^aMean age (SD): 38.2 (9.1) years.

^bMean age (SD): 35.9 (9.2) years.

^cCognitive status during the study was classified as improved, if 6mCCI was sustained until end of study (regardless whether 6mCCD status was met at an earlier visit-window). 6mCCD is defined as a decrease from baseline in SDMT score by ≥ 4 -point sustained for ≥ 6 months. 6mCCI is defined as an increase from baseline in SDMT by ≥ 4 points sustained for ≥ 6 months. 6mCCD, 6-month confirmed cognitive decline; 6mCCI, 6-month confirmed cognitive improvement; SDMT, Symbol Digit Modalities Test; SD, standard deviation; SE, standard error.

Table 1: Effect of ofatumumab versus teriflunomide on cognitive processing speed

Conclusion: Ofatumumab was associated with more clinically meaningful improvements in CPS versus teriflunomide when measured by change in SDMT in both the overall and RD populations. Early treatment initiation with ofatumumab may enhance CPS improvement in patients with RMS by efficiently suppressing inflammation. **Disclosure:** The study was supported by Novartis Pharma AG, Switzerland. The detailed author disclosures will be presented in the subsequent presentation.

OPR-131

Effects of evobrutinib, a Bruton's tyrosine kinase inhibitor, on slowly expanding lesions: a marker of tissue loss in MS

D. Arnold¹, C. Elliott¹, X. Montalban², E. Martin³, Y. Hyvert⁴, D. Tomic⁵

¹ NeuroRx Research, Montreal, QC, Canada,

² Department of Neurology-Neuroimmunology, Centre d'Esclerosi Múltiple de Catalunya (Cemcat), Hospital Universitari Vall d'Hebron, Barcelona, Spain,

³ EMD Serono Research & Development Institute, Inc., Billerica, MA, United States of America., an affiliate of Merck KGaA, ⁴ Merck Healthcare KGaA, Darmstadt, Germany, ⁵ Ares Trading SA, Eysins, Switzerland, an affiliate of Merck KGaA

Background and aims: Slowly expanding lesions (SELs) are chronically active, demyelinated multiple sclerosis (MS) lesions, likely driven by sustained microglia/macrophage activity, resulting in irreversible neural tissue damage and axonal loss. Objective: evaluate the effect of evobrutinib, a Bruton's tyrosine kinase inhibitor (BTKi), vs comparator on SEL volume from baseline to Week (W)48 in a Phase II trial (NCT02975349) in relapsing MS.

Methods: SELs were identified, via magnetic resonance imaging, as radially expanding areas of pre-existing T2 lesions (≥ 10 contiguous voxels; $\sim 30\text{mm}^3$). SEL volume analysis, stratified by baseline T2 lesion volume tertiles, was based on W48/end-of-treatment values (completers and discontinuers); treatment effect was analysed via stratified Hodges–Lehman estimate of distribution shift and stratified Wilcoxon rank-sum test. Evobrutinib dose groups (25mg once-daily [QD], n=50; 75mg QD, n=51; 75mg twice-daily [BID], n=53) were compared with placebo/evobrutinib 25mg QD (n=53; Table).

Results: Relative to comparator, SEL volume decreased with increasing evobrutinib dose (25mg QD, -136.5mm^3 [95% CI: $-618.0;309.0$], $p=0.505$; 75mg QD, -246.0mm^3 [$-712.0;97.0$], $p=0.192$; 75mg BID, -474.5mm^3 [$-1,098.0;-3.0$], $p=0.047$). SEL volume was significantly reduced for evobrutinib high-dose (75mg QD + BID) vs low-dose (placebo + evobrutinib 25mg QD) within these subgroups: baseline EDSS ≥ 3.5 (-652.0mm^3 [95% CI: $-1,507.0;-100.0$], $p=0.020$); relapsing-remitting MS (-317.0mm^3 [$-731.5;-29.0$], $p=0.025$); longer disease duration ($>=8.5$ years; -729.3mm^3 [$-1,706.5;-20.0$], $p=0.040$).

Conclusion: Evobrutinib reduces SEL volume in a dose-dependent manner in relapsing MS. The reduction is especially apparent in patients with more advanced disease. This is the first evidence that a BTKi impacts brain lesions associated with chronic inflammation and tissue loss, potentially via microglia.

Disclosure: Study was sponsored by Merck Healthcare KGaA (CrossRef Funder ID: 10.13039/100009945), detailed author disclosures will be included in the presentation.

	Placebo/Evobrutinib 25 mg QD (n=53)	Evobrutinib 25 mg QD (n=50)	Evobrutinib 75 mg QD (n=51)	Evobrutinib 75 mg BID (n=53)
Sex, n (%)				
Male	14 (26.4)	18 (36.0)	16 (31.4)	17 (32.1)
Female	39 (73.6)	32 (64.0)	35 (68.6)	36 (67.9)
Age, years (mean \pmSD)	41.6 \pm 10.8	42.4 \pm 9.4	42.9 \pm 10.1	42.2 \pm 11.5
Time since MS onset, years, n (%)				
<8.5 years	32 (60.4)	26 (52.0)	20 (39.2)	23 (43.4)
≥ 8.5 years	21 (39.6)	23 (46.0)	31 (60.8)	30 (56.6)
Type of MS				
RRMS	47 (88.7)	42 (84.0)	43 (84.3)	47 (88.7)
SPMS	6 (11.3)	8 (16.0)	8 (15.7)	6 (11.3)
Number of relapses in 2 years pre-randomisation, n (%)				
<=1 relapse (non-HDA)	26 (49.1)	27 (54.0)	18 (35.3)	25 (47.2)
≥ 2 relapses (HDA)	27 (50.9)	23 (46.0)	33 (64.7)	28 (52.8)
EDSS score, n (%)				
<=3	27 (50.9)	28 (56.0)	22 (43.1)	28 (52.8)
≥ 3.5	26 (49.1)	22 (44.0)	29 (56.9)	25 (47.2)
T2 lesion volume, cc (mean \pmSD)	15.9 \pm 12.6	13.8 \pm 11.7	14.0 \pm 12.2	19.0 \pm 13.5

mITT analysis set.

BID, twice daily; EDSS, Expanded Disability Status Scale; HDA, high disease activity; mITT, modified intention-to-treat; MS, multiple sclerosis; QD, once daily; RRMS, relapsing-remitting MS; SD, standard deviation; SPMS, secondary-progressive MS.

Table: Baseline characteristics

OPR-132

Tracking the immune response to SARS-CoV-2 mRNA vaccines in ofatumumab treated RMS patients in a multicenter study

T. Ziemssen¹, B. Ettle², M. Groth², T. Bopp³

¹ Department of Neurology, Center of Clinical Neuroscience, Carl Gustav Carus University Clinic, University Hospital of Dresden, Dresden, Germany, ² Novartis Pharma GmbH, Roonstr. 25, Nuernberg, Germany, ³ Institute for Immunology, University Medical Center of the Johannes Gutenberg-University, Mainz, Germany

Background and aims: Initial and booster vaccination with the newly developed SARS-CoV-2 mRNA vaccines efficiently protect healthy individuals against COVID-19. As only limited data is available for Multiple Sclerosis (MS) patients with immunosuppressive treatment, this study aims to comprehend the impact of ofatumumab treatment on mounting cellular and humoral immune responses to SARS-CoV-2 mRNA vaccines.

Methods: KYRIOS is an open-label, two-cohort study including 40 MS patients at 8 sites in Germany. Patients receive initial or booster SARS-CoV-2 mRNA vaccination either before (cohort 1) or at least 4 weeks after starting ofatumumab treatment (cohort 2). The impact of ofatumumab treatment on development of SARS-CoV-2 reactive T-cells (primary endpoint) and neutralizing antibodies (secondary endpoint) will be evaluated. Furthermore, immune responses will be monitored and phenotypically described for up to 18 months.

Results: Results of an interim analysis show that SARS-CoV-2 mRNA vaccines can induce cellular and humoral immune responses in ofatumumab-treated patients. Immune responses could be detected as soon as 1 week after the initial vaccination cycle for all patients receiving their initial SARS-CoV-2 vaccines during stable ofatumumab treatment (n=4) or before ofatumumab initiation (n=5). The interim analysis further shows the effect of ofatumumab treatment on development of immune responses after booster vaccines (n=23).

Conclusion: The KYRIOS study demonstrates for the first time that ofatumumab treated patients can mount specific immune responses towards SARS-CoV-2 mRNA vaccines. The results further suggest that both, humoral and cellular immune response, need to be considered for interpretation of vaccine efficacy and are in line with other recently published studies.

Disclosure: This study is sponsored by Novartis Pharma Vertriebs GmbH.

OPR-133

Assessing the immune response to SARS-CoV-2 mRNA vaccines in SPMS patients treated with siponimod (clinical trial)

T. Ziemssen¹, B. Rauser², B. Ettle², M. Groth², T. Bopp³

¹ Department of Neurology, Center of Clinical Neuroscience, Carl Gustav Carus University Clinic, University Hospital of Dresden, Dresden, Germany, ² Novartis Pharma GmbH, Nuernberg, Germany, ³ Institute for Immunology, University Medical Center of the Johannes Gutenberg-University, Mainz, Germany

Background and aims: SARS-CoV-2 mRNA vaccines are a key factor for fighting the COVID-19 pandemic across the globe. However, data are lacking on the efficacy of these vaccines to induce cellular and humoral immune responses in patients with secondary progressive multiple sclerosis (SPMS) on disease-modifying therapies (DMTs) both over time and after a booster vaccination.

Methods: AMA-VACC is prospective, open-label, three-cohort study including 41 multiple sclerosis patients at ten sites in Germany. Cohort 1 receives SARS-CoV-2 mRNA vaccination during continuous siponimod treatment, cohort 2 interrupts siponimod treatment for the purpose of a full vaccination cycle and cohort 3 is vaccinated during continuous treatment with first-line DMTs (dimethylfumarate, glatirameracetate, interferons, teriflunomide) or no current treatment in clinical routine. Development of neutralizing antibodies (primary endpoint) as well as detection of SARS-CoV-2 specific T-cells (secondary endpoint) are assessed after initial and booster vaccination and monitored for up to 6 months.

Results: Results of previous interim analysis showed that the majority of patients treated with siponimod can mount an immune response after SARS-CoV-2 mRNA vaccination. Here, longitudinal data will be presented describing for the first time the level of cellular and humoral immune response for up to 6 months after vaccination and the effect of booster vaccines in siponimod treated patients.

Conclusion: This analysis will provide data on the maintenance of humoral and cellular immune response after SARS-CoV-2 vaccination in siponimod treated patients and enable physicians and patients to make an informed decision on the coordination of SARS-CoV-2 mRNA (booster) vaccination and SPMS treatment.

Disclosure: This study is sponsored by Novartis Pharma GmbH.

OPR-134

Longer-term Safety of Ofatumumab in Patients With Relapsing Multiple Sclerosis

F. Saccà¹, S. Hauser², A. Cross³, K. Winthrop⁴, H. Wiendl⁵, J. Nicholas⁶, S. Meuth⁷, P. Giacomini⁸, R. Zielman⁹, X. Hu¹⁰, A. Gupta¹¹, R. Sullivan¹⁰, V. DeLasHeras¹², W. Su¹⁰, L. Kappos¹³

¹ NSRO Department, University "Federico II" of Naples, Naples, Italy, ² UCSF Weill Institute for Neurosciences, University of California, San Francisco, CA, United States of America, ³ Washington University School of Medicine, Saint Louis, Missouri, United States of America, ⁴ Public Health and Preventive Medicine, Division of Infectious Diseases, Oregon Health and Sciences University, Portland, Oregon, United States of America, ⁵ University of Muenster, Muenster, Germany, ⁶ OhioHealth Multiple Sclerosis Center, Columbus, Ohio, United States of America, ⁷ Department of Neurology, Medical Faculty, Heinrich-Heine-University, Düsseldorf, Germany, ⁸ Department of Neurology and Neurosurgery, Montreal Neurological Institute, McGill University, Montreal, Quebec, Canada, ⁹ Novartis Pharma B.V., Amsterdam, The Netherlands, ¹⁰ Novartis Pharmaceuticals Corporation, East Hanover, NJ, United States of America, ¹¹ Novartis Healthcare Pvt. Ltd., Hyderabad, India, ¹² Novartis Pharma AG, Basel, Switzerland, ¹³ Research Center for Clinical Neuroimmunology and Neuroscience Basel and MS Center, Departments of Head, Spine and Neuromedicine, Clinical Research, Biomedicine and Biomedical Engineering, University Hospital and University of Basel, Basel, Switzerland

Background and aims: In the Phase 3 ASCLEPIOS I/II trials, ofatumumab treatment up to 30 months had favourable safety profile and was generally well-tolerated in relapsing multiple sclerosis (RMS) patients. Here, we aim to assess the longer-term safety and tolerability of ofatumumab treatment for up to 4 years.

Methods: Patients completing the core ASCLEPIOS I/II, APOLITOS and APLIOS trials could enter ALITHIOS, an ongoing, open-label extension study. We analysed the cumulative safety data for up to 4 years with ofatumumab (cut-off: 25-Sep-2021) in the overall (n=1,969), continuous (ofatumumab in core+extension; n=1,292) and newly-switched (teriflunomide core and ofatumumab extension; n=677) groups. The proportion of patients with treatment-emergent adverse events (TEAEs), serious AEs (SAEs), serious infections including opportunistic infections, and malignancies will be assessed. Laboratory parameters including neutrophils, lymphocytes, and serum immunoglobulin (Ig)G and IgM levels and association with serious infections will be analysed.

Results: Baseline demographics and disease characteristics are presented in Table 1. In the previously reported data (cut-off: 29-Jan-2021; treatment for ~3.5 years), 83.8% of patients had ≥1 AEs (exposure-adjusted incidence rate/100 patient-years [EAIR], 148.7) and 9.7% had ≥1 SAEs (EAIR, 4.8) with a low incidence of serious infections (2.9%; EAIR, 1.4) and malignancies (0.6%; EAIR, 0.3). Updated cumulative clinical safety data with ofatumumab for up to 4 years will be presented at the congress.

	Ofatumumab Continuous (N=1292)	Ofatumumab Newly Switched (N=677)		Ofatumumab Overall (N=1969)
		Baseline of Core Study (N=677)	Baseline of Extension Study (N=677)	
Age, years (mean±SD)	38.0±9.06	38.2±9.22	40.1±9.21	38.7±9.16
Age group - n (%)				
18 to 30 years	312 (24.1)	156 (23.0)	116 (17.1)	428 (21.7)
31 to 40 years	438 (33.9)	244 (36.0)	239 (35.3)	677 (34.4)
41 to 55 years	539 (41.7)	277 (40.9)	288 (42.5)	827 (42.0)
> 55 years	3 (0.2)	0	34 (5.0)	37 (1.9)
BMI (kg/m ²)	25.61±6.16	25.69±5.83	25.61±5.85	25.61±6.05
Female, n (%)	889 (68.8)	456 (67.4)	456 (67.4)	1345 (68.3)
Time since diagnosis, years (mean±SD)	5.87±6.31	5.45±6.00	7.33±6.01	6.37±6.25
EDSS score at baseline, (mean±SD)	2.90±1.33	2.77±1.32	2.81±1.46	2.87±1.38
IgG levels at baseline (mean±SD); g/L	10.31± 2.24	10.35±2.09	10.23±2.14	10.28±2.21
IgM levels at baseline (mean±SD); g/L	1.34± 0.65	1.36±0.74	1.14±0.67	1.27±0.66
EDSS, Expanded Disability Status Scale; Gd+ Gadolinium-enhancing, Nfl, neurofilament light chain; OMB, ofatumumab; SD, standard deviation For OMB newly-switched patients, their baseline values from extension study contribute to the overall summary.				

Baseline Demographics and Disease Characteristics

Conclusion: Safety findings for upto 3.5 years showed ofatumumab treatment to be well-tolerated with no new safety risks identified. This additional safety data up to 4 years will inform physicians on the longer-term safety profile of ofatumumab in RMS patients.

Disclosure: The study was supported by Novartis Pharma AG, Switzerland. The detailed author disclosures will be presented in the subsequent presentation.

OPR-135

Efficacy and safety of ocrelizumab in a treatment-naive, early RMS population: 7-year data from the OPERA OLE trials

J. Cerqueira¹, A. Berthele², B. Cree³, M. Filippi⁴, G. Pardo⁵, O. Pearson⁶, A. Traboulsee⁷, T. Ziemssen⁸, T. Vollmer⁹, C. Bernasconi¹⁰, J. Coulibaly¹¹, C. Mandel¹², J. Overell¹⁰, E. Havrdova¹³

¹ Life and Health Sciences Research Institute, School of Medicine, University of Minho, Braga, Portugal,

² Department of Neurology, School of Medicine, Technical University of Munich, Munich, Germany, ³ Department of Neurology, UCSF Weill Institute for Neurosciences, University of California San Francisco, San Francisco, CA, United States of America, ⁴ Neurology Unit, Neurophysiology Service, Neurorehabilitation Unit, Neuroimaging Research Unit, Division of Neuroscience, IRCCS San Raffaele Scientific Institute, Milan, Italy, ⁵ Multiple Sclerosis Center of Excellence, Oklahoma Medical Research Foundation, Oklahoma City, OK, United States of America, ⁶ Department of Neurology, Morrision Hospital, Swansea, United Kingdom, ⁷ Department of Neurology, University of British Columbia, Vancouver, CA, Canada, ⁸ Center of Clinical Neuroscience, Department of Neurology, University Clinic Carl Gustav Carus, Dresden University of Technology, Dresden, Germany, ⁹ Department of Neurology, Rocky Mountain Multiple Sclerosis Center at Anschutz Medical Campus, University of Colorado Denver, Denver, CO, United States of America, ¹⁰ F. Hoffmann-La Roche Ltd, Basel, Switzerland, ¹¹ F. Hoffmann-La Roche Ltd, Abidjan, Côte d'Ivoire, ¹² Genentech Inc., San Francisco, CA, United States of America, ¹³ Department of Neurology and Center of Clinical Neuroscience, General University Hospital and Charles University, Prague, Czech Republic

Background and aims: The benefits and risks of highly effective therapy as a first-line treatment early in relapsing multiple sclerosis (RMS) should inform evidence-based therapeutic decisions; this subgroup analysis examined disease activity and progression in a treatment-naive, early (diagnosis ≤ 2 years) RMS subpopulation treated with ocrelizumab (OCR) over >7 years ($n=756$), from the Phase III OPERA trials (NCT01247324/NCT01412333).

Methods: Participants were randomised to OCR or interferon (IFN)-beta 1a during the 96-week double-blind period (DBP). During open-label extension (OLE), participants continued OCR (OCR-OCR) or switched to OCR (IFN-OCR). Efficacy endpoints included no evidence of disease activity (NEDA) with MRI rebaselining at Week (W)24 (absence of: Protocol-defined relapses [PDR], 24W-confirmed disability progression [24W-CDP], contrast-enhancing T1-weighted and new/enlarging T2-weighted lesions). Safety measures included incidence/nature of adverse events (AEs).

Results: Of $n=756$ (OCR 375; IFN 381) analysed participants, 70% remained on treatment for ≥ 7.4 years (OCR 73%; IFN 67%). Versus IFN, higher proportions of OCR-treated participants at W96 had NEDA (72% vs 44%; $p<0.001$); no 24W-CDP (92% vs 88%; $p=0.086$); no

evidence of MRI activity (95% vs 62%; $p<0.001$); no PDR (83% vs 73%; $p=0.0015$). OCR-OCR participants maintained benefits through OLE W286 vs IFN-OCR: NEDA (51% vs 28%; $p<0.001$); no 24W-CDP (81% vs 76%; $p=0.14$); no evidence of MRI activity (90% vs 56%; $p<0.001$); no PDR (76% vs 66%; $p=0.0032$ [Table 1]). AE, serious AE and serious infection rates over 7 years remained similar to the DBP (Table 2).

Table 1. Proportion of participants with NEDA and its components at Week 96 and OLE Week 286

Proportion of participants (%)	DBP (Week 96)			DBP+OLE (Week 286) ^a		
	IFN	OCR	P-value	IFN-OCR	OCR-OCR	P-value
With NEDA	43.93	72.46	<0.001	28.00	50.97	<0.001
With no 24W-CDP	88.45	92.27	0.086	76.38	80.80	0.1403
With no PDR	72.70	82.67	0.0015	66.14	76.27	0.0032
With no evidence of MRI activity	62.20	94.93	<0.001	56.17	89.60	<0.001

^aClinical cut-off date: 27 November 2020.

24W-CDP, 24-week confirmed disability progression; DBP, double-blind period; IFN, interferon;

NEDA, no evidence of disease activity; OCR, ocrelizumab; OLE, open-label extension;

PDR, protocol-defined relapse.

AE	OPERA			OCR all-exposure clinical trials ^a (n=5,688; 21,675 PY)
	DBP (Week 96)		DBP+OLE (Week 286) ^a	
Rate per 100 PY (95% CI)	IFN (n=381; 659.7 PY)	OCR (n=374, 663.7 PY)	OCR (n=668; 4,178.7 PY)	
Any AEs	298 (285–311)	289 (277–303)	201 (197–205)	238 (236–240)
AEs leading to discontinuation	4.4 (2.9–6.3)	1.8 (0.9–3.2)	1.2 (0.9–1.6)	1.0 (0.8–1.1)
SAEs	4.7 (3.2–6.7)	4.2 (2.8–6.1)	6.0 (5.3–6.8)	7.3 (7.0–7.7)
Fatal outcomes	0.15 (0.00–0.84)	0.00 (0.00–0.56)	0.10 (0.03–0.25)	0.21 (0.15–0.28)
Malignancies	0.15 (0.00–0.84)	0.30 (0.04–1.09)	0.50 (0.31–0.77)	0.48 (0.39–0.58)
Infections and infestations	66.85 (60.75–73.40)	84.10 (77.25–91.35)	69.76 (67.25–72.34)	72.68 (71.55–73.83)
Serious infections	1.97 (1.05–3.37)	0.30 (0.04–1.09)	1.36 (1.03–1.77)	2.25 (2.06–2.46)

^aClinical cut-off date: 27 November 2020.

AE, adverse event; CI, confidence interval; DBP, double-blind period; IFN, interferon;

OCR, ocrelizumab; OLE, open-label extension; SAE, serious adverse event; PY, patient years.

Table 2: Rates of AEs per 100 patient years (PY) in the DBP, DBP+OLE and the OCR all-exposure population (subsets of the safety population, $n=755$)

Conclusion: In this treatment-naive, early RMS population, long-term safety and efficacy data support the use of ocrelizumab as first-line therapy.

Disclosure: Sponsored by F. Hoffmann-La Roche Ltd; writing and editorial assistance was provided by Articulate Science, United Kingdom.

MS and related disorders: Biomarkers and MRI in neuroinflammatory diseases

OPR-136

Serum Glial Fibrillary Acidic Protein: A Biomarker of Disease Progression in Multiple Sclerosis

C. Barro ¹, B. Healy ², Y. Liu ², S. Saxena ¹, A. Paul ¹, M. Polgar-Turcsanyi ³, C. Guttmann ⁴, R. Bakshi ³, H. Kropshofer ⁵, H. Weiner ³, T. Chitnis ³

¹ Ann Romney Center for Neurologic Diseases, Brigham and Women's Hospital, Boston, MA, United States of America, Department of Neurology, Harvard Medical School, Boston, MA, United States of America, ² Ann Romney Center for Neurologic Diseases, Brigham and Women's Hospital, Boston, MA, United States of America, Department of Neurology, Harvard Medical School, Boston, MA, United States of America, Massachusetts General Hospital Biostatistics Center, Boston, MA, United States of America, ³ Ann Romney Center for Neurologic Diseases, Brigham and Women's Hospital, Boston, MA, United States of America, Department of Neurology, Harvard Medical School, Brigham Multiple Sclerosis Center, Department of Neurology, Brigham and Women's Hospital, Boston, MA, United States of America, ⁴ Ann Romney Center for Neurologic Diseases, Brigham and Women's Hospital, Boston, MA, United States of America, Center for Neurological Imaging, Department of Radiology, Brigham and Women's Hospital, Boston, MA, United States of America, ⁵ Novartis Pharmaceuticals Corporation

Background and aims: Neurodegeneration and astrocytic activation are pathological hallmarks of progressive multiple sclerosis (MS) and can be quantified by serum neurofilament light chain (sNfL) and glial fibrillary acidic protein (sGFAP). We investigated sNfL and sGFAP as tools for stratifying progressive MS patients based on progression and disease activity status.

Methods: sNfL and sGFAP were analyzed in 259 progressive MS patients within 6-months from first confirmed EDSS \geq 3 corresponding with our "baseline". Progressive patients were classified as "active/non-active" based on new brain/spinal cord lesions or relapses in the two years prior to baseline or during follow-up. Statistical analysis on log-transformed sGFAP/sNfL assessed the baseline association with demographic, clinical, MRI features as well as associations with future disability and cognition.

Results: Baseline sNfL was higher in progressive patients with disease activity during the first two years of follow-up ($\beta=1.17$, $p=0.042$) and during the entire follow-up available ($\beta=1.2$, $p=0.013$). Neither sNfL nor sGFAP discriminated between active status prior to baseline. Baseline sGFAP levels were positively associated with higher risk of 6-months confirmed disease progression (6mCDP, adjusted-HR:1.71). The association was stronger in patients with low

sNfL (adjusted-HR:2.44). The change, but not the absolute value of sNfL, was prognostic for 6mCDP (adjusted-HR:1.46, $p=0.003$). Elevated sNfL levels were associated with future cognitive decline ($\beta= -0.79$, $p=0.028$).

Table. Association between baseline levels of biomarkers and 6-month confirmed progression on the EDSS.

Group	Predictor	Association with confirmed progression	Adjusted association with confirmed progression
All	sNfL (continuous)	1.04 (0.79, 1.38); $p=0.782$	1.11 (0.85, 1.49); $p=0.488$
	sNfL		
	Quintile 1	Reference	Reference
	Quintile 2	1.75 (1.07, 2.87); $p=0.027$	1.72 (1.04, 2.84); $p=0.035$
	Quintile 3	1.18 (0.69, 2.04); $p=0.544$	1.16 (0.66, 2.05); $p=0.601$
	Quintile 4	1.04 (0.60, 1.78); $p=0.900$	1.08 (0.61, 1.89); $p=0.799$
Low sGFAP	sNfL (continuous)	1.10 (0.74, 1.64); $p=0.643$	1.20 (0.67, 1.89); $p=0.627$
	sNfL		
	Quintile 1	Reference	Reference
	Quintile 2	2.41 (1.24, 4.69); $p=0.009$	2.09 (1.04, 4.21); $p=0.040$
	Quintile 3	1.27 (0.60, 2.69); $p=0.537$	1.12 (0.50, 2.52); $p=0.782$
	Quintile 4	1.29 (0.55, 3.04); $p=0.556$	1.32 (0.52, 3.33); $p=0.556$
All	sGFAP (continuous)	1.47 (1.05, 2.05); $p=0.023$	1.71 (1.19, 2.45); $p=0.004$
	sGFAP		
	Quintile 1	Reference	Reference
	Quintile 2	1.27 (0.74, 2.18); $p=0.390$	1.33 (0.77, 2.29); $p=0.311$
	Quintile 3	1.17 (0.69, 1.99); $p=0.568$	1.34 (0.77, 2.32); $p=0.305$
	Quintile 4	1.48 (0.89, 2.48); $p=0.134$	1.61 (0.94, 2.75); $p=0.084$
Low sNfL	sGFAP (continuous)	1.67 (1.00, 2.81); $p=0.052$	2.24 (1.26, 3.98); $p=0.006$
	sGFAP		
	Quintile 1	Reference	Reference
	Quintile 2	2.01 (1.04, 3.88); $p=0.037$	2.10 (1.07, 4.14); $p=0.032$
	Quintile 3	1.59 (0.82, 3.09); $p=0.173$	2.35 (1.11, 5.00); $p=0.026$
	Quintile 4	2.02 (1.06, 3.84); $p=0.033$	2.01 (1.02, 3.98); $p=0.044$
All	sGFAP (continuous)	1.47 (1.05, 2.05); $p=0.023$	1.71 (1.19, 2.45); $p=0.004$
	sGFAP		
	Quintile 1	Reference	Reference
	Quintile 2	1.27 (0.74, 2.18); $p=0.390$	1.33 (0.77, 2.29); $p=0.311$
	Quintile 3	1.17 (0.69, 1.99); $p=0.568$	1.34 (0.77, 2.32); $p=0.305$
	Quintile 4	1.48 (0.89, 2.48); $p=0.134$	1.61 (0.94, 2.75); $p=0.084$
Low sNfL	sGFAP (continuous)	1.67 (1.00, 2.81); $p=0.052$	2.24 (1.26, 3.98); $p=0.006$
	sGFAP		
	Quintile 1	Reference	Reference
	Quintile 2	2.01 (1.04, 3.88); $p=0.037$	2.10 (1.07, 4.14); $p=0.032$
	Quintile 3	1.59 (0.82, 3.09); $p=0.173$	2.35 (1.11, 5.00); $p=0.026$
	Quintile 4	2.02 (1.06, 3.84); $p=0.033$	2.01 (1.02, 3.98); $p=0.044$

Legend: Estimates are presented as hazard ratio and 95% confidence interval from Cox regression model. Adjusted analyses included the measure of interest and age, sex, EDSS, relapse and treatment. Low sGFAP: only patients with sGFAP levels below the median; Low sNfL: only patients with sNfL levels below the median; sGFAP: serum glial fibrillary acidic protein; sNfL: serum neurofilament light chain.

Conclusion: Higher levels of sGFAP were an indicator of progression, whereas sNfL reflected acute disease activity in our progressive MS cohort. Thus, sGFAP and sNfL levels may be used to stratify progressive MS patients at enrollment in clinical research studies and clinical trials.

Disclosure: Postdoctoral fellowship from the Swiss National Science Foundation (P400PM_191077 to CB); Department of Defense (W81XWH1810648 to TC); Novartis Pharmaceuticals Corporation.

OPR-137

A Highly Sensitive Proteomic Immunoassay to Identify Novel Serum Biomarkers for Multiple Sclerosis Disease Progression

Z. Van Lierop¹, S. In 't Veld², S. Noteboom³, E. Willemse⁴, M. Schoonheim³, M. Steenwijk³, J. Geurts³, B. Uitdehaag¹, J. Killestein¹

¹ Neurology Department, Amsterdam UMC location VUmc, Amsterdam, The Netherlands, ² Clinical Chemistry Department, Amsterdam UMC location VUmc, Amsterdam, The Netherlands, ³ Anatomy and Neurosciences Department, Amsterdam UMC location VUmc, Amsterdam, The Netherlands, ⁴ Multiple Sclerosis Centre, University Hospital of Basel, Basel, Switzerland

Background and aims: Progression independent of relapse activity (PIRA) is common in relapsing remitting multiple sclerosis (RRMS), even under high-efficacious disease modifying treatment such as natalizumab, yet specific blood biomarkers are currently lacking. Our objective was to identify novel biomarkers associated with PIRA using a proteomics approach.

Methods: In this longitudinal cohort study of 84 natalizumab-treated RRMS patients, 1,472 proteins were assessed using the Olink Explore panel (Proximity Extension Assay) at baseline (prior to natalizumab initiation) and after 3 months and 24 months of natalizumab treatment. Annual clinical and radiological data on disease activity and progression were collected for a median of 5.2 years, including relapses, Expanded Disability Status Scale (EDSS), 9-hole peg test, timed 25-foot walk test and lesion, whole brain, ventricle and thalamus volume by Freesurfer's Sequence Adaptive Multimodal SEGmentation (SAMSEG) tool. EDSS plus status (progressor or non-progressor) was determined between year 1 and last follow-up, correcting for relapse associated worsening. Relevant proteins were selected based on statistically significant effects on EDSS-plus status and brain atrophy measures.

Results: EDSS plus progressors (n=40) and non-progressors (n=44) showed comparable low rates of clinical and radiological disease activity at baseline and follow-up. Up to 3 serum proteins were found to be significantly up- or downregulated in progressors compared to non-progressors at the 3 and 24 month timepoint, including some involved in the complement pathway and myelination. Additional proteins were significantly associated to and predictive of brain atrophy.

Conclusion: We identified several potential serum biomarkers associated with PIRA and brain atrophy in natalizumab-treated RRMS.

Disclosure: Nothing to disclose.

OPR-138

Monoaminergic network abnormalities: a fingerprint for multiple sclerosis-related fatigue and depression

A. Carotenuto¹, P. Valsasina¹, P. Preziosa¹, D. Mistri¹, M. Rocca², M. Filippi²

¹ Neuroimaging Research Unit, Division of Neuroscience, IRCCS San Raffaele Scientific Institute, Milan, Italy,

² Neuroimaging Research Unit, Division of Neuroscience, and Neurology Unit, IRCCS San Raffaele Scientific Institute, and Vita-Salute San Raffaele University, Milan, Italy

Background and aims: Fatigue and depression are extremely frequent in MS; however, their pathophysiological correlates are not completely unveiled. We explored monoaminergic network functional abnormalities in MS patients and their correlation with fatigue and depression by applying PET-constrained independent component analysis (ICA) to resting state (RS) functional MRI (fMRI) data.

Methods: We enrolled 213 MS patients and 62 healthy controls (HC), who underwent neurological, fatigue, depression and RS fMRI assessment. We excluded patients with cognitive impairment assessed through the symbol digit modality test and patients with depression or fatigue due to disease-modifying treatments. Patterns of dopamine, noradrenaline- and serotonin-dependent RS functional connectivity (FC) were derived by ICA, constrained to PET atlases for dopamine, noradrenaline and serotonin transporters, previously obtained in HC's brain.

Results: Compared to HC, MS patients showed abnormalities in all three explored monoaminergic networks, mostly with decreased monoamine-dependent RS FC in frontal regions and subcortical areas including the cerebellum and thalamus, and increased RS FC in temporoparieto-occipital cortical areas, including bilateral precuneus. MS-related fatigue was associated with decreased dopamine-dependent RS FC in the left thalamus and left cerebellum, and increased serotonin-dependent RS FC in the left middle occipital gyrus. MS-related depression was associated with more distributed abnormalities involving the three explored monoaminergic networks, resulting in overall reduced monoamine-dependent RS fMRI FC in the frontal lobe, limbic areas and precuneus.

Conclusion: MS patients presented diffuse monoaminergic network functional dysregulation. Specific alterations in these networks were associated with fatigue and depression, providing a pathological fingerprint for these bothersome symptoms and putative targets for their treatment.

Disclosure: Antonio Carotenuto was supported by a MAGNIMS/ECTRIMS research fellowship.

OPR-139

MAGNON – Contribution of Lublin Criteria and quantitative MRI-Analysis for daily clinical routine of MS Patients

O. Hoffmann¹, M. Jankovic², S. Schmidt³, M. Groth³

¹ St. Josefs-Krankenhaus Potsdam-Sanssouci, Potsdam, Germany, ² Sauerlandklinik Hachen, Sundern, Germany,

³ Novartis Pharma GmbH, Clinical Research Neuroscience, Nuremberg, Germany

Background and aims: Revised Lublin criteria provide a definition of remitting and progressing Multiple Sclerosis to classify disease activity of patients with Secondary Progressive Multiple Sclerosis (SPMS). However, Lublin criteria are only rarely used in clinical practice, like quantitative and standardized MRI analyses, which are often not part of standard routine care in patient management. MAGNON aims to evaluate if standardized quantification of MRI data and assessment of MS patients based on the Lublin criteria could help to classify disease activity.

Methods: 1,000 MRI scans of patients with SPMS or suspected SPMS will be provided by 50 centers in Germany between 2020–2022. The analysis of standardized MRI data will comprise a volumetric quantification of brain and thalamic volumes as well as T2-lesion-volume and number using a centralised automatic processing pipeline (Biometrica MS[®], jung diagnostics GmbH). Percentage brain volume change is computed when follow-up scans are available. The value of standardized MRI analysis and the impact on patient assessment, including potential changes in Lublin classification, is evaluated.

Results: Latest interim analysis data (n=650) show that already one stand-alone standardized MRI scan can provide insights on disease activity and progression. Moreover, physicians stated that already one stand-alone MRI suggested a change in MS treatment for about 40% of their patients with suspected SPMS.

Conclusion: MAGNON interim results indicate that quantification of lesion volume as well as brain and thalamic atrophy on routine MRI may facilitate the individual assessment of disease activity and progression according to the Lublin criteria and thus enhance individualized patient care.

Disclosure: This data collection is funded by Novartis Pharma GmbH, Germany.

OPR-140

Exploring in vivo multiple sclerosis brain microstructural damage through T1w/T2w-ratio: a multicenter study

M. Margoni¹, E. Pagani¹, A. Meani¹, L. Storelli¹, S. Mesaros², J. Drulovic², F. Barkhof³, H. Vrenken³, A. Gallo⁴, A. Bisecco⁴, D. Pareto⁵, J. Sastre-Garriga⁶, O. Ciccarelli⁷, M. Yiannakas⁷, J. Palace⁸, P. Preziosa¹, M. Rocca⁹, M. Filippi⁹

¹ Neuroimaging Research Unit, Division of Neuroscience, IRCCS San Raffaele Scientific Institute, Milan, Italy, ² Clinic of Neurology, Faculty of Medicine, University of Belgrade, Belgrade, Serbia, ³ Radiology and Nuclear Medicine, and MS Center Amsterdam, Amsterdam Neuroscience, Amsterdam UMC, Vrije Universiteit Amsterdam, Amsterdam, The Netherlands, ⁴ Department of Advanced Medical and Surgical Sciences, and 3T MRI-Center, University of Campania “Luigi Vanvitelli”, Naples, Italy, ⁵ Section of Neuroradiology, Department of Radiology, Hospital Universitari Vall d’Hebron, Barcelona, Spain, ⁶ Department of Neurology/Neuroimmunology, Multiple Sclerosis Centre of Catalonia, Hospital Universitari Vall d’Hebron, Barcelona, Spain, ⁷ NMR Research Unit, Queen Square MS Centre, Department of Neuroinflammation, UCL Queen Square Institute of Neurology, London, United Kingdom, ⁸ Nuffield Department of Clinical Neurosciences, University of Oxford, Oxford, United Kingdom, ⁹ Neuroimaging Research Unit, Division of Neuroscience, and Neurology Unit, IRCCS San Raffaele Scientific Institute, and Vita-Salute San Raffaele University, Milan, Italy

Background and aims: The T1-weighted (w)/T2w-ratio may be clinically feasible to investigate microstructural damage in multiple sclerosis (MS). The aims of this study were to evaluate white matter (WM) and gray matter (GM) T1w/T2w-ratio in healthy controls (HC) and MS patients, and its association with clinical disability.

Methods: In this cross-sectional study, 270 HC and 434 MS patients were retrospectively selected from seven European sites. T1w/T2w-ratio was obtained from brain T2w and T1w scans after intensity calibration using eyes and temporal muscle.

Results: In HC, T1w/T2w-ratio increased until 50-60 years in WM and GM. Compared to HC, T1w/T2w-ratio was significantly lower in lesions of all phenotypes, and in normal-appearing (NA) WM and cortex of relapsing-remitting (RR) and secondary progressive (SP) MS ($p \leq 0.026$), but it was significantly higher in the striatum and pallidum of RR, SP and primary progressive (PP) MS ($p \leq 0.04$). In relapse-onset MS, T1w/T2w-ratio was significantly lower in lesions and NAWM already at Expanded Disability Status Scale [EDSS] < 3.0 and in the cortex only for EDSS ≥ 3.0 ($p \leq 0.02$). Conversely, T1w/T2w-ratio was significantly higher in the striatum and pallidum for EDSS ≥ 4.0 ($p \leq 0.005$). In PPMS, striatum and pallidum showed significantly higher T1w/T2w-ratio beyond EDSS = 6.0 ($p \leq 0.001$). In MS, longer disease duration, higher EDSS, higher brain lesional volume, and lower normalized brain volume were associated with lower

lesional and cortical T1w/T2w-ratio and a higher T1w/T2w-ratio in the striatum and pallidum (β from -1.17 to 0.29, $p < 0.04$).

Conclusion: T1w/T2w-ratio is a clinically relevant marker sensitive to demyelination, neurodegeneration, and iron accumulation occurring in the different MS phases.

Disclosure: MM is supported by a MAGNIMS/ECTRIMS research fellowship. FB is supported by the NIHR biomedical research centre at UCLH. This work is partially supported by the Ministry of Education and Science, Republic of Serbia (project 175031).

OPR-141

CYBA genotypes may influence disease severity and recovery in patients with Guillain Barré syndrome

A. Törnelli^{1,*}, N. Lagerström^{2,*}, N. Mossberg³, R. Kiffin¹, O. Andresen², M. Axelsson², K. Hellstrand¹, A. Martner¹
¹ Sahlgrenska Center for Cancer Research, Department of Infectious Diseases, Institute of Biomedicine, Sahlgrenska Academy, University of Gothenburg, Gothenburg, Sweden, ² Department of Clinical Neuroscience, Institute of Neuroscience and Physiology, Sahlgrenska Academy, University of Gothenburg, Gothenburg, Sweden, ³ GHP Neuro Center, Calanderska Hospital, Gothenburg, Sweden, * contributed equally to this paper

Background and aims: The NOX2 enzyme expressed by myeloid cells, including inflammatory M1 macrophages, generates potentially neurotoxic reactive oxygen species (ROS). Single nucleotide polymorphisms (SNP) within the gene encoding the functional NOX2 subunit CYBA impact on the magnitude of NOX2-derived ROS formation from myeloid cells. We have recently reported that genetic variation at CYBA influences disease severity and time to progression among patients with multiple sclerosis (Törnelli et al., *Eur J Neurol*, in press 2022). In this retrospective study, we determined the potential impact of variants of CYBA SNPs (rs1049254 and rs4673) for severity and recovery time among patients with Guillain-Barré syndrome (GBS).

Methods: 100 patients with GBS were followed for median 15 (range 0.5–86) months with clinical parameters sequentially recorded. 31% of the patients were female, and the median age at diagnosis was 52 years (range 17–85). DNA was isolated from serum samples for genotyping at rs1049254 and rs4673 using the TaqMan SNP genotyping kit.

Results: CYBA alleles linked to reduced NOX2-derived ROS formation, i.e. rs1049254/G and rs4673/A, were associated with reduced likelihood of requirement of assisted ventilation ($p=0.01$, Fisher's exact test, Figure 1A). Additionally, a higher frequency of low-ROS alleles was associated with shorter time to independent walking ($p < 0.001$, log-rank test, Figure 1B).

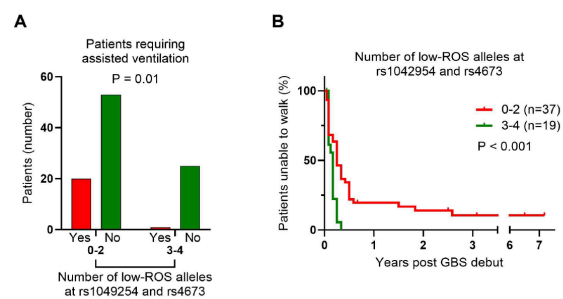


Figure 1: Patients with Guillain Barré syndrome carrying 3-4 low-ROS alleles rs1049254/G and rs4673/A experienced reduced likelihood of requirement of assisted ventilation (A) and a shorter time to independent walking (B).

Conclusion: These results implicate NOX2-derived ROS in GBS pathophysiology and suggest that patients carrying low-ROS CYBA alleles show favorable outcomes in terms of disease severity and in the phase of recovery.

Disclosure: None of the authors report conflicting interests. The study was supported by Swedish State via the ALF agreement (grant no. ALFGBG-724881) and the Sahlgrenska Academy at University of Gothenburg.

Cerebrovascular diseases: Basic and translational stroke research

OPR-142

IPSC-derived mural cells to model the effects of hyperglycemia on the neurovascular unit

E. Abati¹, G. Rocha², H. Slevén², Z. Cader²

¹ Department of Pathophysiology and Transplantation (DEPT), University of Milan, Milan, Italy, ² Nuffield Department of Clinical Neurosciences, University of Oxford, John Radcliffe Hospital, Oxford OX3 9DU, United Kingdom

Background and aims: The neurovascular unit (NVU) is a functional domain that constitutes the blood-brain barrier and contributes to a variety of trophic and signaling functions. Recent studies have highlighted a potential role of non-neuronal NVU constituents, such as mural cells, in the development of cognitive impairment. Moreover, a link between vascular risk factors for cognitive impairment, namely type 2 diabetes, and neurovascular dysfunction has been established. The aims of this project are to establish an in vitro model of mural cells (pericytes and vascular smooth muscle cells (VSMCs)) derived from induced pluripotent stem cells (iPSCs) and to assess the effects of changes in glucose homeostasis on mural cells' functionality.

Methods: We used a two-step protocol to differentiate neural crest cells and then mural cells from iPSCs. We also assessed cell contractility in response to endothelin-1, a potent vasoconstrictor, under basal conditions and following hyperglycaemic (25 mM), normoglycaemic (5.5 mM) and hypoglycaemic (0 mM) conditioning for 24 hours.

Results: We managed to obtain a mixed population of mural cells, although it was not possible to differentiate two distinct populations of pericytes and VSMCs. The cells were indeed able to contract in reaction to an endothelial vasoconstrictor stimulus. Contractile response seemed to be better after normoglycaemic conditioning compared to hypo- and hyperglycaemic one.

Conclusion: Further studies are needed in order to better characterize differences between pericytes and VSMCs that could be translated in more efficient differentiation protocols. Nevertheless, our preliminary results seem to confirm a potential relationship between impairment in glucose homeostasis and mural cells dysfunction.

Disclosure: The authors have nothing to disclose.

OPR-143

The Renin-Angiotensin-Aldosterone-System modulates astrocytes and their crosstalk with microglia and neurons

D. Olschewski¹, F. Lange¹, C. Kulka¹, N. Nazarzadeh¹, S. Blaschke¹, J. Abraham³, R. Merkel³, B. Hoffmann³, G. Fink¹, G. Fink², M. Schroeter¹, M. Schroeter², M. Rueger¹, M. Rueger², S. Vay¹

¹ Department of Neurology, University of Cologne, Faculty of Medicine and University Hospital Cologne, Cologne, Germany, ² Cognitive Neuroscience, Institute of Neuroscience and Medicine (INM-3), Research Centre Juelich, Juelich, Germany, ³ Department of Mechanobiology, Institute of Biological Information Processing (IBI-2), Research Centre Juelich, Juelich, Germany.

Background and aims: Astrocytes are the most abundant central nervous system (CNS) cell type and are fundamentally involved in homeostasis, neuroprotection, and synaptic plasticity. The renin-angiotensin-aldosterone system regulates arterial blood pressure through endothelial cells and perivascular musculature. Moreover, astrocytes express angiotensin II type 1 and 2 receptors. However, their role in astrocytic function has not yet been elucidated. We hypothesized that the angiotensin II receptors impact astrocyte function as revealed in an in vitro system mimicking cerebral ischemia.

Methods: Astrocytes were exposed to telmisartan or PD123319 (angiotensin II type 1 and 2 receptor-blockers) under normal conditions (control) or deprivation from oxygen and glucose (OGD). Conditioned medium (CM) of astrocytes was harvested to elucidate astrocyte-mediated indirect effects on microglia and cortical neurons.

Results: Telmisartan increased the survival of astrocytes during acute and prolonged ischemic conditions in vitro without affecting their proliferation rate or disturbing their expression of S100A10, a marker of activation. PD123319 resulted in both increased expression of S100A10 and proliferation rate. The CM of telmisartan-stimulated astrocytes reduced the expression of pro-inflammatory mediators in microglia, while PD123319-stimulated astrocytes increased the expression of pro-inflammatory markers in microglia with simultaneous reduction of anti-inflammatory markers. Increased neuronal activity was observed after treatment of neurons with CM of telmisartan- as well as PD123319-stimulated astrocytes.

Conclusion: Data show that angiotensin II receptors have functional relevance for astrocytes and modulate both astrocytes' phenotype and functionality. The effects of modulation of angiotensin II receptors on astrocytes might potentially serve as a therapeutic target in human stroke.

Disclosure: The authors declare that the research was conducted in the absence of any commercial or financial relationships that could be construed as a potential conflict of interest.

OPR-144

Electrocorticographic band changes during infarct progression and spreading depolarizations in gyrencephalic brain

R. Díaz Peregrino ¹, M. Kentar ¹, C. Trenado Colín ², R. Sánchez Porras ³, J. Woitzik ³, E. Santos Marcial ³
¹ Department of Neurosurgery, Heidelberg University Hospital, Heidelberg, Germany, ² Institute of Clinical Neuroscience and Medical Psychology, Heinrich Heine University, Düsseldorf, Germany, ³ Department of Neurosurgery, Oldenburg University, Oldenburg, Germany

Background and aims: Characterization of temporal and anatomical electrocorticographic changes occurring after a Middle Cerebral Artery occlusion (MCAo), including those caused by Spreading Depolarizations (SDs) as outcome biomarkers.

Methods: The left medial cerebral arteries were clipped in six Landrace swine. Five electrodes were placed bilaterally over the parietal and frontal cortex corresponding to the irrigation territory of the MCA and the Anterior Cerebral Artery (ACA). Five-minute ECoG signal segments were obtained before, 0, 4, 8, and 12 hours after the artery occlusion, and before, during, and after the negative DC shift of SDs. The power spectrum of signals was decomposed into the delta, theta, alpha, beta, and gamma bands.

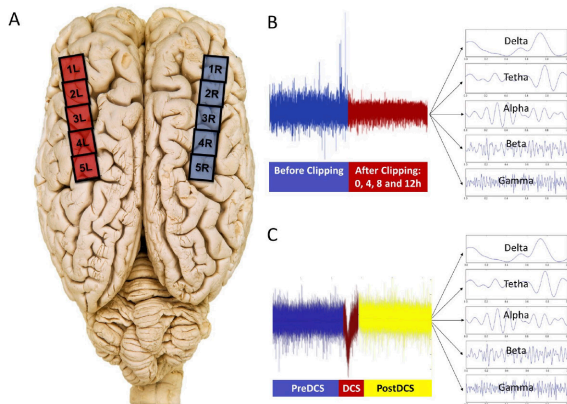


Figure 1. (A) Placement of the electrodes: The electrodes were placed over the frontal and parietal cortex. Channels 1L-5L recorded the left insulted hemisphere. Channels 1R-5R gathered the signal information from the right healthy hemisphere. (B) Effects of the MCAo over the brain electrical activity: Five-minutes signal segments were obtained before, 0, 4, 8, and 12 hours after the artery occlusion. (C) Effects of SDs over the brain electrical activity: The SD signal was assessed 5 min before (preDCS), during (DCS), and 5 min after the negative DC shift (postDCS). The power spectrum of signals was decomposed into the delta, theta, alpha, beta, and gamma bands

Figure 1. Placement of the electrodes and signal gathering

Results: After the artery clipping, channels located near to the MCAo (nMCAo) registered permanent power drop in all the frequencies. Channels far from the MCAo (fMCAo), coinciding with the penumbra, exhibited constant shrinkage of fast waves mainly alpha, and progressive decline in delta and theta. After 8 hours, the ACA channel recorded power decay in all the frequencies except gamma. During the DC shift, all brain oscillations were abated at MCA and ACA channels. Delta, theta, and alpha remained collapsed in the fMCAo channels, whereas no power reductions were observed in the ACA channel after the DC shift.

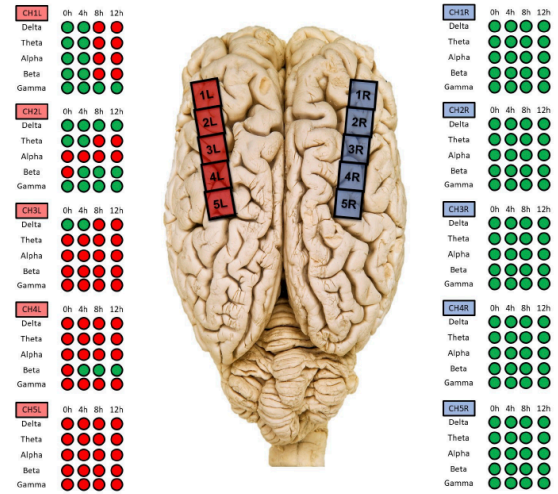


Figure 2. Frequency power in the left and right channels after the middle cerebral artery occlusion (MCAo): The 5-minute signal segment before MCAo was used as the baseline to compare the changes in frequency power at time points 0h, 4h, 8h, and 12h. The statistically significant drop in power of the frequencies is represented as red light ($p \leq 0.05$). The green light represents no modification in the power of the brainwaves. Channels near to the MCAo (nMCAo): CH5L and CH4L; Channels far from the MCAo (fMCAo): CH3L and CH2L; ACA channel: CH1L

Figure 2. Frequency power in the left and right channels after the middle cerebral artery occlusion (MCAo)

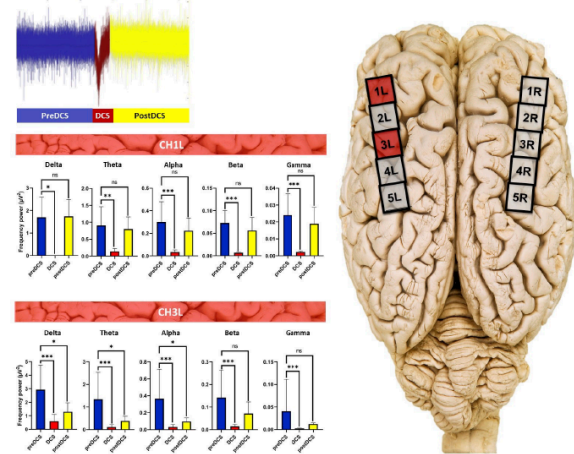


Figure 3. Frequency power in the left channels during and after the DC shift of the SDs: The 5-minutes signal segment before the negative DC shift (preDCS) was used as the baseline to compare the variations in frequency power at the negative DC shift (DCS) and after the DC shift (postDCS) segments. The p-value notation: * is equal to ≤ 0.05 ; ** is equal to ≤ 0.01 ; *** is equal to ≤ 0.001 ; **** is equal to ≤ 0.0001 . Channels near to the MCAo (nMCAo): CH5L and CH4L; Channels far from the MCAo (fMCAo): CH3L and CH2L; ACA channel: CH1L

Figure 3. Frequency power in the left channels during and after the DC shift of the SDs

Conclusion: ECoG can identify the penumbra zone and monitor infarct progression. Secondary brain injury was observed in the irrigation territory of ACA after 8 hours of blood constraints at MCA. SDs generate drastic frequency disturbances regardless of the cortical location, causing sequelae at the presumable salvable brain tissue.

Disclosure: Nothing to disclose.

OPR-145

Thrombo-CARE - histological and immunohistochemical analysis of clots to differentiate stroke etiology

D. Schwarzenhofer¹, T. Von Oertzen¹, S. Weis², M. Sonnberger³, H. Wagner⁴, H. Philipp⁴, B. Grubauer⁴, J. Wagner¹

¹ Department of Neurology¹ Neuromed Campus Kepler University Hospital, Linz, Austria, ² Department of Neuropathology Neuromed Campus Kepler University Hospital, Linz, Austria, ³ Department of Neuroradiology Neuromed Campus Kepler University Hospital, Linz, Austria, ⁴ Kompetenzzentrum für Klinische Studien (KKS Linz) am Zentrum für Klinische Forschung (ZKF), Linz, Austria

Background and aims: Despite extensive diagnostic efforts, etiology of stroke remains unclear in about 20% of patients. The establishment of mechanical thrombectomy offers the possibility to enhance etiological determination by histological and immunohistochemical analysis of retrieved thrombotic material.

Methods: Clots from 200 consecutive patients undergoing mechanical thrombectomy in a neurovascular center were investigated by Hematoxylin and Eosin, CD3 and CD45 staining. Semiquantitative and computer-based automatic image analysis defined histological composition and relative fractions of immune stained areas. Results were initially correlated with strokes of known etiology. Subsequently, thrombi of unknown source were characterized with regard to their (immuno-)histological profile attempting etiological classification.

Results: 198 samples were accessible for analysis. Mixed histology appeared in 123 (62%), thrombocyte/fibrin-rich in 45 (23%) and erythrocyte-rich histology in 18 (9%) patients. Etiology was classified as cardio-embolic in 87 (44%), arterio-embolic in 37 (19%) and undetermined in 26 (13%) patients. 20 patients with cardio-embolic stroke had thrombocyte/fibrin-rich clots, five patients with arterio-embolic stroke. eight patients with arterio-embolic stroke had erythrocyte-rich clots, one patient with cardio-embolic stroke. Associations between histology and etiological groups were significant ($p=0.0061$). Associations between immune staining and all etiological groups were not significant. Clots from embolic strokes of undetermined source (ESUS) presented similar histological features as cardio-embolic ones.

Conclusion: Erythrocyte-rich thrombi were significantly associated with arterio-embolic stroke, thrombocyte/fibrin-rich thrombi with cardio-embolic stroke. Many patients with ESUS shared similar histological clot features as cardio-embolic strokes. Patients with ESUS and thrombocyte/fibrin-rich clots especially require long-term cardiac rhythm monitoring and may benefit from oral anticoagulation.

Disclosure: Nothing to disclose.

OPR-146

Distribution of five clinically important neuroglial proteins in the human brain

K. Sjölin¹, K. Kultima², A. Larsson², E. Freyhult³, C. Zjukovskaja¹, K. Alkass⁴, J. Burman¹

¹ Department of Medical Sciences, Neurology, Uppsala University Hospital, Uppsala, Sweden, ² Department of Medical Sciences, Clinical Chemistry, Uppsala University Hospital, Uppsala, Sweden, ³ Department of Cell and Molecular Biology, Uppsala University, Uppsala, Sweden, ⁴ Forensic Medicine Laboratory, Department of Oncology-Pathology, Karolinska Institute, Stockholm, Sweden

Background and aims: Glial fibrillary acidic protein (GFAP), myelin basic protein (MBP), neurofilament light chain (NFL), Tau and ubiquitin carboxy-terminal hydrolase L1 (UCHL1) are five neuroglial proteins that are used as biomarkers of tissue damage in the nervous system. There is incomplete knowledge of their quantitative distribution in the CNS, limiting the interpretability of circulating levels of these proteins. The aim with this study was to quantitate the concentration of GFAP, MBP, NFL, Tau and UCHL1 in different anatomical regions in the CNS, thereby creating a map of how these proteins are distributed in the human brain and spinal cord.

Methods: Tissue homogenates from 17 selected anatomical regions in the CNS, from ten deceased donors were analysed with ELISA for each protein of interest. When appropriate, the protein concentrations were adjusted for post-mortem interval.

Results: The concentration of GFAP, MBP, NFL, Tau and UCHL1 varied substantially between different CNS regions. The concentration of MBP were tenfold higher in white matter compared with cerebral cortex, whereas Tau showed an inverse pattern. GFAP, NFL and Tau displayed an anteroposterior gradient in cerebral white matter. The cerebellum had relatively low concentrations of all the investigated proteins.

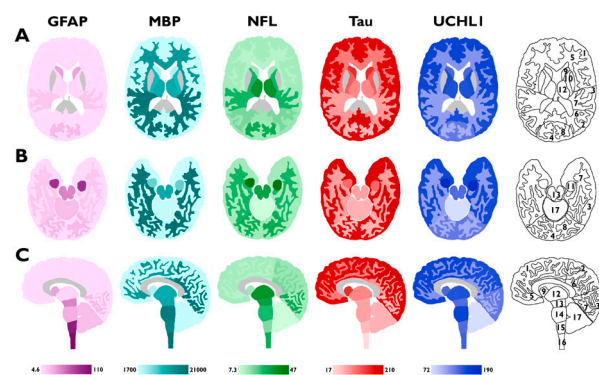


Figure 1 A-C. (A) axial cranial, (B) axial caudal, and (C) sagittal sections of the CNS. The bar below every section shows the colour gradient used between the minimum and maximum value for each neuroglial protein. Darker colour represents higher values.

Conclusion: This study investigated the tissue content of GFAP, MBP, NFL, Tau and UCHL1 in different anatomical CNS regions, and the results show a substantial variation between CNS regions and investigated proteins. This information can be used as a reference when interpreting circulating levels of these proteins in relation to localisation and extent of a CNS damaging disease.

Disclosure: The authors reports no competing interests.

OPR-147

Circulating endothelial progenitor cells (cEPC) as a putative predictive cellular biomarker in Moyamoya arteriopathy

G. Pollaci, G. Gorla, T. Carrozzini, A. Potenza, S. Nava, I. Canavero, L. Gatti, A. Bersano
Neurology IX Unit, UCV, Fondazione IRCCS Istituto Neurologico Carlo Besta, Milan, Italy

Background and aims: Moyamoya arteriopathy (MA) is a rare cerebrovascular disorder characterized by ischemic/hemorrhagic strokes. The pathophysiology is unknown. Circulating endothelial progenitor cells (cEPC) have been hypothesized to contribute to vascular remodeling of MA. Our aim is to evaluate if % cEPC could be used as a cellular prognostic or predictive biomarker in MA patients.

Methods: 75 MA patients of GEN-O-MA project, 34 healthy donors (HD) and 20 subjects with unrelated diseases (ACVD) were recruited. Clinical data and peripheral blood samples were collected. Percentage of cEPC ($(\text{cEPC}/(\mu\text{l}))/(\text{WBC}/(\mu\text{l})) \times 100$), defined as CD45dimCD133+CD34+, was measured by FACS.

Results: Our previous comparison did not show significant differences of % cEPC in peripheral blood of MA, HD and ACVD. Nevertheless, the selection of a patient subgroup (Caucasian, adults, with a pre-surgical sampling) resulted in a substantial decrease of % cEPC in MA as compared to HD. Here, such an evidence became more significant as far as the size of MA subgroup raised. Pediatric patients instead exhibited an increase in % cEPC as compared to age/sex matched HD. Moreover, an analysis was performed to correlate % cEPC value to clinical features, prognosis and disease severity within the MA group.

Conclusion: Our findings suggest that % cEPC value could be a promising “circulating cellular biomarker” for a better patient stratification in MA. The validation of these results on a larger population could provide a new reliable biological marker in support to neuroimaging data, to date the only available prognostic tool for MA patient management.

Disclosure: Nothing to disclose.

Neurogenetics 2

OPR-148

Repeat expansion size predicts age of onset in RFC1 CANVAS and disease spectrum

R. Currò^{1,2}, N. Dominik², D. Pareyson³, A. Brusco⁴, F. Taroni³, F. Manganelli⁵, C. Tassorelli¹, P. Mandich⁶, M. Jokela⁷, J. Infante⁸, G. Ravenscroft⁹, R. Roxburgh¹⁰, F. Santorelli¹¹, G.M. Fabrizi¹², C. Briani¹³, A. Başak¹⁴, M. Strupp¹⁵, A. Hartmann¹⁶, M. Synofzik¹⁷, M. Hadjivassiliou¹⁸, T. Stojkovic¹⁹, M.M. Reilly², H. Houlden², A. Cortese²

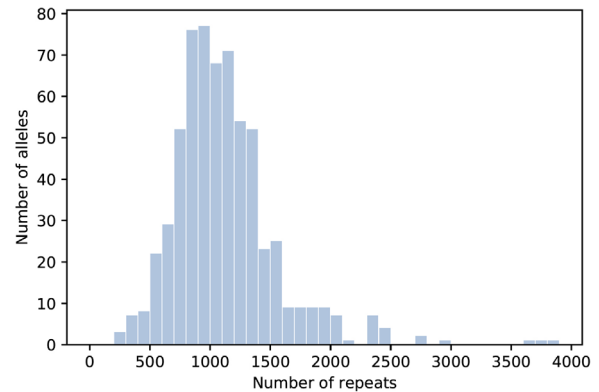
¹ Department of Brain and Behavioral Sciences, University of Pavia, Pavia, Italy, ² Department of Neuromuscular Diseases, UCL Queen Square Institute of Neurology, London, United Kingdom, ³ Fondazione IRCCS Istituto Neurologico Carlo Besta, Milan, Italy, ⁴ Department of Medical Sciences, University of Torino, Turin, Italy, ⁵ Università Federico II di Napoli, Naples, Italy, ⁶ DINOEMI, University of Genoa, Genova, Italy, ⁷ Neuromuscular Research Center, Department of Neurology, Tampere University, Tampere, Finland, ⁸ University Hospital Marqués de Valdecilla- IDIVAL, University of Cantabria, Santander, Spain, ⁹ Neurogenetic Diseases Group, Centre for Medical Research, QEII Medical Centre, University of Western Australia, Nedlands, Australia, ¹⁰ Centre for Brain Research, University of Auckland, Auckland, New Zealand, ¹¹ Molecular Medicine, IRCCS Fondazione Stella Maris, Pisa, Italy, ¹² Department of Neuroscience, Biomedicine and Movement Sciences, University of Verona, Verona, Italy, ¹³ Department of Neuroscience, University of Padova, Padova, Italy, ¹⁴ Suna and İnan Kırac Foundation, Neurodegeneration Research Laboratory, KUTTAM, Koç University School, Istanbul, Turkey, ¹⁵ Department of Neurology, University Hospital, Ludwig Maximilians University, Munich, Germany, ¹⁶ Department of Psychiatry, Psychotherapy and Psychosomatics, University of Halle, Halle, Germany, ¹⁷ Hertie-Institute for Clinical Brain Research, Tübingen, Germany, ¹⁸ Sheffield Teaching Hospitals NHS Trust and University of Sheffield, Sheffield, United Kingdom, ¹⁹ Institute of Myology, Pitié-Salpêtrière Hospital, APHP, Sorbonne University, Paris, France

Background and aims: Biallelic repeat expansions in RFC1 have been identified as the cause of cerebellar ataxia, neuropathy, vestibular areflexia syndrome (CANVAS). Based on the first descriptions, RFC1 disease has variable phenotype, onset and progression, however the factors underlying this heterogeneity are still largely unknown.

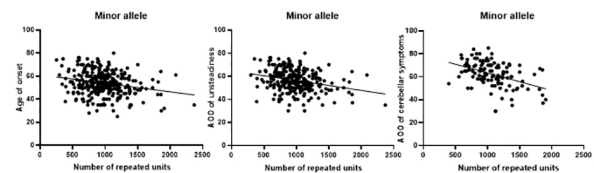
Methods: We investigated the effect of the repeat expansion size on age at onset, clinical phenotype and disease course in a multicenter cohort of 316 patients with biallelic AAGGG RFC1 repeat expansions confirmed by Southern Blotting. Furthermore, we assessed the stability of the repeat during intergenerational transmission in 19 families.

Results: Median age at onset of imbalance was 55 years and median disease duration at last follow-up was 10 years. At last examination, 45% of patients showed a full-blown CANVAS, 16% isolated sensory neuropathy and 39% neuropathy with

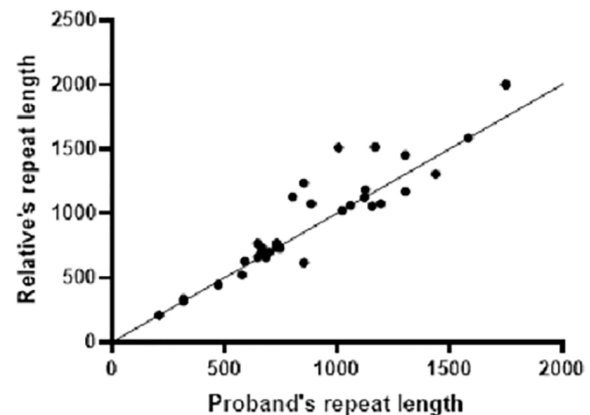
cerebellar or vestibular involvement. RFC1 expansion ranged from 249 to 3,885 repeats. An inverse correlation, which was stronger for the smaller allele, was observed between the repeat size and age at neurological onset. A larger expansion was also predictive of a more complex phenotype and a faster progression to disabling manifestations. RFC1 expansion appeared stable during parental transmission, with no or minimal variation in most cases.



Distribution of the size of the AAGGG repeat expansions in our cohort.



Correlation between the size of the minor RFC1 allele and age of onset, age at onset of unsteadiness and age at onset of cerebellar symptoms.



Relationship between the repeat length in probands and first-degree relatives.

Conclusion: RFC1 disorder shows heterogeneous clinical presentation and disease course. A smaller expansion has a favorable prognostic role and is associated with later disease onset, later appearance of cerebellar symptoms and delayed need for walking aids. Southern blotting is recommended after PCR screening in all RFC1 positive cases to better inform patients on their prognosis.

Disclosure: EAN Research Fellowship 2021.

OPR-149

Brain metabolic profile and longitudinal changes in the presymptomatic phase of GRN-associated frontotemporal dementia

D. Saracino¹, L. Sellami¹, H. Boniface², M. Locatelli², M. Pelegrini², A. Funkiewiez³, M. Houot⁴, D. Rinaldi¹, K. Dorgham⁵, F. Pasquier⁶, M. Chastan⁷, A. Hitzel⁸, J. Pariente⁹, A. Pallardy¹⁰, E. Guedj¹¹, M. Didic¹², A. Kas², M. Habert², I. Le Ber¹

¹ Sorbonne Université, Paris Brain Institute – Institut du Cerveau – ICM, Inserm U1127, CNRS UMR 7225, APHP – Hôpital Pitié-Salpêtrière, Paris, France, ² Laboratoire d’Imagerie Biomedicale (LIB), Centre d’Acquisition et Traitement d’Images (CATI), APHP – Hôpital Pitié-Salpêtrière, Paris, France, ³ Reference Center for Rare or Early Dementias, IM2A, Département de Neurologie, AP-HP – Hôpital Pitié-Salpêtrière, Paris, France, ⁴ Sorbonne Université, Paris Brain Institute – Institut du Cerveau – ICM, Center of Excellence of Neurodegenerative Disease (CoEN), APHP – Hôpital Pitié-Salpêtrière, Paris, France, ⁵ Sorbonne Université, INSERM, Centre d’Immunologie et des Maladies Infectieuses-Paris (CIMI-Paris), Paris, France, ⁶ Univ Lille, Inserm U1171, CHU Lille, DistAlz, LiCEND, CNR-MAJ, Lille, France, ⁷ Centre Henri Becquerel, CHU Charles Nicolle, Rouen, France, ⁸ Département de Médecine Nucléaire, CHU de Toulouse, Toulouse, France, ⁹ Département de Neurologie, CHU de Toulouse, Toulouse, France, ¹⁰ Département de Médecine Nucléaire, CHU de Nantes, Nantes, France, ¹¹ Département de Médecine Nucléaire, APHM, CNRS, Centrale Marseille, Institut Fresnel, Hôpital Timone, Aix Marseille Univ, Marseille, France, ¹² Service de Neurologie et Neuropsychologie, APHM Hôpital Timone, Aix Marseille Univ, Marseille, France

Background and aims: Progranulin gene (GRN) mutations are among the main genetic causes of frontotemporal dementia (FTD). Previous biomarker-based studies shed light on pathophysiological changes occurring during the presymptomatic phase. FDG-PET may be useful to capture early signs of brain dysfunction, before structural changes; however, there is a lack of longitudinal investigations assessing brain metabolic changes in GRN-associated FTD. This study aimed at characterizing the dynamic profile of brain hypometabolism in presymptomatic GRN carriers and its position in preclinical pathochronology.

Methods: This prospective study analysed 27 presymptomatic GRN carriers and 31 demographically comparable non-carriers issued from the Predict-PGRN study (NCT04014673). Participants were evaluated over 5 years with cognitive/behavioral assessments, plasma neurofilament measurements, brain MRI and FDG-PET imaging. PET data were analysed with voxel-wise comparisons, metabolic percent annual changes maps (PET-PAC) and region of interest-based approach.

Results: The median age at inclusion was 42 years, ≥ 15 years before expected disease onset. Since their inclusion, carriers displayed significant hypometabolism involving superior and middle temporal gyri, in absence of cortical

atrophy or any cognitive changes. During follow-up accelerated metabolic decline (up to 20%/year) occurred in the lateral temporal region, as well as in temporal pole and superior occipital gyrus. Metabolic changes in temporal cortex were associated with increase in neurofilaments.

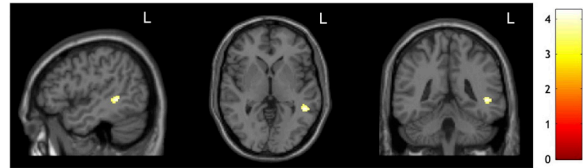


Figure 1: Cross-sectional voxel-wise analysis of brain glucose metabolism in presymptomatic GRN carriers compared to controls at baseline, showing a cluster of hypometabolism in the left middle temporal gyrus ($p < 0.001$, uncorrected).

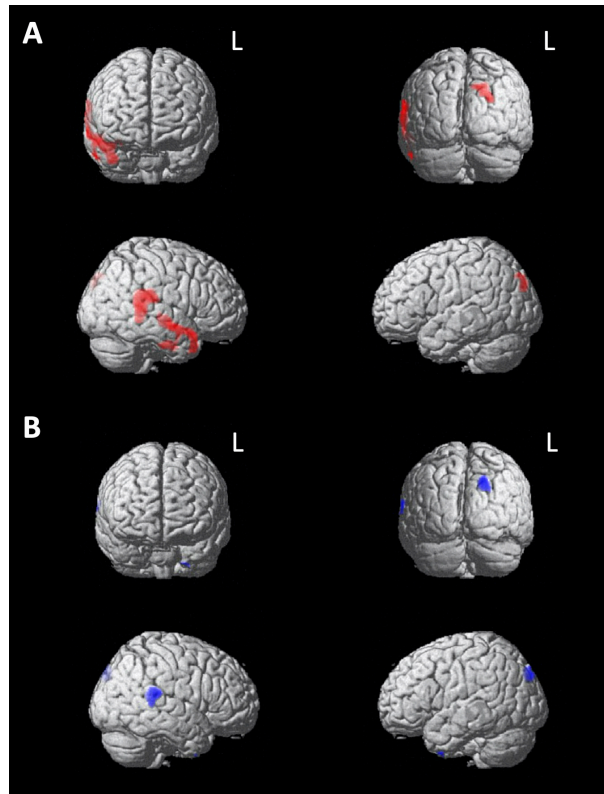


Figure 2: Longitudinal decrease of glucose metabolism in carriers during the 5-year follow-up, peaking in right superior/middle temporal lobe, from pairwise voxel-based t-tests (A) and PET-PAC maps (B) ($p < 0.001$, FDR cluster-level corrected).

Conclusion: Brain metabolic changes are present since the earliest phases of GRN disease. They highlight the lateral temporal lobe as hub of lesional accumulation, heralding subsequent spreading and neurodegeneration. Their annualised change rates may serve as valuable biomarkers to assess the efficacy of therapeutic trials in presymptomatic carriers.

Disclosure: The research leading to these results was partially funded by “Investissements d’avenir” ANR-11-INBS-0011 and the Programme Hospitalier de Recherche Clinique (PHRC) Predict-PGRN (to ILB, promotion by AP-HP).

OPR-150

Whole exome sequencing in 444 families with rare paediatric neurological disorders in Central Asia and Transcaucasia

R. Kaiyrzhanov¹, K. Salayev², M. Ganieva³, B. Sukhudyay⁴, N. Tabatadze⁵, U. Guliyeva⁶, E. Kurua⁵, S. Gulieva⁶, C. Shashkin⁷, Z. Tavadyan⁸, A. Gevorgyan⁴, M. Isoqova³, N. Kuyumjyan⁹, N. Asilova³, A. Hakobyan¹⁰, M. Kekenadze¹¹, Z. Aynur¹², R. Ibadova¹³, M. Beridze¹¹, N. Tatishvili¹⁴, N. Zharkinbekova¹, S. Khachatryan⁸, G. Melikishvili⁵, R. Maroofian¹⁵, H. Houlden¹⁵

¹ South Kazakhstan Medical Academy, Department of Neurology, Shymkent, Kazakhstan, ² Azerbaijan Medical University, Department of Neurology, Baku, Azerbaijan, ³ Department of Neurology, Avicenna Tajik State Medical University, Dushanbe, Tajikistan, ⁴ Arabkir Joint Medical Center and Institute of Child and Adolescent Health, Yerevan, Armenia, ⁵ Department of Pediatrics, MediClubGeorgia Center, Tbilisi, Georgia, ⁶ MediClub Hospital, Baku, Azerbaijan, ⁷ International Research Institute of Postgraduate Education, Kazakhstan, Almaty, ⁸ Sleep and Movement Disorders Center, Somnus Neurology Clinic, Yerevan, Armenia, ⁹ Surb Astvatsamayr Pediatric Hospital, Yerevan, Armenia, ¹⁰ Department of Neurology Yerevan State Medical University, Yerevan, Armenia, ¹¹ Tbilisi State Medical University, Tbilisi, Georgia, ¹² Neuron medical center, Baku, Azerbaijan, ¹³ Neurology department, Hb Guven Clinic, Baku, Azerbaijan, ¹⁴ David Tvildiani Medical University, Tbilisi, Georgia, M. Iashvili Children's Central Hospital - Neuroscience, Tbilisi, Georgia, ¹⁵ University College London, Institute of Neurology, Department of Neuromuscular Disorders, London, United Kingdom

Background and aims: Little is known about the genetics of rare paediatric neurological disorders (RPND) in Central Asia and Transcaucasia (CAT). Additionally, ethnic groups from CAT are largely underrepresented in reference population genetic databases. Here, we report the results of proband and trio research whole-exome sequencing (WES) in 444 families with RPND from five CAT countries.

Methods: In 2018 the “University College London (UCL)-Central Asia-Transcaucasia disease diversity project” was initiated, and hitherto, ~2,000 families with RPND from CAT have been recruited. To date, proband or trio research WES data is available from 444 families. WES, variant filtering, dynamic re-analysis of WES data, and variant confirmation/segregation analysis by Sanger sequencing were performed at UCL as previously described (PMID: 29343805).

Results: Almost half of the cohort (47%) were probands from consanguineous unions mostly originating from Azerbaijan and Tajikistan (Figure 1). Families with multiple affected members made of 14% of the cohort. A mean age of the probands at the time of recruitment was 8.7±7.5 years. Clinical phenotypes were classified into 5 diagnostic categories (Table 1). Trio WES was performed on 36% of

families while proband WES was done in 64%. Overall 179 families (40%) received a molecular diagnosis with causative variants identified in known disease-associated genes (Figure 1, Table 1). Firm novel genes were found in 2% and putative candidate genes were identified in 8% of the families (Table 2). Several actionable genes improved clinical management.

Figure 1 The results of research WES in 444 families with rare paediatric neurological disorders in CAT

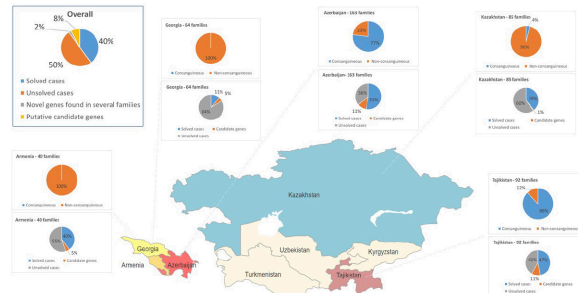


Table 1 Diagnostic categories and known disease genes found in the CAT cohort

Diagnostic categories	Established disease-associated genes with segregated pathogenic and likely pathogenic variants found in the CAT cohort
<ul style="list-style-type: none"> Global developmental delay/intellectual disability (GDD/ID) GDD/ID with epilepsy GDD/ID with autism spectrum disorder (ASD) ASD GDD with regression Microcephaly Syndromic GDD/ID Epileptic encephalopathy/structural epilepsy GDD/ID with complex neurological phenotype 	<p>Overall 341 families</p> <ul style="list-style-type: none"> PIAS3B (2 families), TPST1 (8 families), SCY119 (2 families), C-ORF153 (family), PPT1 (2 families), SINGAP1 (2 families), CACNA1A (2 families), AOCGR1 (2 families), VPS36 (2 families), MED13 (2 families), HNF1P1 (3 families), CLD1 (3 families), ARI1 (2 families), SPIN1A2, MFSD1, GRIN1, GRIN2B, LAMA2, C2orf172, RASGEF1B, SPSPEC1, EPMA2, PI16V2, CEM1E, PPT1, ZFR1, ANK1, SC2B3A, ALG12, B9P1, MECP1, GRIN3B, TSPAN1, CHST1, POU3F1, GANCB, APPA, KCNE1, ERFEL, TSC2, PTPRK1A, MET, FOXRED1, TUBB3A (homologous), ALDH4L1, DOC, G3BP2, FDD1, PA13, ALG11, FROCH3, CIMP1, ANK1, KCTD11, NDU1B, NDU1A, NDU1, SLC6A1, SLC6A2, SLC6A3, SLC6A4, SLC6A5, SLC6A6, SLC6A7, SLC6A8, SLC6A9, SLC6A10, SLC6A11, SLC6A12, SLC6A13, SLC6A14, SLC6A15, SLC6A16, SLC6A17, SLC6A18, SLC6A19, SLC6A20, SLC6A21, SLC6A22, SLC6A23, SLC6A24, SLC6A25, SLC6A26, SLC6A27, SLC6A28, SLC6A29, SLC6A30, SLC6A31, SLC6A32, SLC6A33, SLC6A34, SLC6A35, SLC6A36, SLC6A37, SLC6A38, SLC6A39, SLC6A40, SLC6A41, SLC6A42, SLC6A43, SLC6A44, SLC6A45, SLC6A46, SLC6A47, SLC6A48, SLC6A49, SLC6A50, SLC6A51, SLC6A52, SLC6A53, SLC6A54, SLC6A55, SLC6A56, SLC6A57, SLC6A58, SLC6A59, SLC6A60, SLC6A61, SLC6A62, SLC6A63, SLC6A64, SLC6A65, SLC6A66, SLC6A67, SLC6A68, SLC6A69, SLC6A70, SLC6A71, SLC6A72, SLC6A73, SLC6A74, SLC6A75, SLC6A76, SLC6A77, SLC6A78, SLC6A79, SLC6A80, SLC6A81, SLC6A82, SLC6A83, SLC6A84, SLC6A85, SLC6A86, SLC6A87, SLC6A88, SLC6A89, SLC6A90, SLC6A91, SLC6A92, SLC6A93, SLC6A94, SLC6A95, SLC6A96, SLC6A97, SLC6A98, SLC6A99, SLC6A100, SLC6A101, SLC6A102, SLC6A103, SLC6A104, SLC6A105, SLC6A106, SLC6A107, SLC6A108, SLC6A109, SLC6A110, SLC6A111, SLC6A112, SLC6A113, SLC6A114, SLC6A115, SLC6A116, SLC6A117, SLC6A118, SLC6A119, SLC6A120, SLC6A121, SLC6A122, SLC6A123, SLC6A124, SLC6A125, SLC6A126, SLC6A127, SLC6A128, SLC6A129, SLC6A130, SLC6A131, SLC6A132, SLC6A133, SLC6A134, SLC6A135, SLC6A136, SLC6A137, SLC6A138, SLC6A139, SLC6A140, SLC6A141, SLC6A142, SLC6A143, SLC6A144, SLC6A145, SLC6A146, SLC6A147, SLC6A148, SLC6A149, SLC6A150, SLC6A151, SLC6A152, SLC6A153, SLC6A154, SLC6A155, SLC6A156, SLC6A157, SLC6A158, SLC6A159, SLC6A160, SLC6A161, SLC6A162, SLC6A163, SLC6A164, SLC6A165, SLC6A166, SLC6A167, SLC6A168, SLC6A169, SLC6A170, SLC6A171, SLC6A172, SLC6A173, SLC6A174, SLC6A175, SLC6A176, SLC6A177, SLC6A178, SLC6A179, SLC6A180, SLC6A181, SLC6A182, SLC6A183, SLC6A184, SLC6A185, SLC6A186, SLC6A187, SLC6A188, SLC6A189, SLC6A190, SLC6A191, SLC6A192, SLC6A193, SLC6A194, SLC6A195, SLC6A196, SLC6A197, SLC6A198, SLC6A199, SLC6A200, SLC6A201, SLC6A202, SLC6A203, SLC6A204, SLC6A205, SLC6A206, SLC6A207, SLC6A208, SLC6A209, SLC6A210, SLC6A211, SLC6A212, SLC6A213, SLC6A214, SLC6A215, SLC6A216, SLC6A217, SLC6A218, SLC6A219, SLC6A220, SLC6A221, SLC6A222, SLC6A223, SLC6A224, SLC6A225, SLC6A226, SLC6A227, SLC6A228, SLC6A229, SLC6A230, SLC6A231, SLC6A232, SLC6A233, SLC6A234, SLC6A235, SLC6A236, SLC6A237, SLC6A238, SLC6A239, SLC6A240, SLC6A241, SLC6A242, SLC6A243, SLC6A244, SLC6A245, SLC6A246, SLC6A247, SLC6A248, SLC6A249, SLC6A250, SLC6A251, SLC6A252, SLC6A253, SLC6A254, SLC6A255, SLC6A256, SLC6A257, SLC6A258, SLC6A259, SLC6A260, SLC6A261, SLC6A262, SLC6A263, SLC6A264, SLC6A265, SLC6A266, SLC6A267, SLC6A268, SLC6A269, SLC6A270, SLC6A271, SLC6A272, SLC6A273, SLC6A274, SLC6A275, SLC6A276, SLC6A277, SLC6A278, SLC6A279, SLC6A280, SLC6A281, SLC6A282, SLC6A283, SLC6A284, SLC6A285, SLC6A286, SLC6A287, SLC6A288, SLC6A289, SLC6A290, SLC6A291, SLC6A292, SLC6A293, SLC6A294, SLC6A295, SLC6A296, SLC6A297, SLC6A298, SLC6A299, SLC6A300, SLC6A301, SLC6A302, SLC6A303, SLC6A304, SLC6A305, SLC6A306, SLC6A307, SLC6A308, SLC6A309, SLC6A310, SLC6A311, SLC6A312, SLC6A313, SLC6A314, SLC6A315, SLC6A316, SLC6A317, SLC6A318, SLC6A319, SLC6A320, SLC6A321, SLC6A322, SLC6A323, SLC6A324, SLC6A325, SLC6A326, SLC6A327, SLC6A328, SLC6A329, SLC6A330, SLC6A331, SLC6A332, SLC6A333, SLC6A334, SLC6A335, SLC6A336, SLC6A337, SLC6A338, SLC6A339, SLC6A340, SLC6A341, SLC6A342, SLC6A343, SLC6A344, SLC6A345, SLC6A346, SLC6A347, SLC6A348, SLC6A349, SLC6A350, SLC6A351, SLC6A352, SLC6A353, SLC6A354, SLC6A355, SLC6A356, SLC6A357, SLC6A358, SLC6A359, SLC6A360, SLC6A361, SLC6A362, SLC6A363, SLC6A364, SLC6A365, SLC6A366, SLC6A367, SLC6A368, SLC6A369, SLC6A370, SLC6A371, SLC6A372, SLC6A373, SLC6A374, SLC6A375, SLC6A376, SLC6A377, SLC6A378, SLC6A379, SLC6A380, SLC6A381, SLC6A382, SLC6A383, SLC6A384, SLC6A385, SLC6A386, SLC6A387, SLC6A388, SLC6A389, SLC6A390, SLC6A391, SLC6A392, SLC6A393, SLC6A394, SLC6A395, SLC6A396, SLC6A397, SLC6A398, SLC6A399, SLC6A400, SLC6A401, SLC6A402, SLC6A403, SLC6A404, SLC6A405, SLC6A406, SLC6A407, SLC6A408, SLC6A409, SLC6A410, SLC6A411, SLC6A412, SLC6A413, SLC6A414, SLC6A415, SLC6A416, SLC6A417, SLC6A418, SLC6A419, SLC6A420, SLC6A421, SLC6A422, SLC6A423, SLC6A424, SLC6A425, SLC6A426, SLC6A427, SLC6A428, SLC6A429, SLC6A430, SLC6A431, SLC6A432, SLC6A433, SLC6A434, SLC6A435, SLC6A436, SLC6A437, SLC6A438, SLC6A439, SLC6A440, SLC6A441, SLC6A442, SLC6A443, SLC6A444, SLC6A445, SLC6A446, SLC6A447, SLC6A448, SLC6A449, SLC6A450, SLC6A451, SLC6A452, SLC6A453, SLC6A454, SLC6A455, SLC6A456, SLC6A457, SLC6A458, SLC6A459, SLC6A460, SLC6A461, SLC6A462, SLC6A463, SLC6A464, SLC6A465, SLC6A466, SLC6A467, SLC6A468, SLC6A469, SLC6A470, SLC6A471, SLC6A472, SLC6A473, SLC6A474, SLC6A475, SLC6A476, SLC6A477, SLC6A478, SLC6A479, SLC6A480, SLC6A481, SLC6A482, SLC6A483, SLC6A484, SLC6A485, SLC6A486, SLC6A487, SLC6A488, SLC6A489, SLC6A490, SLC6A491, SLC6A492, SLC6A493, SLC6A494, SLC6A495, SLC6A496, SLC6A497, SLC6A498, SLC6A499, SLC6A500, SLC6A501, SLC6A502, SLC6A503, SLC6A504, SLC6A505, SLC6A506, SLC6A507, SLC6A508, SLC6A509, SLC6A510, SLC6A511, SLC6A512, SLC6A513, SLC6A514, SLC6A515, SLC6A516, SLC6A517, SLC6A518, SLC6A519, SLC6A520, SLC6A521, SLC6A522, SLC6A523, SLC6A524, SLC6A525, SLC6A526, SLC6A527, SLC6A528, SLC6A529, SLC6A530, SLC6A531, SLC6A532, SLC6A533, SLC6A534, SLC6A535, SLC6A536, SLC6A537, SLC6A538, SLC6A539, SLC6A540, SLC6A541, SLC6A542, SLC6A543, SLC6A544, SLC6A545, SLC6A546, SLC6A547, SLC6A548, SLC6A549, SLC6A550, SLC6A551, SLC6A552, SLC6A553, SLC6A554, SLC6A555, SLC6A556, SLC6A557, SLC6A558, SLC6A559, SLC6A560, SLC6A561, SLC6A562, SLC6A563, SLC6A564, SLC6A565, SLC6A566, SLC6A567, SLC6A568, SLC6A569, SLC6A570, SLC6A571, SLC6A572, SLC6A573, SLC6A574, SLC6A575, SLC6A576, SLC6A577, SLC6A578, SLC6A579, SLC6A580, SLC6A581, SLC6A582, SLC6A583, SLC6A584, SLC6A585, SLC6A586, SLC6A587, SLC6A588, SLC6A589, SLC6A590, SLC6A591, SLC6A592, SLC6A593, SLC6A594, SLC6A595, SLC6A596, SLC6A597, SLC6A598, SLC6A599, SLC6A600, SLC6A601, SLC6A602, SLC6A603, SLC6A604, SLC6A605, SLC6A606, SLC6A607, SLC6A608, SLC6A609, SLC6A610, SLC6A611, SLC6A612, SLC6A613, SLC6A614, SLC6A615, SLC6A616, SLC6A617, SLC6A618, SLC6A619, SLC6A620, SLC6A621, SLC6A622, SLC6A623, SLC6A624, SLC6A625, SLC6A626, SLC6A627, SLC6A628, SLC6A629, SLC6A630, SLC6A631, SLC6A632, SLC6A633, SLC6A634, SLC6A635, SLC6A636, SLC6A637, SLC6A638, SLC6A639, SLC6A640, SLC6A641, SLC6A642, SLC6A643, SLC6A644, SLC6A645, SLC6A646, SLC6A647, SLC6A648, SLC6A649, SLC6A650, SLC6A651, SLC6A652, SLC6A653, SLC6A654, SLC6A655, SLC6A656, SLC6A657, SLC6A658, SLC6A659, SLC6A660, SLC6A661, SLC6A662, SLC6A663, SLC6A664, SLC6A665, SLC6A666, SLC6A667, SLC6A668, SLC6A669, SLC6A670, SLC6A671, SLC6A672, SLC6A673, SLC6A674, SLC6A675, SLC6A676, SLC6A677, SLC6A678, SLC6A679, SLC6A680, SLC6A681, SLC6A682, SLC6A683, SLC6A684, SLC6A685, SLC6A686, SLC6A687, SLC6A688, SLC6A689, SLC6A690, SLC6A691, SLC6A692, SLC6A693, SLC6A694, SLC6A695, SLC6A696, SLC6A697, SLC6A698, SLC6A699, SLC6A700, SLC6A701, SLC6A702, SLC6A703, SLC6A704, SLC6A705, SLC6A706, SLC6A707, SLC6A708, SLC6A709, SLC6A710, SLC6A711, SLC6A712, SLC6A713, SLC6A714, SLC6A715, SLC6A716, SLC6A717, SLC6A718, SLC6A719, SLC6A720, SLC6A721, SLC6A722, SLC6A723, SLC6A724, SLC6A725, SLC6A726, SLC6A727, SLC6A728, SLC6A729, SLC6A730, SLC6A731, SLC6A732, SLC6A733, SLC6A734, SLC6A735, SLC6A736, SLC6A737, SLC6A738, SLC6A739, SLC6A740, SLC6A741, SLC6A742, SLC6A743, SLC6A744, SLC6A745, SLC6A746, SLC6A747, SLC6A748, SLC6A749, SLC6A750, SLC6A751, SLC6A752, SLC6A753, SLC6A754, SLC6A755, SLC6A756, SLC6A757, SLC6A758, SLC6A759, SLC6A760, SLC6A761, SLC6A762, SLC6A763, SLC6A764, SLC6A765, SLC6A766, SLC6A767, SLC6A768, SLC6A769, SLC6A770, SLC6A771, SLC6A772, SLC6A773, SLC6A774, SLC6A775, SLC6A776, SLC6A777, SLC6A778, SLC6A779, SLC6A780, SLC6A781, SLC6A782, SLC6A783, SLC6A784, SLC6A785, SLC6A786, SLC6A787, SLC6A788, SLC6A789, SLC6A790, SLC6A791, SLC6A792, SLC6A793, SLC6A794, SLC6A795, SLC6A796, SLC6A797, SLC6A798, SLC6A799, SLC6A800, SLC6A801, SLC6A802, SLC6A803, SLC6A804, SLC6A805, SLC6A806, SLC6A807, SLC6A808, SLC6A809, SLC6A810, SLC6A811, SLC6A812, SLC6A813, SLC6A814, SLC6A815, SLC6A816, SLC6A817, SLC6A818, SLC6A819, SLC6A820, SLC6A821, SLC6A822, SLC6A823, SLC6A824, SLC6A825, SLC6A826, SLC6A827, SLC6A828, SLC6A829, SLC6A830, SLC6A831, SLC6A832, SLC6A833, SLC6A834, SLC6A835, SLC6A836, SLC6A837, SLC6A838, SLC6A839, SLC6A840, SLC6A841, SLC6A842, SLC6A843, SLC6A844, SLC6A845, SLC6A846, SLC6A847, SLC6A848, SLC6A849, SLC6A850, SLC6A851, SLC6A852, SLC6A853, SLC6A854, SLC6A855, SLC6A856, SLC6A857, SLC6A858, SLC6A859, SLC6A860, SLC6A861, SLC6A862, SLC6A863, SLC6A864, SLC6A865, SLC6A866, SLC6A867, SLC6A868, SLC6A869, SLC6A870, SLC6A871, SLC6A872, SLC6A873, SLC6A874, SLC6A875, SLC6A876, SLC6A877, SLC6A878, SLC6A879, SLC6A880, SLC6A881, SLC6A882, SLC6A883, SLC6A884, SLC6A885, SLC6A886, SLC6A887, SLC6A888, SLC6A889, SLC6A890, SLC6A891, SLC6A892, SLC6A893, SLC6A894, SLC6A895, SLC6A896, SLC6A897, SLC6A898, SLC6A899, SLC6A900, SLC6A901, SLC6A902, SLC6A903, SLC6A904, SLC6A905, SLC6A906, SLC6A907, SLC6A908, SLC6A909, SLC6A910, SLC6A911, SLC6A912, SLC6A913, SLC6A914, SLC6A915, SLC6A916, SLC6A917, SLC6A918, SLC6A919, SLC6A920, SLC6A921, SLC6A922, SLC6A923, SLC6A924, SLC6A925, SLC6A926, SLC6A927, SLC6A928, SLC6A929, SLC6A930, SLC6A931, SLC6A932, SLC6A933, SLC6A934, SLC6A935, SLC6A936, SLC6A937, SLC6A938, SLC6A939, SLC6A940, SLC6A941, SLC6A942, SLC6A943, SLC6A944, SLC6A945, SLC6A946, SLC6A947, SLC6A948, SLC6A949, SLC6A950, SLC6A951, SLC6A952, SLC6A953, SLC6A954, SLC6A955, SLC6A956, SLC6A957, SLC6A958, SLC6A959, SLC6A960, SLC6A961, SLC6A962, SLC6A963, SLC6A964, SLC6A965, SLC6A966, SLC6A967, SLC6A968, SLC6A969, SLC6A970, SLC6A971, SLC6A972, SLC6A973, SLC6A974, SLC6A975, SLC6A976, SLC6A977, SLC6A978, SLC6A979, SLC6A980, SLC6A981, SLC6A982, SLC6A983, SLC6A984, SLC6A985, SLC6A986, SLC6A987, SLC6A988, SLC6A989, SLC6A990, SLC6A991, SLC6A992, SLC6A993, SLC6A994, SLC6A995, SLC6A996, SLC6A997, SLC6A998, SLC6A999, SLC6A1000, SLC6A1001, SLC6A1002, SLC6A1003, SLC6A1004, SLC6A1005, SLC6A1006, SLC6A1007, SLC6A1008, SLC6A1009, SLC6A1010, SLC6A1011, SLC6A1012, SLC6A1013, SLC6A1014, SLC6A1015, SLC6A1016, SLC6A1017, SLC6A1018, SLC6A1019, SLC6A1020, SLC6A1021, SLC6A1022, SLC6A1023, SLC6A1024, SLC6A1025, SLC6A1026, SLC6A1027, SLC6A1028, SLC6A1029, SLC6A1030, SLC6A1031, SLC6A1032, SLC6A1033, SLC6A1034, SLC6A1035, SLC6A1036, SLC6A1037, SLC6A1038, SLC6A1039, SLC6A1040, SLC6A1041, SLC6A1042, SLC6A1043, SLC6A1044, SLC6A1045, SLC6A1046, SLC6A1047, SLC6A1048, SLC6A1049, SLC6A1050, SLC6A1051, SLC6A1052, SLC6A1053, SLC6A1054, SLC6A1055, SLC6A1056, SLC6A1057, SLC6A1058, SLC6A1059, SLC6A1060, SLC6A1061, SLC6A1062, SLC6A1063, SLC6A1064, SLC6A1065, SLC6A1066, SLC6A1067, SLC6A1068, SLC6A1069, SLC6A1070, SLC6A1071, SLC6A1072, SLC6A1073, SLC6A1074, SLC6A1075, SLC6A1076, SLC6A1077, SLC6A1078, SLC6A1079, SLC6A1080, SLC6A1081, SLC6A1082, SLC6A1083, SLC6A1084, SLC6A1085, SLC6A1086, SLC6A1087, SLC6A1088, SLC6A1089, SLC6A1090, SLC6A1091, SLC6A1092, SLC6A1093, SLC6A1094, SLC6A1095, SLC6A1096, SLC6A1097, SLC6A1098, SLC6A1099, SLC6A1100, SLC6A1101, SLC6A1102, SLC6A1103, SLC6A1104, SLC6A1105, SLC6A1106, SLC6A1107, SLC6A1108, SLC6A1109, SLC6A1110, SLC6A1111, SLC6A1112, SLC6A1113, SLC6A1114, SLC6A1115, SLC6A1116, SLC6A1117, SLC6A1118, SLC6A1119, SLC6A1120, SLC6A1121, SLC6A1122, SLC6A1123, SLC6A1124, SLC6A1125, SLC6A1126, SLC6A1127, SLC6A1128, SLC6A1129, SLC6A1130, SLC6A1131, SLC6A1132, SLC6A1133, SLC6A1134, SLC6A1135, SLC6A1136, SLC6A1137, SLC6A1138, SLC6A1139, SLC6A1140, SLC6A1141, SLC6A1142, SLC6A1143, SLC6A1144, SLC6A1145, SLC6A1146, SLC6A1147, SLC6A1148, SLC6A1149, SLC6A1150, SLC6A1151, SLC6A1152, SLC6A1153, SLC6A1154, SLC6A1155, SLC6A1156, SLC6A1157, SLC6A1158, SLC6A1159, SLC6A1160, SLC6A1161, SLC6A1162, SLC6A1163, SLC6A1164, SLC6A1165, SLC6A1166, SLC6A1167, SLC6A1168, SLC6A1169, SLC6A1170, SLC6A1171, SLC6A1172, SLC6A1173, SLC6A1174, SLC6A1175, SLC6A1176, SLC6A1177, SLC6A1178, SLC6A1179, SLC6A1180, SLC6A1181, SLC6A1182, SLC6A1183, SLC6A1184, SLC6A1185, SLC6A1186, SLC6A1187, SLC6A1188, SLC6A1189, SLC6A1190, SLC6A1191, SLC6A1192, SLC6A1193, SLC6A1194, SLC6A1195, SLC6A1196, SLC6A1197, SLC6A1198, SLC6A1199, SLC6A1200, SLC6A1201, SLC6A1202, SLC6A1203, SLC6A1204, SLC6A1205, SLC6A1206, SLC6A1207, SLC6A1208, SLC6A1209, SLC6A1210, SLC6A1211, SLC6A1212, SLC6A1213, SLC6A1214, SLC6A1215, SLC6A1216, SLC6A1217, SLC6A1218, SLC6A1219, SLC6A1220, SLC6A1221, SLC6A1222, SLC6A1223, SLC6A1224, SLC6A1225, SLC6A1226, SLC6A1227, SLC6A1228, SLC6A1229, SLC6A1230, SLC6A1231, SLC6A1232, SLC6A1233, SLC6A1234, SLC6A1235, SLC6A1236, SLC6A1237, SLC6A1238, SLC6A1239, SLC6A1240, SLC6A1241, SLC6A1242, SLC6A1243, SLC6A1244, SLC6A1245, SLC6A1

OPR-151

Long-term clinical benefit of idebenone in LHON: Results from the prospective, natural history-controlled LEROS study

T. Klopstock¹, L. Tomasso², X. Llòria², V. Carelli³, P. Yu Wai Man⁴, on behalf of the LEROS study group

¹ Department of Neurology, Friedrich-Baur-Institute, University Hospital of the Ludwig-Maximilians-University, Munich, Germany, ² Chiesi Farmaceutici S.p.A., Parma, Italy, ³ IRCCS Istituto di Scienze Neurologiche di Bologna, Bologna, Italy, ⁴ Moorfields Eye Hospital, London, United Kingdom

Background and aims: Idebenone is approved in Europe for treating Leber's hereditary optic neuropathy (LHON) – a rare mitochondrial disorder resulting in vision loss. Controlled data detailing long-term treatment is sparse.

Methods: Patients with LHON onset ≤ 5 years prior were enrolled and stratified by time since onset: subacute/dynamic (≤ 1 year) and chronic (> 1 year). The primary outcome measure was clinically relevant benefit (CRB=clinically relevant recovery and/or stabilisation of visual acuity [VA]) from baseline after 12 months of treatment. Data from 181 patients treated up to 24 months were compared to an external natural history (NH) cohort (372 patients), matched by time since disease onset.

Results: The primary endpoint was met (42.3% CRB in treated subacute/dynamic eyes at 12 months [60/142] vs 20.7% [40/193] in matched NH cohort eyes [$p=0.0020$]); this difference was maintained after 24 months (52.9% [64/121] vs 36.0% [27/75] [$p=0.0297$]). A similar result was observed in chronic patients at 12 months (50.3% [72/143] vs 38.6% [59/153] [$p=0.0087$]). In subacute/dynamic eyes, CRB was largely driven by stabilisation of VA at 12 months (64.5% [20/31] vs 22.5% [9/40] [$p=0.0005$]), while in chronic eyes by recovery of VA (32.9% [47/143] vs 19.6% [30/153] [$p=0.0034$]).

Conclusion: In LEROS, long-term treatment with idebenone resulted in prolonged clinical benefit in patients with LHON. This benefit was largely driven by preventing significant VA loss in the subacute/dynamic phase, and by VA recovery in the chronic phase.

Disclosure: TK has received research support and personal fees from Santhera Pharmaceuticals and Chiesi GmbH. LT and XL are employees of Chiesi Farmaceutici S.p.A. LEROS was funded by Santhera Pharmaceuticals. TK, VC, PYWM: Research support and/or compensation from Santhera Pharmaceuticals, Chiesi GmbH and GenSight Biologics. LT, XL: Employees of Chiesi Farmaceutici S.p.A.

Neuro-oncology 2

OPR-152

CAR T-cell therapy in BologNa - NEUrotoxicity TRreatment and Assessment in Lymphoma: the CARBON-NEUTRAL study

M. Guarino ¹, U. Pensato ², G. Amore ³, L. Muccioli ³, F. Rondelli ¹, R. D'Angelo ¹, R. Rinaldi ¹, S. Sammali ³, M. Nicodemo ¹, S. Mondini ¹, L. Sambati ¹, R. Santoro ¹, A. Farolfi ⁴, L. Spinardi ⁵, L. Faccioli ⁵, E. Pierucci ⁶, B. Casadei ⁷, P. Zinzani ⁷, P. Cortelli ¹, F. Bonifazi ⁷
¹ IRCCS Istituto delle Scienze Neurologiche di Bologna, Bologna, Italy, ² IRCCS Humanitas Research Hospital -, via Manzoni 56, 20089 Rozzano, Milan, Italy, ³ Dipartimento di Scienze Biomediche e Neuromotorie, Università di Bologna, Bologna, Italy, ⁴ Division of Nuclear Medicine, IRCCS Azienda Ospedaliero-Universitaria di Bologna, Bologna, Italy, ⁵ Diagnostic and Interventional Neuroradiology Unit - S.Orsola-Malpighi Hospital, Bologna, Italy, ⁶ Intensive Therapy Unit- S.Orsola-Malpighi Hospital, Bologna, Italy, ⁷ IRCCS Azienda Ospedaliero-Universitaria di Bologna, Istituto di Ematologia "Seràgnoli", Bologna, Italy

Background and aims: To investigate clinical, laboratory and instrumental characteristics of chimeric antigen receptor (CAR) T-cells therapy-related neurotoxicity.

Methods: In this prospective, monocentric study, consecutive patients affected by refractory B-cell non-Hodgkin lymphoma were included. Patients were comprehensively screened (neurological examination, EEG, brain MRI, nerve conduction study, neuropsychological evaluation) before infusion. From the day of CAR T-cells infusion, patients underwent serial examinations to monitor development of neurotoxicity (Figure 1).

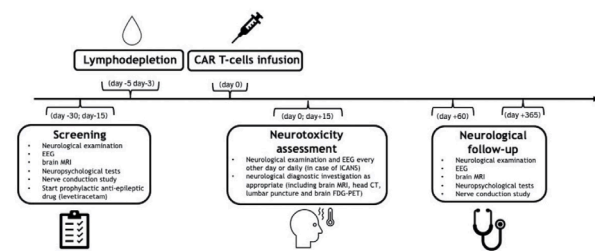


Figure 1: Neurological assessment protocol comprehensive of screening, toxicity monitoring and follow-up.

Results: Of 103 consecutive patients candidate to receive anti-CD19 CAR T-cells infusion, 45% (n=46) were treated and included in the study (Figure 2). Median age at infusion was 56.5 years and 13 patients (28%) were females. Seventeen patients (37%) developed neurotoxicity characterized by encephalopathy frequently associated with language disturbances (65%) and frontal lobe dysfunction (65%). A predominant frontal lobe involvement was also supported by ancillary tests (EEG, neuropsychological

evaluation and brain FDG-PET). Median time at onset and duration were five and eight days, respectively. EEG abnormalities at baseline represented a negative prognostic factor (OR=10.027; CI=1.509-66.628; p=0.017). Notably, CRS was invariably present prior to or concomitant with neurotoxicity, and all patients who exhibited severe CRS developed neurotoxicity. A strong correlation between CRS and neurotoxicity was observed in all clinical and laboratory explored parameters (Figure 3). Fourteen patients had complete neurological resolution, whereas three patients died secondary to systemic complications, of whom only one with neurotoxicity (fulminant cerebral oedema).

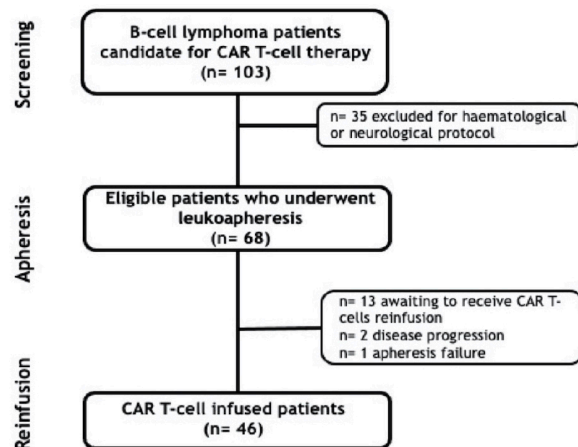


Figure 2: Eligibility flow chart of patients with B-cell lymphoma who received CAR T-cell therapy.

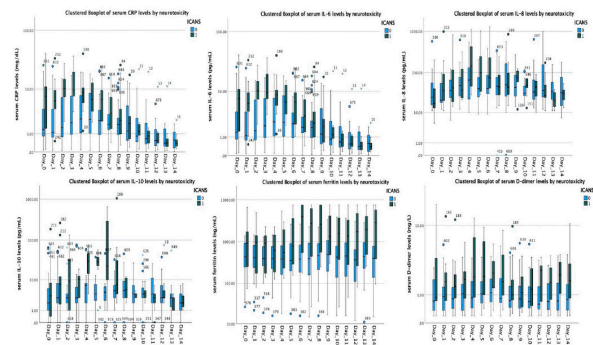


Figure 3: Serum level of CRP, IL-6, IL-8, IL-10, ferritin and D-dimer during the first two-weeks from CAR T-cells infusion in ICANS patients (blue boxes) and patient who did not develop neurotoxicity (green boxes).

Conclusion: Neurotoxicity related to CAR T-cell therapy exhibits a distinctive clinical and investigative signature, namely frontal predominant encephalopathy, and is strictly related to CRS, arguably involving cytokine-mediated neuroinflammatory mechanisms.

Disclosure: Nothing to disclose.

OPR-153

Neratinib for treatment of leptomeningeal metastases from HER2-positive breast cancer in extended access program

A. Pellerino¹, F. Bruno¹, R. Manna², E. Muscolino¹, P. Botta¹, R. Palmiero¹, R. Rudà³, R. Soffiotti¹

¹ Division of Neuro-Oncology, Department of Neuroscience, University and City of Health and Science Hospital, Turin, Italy, ² Department of Medical, Surgical Sciences and Advanced Technologies GF Ingrassia, University of Catania, Catania, Italy, ³ Department of Neurology, Castelfranco Veneto and Treviso Hospital, Treviso, Italy

Background and aims: The aim of the study was to evaluate the activity of neratinib in leptomeningeal metastases (LM) from HER2-positive breast cancer (BC) after the failure of multiple treatments.

Methods: Adult patients with a newly diagnosed LM (LANO criteria) from HER2-positive BC with KPS ≥ 60 were included. Coexistence of BM that have or not received radiotherapy and previous antineoplastic drugs for systemic disease were allowed, with the exclusion of lapatinib. Primary endpoint was the overall survival (OS). Secondary endpoints were progression-free survival (PFS), neurological benefit, radiological response, and tolerability.

Results: Nine patients have been enrolled with a median age of 44 years, and a median KPS of 80. Median time since LM onset from the diagnosis of primary BC was 42 months, after a median number of adjuvant treatments before LM of 3. Three patients developed LM alone, and other 6 had LM associated with BM. Six-months and 1-year OS were 66.7% and 22.3%, respectively, with a median OS of 8 months (95%CI 3-13*). Median PFS was 3.5 months (95%CI 2-6) after the start of treatment. A neurological improvement was reported in 2/9 patients (22.2%), while in other 4/9 patients (44.5%) was achieved a neurological stabilization lasting for a median time of 5 months (95%CI 2-19). The best radiological response was a stable disease in 5/9 patients (55.6%). A CSF clearance was observed in 1 patient (11.1%). Two patients (22.2%) had mild diarrhea correlated with neratinib.

Conclusion: Neratinib might be a safe and effective treatment in LM from heavily pretreated HER2-positive BC

Disclosure: The Authors declare that have no conflict of interest.

OPR-154

Long term neurological safety in B-cell lymphoma patients treated with CAR T-cell therapy: a prospective cohort study

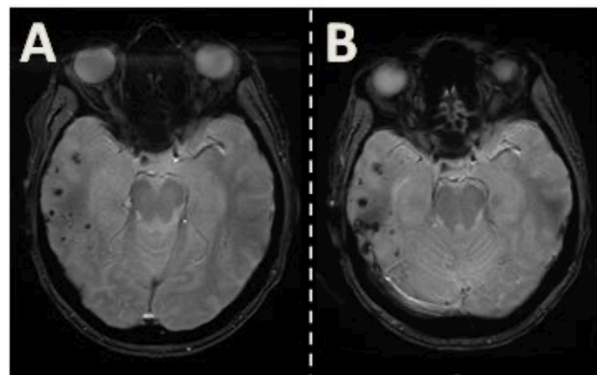
R. Ursu¹, D. Maillat¹, C. Belin¹, C. Moroni², S. Cuzzubbo³, V. Vernier¹, L. Sirven-Villaras¹, C. Carreau¹, R. Di Blasi⁴, C. Thieblemont⁴, A. Carpentier¹

¹ Assistance Publique-Hôpitaux de Paris (AP-HP), Hôpital Saint-Louis, Paris, France, ² Université de Lille, ULR 4072 – PSITEC – Psychologie: Interactions, Temps, Emotions, Cognition, Lille, France, ³ Université de Paris, Paris Diderot, Paris, France, ⁴ Service d'Hémo-Oncologie, Hôpital Saint-Louis, Assistance Publique-Hôpitaux de Paris (AP-HP), Paris, France

Background and aims: Anti-CD19 CAR T-cell therapy has transformed the standard of care for patients with relapsed and refractory hematologic malignancies, but is frequently associated with acute neurotoxicity. Yet, long-term neurological safety is still unknown.

Methods: We here report a long-term, prospective, follow-up study of an adult patient population with aggressive B-cell lymphoma, treated with CAR – T cell therapy in our center between October 2018 and August 2019. All patients underwent neurological examination, neuropsychological assessment, cerebral MRI and completed self-administrated questionnaires, both at baseline and two-years after CAR T-cells infusions.

Results: 52 patients were included, 33 had tumour progression or died, leaving 19 disease-free patients for long-term evaluation (at 2 years). None of these patients developed new neurological deficits or MRI changes when compared to baseline. Cognitive performances showed no difference before and two years later after for all evaluated patients, including in patients who had developed acute neurotoxicity after CAR T-cells. In self-questionnaire assessments, anxiety and depression complaints significantly (?) improved at two years when compared to baseline.



Brain MRI: T2* weighted images of patient with multiple micro bleeds at baseline (A) and at two years (B) after CAR T-cell treatment.

Conclusion: This study suggests a long-term neurological safety for CAR-T cell therapy as neither neurocognitive disorders, nor neurologic impairments, nor modifications of cerebral imaging were observed two years after CAR T-cell infusions.

Disclosure: Nothing to disclose.

OPR-155

Risk factors for temozolomide-induced myelotoxicity and effect of dose adjustments on prognosis of glioblastoma patients

N. Grun¹, J. Osinga¹, A. Van der Vegt¹, F. Van den Elzen¹, C. Den Otter¹, T. Postma¹, M. Schuur¹, P. De Witt Hamer², A. Bruynzeel³, F. Lagerwaard³, M. Van Linde⁴, I. Bartelink⁵, B. Lissenberg-Witte⁶, M. Kouwenhoven¹

¹ Department of Neurology, Amsterdam UMC location VUmc, Amsterdam, The Netherlands, ² Department of Neurosurgery, Amsterdam UMC location VUmc, Amsterdam, The Netherlands, ³ Department of Radiotherapy, Amsterdam UMC location VUmc, Amsterdam, The Netherlands, ⁴ Department of Medical Oncology, Amsterdam UMC location VUmc, Amsterdam, The Netherlands, ⁵ Department of Pharmacy, Amsterdam UMC location VUmc, Amsterdam, The Netherlands, ⁶ Department of Biostatistics and Data Science, Amsterdam UMC location VUmc, Amsterdam, The Netherlands

Background and aims: Temozolomide (TMZ) is generally well-tolerated in patients treated for glioblastoma; a malignant primary brain tumor with poor prognosis. Still, 16% of the patients develop severe myelotoxicity during standard first line treatment. In this study, we evaluate risk factors for severe myelotoxicity and prognosis of toxicity-dictated treatment adjustments.

Methods: Retrospective cohort study of patients treated with standard treatment between 2000–2021; 359 patients with glioblastoma were included. We identified risk factors for myelotoxicity by logistic regression, determined decrease in thrombocytes to identify patients at risk for severe thrombocytopenia during chemoradiation with ROC analysis and used Kaplan-Meier analysis for survival analyses.

Results: Females (OR 12,807; [95% CI: 5,488–29,884]) and patients >50 years (OR 3,473 [1,373–8,785]) were at risk for severe myelotoxicity. Females were more at risk for severe thrombocytopenia (OR 9,667 [4,164–22,442]) compared to men. A decrease in thrombocyte counts of $\geq 31.22\%$ identified patients who developed severe thrombocytopenia with a sensitivity of 100% and specificity of 80.5% (AUC 0.952 [0.910–0.994]). The median survival of patients discontinuing adjuvant treatment was reduced compared to patients who received 6 courses TMZ with or without dose reduction (14 vs 21 months; $p=0.004$).

Conclusion: Females and patients >50 years were at risk for myelotoxicity. Patients with a decrease in thrombocytes of $\geq 31.22\%$ during chemoradiation were at risk for severe thrombocytopenia. Discontinuation of adjuvant TMZ treatment negatively impacted prognosis, dose reductions during the adjuvant phase did not affect survival in patients with glioblastoma.

Disclosure: Nothing to disclose.